



Cyclodextrin nanostructures and ocular drug delivery

Blanca Lorenzo-Veiga

Thesis for the degree of Philosophiae Doctor

Supervisors:

Professor Hákon Hrafn Sigurðsson

Professor Þorsteinn Loftsson

Doctoral committee:

Professor Carmen Alvarez-Lorenzo

Professor Einar Stefánsson

Professor Margrét Thorsteinsdóttir

October 2020



UNIVERSITY OF ICELAND
SCHOOL OF HEALTH SCIENCES

FACULTY OF PHARMACEUTICAL SCIENCES

Sýklódextrín nanóagnir fyrir augnlyfjagjöf

Blanca Lorenzo-Veiga

Ritgerð til doktorsgráðu

Leiðbeinendur:

Professor Hákon Hrafn Sigurðsson

Professor Þorsteinn Loftsson

Doktorsnefnd:

Professor Carmen Alvarez-Lorenzo

Professor Einar Stefánsson

Professor Margrét Thorsteinsdóttir

Október 2020



UNIVERSITY OF ICELAND
SCHOOL OF HEALTH SCIENCES

FACULTY OF PHARMACEUTICAL SCIENCES

Thesis for a doctoral degree at the University of Iceland. All right reserved.
No part of this publication may be reproduced in any form without the prior
permission of the copyright holder.

© Blanca Lorenzo-Veiga 2020

ISBN 978-9935-9445-5-9

Printing by Háskólaprent EHF.

Reykjavik, Iceland 2020

Ágrip

Þróun augnlyfja er mjög krefjandi vegna einstakrar byggingar augans og hindrana sem eru á flæði lyfja í gegnum himnur augans. Lítil vatnsleysni margra lyfja of stuttur viðverutími þeirra á yfirborði augans gerir þróun augnlyfjasamsetninga enn erfiðari. Nokkar aðferðir hafa verið reyndar til að auka aðgengi lyfja inn í augað. Sýklódextrín nanóagnir eru áhugaverð nálgun á þessu vandamáli þar sem sýklódextrín hafa mikla getu til að auka vatnsleysni fitusækinna lyfja og hjálpa þeim að komast í gegnum lífrænar himnur. Sýklódextrín nanóagnir auka viðverutíma lyfja á yfirborði augans og valda með því auknu frásogi inn í augað.

Markmið þessa verkefnis var að auka leysni lyfjanna Nepafenac og Natamycin með notkun sýklódextrín flétta og fjölliða sem mynda örkjarna í lausn og auka frásog lyfjanna í gegnum helstu himnur augans.

Nepafenac er bólgueyðandi lyf sem er ávísað gegn bólgum og verkjum sem fylgja augasteinsaðgerðum. Lyfið er torleyst í vatni og kemst illa í gegnum himnur augans. Fléttumyndun lyfsins við sex sýklódextrín í fjölliðulausnum var rannsökuð ásamt því að skoða hvernig nanóagnir mynduðust. Helstu niðurstöður sýndu að HP β -CD jók leysni lyfsins mest og γ -CD stuðlaði að mestri nanóagnamyndum. Fléttumyndum var rannsökuð með leysniferli ásamt DSC, FT-IR og ¹H-NMR aðferðum. Sú flétta sem kom best út var samsett úr 15% (w/v) γ -CD og 8% (w/v) HP β -CD. Sú flétta var þróuð áfram með mismunandi vatnsleysanlegum fjölliðum. Eðlislyfjafræðilegir eiginleikar fléttanna voru rannsakaðir ásamt því að nota mismunandi aðferðir til að meta hæfni þeirra til að koma lyfinu í gegnum himnur og vefi augans. Einnig voru líffræðilegar aðferðir notaðar til að meta virkni, ertingu og eitrunaráhrif lyfjasamsetninganna. Lyfjasamsetningarnar voru bornar saman við Nevanac[®] sem er skráð lyf á markaði og komu þær mun betur út m.t.t. ofangreindra þátta heldur en skráða lyfið.

Natamycin er notað við sveppasýkingum í augum. Notkun þess er þó takmörkuð vegna þess hve torleyst lyfið er og aðgengi þess í augum lélegt. Fjölliðurnar Soluplus[®] og Pluronic[®] P103 voru notaðar til að búa mísellur, blandaðar mísellur og rotaxana í mismunandi lyfjasamsetningum með α -CD. Eðlislyfjafræðilegir eiginleikar fjölliðukerfanna voru rannsakaðir ásamt því nota mismunandi aðferðir til að meta hæfni þeirra til að koma lyfinu í gegnum himnur og vefi augans. Einnig voru líffræðilegar aðferðir notaðar til að meta

virgni, ertingu og eitrunaráhrif lyfjasamsetninganna. Soluplus mísellur reyndust best til að auka leysni lyfsins. Rotaxanar reyndust ekki hentugir til að auka flæði lyfsins inn í vefi augans samanborið við mísellurnar.

Samantekið þá tókst að þróa lyfjasamsetningar fyrir annars vegar Nepafenac og hinsvegar Natamycin sem auka leynsi lyfjanna, hafa hentuga eiginleika fyrir augnlyfjasamsetningar og valda ekki ertingu eða eitrunaráhrifum í einföldum prófunum.

Lykilorð:

Sýkódextrín, mísellur, poly(pseudo)rotaxane, örferjur, augnlyfjagjöf.

Abstract

Ocular drug delivery is very challenging due to the anatomical and physiological barriers of the eye. Poor aqueous solubility of many drugs and short retention time at ocular surfaces makes the formulation of topical dosage forms even more challenging. Several approaches have been reported to enhance drug bioavailability at the ocular tissues. Cyclodextrin-based nanocarriers have been selected due to their well-known capability of cyclodextrins to enhance the solubility of lipophilic drugs and its permeability through biological membranes. They can also prolong the retention time of ophthalmic formulations on the ocular surface and, as a consequence, increase their bioavailability.

The aim of this project was to apply cyclodextrin technology and cyclodextrin-amphiphilic copolymers to enhance the aqueous solubility of two poorly soluble drugs, Nepafenac and Natamycin, as well as their corneal or scleral accumulation.

Nepafenac is a non-steroidal anti-inflammatory drug (NSAID) prescribed for the treatment of pain and inflammation that usually occurred after cataract surgery. Nepafenac has low water solubility and ocular permeability. The complexation of nepafenac with six CDs and various water-soluble polymers was investigated. Results showed that HP β -CD showed the highest solubilizing capacity, while γ -CD led to the highest aggregate formation. Complex formation was investigated and supported by phase solubility analysis, DSC, FT-IR and ¹H-NMR. The optimized complex, which contained 15% (w/v) γ -CD and 8% (w/v) HP β -CD, was selected for additional studies. Nine formulations containing nepafenac/ γ -CD/HP β -CD complexes and various water-soluble polymers were prepared. Physicochemical and rheological characterization, mucoadhesive capacity, ocular tolerance, diffusion studies, corneal and scleral permeability, and anti-inflammatory activity of these formulations were investigated and compared to the marketed nepafenac suspension, Nevanac[®] 3 mg/mL. The formulations displayed zeta potential from -6 to -27 mV, microparticle size in the range of 340-5950 nm, neutral pH and high sclera permeation. Moreover, they were found to be non-toxic and non-irritant. Compared to Nevanac[®], formulations containing poly(vinyl)-alcohol (PVA), methylcellulose (MC) and carboxymethyl cellulose (CMC) presented the best results in relation to sclera accumulation and anti-inflammatory activity.

Natamycin is approved for the treatment of fungal keratitis but its use is restricted due to its low water solubility and low ocular penetration. Soluplus[®] and Pluronic[®] P103 were selected as surfactants to prepare single and mixed micelles and poly(pseudo)rotaxanes for Natamycin encapsulation. Soluplus, Pluronic P103 and a mixture of Soluplus/ Pluronic in ratio 4:1 dispersions were prepared with and without 10% α -CD in 0.9% sodium chloride or buffer pH 6.4. They were investigated in relation to their solubility, particle size, zeta potential, pH, rheological properties, diffusion studies, ocular irritancy, and ex vivo cornea and sclera permeation. All formulations revealed zeta potentials close to zero while differences were found with respect to their size. Soluplus micelles and mixed micelles revealed larger sizes (range 90-150 nm) followed by Pluronic P103 micelles. Soluplus micelles led to the highest Natamycin solubility, followed by Pluronic P103 and their mixed micelles. All formulations were found cytocompatible on murine fibroblasts and did not display irritation. Although Soluplus nanomicelles and poly(pseudo)rotaxanes showed in situ gel behavior at 35 °C and the highest solubilizing capacity, Pluronic and Soluplus poly(pseudo)rotaxanes led to the lowest diffusion rate and corneal and sclera permeation. Moreover, poly(pseudo)rotaxanes of mixed micelles showed intermediate diffusion release and permeability through cornea and sclera comparing to only Soluplus and Pluronic poly(pseudo)rotaxanes.

To conclude, we would like to point out that both optimized Nepafenac formulation and Natamycin-based mixed poly(pseudo)rotaxanes may represent a new approach for topical instillation of drugs to the posterior segment of the eye.

Keywords: Cyclodextrin, micelles, poly(pseudo)rotaxane, nanocarrier, ocular drug delivery.

Acknowledgements

The research work presented in this thesis was developed at the Faculty of Pharmaceutical Science, School of Health Science, the University of Iceland over the years 2016-2018, and at R+D Pharma Group (GI-1645), Faculty of Pharmacy, University of Santiago de Compostela over a twelve-month period in 2018-2019, with financial support from Professor Thorsteinn Loftsson, Erasmus+ traineeship Grant (IS-SM2018-81075) and Berthóra and Thorsteins Thorsteinssonar fund.

First, I would like to express my most sincere appreciation to my main supervisor, Professor Hákon Hrafn Sigurðsson, and Professor Þorsteinn Loftsson, for all the knowledge taught as well as their support, advice, and kindness. For allowing me to start a privileged path with them that allowed me to grow academically, professionally, and personally. Secondly, I would like to thank Professor Carmen Alvarez-Lorenzo for her guidance, dedication, and patience. I would also like to thank all the members of her research group, R+D Pharma Group, and especially to Maria, Ángela, Fernando, and Andrea for their help, kindness, and friendship. I am grateful to have had the opportunity to work with all these talented people to whom I admire deeply. Moreover, I am eternally grateful to Dr. Patricia Diaz-Rodriguez for her guidance, help, and co-work in vitro cell assays.

I would like to thank my doctoral committee for their kindness and advice throughout the dissertation.

Many thanks to my colleagues and friends in Iceland, for their loyalty and encouragement throughout these years, especially to Sigrún Sigurðardóttir, Auður Ágústsdóttir, Maria Folguera, Margarida, Xixia, Sebastian, Vivien, Flor, Manisha, Pui, May, and Zoltan.

I extend my special appreciation to my friends community pharmacists in Vigo, especially to Raquel and her staff, Floro and Berbes Group, for their knowledge, support, friendship, and advice during my years as a community pharmacist.

Last but not least, I am very grateful to my beloved family, my parents, my grandmother, sister, brother-in-law, and my best friend Arancha for their love, advice and endless support all these years. Special thanks to my sister, Beatriz, and my brother-in-law, Savo, for being always there for me and

encourage me to follow an academic career. Thank you to my boyfriend, Tómas, and his family for their kindness and love during my years in Iceland. Takk fyrir.

Finally, I would also like to thank other people that I did not mention here, but who helped me to conduct my research.

Contents

Ágrip	v
Abstract	vii
Acknowledgements.....	ix
Contents	xi
List of abbreviations	xiv
List of figures.....	xviii
List of tables	xxi
List of original papers.....	xxiii
Declaration of contribution	xxiv
1 Introduction	1
1.1 Anatomy, physiology, barriers and common diseases affecting the eye	1
1.1.1 Anterior segment.....	3
1.1.2 Posterior segment	7
1.2 Routes of drug administration	9
1.3 Viscosity modifier polymers	10
1.3.1 Polyvinylpyrrolidone (PVP).....	12
1.3.2 Poly(vinyl)alcohol (PVA).....	12
1.3.3 Cellulose derivatives	13
1.3.4 Tyloxapol	13
1.3.5 Sodium alginate (SA)	13
1.3.6 Sodium hyaluronate (HA).....	14
1.4 Novel drug delivery systems	14
1.5 Cyclodextrins as solubilizers and penetration enhancers	19
1.6 CD-based ophthalmic formulations for topical drug delivery to the eye	23
1.6.1 CD aggregates	23
1.6.2 Poly(pseudo)rotaxanes	25
2 Aims.....	27
3 Materials and methods	28
3.1 Materials.....	28
3.2 Quantitative analysis.....	29

3.2.1	Nepafenac quantification method.....	29
3.2.2	Natamycin quantification method	30
3.3	Solubility studies	30
3.3.1	Phase-solubility studies of nepafenac.....	30
3.3.2	Solubility of nepafenac eye drops	31
3.3.3	Solubility tests of natamycin	32
3.4	Nepafenac/CD aggregates.....	33
3.4.1	Moisture content of CDs.....	33
3.4.2	Chemical stability of nepafenac.....	33
3.4.3	Preparation of inclusion complexes.....	34
3.4.4	Solid state characterization of nepafenac/CD complexes	34
3.5	Formulations	36
3.5.1	Optimization of nepafenac eye drops.....	36
3.5.2	Natamycin micelles and poly(pseudo)rotaxanes.....	37
3.6	Rheological analysis	38
3.7	HET-CAM	39
3.8	In vitro diffusion studies.....	39
3.9	Ex-vivo cornea and sclera permeability studies.....	40
3.10	Statistical Analysis	41
4	Results and discussion	43
4.1	Nepafenac-loaded cyclodextrin/polymer aggregates.....	43
4.1.1	Stability of nepafenac after a heating method.....	43
4.1.2	Phase-solubility studies	43
4.1.3	Effect of ternary complexes on nepafenac/CD complex solubility	45
4.1.4	Solid-state characterization of nepafenac/CD Inclusion complexes	47
4.2	Nepafenac eye drops	50
4.2.1	Solubility of nepafenac eye drops and their characterization.....	50
4.2.2	Rheological analysis.....	53
4.2.3	Mucoadhesive studies	54
4.2.4	HET-CAM and cytocompatibility tests.....	55
4.2.5	In vitro diffusion studies	57
4.2.6	Ex vivo corneal and scleral permeability studies.....	58
4.2.7	Anti-inflammatory activity	61
4.3	Natamycin micelles and poly(pseudo)rotaxanes	63
4.3.1	Micelles preparation and natamycin solubilization	63
4.3.2	Poly(pseudo)rotaxane formation	70

4.3.3 Rheological properties.....	71
4.3.4 HET-CAM assay.....	73
4.3.5 Natamycin diffusion	74
4.3.6 Ex vivo permeation assay	77
5 Summary and conclusions.....	81
References	83
Paper I.....	101
Paper II.....	102
Paper III.....	103
Appendix	105

List of abbreviations

HP α -CD	2-hydroxypropyl-alpha-cyclodextrin
HP β -CD	2-hydroxypropyl-beta-cyclodextrin
γ -CD	2-hydroxypropyl-gamma-cyclodextrin
α -CD	alpha-cyclodextrin
P _{app}	apparent permeability coefficient
BAK	benzalkonium chloride
β -CD	beta-cyclodextrin
BAB	blood-aqueous barrier
BRB	blood–retinal barrier
BCOP	bovine corneal opacity and permeability
CMC	carboxymethylcellulose
CDPPR	CDs-based poly(pseudo)rotaxanes
$\Delta\delta$	chemical shifts
CAM	chorio-allantoic membrane
CE	complexation efficiency
CMC	critical micelle concentration
CDs	cyclodextrins
DSC	differential scanning calorimetry

DM β -CD	di-methyl-beta-cyclodextrin
DMEM	dulbecco's modified eagle medium
DPBS	dulbecco's phosphate-buffered saline
EDTA	ethylenediamine-tetraacetic acid disodium salt dihydrate
FBS	fetal bovine serum
FDA	Food and Drug Administration
FT-IR	fourier transform infra-red spectroscopy
γ -CD	gamma-cyclodextrin
GRAS	generally recognized as safe
HET-CAM	hen's egg test on chorio-allantoic membrane
HPLC	high-performance liquid chromatography
HEC	hydroxyethyl cellulose
HPC	hydroxypropyl cellulose
HPMC	hydroxypropylmethylcellulose
IL-1ra	interleukin 1 receptor antagonist
IL-6	interleukin 6
IOP	intraocular pressure
S ₀	intrinsic solubility of the drug
IS	irritation score
SDS	lauryl sulfate sodium salt
LPS	lipopolysaccharides

log P	log partition coefficient
EC50	median effective concentration
MC	methyl cellulose
MIC 90	minimal inhibitory concentration
PMA	phorbol 12-myristate 13-acetate
PBS	phosphate-buffered saline
PCL	poly (E-caprolactone)
PEO-PPO- PEO	poly (ethylene oxide)-poly (propylene oxide)-poly (ethylene oxide)
PEG	poly(ethylene glycol)
PLGA	poly(lactic-co-glycolic acid)
PVA	poly(vinyl alcohol)
PDI	polydispersion index
PEG	polyethylene glycol
PVP	polyvinylpyrrolidone
PGE2	prostaglandin E2
RAME β -CD	randomly methylated beta-cyclodextrin
RPE	retinal pigmented epithelium
SEM	scanning electron microscopy
SA	sodium alginate
NaCMC	sodium carboxymethylcellulose

HA	sodium hyaluronate
SDF	solid drug fraction
K_s	stability constant
SD	standard deviation
SB β -CD	sulfobutyloxy-beta-cyclodextrin
TEM	transmission electron microscope analysis
UV	ultraviolet spectroscopy

List of figures

Figure 1. A schematic diagram of the eye.....	2
Figure 2. Representation of some ocular diseases that affect both eye chambers.....	3
Figure 3. A cross-sectional view of the corneal structure.....	4
Figure 4. A cross-sectional view of the cornea epithelial cell layer.....	5
Figure 5. Schematic illustration of the structure of the tear film.....	6
Figure 6. Cross-section of the human retina.....	8
Figure 7. Schematic illustration of routes of ocular administration.....	9
Figure 8. Schematic representation of various ocular nanotechnology-based ocular delivery systems.....	15
Figure 9. Chemical structure and molecular shape of natural cyclodextrins (α -, β -, γ -CDs).....	19
Figure 10. Phase-solubility profile of one drug in the presence of CD.....	20
Figure 11. Schematic illustration of drug penetration into the eye after topical instillation of aqueous cyclodextrin (CD) eye drop solution in the tear film.....	22
Figure 12. Drug/CD complex formation (1:1).....	23
Figure 13. Schematic illustration of poly(pseudo)rotaxane of α -CD and PEO-PPO-PEO triblock copolymers.....	25
Figure 14. Phase-solubility diagram of nepafenac at 25 °C in various CDs aqueous solutions. Results are expressed as mean (n=3).....	44
Figure 15. Effect of cyclodextrins and hydrophilic polymers on the apparent solubility of nepafenac.....	46
Figure 16. FT-IR spectra of (a) pure nepafenac, (b) pure HP β CD, (c) pure γ -CD and (d) freeze-dried nepafenac/15% γ -CD/8%HP β -CD complex.....	47

Figure 17. DSC curves of (a) pure nepafenac, (b) pure γ -CD, (c) pure HP β -CD, (d) freeze-dried nepafenac and mixture of 15% γ -CD/ 2.5%HP β -CD complex, (e) freeze-dried of nepafenac/ 15% γ -CD/ 5%HP β -CD complex and (f) freeze-dried nepafenac/ 15% γ -CD/ 8%HP β -CD complex.....	48
Figure 18. Dependence of viscosity on shear rate conditions of eye drops determined at 37 °C.....	53
Figure 19. Evolution of storage (G' , solid symbols) and loss (G'' , open symbols) moduli as a function of angular frequency (rad/s).....	54
Figure 20. Pictures of the HET-CAM test recorded after 5 min contact with nepafenac formulations.....	56
Figure 21. Viability of BALB/3T3 cells after 24 hours of exposure to ophthalmic formulations A1–A9 and Nevanac at various concentrations and control.....	57
Figure 22. Nepafenac diffusion test through cellulose acetate membrane at 37 °C from eye drop formulations A1 to A9.....	58
Figure 23. Nepafenac permeated through (a) bovine cornea and (b) sclera measured in the receptor chamber as a function of time.....	59
Figure 24. Nepafenac accumulated on the surface and inside (a) cornea and (b) sclera after 6 hours exposition.....	61
Figure 25. Effect of ophthalmic formulations on levels of (a) IL-1ra, (b) IL-6, and (c) prostaglandin E2 (PGE2) in macrophages.....	63
Figure 26. Apparent solubility of natamycin in Soluplus and Pluronic P 103 dispersions (0, 0.01, 0.1, 1, 2, 3, 4 and 5% w/v) prepared in 0.9% NaCl at 25 °C	65
Figure 27. Modification of the absorbance of natamycin-loaded Pluronic P103 10%(w/v) nanomicelle formulations after 30-fold and 60-fold dilution in 0.9% NaCl or pH 6.4 buffer.....	66
Figure 28. Apparent solubility of natamycin in micelle dispersions of 10% (w/v) of Soluplus and Pluronic P103 and their mixtures (Soluplus: Pluronic P103) prepared at various volume ratios in 0.9% NaCl and pH 6.4 buffer. Total copolymer concentration was 10% w/v in all cases.....	68

Figure 29. Schematic illustration of single and mixed nanomicelles formed by self-assembly of the amphiphilic block copolymers, and the CD-based poly(pseudo)rotaxanes.....69

Figure 30. The apparent solubility of natamycin without α -CD and containing 5-10% (w/v) in 0.9% NaCl and pH 6.4 buffer at 25 °C70

Figure 31. Evolution at 25° C of appearance of (A) Soluplus 10% (left) and Pluronic P103 10% (right) dispersions in 0.9% NaCl; (B)(Poly(pseudo)rotaxane formation after addition of 10 % α CD to Soluplus (left), Soluplus/ Pluronic P103 in ratio (4:1) (in the middle) and Pluronic P103 dispersions (right) in pH 6.4 buffer after storage for 12h at room temperature.....71

Figure 32. Evolution of the storage (G') and the loss (G'') moduli as a function of the temperature of (A, B) unloaded and (C, D) drug-loaded copolymer dispersions and their mixtures with and without α -CD poly(pseudo)rotaxanes in 0.9% NaCl (left) and pH 6.4 buffer (right).....72

Figure 33. Photographs of HET-CAM tests of Soluplus and Pluronic P103 formulations. Negative and positive controls refer to 0.9% NaCl and 0.1 N NaOH, respectively.....74

Figure 34. Natamycin diffusion test at 37 °C from Soluplus and Pluronic micelles, Soluplus: Pluronic P103 4:1 vol/vol mixed micelles, and poly(pseudo)rotaxanes in 0.9% NaCl (left) and pH 6.4 buffer (right).....75

Figure 35. The amount of natamycin accumulated inside bovine cornea (a, b) and sclera (c, d) after addition of Soluplus and Pluronic micelles, Soluplus: Pluronic P103 4:1 vol/vol mixed micelles and their poly(pseudo)rotaxanes in 0.9% NaCl (left) and pH 6.4 buffer (right) after 6 hours experimentation.....77

Figure 36. The amount of natamycin permeated through bovine sclera and measured in the receptor chamber as a function of time. Natamycin was formulated in Soluplus and Pluronic micelles, Soluplus: Pluronic P103 4:1 vol/vol mixed micelles, and their poly(pseudo)rotaxanes in 0.9% NaCl (left) and pH 6.4 buffer (right).....79

List of tables

Table 1. Physicochemical characteristics and properties of hydrophilic polymers tested.....	10
Table 2. Typical nanotechnology-based formulations.....	18
Table 3 Currently marketed CDs-based ophthalmic formulations.....	24
Table 4. Polymers used to prepare nepafenac eye drop formulations and their percentages.....	31
Table 5. The polymer composition of the preliminary eye drop formulations.....	34
Table 6. Nepafenac concentrations in an aqueous solution containing 1% (w/v) γ -CD after heating by sonication.....	43
Table 7. Values of the apparent stability constant ($K_{1:1}$) and complexation efficiency (CE).....	44
Table 8. Variation of $^1\text{H-NMR}$ chemical shift, expressed in ppm, of free γ CD alone and nepafenac/ γ -CD complex.....	49
Table 9. Variation of $^1\text{H-NMR}$ chemical shift, expressed in ppm, of free HP β CD alone and nepafenac/ HP β CD complex.....	50
Table 10. Apparent drug solubility, zeta potential, and pH of nepafenac eye drop suspensions.....	51
Table 11. Particle size results of aqueous nepafenac eye drop formulations. Formulations were diluted with MilliQ water.....	52
Table 12. Mucoadhesive strength of ophthalmic formulations on ex vivo bovine cornea.....	55
Table 13. The pH, size and zeta potential of unloaded micelles of Soluplus and Pluronic P103 and their mixtures prepared at various volume ratios in 0.9% NaCl and pH 6.4 buffer.....	64
Table 14. Parameters that characterize the capacity of Soluplus dispersions in 0.9% NaCl to solubilize natamycin estimated using Eqs. (3)–(7). (NAT: natamycin; χ : molar solubilization capacity; P: partition coefficient; PM: molar partition coefficient; ΔG : standard-free Gibbs energy of solubilization; mf: the molar fraction of drug encapsulated inside the micelle).*Data from solubility experiments carried out in pH 6.4 buffer.....	67

Table 15. Parameters that characterize the capacity of Pluronic P103 dispersions in 0.9% NaCl to solubilize natamycin estimated using Eqs. (3)–(7). (NAT: natamycin; χ : molar solubilization capacity; P: partition coefficient; PM: molar partition coefficient; ΔG : standard-free Gibbs energy of solubilization; mf: the molar fraction of drug encapsulated inside the micelle). *Data from solubility experiments carried out in pH 6.4 buffer.....67

Table 16. Natamycin diffusion coefficients from Soluplus and Pluronic micelles, Soluplus: Pluronic P103 4:1 vol/vol mixed micelles and poly(pseudo)rotaxanes in 0.9% NaCl and pH 6.4 buffer.....76

Table 17. Transcleral steady-state flux (J) and permeability coefficients (P_{app}) estimated for natamycin formulated in Soluplus and Pluronic micelles, Soluplus: Pluronic P103 4:1 vol/vol mixed micelles, and poly(pseudo)rotaxanes in 0.9% NaCl and pH 6.4 buffer.....79

List of original papers

This thesis is based on the following original publications, which are referred to in the text by their Roman numerals (I-V):

- I. Lorenzo-Veiga B, Sigurdsson HH, Loftsson T. Nepafenac-Loaded Cyclodextrin/Polymer Nanoaggregates: A New Approach to Eye Drop Formulation. *Materials (Basel)*. 2019;12(2).
- II. Lorenzo-Veiga B, Diaz-Rodriguez P, Alvarez-Lorenzo C, Loftsson T, Sigurdsson HH. In Vitro and Ex Vivo Evaluation of Nepafenac-Based Cyclodextrin Microparticles for Treatment of Eye Inflammation. *Nanomaterials (Basel)*. 2020;10(4):E709.
- III. Lorenzo-Veiga B, Sigurdsson HH, Loftsson T, Alvarez-Lorenzo C. Cyclodextrin(-)Amphiphilic Copolymer Supramolecular Assemblies for the Ocular Delivery of Natamycin. *Nanomaterials (Basel)*. 2019;9(5).

Declaration of contribution

The doctoral student, Blanca Lorenzo-Veiga, with the supervision of her tutor, doctoral committee and co-authors of each study, planned and carried out her research studies, drafted the original manuscripts gathering results and conclusions as appropriate and wrote this thesis.

1 Introduction

Ocular disorders are known to affect the quality of life and might lead to blindness and visual loss (Thevi et al., 2012; Weng et al., 2017). Glaucoma, age-related macular degeneration, diabetic retinopathy, and cataracts are the primary cause of blindness in the elderly, both in developing and developed countries. According to recent epidemiology data, it is estimated that more than 2 billion people around the world suffer from visual impairment or blindness (Bourne et al., 2017; Flaxman et al., 2017; Fricke et al., 2018).

Based on estimations from The Vision Loss Expert Group, the number of blind people is expected to increase to 115 million by 2050 (Varma et al., 2016).

Nowadays, ocular drug delivery is considered a challenge due to the multiple hurdles provided by the protective barriers of the eye that lead to low ocular bioavailability, less than 5%.

Improved ocular bioavailability remains as one of the main objectives in the development of any ophthalmic formulation. Considering that the addition of viscosity enhancers or mucoadhesive polymers prolong residence time but slightly enhance ocular bioavailability, other approaches based on nanoparticulate or colloidal drug delivery systems are needed to improve ocular absorption and reduce side effects (Ali et al., 2016).

This review summarizes the main features of eye anatomy and common eye disorders. Routes of drug administration, its barriers, and strategies to increase ocular absorption are also described. Furthermore, most recent literature on new developments using cyclodextrin-based nanocarriers for topically drug delivery is also included.

1.1 Anatomy, physiology, barriers and common diseases affecting the eye

The eye is a complex and sensitive organ that is organized into two segments: anterior and posterior segments (**Figure 1**).

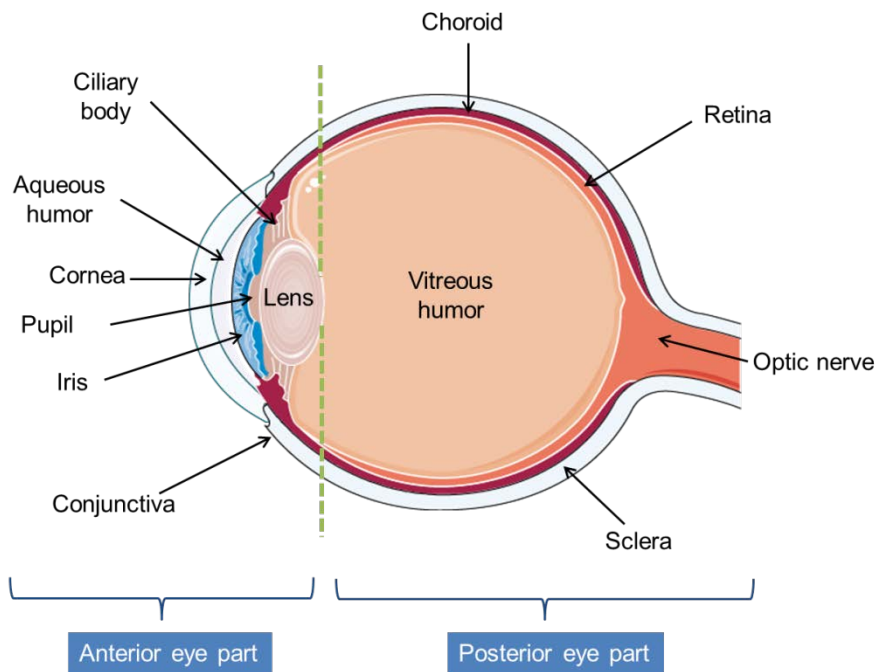


Figure 1. A schematic diagram of the eye. This figure was created using Servier Medical Art by Servier, which is licensed under a Creative Commons Attribution 3.0 Unported License; <https://smart.servier.com>.

The anterior segment includes the exterior part of the eye. It consists of the cornea, conjunctiva, iris, pupil, ciliary body, lens, and aqueous humor that fills the anterior eye tissue space. While the posterior segment is composed of the internal eye structure, which includes sclera, retina, choroid, optic nerve, and vitreous humor that fills the space between the retina and ciliary body (Bachu et al., 2018; Sahoo et al., 2008; Kang-Mieler et al., 2014). Both eye chambers can suffer several eye diseases (**Figure 2**).

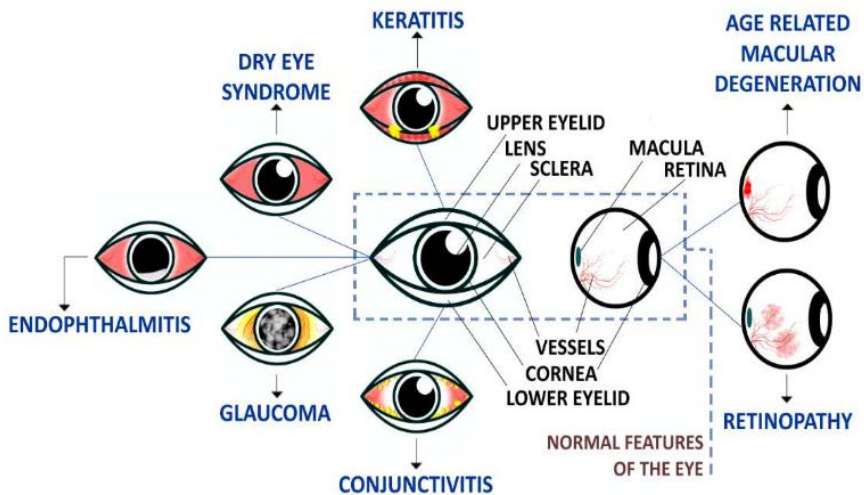


Figure 2. Representation of some ocular diseases that affect both eye chambers. Reproduced with permission from Chaudhari et al. (2019).

The most common disorders at the anterior chamber include keratitis, conjunctivitis, and cataract. In contrast, the most frequent diseases that affect the back of the eye are macular degradation, retinitis, diabetic retinopathy, diabetic macular edema, and endophthalmitis. Uveitis and glaucoma can affect both anterior and posterior eye tissues (Malhotra et al., 2011; Srinivasarao et al., 2019).

1.1.1 Anterior segment

The cornea is the primary barrier of the eye. It is transparent with no blood vessels and contains cellular and extracellular matrix components. It is located in front of the iris and consists of 5 layers: epithelium, Bowman's layer, stroma, Descemet's membrane, and endothelium (Sridhar, 2018; Barar et al., 2008)(**Figure 3**).

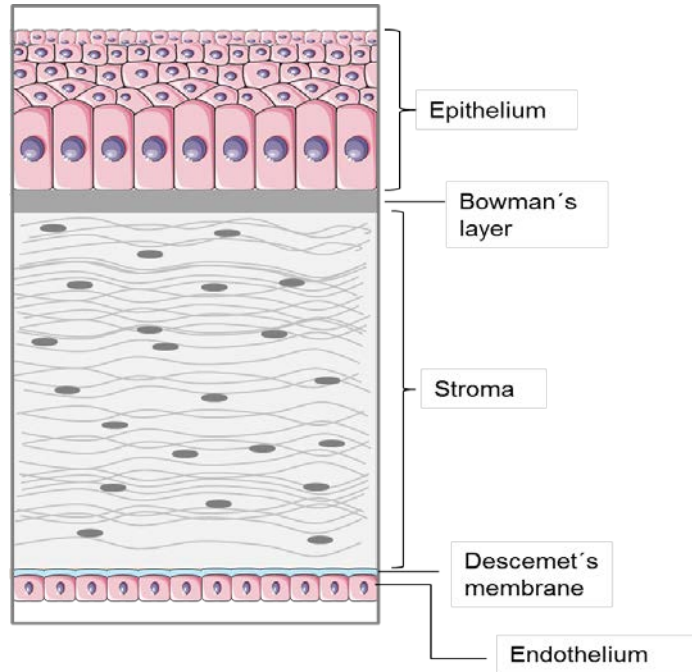


Figure 3. A cross-sectional view of the corneal structure. This figure was created using Servier Medical Art by Servier, which is licensed under a Creative Commons Attribution 3.0 Unported License; <https://smart.servier.com>.

Drugs can penetrate the eye by corneal or non-corneal routes. The corneal route follows this path: the cornea > aqueous humor > intraocular tissues (Chastain et al., 2016; Novack & Robin, 2016; Hughes et al., 2005).

Depending on their molecular weight and hydrophobicity, drugs penetrate the cornea epithelium through a paracellular or transcellular route (Rabinovich-Guilatt et al., 2004). Corneal epithelium (**Figure 4**) is the most critical part of drug absorption due to the connection of several layers of corneal epithelial cells by tight junctions, which serve as a barrier for small molecules and restrict diffusion of large molecules through paracellular route (Barar et al., 2008).

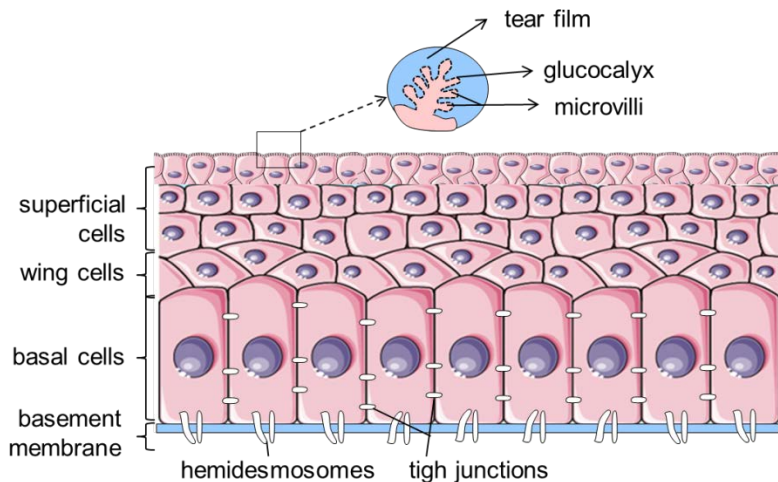


Figure 4. A cross-sectional view of the cornea epithelial cell layer. This figure was created using Servier Medical Art by Servier, which is licensed under a Creative Commons Attribution 3.0 Unported License; <https://smart.servier.com>.

Apart from the molecular weight, drug charge and log partition coefficient ($\log P$) affect permeability. The optimal $\log P$ of the drug to penetrate the eye is in the range 1-3 (Macha et al., 2003). The cornea surface is generally negatively charged under their isoelectric point, hence, cationic compounds permeate easier through the cornea than anionic ones. Moreover, only small molecules with adequate values of $\log P$ can efficiently penetrate. Additionally, transmembrane efflux pumps also contribute to low bioavailability of drugs applied to the cornea (Srinivasarao et al., 2019).

The stroma is a highly hydrophilic tissue containing mainly corneal fibroblasts and water and performs as a limiting barrier for most hydrophobic drugs.

The corneal endothelium is responsible for maintaining regular corneal hydration and possesses tighter junctions than cornea epithelium.

The tear film is a three-layer structure (outer lipid layer, middle aqueous layer and inner mucous layer) which its primary function is the protection of the corneal surface from external damage (**Figure 5**).

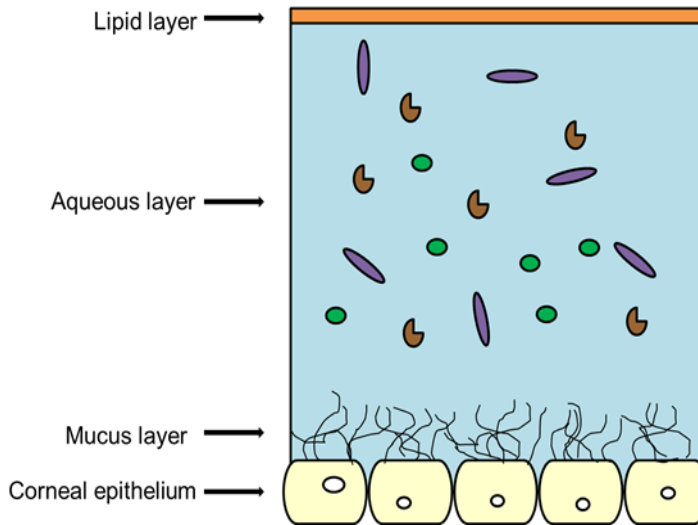


Figure 5. Schematic illustration of the structure of the tear film. This figure was created using Servier Medical Art by Servier, which is licensed under a Creative Commons Attribution 3.0 Unported License; <https://smart.servier.com>.

The outer layer of the tear contains lipids that prevent tear evaporation from the meibomian glands. The middle layer contains proteins, electrolytes and water mainly produced by the lacrimal gland. The innermost layer is the mucous layer that is composed of secreted mucins, electrolytes, and water produced by the conjunctival goblet cells. Along with the aqueous humor, the tear film provides the nutrients to the cornea (Moiseev et al., 2019).

Non-corneal routes were also considered interesting for targeting the back of the eye. They follow this path: conjunctiva > sclera > choroid > posterior tissues (Hughes et al., 2005; Awwad et al., 2017). The **conjunctiva** is a thin and transparent mucus membrane that covers the anterior cavity of the eye (including the sclera) and the inner surface of the eyelids. It contains epithelial cells, goblet cells and basal lamina. It is a high vascularized tissue that is organized into three parts (palpebral, bulbar and fornix). Its key functions include tear film formation and eye protection from microorganisms (Takahashi et al., 2013). It has greater intercellular spaces than the cornea, therefore, the conjunctiva is generally more permeable than the cornea.

Nevertheless, the drug absorption is still deficient due to blood capillaries and lymphatics that can deliver the drug into the systemic blood. The conjunctival surface area is higher than the surface area of the cornea. Tight junctions are also the main barrier to drug penetration across conjunctiva.

Low molecular weight hydrophobic molecules pass through the transcellular **route** and showed higher bioavailability compared to hydrophilic molecules (Srinivasarao et al., 2019).

The pupil is an opening within the iris that allows light to reach the retina.

The **aqueous humor** is the clear fluid that fills the space after the cornea and in front of the iris. Its primary function includes maintaining intraocular pressure (IOP) and to provide oxygen and nutrients to the anterior segment of the eye. It is protected by the blood-aqueous barrier that acts as a barrier that limits the crossing from the anterior to the posterior segment of the eye due to aqueous humor drainage (Dubald et al., 2018).

Iris and ciliary body are dynamic barriers. Along with the choroid, they are part of the uvea that is responsible for drug dilution after systemic administration. **Iris** is a circular and thin structure that controls the amount of light entering the eye. It is made of two layers: pigmented fibrovascular layer or stroma and pigmented epithelial cells. It separates the anterior and posterior segments of the eye. **The ciliary body** is a structure that contains ciliary muscles and ciliary epithelium. It is located behind the iris, and its primary function is to focus the lens (Malhotra et al., 2011).

The **lens** is transparent and it can be replaced if necessary. It focuses light rays onto the retina, and it is composed of collagens, laminins and negatively charged proteoglycans becoming the diffusion rates of neutral molecules higher compared to anionic molecules (Winkler et al., 2001).

1.1.2 Posterior segment

After crossing the conjunctiva, the drug needs to pass the sclera (Gaudana et al., 2010). The **sclera** is the white part of the eyes that provide protection and maintain the structural integrity of the eye globe. It contains mucopolysaccharides and collagen fibers. It is divided into three layers: episclera, sclera stroma and lamina fusca. Drug permeation through the sclera is considered higher than through the cornea and the conjunctiva. An increase in molecular weight, radius ratio, or hydrophobicity decreases drug permeability through the sclera. Differently to the cornea, negative molecules penetrate better to the sclera since the sclera matrix is made of negatively charged proteoglycans (Geroski & Edelhauser, 2001; Cholkar et al., 2013; Ambati et al., 2000).

The choroid is a vascular layer located between sclera and retina. It contains connective tissue, fibroblasts, melanocytes, and local

immunocompetent cells. The main functions of the choroid are to supply oxygen and nutrients to the retina, help in light absorption, and modulate the intraocular pressure via control of the blood flow. It is also responsible for aqueous humor drainage from the anterior segment. The choroid is supported by a Brunch's membrane that acts as a barrier.

The optic nerve, known as cranial nerve, links the eye to the brain.

The retina consists of a network of different types of cells, such as retinal pigmented epithelium (RPE), photoreceptors (rods and cones), horizontal, bipolar, amacrine, and ganglion cells (**Figure 6**).

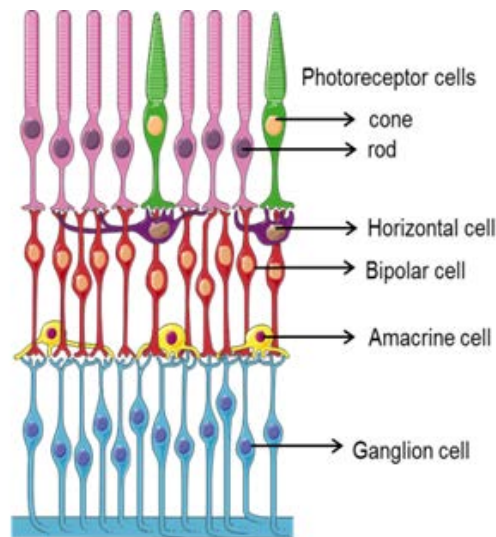


Figure 6. Cross-section of the human retina. This figure was created using Servier Medical Art by Servier, which is licensed under a Creative Commons Attribution 3.0 Unported License; <https://smart.servier.com>.

The macula is an oval pigmented area located in the retina. Its center is called the fovea, and it is responsible for clear vision. **Retinal pigmented epithelium (RPE)** divides the outer retina and choroidal capillaries and forms the outer blood-retinal barriers (Geroski & Edelhauser, 2001).

Vitreous humor is a transparent viscous fluid that contains mostly water, hyaluronic acid, and collagen fibrils. It fills the space between retina and lens.

Regarding permeation through the retina and vitreous humor, the charge of the drugs affects their diffusion, making anionic compounds diffuse without restrictions while cationic molecules are retained. Moreover, at both blood-aqueous and blood-retina barriers, permeation is limited due to tight junctions

that restrict the penetration of molecules into the intraocular tissues (Eye physiology; Xu et al., 2013).

1.2 Routes of drug administration

Therapeutics can be administered to the eye through different routes of administration. The most frequent routes are shown in **Figure 7**.

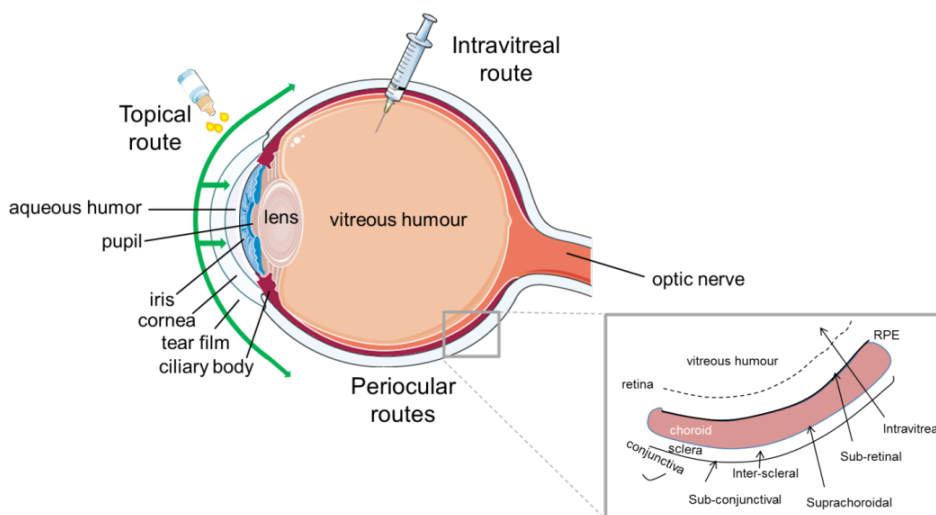


Figure 7. Schematic illustration of routes of ocular administration. This figure was created using Servier Medical Art by Servier, which is licensed under a Creative Commons Attribution 3.0 Unported License; <https://smart.servier.com>.

From a drug delivery point of view, barriers to ocular drug delivery depend on the route of administration. Generally, ocular drug delivery can be achieved by topical, periocular, intravitreal, and systemic routes (Gaudana et al., 2009). The choice of the administration route depends on the interested target that usually is the anterior or posterior segment of the eye (mostly retina and vitreous,) precorneal tissues (i.e., conjunctiva) or cornea. Diseases that affect the eye surface are mainly treated through topical instillation and subconjunctival injections. In contrast, more invasive routes (i.e., intravitreal and subretinal injections) are usually needed for the treatment of more profound intraocular diseases.

The topical route is less invasive, displays high patient compliance, and allows self-medication. It is the preferred route for treatment of keratitis, uveitis, conjunctivitis, scleritis, episcleritis, and blepharitis. Nevertheless, it leads to the very low bioavailability (less than 5%) due to the precorneal

factors (i.e., eye blinking, tear film, tear turnover, solution drainage, and lacrimation), static barriers (layers of the cornea, sclera, and retina, blood-aqueous barrier and blood-retinal barrier) and dynamic barriers (tear dilution, lymphatic clearance, choroid and conjunctiva blood flow (Gaudana et al., 2009; Patel et al., 2013)).

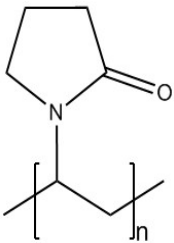
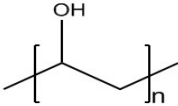
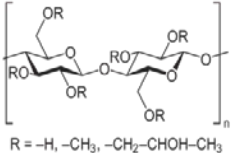
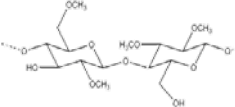
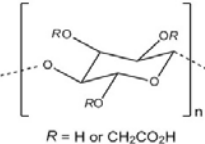
Another alternative route of drug administration is intravitreal injections. Nevertheless, the intravitreal route is considered painful and requires medical assistance, which leads to poor patient compliance. Additionally, their use is associated with discomfort and severe side effects such as the risk of cataract, retinal detachment, and endophthalmitis. Over the last years, periocular routes had emerged as a less invasive alternative to treat diseases that impact the posterior segment of the eye. It includes transscleral, intrascleral, retrobulbar, and peribulbar administration (Raghava et al., 2004). Another non-invasive route with less patient compliance is the systemic route. This route can be used for the treatment of scleritis, episcleritis, cytomegalovirus retinitis, and posterior uveitis. Low bioavailability, toxicity after high doses, blood-aqueous barrier (BAB), and blood-retinal barriers (BRB) are the main limitations (Kim, 2014; Shah et al., 2010; Jiang et al., 2018). Effective and non-invasive therapies for self-medication are needed. In this thesis, the use of cyclodextrin based nanoparticle eye drops for targeting the eye has been proposed as a promising alternative to invasive injections.

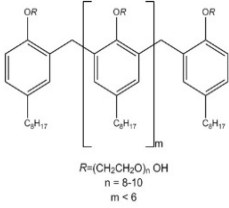
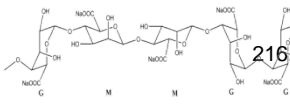
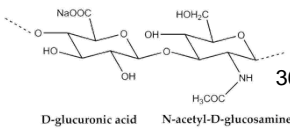
1.3 Viscosity modifier polymers

Polymers are widely used in the preparation of eye drops due to their viscous properties, which allow formulations to be optimized by prolonging the contact time of the formulation with the cornea and epithelium of the conjunctiva. Frequently, ophthalmic formulations use a combination of polymers, such as mucoadhesive polymers and viscosity modifier polymers (Kharenko et al., 2009; Dubashynskaya et al., 2019). Some examples of polymers used in this thesis are summarized in **Table 1**.

Table 1. Physicochemical characteristics and properties of hydrophilic polymers tested (Muankaew et al., 2014; Ludwig, 2005; Lorenzo-Veiga et al., 2019).

DRUG	CHEMICAL STRUCTURE	MOLECULAR WEIGHT	SOLUBILITY IN WATER (MG/ML)	CHARGE	PROPERTIES
------	--------------------	------------------	-----------------------------	--------	------------

PVP		40KDa	Soluble 100 mg/ml	Non-ionic	Synthetic polymer Inert Adhesive/cohesive properties Protective-colloid action Detoxifying properties
PVA		44.053 g/mol	Soluble	Non-Ionic	Synthetic polymer Film form Chemical resistance Biodegradability Safe Stable
HPMC	 <p>R = -H, -CH₃, -CH₂-CHOH-CH₃</p>	26KDa	Soluble in cold water	Non-ionic	Biocompatible Synthetic polymer Viscosity enhancer Thermoresponsive polymers Film-forming agent
MC		658.735 g/mol	Soluble	Non-ionic	Synthetic polymer Viscosity modifier Thermoresponsive polymers
CMC	 <p>R = H or CH₂CO₂H</p>	262.19 g/mol	Soluble 20 mg/ml	Negative	Synthetic polymer Viscosity enhancer Biocompatibility Biodegradability Low immunogenicity Thermoresponsive polymers

Tyloxapo I	 <p style="text-align: center;"> $R = (CH_2CH_2O)_n OH$ $n = 8-10$ $m < 6$ </p>	298.4 g/mol	Miscible	Non-ionic	Emulsifier Detergent properties Permeability enhancer Prolong corneal retention Able to form micelles
SA		216.121g/mol	Slowly in water	Negative	Natural polymer Ion-sensitive polymer Non toxic Biodegradable Penetration enhancer Mucoadhesive properties Gelling agent
HA	 <p style="text-align: center;"> D-glucuronic acid N-acetyl-D-glucosamine </p>	360 KDa	Soluble	Negative	Biocompatible Natural polymer Viscoelastic properties Humectant/ lubricant

1.3.1 Polyvinylpyrrolidone (PVP)

Polyvinylpyrrolidone (PVP) is a class of synthetic polymers that have broad applications in the biomedical field, improving the formulation of poorly water-soluble drugs. It can be used as a complexing agent improving the solubility of hydrophobic drugs. It is highly biocompatible with the vitreous and is employed in the production of hydrogels that can be used as vitreous substitutes. In some ophthalmic formulations, it is used as a viscosity enhancer, stabilizing, or suspending agent (Kadajji & Betageri, 2011).

1.3.2 Poly(vinyl)alcohol (PVA)

It is a synthetic polymer that currently has numerous applications in the pharmaceutical industry, for example, in the production of PVA hydrogels. In

ophthalmic formulations, it is used in artificial tears and to prepare hydrogel contact lenses (Gajra et al., 2011). Moreover, a combination of PVA and cyclodextrins is an effective drug delivery procedure (Xu et al., 2010).

1.3.3 Cellulose derivatives

They have been widely used as viscosity enhancers in ophthalmic formulations and wetting agents in artificial tears, increasing the contact time with the ocular surface (Ludwig, 2005).

Some cellulose-ethers, e.i. hydroxypropylmethyl cellulose (HPMC) and hydroxypropyl cellulose (HPC), also exhibit surface-active properties, interact with components of the tear film, and alter the physicochemical parameters governing the tear film stability (Benedetto et al., 1975). Sodium carboxymethylcellulose (NaCMC) is the cellulose derivative that exhibits the highest a mucoadhesive capacity (Ludwig, 2005). Methylcellulose (MC) showed wound healing properties, and it has been used as a tear substitute in dry eye syndrome (Lin & Boehnke, 1999).

Sensoy et al. (2009) developed bioadhesive sulfacetamide sodium microspheres using a mixture of polymers, such as pectin, polycarbophil, and HPMC at different ratios and showed to increase residence time on the ocular surface and to enhance treatment efficacy of ocular keratitis.

1.3.4 Tyloxapol

Tyloxapol, also known as Triton WD-1339, belongs to polyoxyethylene non-ionic surfactants. It is considered a safe detergent, so it has been widely used as an ophthalmic excipient (Kristl et al., 2008; Kuo et al., 2006). It has been used to prepared eye drops containing nepafenac (Lorenzo-Veiga et al., 2019), irbesartan (Muankaew et al., 2014) or prostaglandin F₂ α analog (Patent EP2937076A1).

1.3.5 Sodium alginate (SA)

Sodium alginate is a copolymer of (1,4) linked β -D-mannuronic (M) acid and α -1,4-linked-L-glucuronic acid (G)parts. It is found in marine brown algae and soil bacteria (Szekalska et al., 2016). This copolymer is biodegradable, biocompatible, non-toxic, and it is also a food additive considered as safe (GRAS) by the FDA (Borba et al., 2016). It is an excellent penetration enhancer due to its carboxylic groups. Increasing the concentration of this natural polysaccharide led to solutions with high bioadhesive properties even better than other mucoadhesive polymers as poly (acrylic acid) or hydroxyethyl cellulose (Khan et al., 2015). SA was involved in the formation

of different drug delivery systems for the ocular application alone or in combination with other materials as chitosan or cellulose derivatives (Gupta et al., 2015; Liu et al., 2006). Gatifloxacin based sodium alginate and sodium carboxymethylcellulose displayed higher mucoadhesive capacity after increasing the concentration of these two polymers (Kesavan et al., 2010).

1.3.6 Sodium hyaluronate (HA)

Sodium hyaluronate (HA) has been widely studied in different pharmaceutical applications. In ocular therapy, this natural polysaccharide demonstrated excellent mucoadhesive properties, non-toxicity, biocompatibility, biodegradability, and viscoelastic behavior. It is available in a broad molecular range between 1000 to 10,000,000 Da and commercialized as sodium salt (Kleiter et al., 2004; Guter & Breunig, 2017; Salzillo et al., 2016). Furthermore, it is present in different ocular tissues in the eye as a vitreous, lacrimal gland, corneal epithelium, conjunctiva, and also, at the tear fluid. HA eye drops have been widely investigated for the treatment of dry eye due to its carboxylic groups that confer them a high water accumulation capability (Kim et al., 2017). Moreover, other ophthalmic pathologies in which were successfully used are retinitis pigmentosa, macular dystrophy, diabetic retinopathy, and after ocular surgery, wound healing.

1.4 Novel drug delivery systems

Due to the protective barriers of the eye, both static and dynamic, reaching the target site and conserving the therapeutic concentration at this location is very difficult, making ocular drug delivery one of the most challenging areas in pharmaceutics (Weng et al., 2017; Maharjan et al., 2019).

Traditional dosage forms (i.e., ophthalmic solutions, suspensions, emulsions, and ointments) have shown low bioavailability, non-specific tissue distribution, and unable to control drug release profiles. To overcome these limitations, nanotechnology-based novel ophthalmic formulations have emerged for the effective treatment of ocular diseases for both anterior and posterior segment (Bhattacharjee et al., 2019; Bravo-Osuna et al., 2016). The most widely used nanocarriers to treat ocular diseases are summarized in

Figure 8.

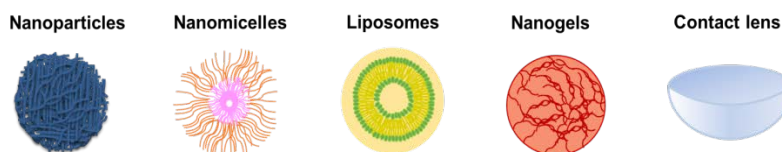


Figure 8. Schematic representation of various ocular nanotechnology-based ocular delivery systems.

In recent years, nanotechnology, specifically, nanosystems, have been widely used in the field of ocular drug administration since its numerous advantages include the protection of molecules, controlled release of drugs, improvement in drug permeability through tissues, ability to adhere to a tissue that surrounds the eye preventing the formulations from being eliminated by the eye's defense mechanisms and increasing the bioavailability of the drug (Srinivasarao et al., 2019).

Nanoparticles are colloidal drug carriers with a size comprised between 10 to 1000 nm (Cholkar et al., 2014). There are different types of nanoparticles used in ophthalmology composed of lipids, proteins, natural or synthetic polymers. Structurally, they can be classified as nanocapsules or nanospheres depending on whether the drug is confined inside the polymeric shell or uniformly distributed (Patel, et al., 2013).

They have been widely used to target the anterior and posterior segments of the eyeball. The optimal size of nanoparticles for ocular delivery is considered between 50 to 400 nm, where they have the ability to overcome physiological barriers (Almeida et al., 2014). They can be loaded with lipophilic (Losa et al., 1993) or hydrophilic (Losa et al., 1991) drugs. Improved ocular bioavailability was observed with ibuprofen nanoparticles in the aqueous humor of rabbit eyes when compared with ibuprofen aqueous eye drops (Pignatello et al., 2002). Furthermore, other anti-inflammatory drugs such as flurbiprofen and indomethacin were used to treat the anterior segment; moreover, they were able to improve the bioavailability of the drug (Bachu et al., 2018). Polymers as chitosan, polyethylene glycol (PEG), and hyaluronic acid are widely employed to increase the precorneal residence time of nanoparticles due to their bioadhesive properties (Patel et al., 2013). Musumeci et al. (2013) demonstrated that PLGA-PEG nanoparticles loaded melatonin showed better results, lowering intraocular pressure (IOP) compared to solely PLGA nanoparticles-loaded melatonin.

Nanomicelles are amphiphilic molecules with size from 5 to 200 nm (Bachu et al., 2018). Depending on the molecular weight of the core and corona forming blocks, they can have different shapes (spherical, cylindrical, or star-shaped) (Vaishya et al., 2014). They are used as safe alternatives for ocular drug delivery due to their ability to formulate hydrophobic drugs into a

clear aqueous solution (Velagaleti et al., 2010). Their main advantages are the high drug encapsulation capacity and that they are formed spontaneously. Vaishya et al. (2014) carried out a comprehensive review concerning micelles for ocular drug delivery.

Alvarez-Rivera et al. (2016) prepared nanomicelles with Soluplus[®], a polyethylene glycol, polyvinyl acetate, and polyvinyl caprolactam-based graft copolymer, to encapsulate α -lipoic acid. They showed enhanced solubility, stability, and corneal permeability of α -lipoic acid compared to marketed eye drops Tioretin[®] A. Nanomicelles using copolymers was also investigated for gene delivery for treating corneal diseases. Liaw et al. (2001) have used a non-ionic copolymeric system, poly (ethylene oxide)-poly (propylene oxide)-poly (ethylene oxide) (PEO-PPO-PEO), for ocular gene delivery.

Pepić et al. (2010) designed and characterized dexamethasone-loaded nanomicellar formulation with chitosan and Pluronic F127. They showed highly improved ocular bioavailability compared to ordinary dexamethasone suspension.

Liposomes are spherical lipid vesicles with phospholipids bilayers at the central aqueous core. This biphasic character allows them to encapsulate both lipophilic and hydrophilic drugs (Cholkar et al., 2014). They have been widely investigated in ophthalmology due to their low toxicity, biodegradability, and biocompatibility. Regarding their size and number of bilayers, they can be classified in small unilamellar (10-100 nm), large unilamellar (100-300 nm), and multilamellar vesicles. The surface charge affects liposome stability. Hence, cationic liposomes demonstrated better corneal permeation (Achouri et al., 2013). This was investigated by Law et al. (2000) on positively charged and neutral liposomes loaded with acyclovir. Nowadays, there are some marketed liposome formulations like Tear[®] and Visudyne[®].

Hydrogels are crosslinked polymeric 3D networks in water. They have high potential applications in drug delivery. Hydrophilicity, flexibility, and elasticity make them a convenient option for ocular drug delivery (Maharjan et al., 2019; Hoare & Kohane, 2008).

Their ability to respond to different external stimuli such as temperature, pH, and ionic strength makes them very promising alternatives in ocular drug delivery since they show sustained drug release from the hydrogel once the hydrogel is instilled upon the blinking eye (Fathi et al., 2015). Moreover, other applications of hydrogels in ophthalmology include implants and contact

lenses, which were widely investigated by Alvarez-Lorenzo group (Alvarez-Rivera et al., 2019; Alvarez-Lorenzo et al., 2006; Hiratani & Alvarez-Lorenzo, 2002).

Contact lenses are hydrogels, systems consisting of a three-dimensional polymeric network capable of holding a significant volume of water, placed on the surface of the eye and prevent drug loss since they remain in the eye despite the blinking. They allow the improvement of the drug efficiency and reduce the systemic side effects concerning other administration routes (Ako-Adounvo et al., 2014). Nanoparticles-loaded into contact lenses is considered as an alternative because they can maximize drug retention and improve corneal drug permeation (Sahoo et al., 2008).

The **ocular inserts** or **polymeric films** are solid or semi-solid, flexible, and biologically inert polymeric devices that are placed in the cul-de-sac or in the conjunctival sac to prolong the release of medications (Kumari et al., 2010). They can have various shapes and sizes and are made of polymers that can contain the drug or can be subsequently included in the polymeric material. Depending on their solubility, they can be classified as soluble, insoluble, or bioerodible. Their main advantages include the controlled release of the drug for more extended periods and constant rates, decrease the frequency of instillation and increase absorption since they will increase the time of ocular residence, avoiding a high washing out of the drug in the tear fluid. All these advantages mean that they can overcome the problems related to conventional eye drops, which have a low precorneal contact time and low bioavailability due to precorneal factors such as drainage and tearing. Besides, by reducing the frequency of administration, they allow their self-administration and improvement of patient adherence. Among its drawbacks are the costs of manufacturing and the possible interference of vision.

The first eye insert was designed in the 1980s to treat glaucoma and contained PVA soaked in pilocarpine (The concept of ocular inserts as drug delivery systems: An overview). Some products that use currently marketed inserts include Ocusert[®], Ocufit[®] SR, and Minidisc[®]. Recently, Tighsazzadeh et al. (2019) developed erodible polymeric films of hyaluronic acid (HA) and hydroxypropyl methylcellulose (HPMC) using timolol maleate as a model drug for glaucoma treatment. The results confirmed prolonged release profiles and excellent biocompatibility in HeLa cells, becoming promising delivery systems for glaucoma treatment. Souza et al. (2016) studied the use of chitosan inserts for improving the bioavailability of brimonidine tartrate to

treat glaucoma. The inserts were biocompatible, well-tolerated in vivo, and displayed a high release of brimonidine.

Although pharmacological therapies based on nanometer-scale carriers have been extensively investigated for the treatment of ocular diseases, only a few are in clinical trials (**Table 2**) (Bachu et al., 2018).

Table 2. Typical nanotechnology-based formulations.

FORMULATION	PAYLOAD	TARGET	CLINICAL STAGE	REF.
Nanoparticle	Gene	Anterior eye segment	Preclinical	(Jiang et al., 2012)
Hydrogel	Diclofenac	Anterior eye segment	Preclinical	(Zhang et al., 2016)
Nanowafer	Axitinib	Anterior eye segment	Preclinical	(Yuan et al., 2015)
Hydrogel	Ganciclovir	Anterior eye segment	Market	(Chou & Hong, 2014)
Liposome	Coenzyme – Q10	Anterior eye segment	Preclinical	(Zhang & Wang, 2009)
Hydrogel	Bevacizumab	Posterior eye segment	Preclinical	(Tyagi et al., 2013)
Nanoparticle	Latanoprost acid	Posterior eye segment	Preclinical	(Natarajan et al., 2014)
Micelle	Triamcinolone acetonide	Posterior eye segment	Preclinical	(Jiang et al., 2012)
Liposome	Gene	Posterior eye segment	Preclinical	(Chen et al., 2013)
Nanoparticle	Gene	Posterior eye segment	Preclinical	(Rajala et al., 2014)

In next sections, we will provide a detailed description of current knowledge of cyclodextrins as drug delivery systems focuses on ocular diseases. Products currently marketed and last research studies are also discussed.

1.5 Cyclodextrins as solubilizers and penetration enhancers

Cyclodextrins are cyclic oligosaccharides with D-glucopyranose units linked by α -(1, 4) glycosidic unions. They are considered promising excipients because their outer hydrophilic part (with primary and secondary hydroxyl functional groups) and their hydrophobic corona (with CH_2 groups), they can encapsulate hydrophobic drugs in their cavity. The most prevalent cyclodextrins are α -, β - and γ -CD, and they are known as native cyclodextrins (Popielec & Loftsson, 2017; Jacob & Nair, 2018)(Figure 9). However, due to their better solubilizing capacity, their derivatives, Methyl- (Me β -CD and Me γ -CD), hydroxypropyl- (HP α -CD, HP β -CD, and HP γ -CD), and sulfobutyl ether (SEB β -CD) have been more commonly used in the pharmaceutical industry (Loftsson, 2002).

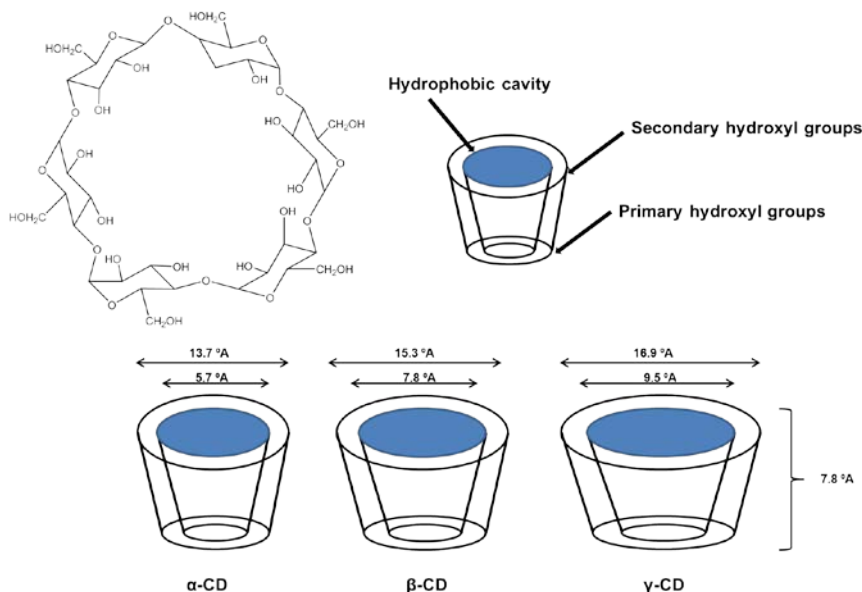


Figure 9. Chemical structure and molecular shape of natural cyclodextrins (α -, β -, γ -CDs).

In this industry, they are widely used as solubilizers (i.e., class II and IV drugs), penetration enhancers, excipients, stabilizers, and food additives because they are biocompatible and are considered to be safety excipients. Besides, they are accepted by the FDA and listed as inactive ingredients. Its main characteristic relies on its ability to form inclusion complexes by encapsulating small molecules and even biomolecules, such as proteins or peptides, in its cavity, forming a torus like structure (Conceicao et al., 2018; Jansook et al., 2018; Liu et al., 2018; Loftsson & Duchêne, 2007).

One of the most common methods to determine the stability constant (K_S), the stoichiometry of the inclusion complex and complexation efficiency (CE) for CD complexes is a phase-solubility study, described by Higuchi et al. They predict the mutual effect on the components on their apparent solubility in drug/ CD solutions based on an isothermal saturation method. Equilibrium concentrations of drug vs. real concentration of CDs are plotted to determine the phase-solubility profile and its type (**Figure 10**)(Higuchi & Connors, 1965).

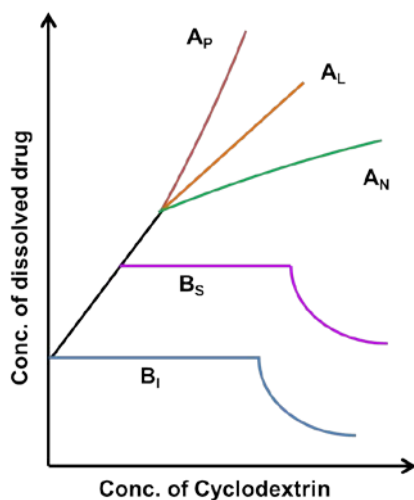


Figure 10. Phase-solubility profile of one drug in the presence of CD.

Phase solubility diagrams are divided into A- and B-type diagrams (**Figure 10**). A-type diagrams represent the formation of highly soluble complexes, whereas in B-type diagrams, the solubility of the complexes in the aqueous complexation media is limited. A-types can be divided into three subtypes, A_L , A_P , and A_N . B-type diagrams can be divided into two subtypes, B_S and B_I . There is a direct correlation between the rise of drug concentration and the rise of CD concentration when A_L occurs. The A_P -type emerges when CD exists at a higher concentration than the drug, showing a deviation from linearity in an upward trend. The A_N -type refers to the bulk change of the solvent due to the solubilizing agent. In B-type diagrams, the B_S indicates that in the complex formed, the total solubility increases by increasing CD concentration until the maximum solubility of the drug is attained (plateau). Hence, if more CD is added, it produces a precipitating complex where dissolution and complexation can appear at any moment if solid drug remains. When the consumption of all solid drug has been completed, the

incorporation of CD decreases the total drug concentration and forms a considerable insoluble inclusion complex. The B_i type is similar to the B_s type except for that the initial inclusion complex is very insoluble (Brewster and Loftsson, 2007; Higuchi & Connors, 1965; Challa et al., 2005).

CD complexation usually involves a 1:1 ratio, although other complexation order can happen (Connors, 1997). In the case of 1:1 complex, the binding constant, K_{1:1}, can be determined from the slope of the curve following this equation:

$$K_{1:1} = \frac{\text{Slope}}{S_0(1-\text{Slope})} \quad (1)$$

where K_{1:1} indicates the affinity of the drug within the CD cavity and is generally between 100–20,000 M⁻¹, and S₀ is the intrinsic solubility of the drug without cyclodextrin. Also, other excipients (i.e., buffer salts or polymers) can increase K_{1:1} while chaotropic factors (i.e., urea) decrease it (Godínez et al., 1997; Muankaew et al., 2014; Muankaew et al., 2018).

The complexation efficiency (CE), which corresponds to the ratio of complex to free CD concentration, can be determined from the phase diagram slope as reported in this equation (Brewster & Loftsson, 2007):

$$CE = \frac{\text{Slope}}{1-\text{Slope}} \quad (2)$$

Factors that could influence the complexation include the type of CDs, cavity size, charge, molar substitution, pH and ionization, formulation bulk, temperature, method of preparation, and addition of additives. Different methods have been suggested to improve the CE of drug-CD, i.e., drug ionization, salt formation, polymer complexes, amorphous form, acid-base complexes, metal complexes, co-solvents and ion-pairing (Cirri et al., 2006; Loftsson and Brewster., 2012).

There are different methods to prepare CDs complexes. In solution, the complexes are frequently prepared by the addition of an excess amount of the drug to an aqueous cyclodextrin solution containing increasing amounts of CDs. Then, the suspension is shaken for several days until it reaches equilibrium and then filtered or centrifuged to form a clear drug/ cyclodextrin complex solution. The total drug concentration is determined by ultraviolet spectrometry (UV) or high-performance liquid chromatography (HPLC) (Challa et al., 2005). Solid complexes can also be prepared by removing the water from the suspension, i.e., by freeze-drying. Other procedures include

co-precipitation, kneading, neutralization, and grinding techniques that have been investigated (Del Valle, 2004).

Furthermore, in solid-state, drug/ CD complexes can be characterized by thermal analysis methods, X-ray diffraction, spectroscopic techniques, or scanning electron microscopy (SEM) (Mura, 2015).

Another application of CDs in formulation development, apart from solubilizers, is their ability to enhance drug permeation through a biological membrane by increasing drug bioavailability at the surface of the biological barrier, where they partition into the membrane. Biological membranes, for example, mucus layers at the ocular membranes, are lipophilic, and only relatively lipophilic molecules can penetrate through the membranes. Excess addition of CDs can lead to restricted drug permeation. The addition of CDs could be the first step to optimize formulations as eye drops. With the formation of inclusion complexes, the drug is dissolved in the tear and concentrates near the cornea. At the same time, the CD remains at the ocular tissue and is usually eliminated through the nasolacrimal pathway (Másson et al., 1999; Biro & Aigner, 2019) (**Figure 11**).

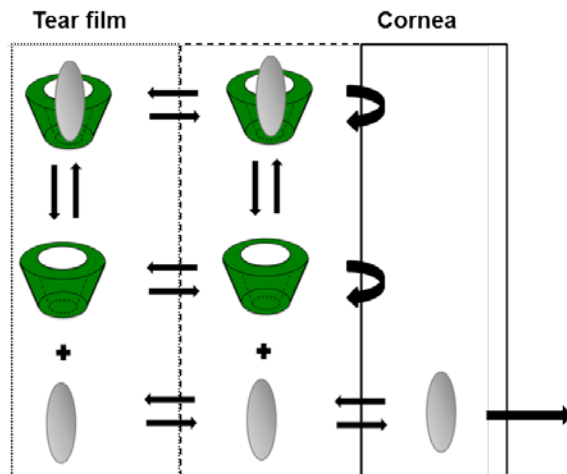


Figure 11. Schematic illustration of drug penetration into the eye after topical instillation of aqueous cyclodextrin (CD) eye drop solution in the tear film. Adapted from (Biro and Aigner, 2019).

1.6 CD-based ophthalmic formulations for topical drug delivery to the eye

1.6.1 CD aggregates

It is already reported that CDs self-assemble in aqueous solution forming nano- or microsized aggregates which are able to solubilize the drug owing to the formation of water-soluble complexes (Messner et al., 2010; Ryzhakov et al., 2016). This phenomenon was firstly introduced by Koichiro et al. (1983) years ago. Also, non-inclusion complexes can take place in aqueous CD solution (Stella et al., 1999). Complex formation is possible owing to Van der Waals forces and hydrophobic interactions between the drug and the CD cavity (Loftsson & Duchêne, 2007; Rodell et al., 2015). CD complex formation is a dynamic process whereby aggregates are constantly formed and disrupted (Loftsson et al., 2005). Dilution is responsible for drug release from complexes (Stella et al., 1999). Since the interaction between the CD and the drug is very fast, most drugs are effortlessly dissociated from CD. Compared to native CDs, derivative CDs (i.e., HP β -CD, DM β -CD, and SE β -CD) demonstrate lower ability to form aggregates due to substitution of -OH groups that impede the ability to form intermolecular hydrogen bonds (Messner et al., 2011). The size of aggregates has been found less than 200 nm, but in some cases, larger aggregates with different shapes (rod, worm-like structure disk, and sheet) can be observed under a light microscope (Brewster & Loftsson, 2007; Jóhannsdóttir et al., 2017).

The most habitual stoichiometry of the complexes is 1:1 (that is complexation of one drug and one cyclodextrin molecule)(**Figure 12**)(Connors, 1997).

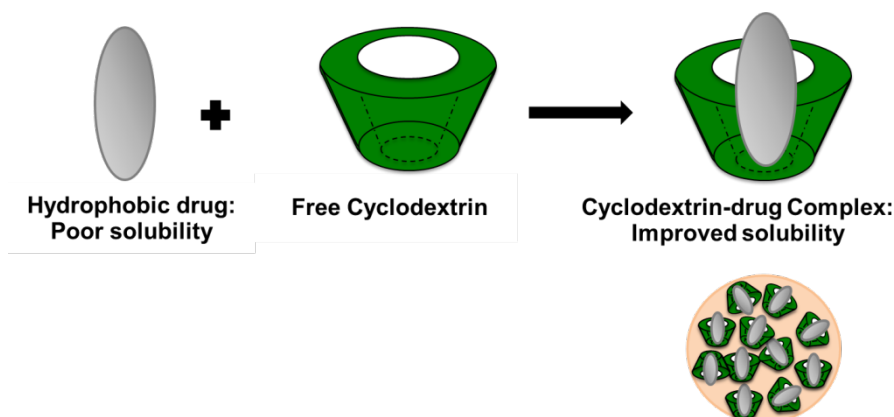


Figure 12 Drug/CD complex formation (1:1).

Nowadays, there are some CDs-based ophthalmic formulations on the market (**Table 3**).

Table 3 Currently marketed CDs-based ophthalmic formulations.

DRUG	CYCLODEXTRIN	TRADE NAME	COMPANY
Chloramphenicol	Randomly methylated β -cyclodextrin (RAMEB-CD)	Clorocil	Oftalder (Portugal)
Diclofenac	2-Hydroxy-propyl-gamma-cyclodextrin (HPG-CD)	Voltaren/ Voltarol	Novartis (Schwitzerland)
Indomethacin	2-Hydroxy-propyl- beta-cyclodextrin (HPB-CD)	Indocid/Indocyllir	Chauvin (UK)/Baush & Lomb(US)
Thimerosal	Beta-cyclodextrin (β -CD)	Vitaseptol	Novartis (Schwitzerland)

Furthermore, during the last decade, several efforts have been made on demonstration of therapeutic drug concentration at the posterior segment of the eye after topical instillation of aqueous eye drops of low viscosity (Loftsson & Stefánsson 2017). After studies in rabbits and test in clinical trials, Loftsson and coworkers designed eye drops containing solid or dissolved drug/cyclodextrin complex aggregates and dissolved drug molecules in an aqueous eye drop media of low viscosity using dorzolamide or dexamethasone as models drugs (Loftsson et al., 2012; Loftsson & Stefánsson, 2002). They showed that these eye drops were able to deliver therapeutic concentration both to anterior and posterior segment of the eye opening a new alternative for less invasive treatment of ophthalmic diseases. Also, they studied the application of these cyclodextrin-based aggregates to deliver larger molecules to the eye using Cyclosporine A as model drug. They

tested in vivo in rabbits and formulations were found not irritation or toxic after topical instillation in rabbit once or twice per day during three months (Jóhannsdóttir et al. 2015; Jóhannsdóttir et al. 2017). Huang et al. (2019) developed microparticles by co-association between 2-hydroxypropyl- γ -cyclodextrin (HP γ -CD)/ loteprednol etabonate complexes through the addition of polysorbate 80 for treatment of ocular uveitis. Results suggested that this microparticle system enhanced the efficacy of the corticosteroids after performing in vivo pharmacokinetics and pharmacodynamics studies. Also, Jansook et al. (2016), revealed the stabilizing effect of the addition of amphiphilic polymer, Pluronic P407, to γ -CD/HP γ -CD complex using two model drugs, a dexamethasone and amphotericin B.

1.6.2 Poly(pseudo)rotaxanes

Cyclodextrin(CD)-based supramolecular systems have attracted great attention as host-guest supramolecular delivery systems, due to their ability to encapsulate guest components forming supramolecular structures in a self-assembly manner able to increase the solubility, controlled drug release and low toxicity, leading to new applications in the biomedical and pharmaceutical field (Liu et al., 2018; Zhang et al., 2013). CDs-based poly(pseudo)rotaxanes (CDPPR) are a family of supramolecular structures where linear polymeric chains penetrate CDs cavities forming "molecular necklaces" and they can easily be de-threaded under certain conditions. The first CDPPR was obtained by Harada et al. (1993) after threading α -CD along the PEO chain to form inclusion complexes. Between the copolymers and long polymers investigated for forming CDPPR, poly(ethylene glycol) (PEG), poly(propylene oxide) (PEO), poly(E-caprolactone) (PCL), Pluronic[®] (PEO-PPO-PEO) have been broadly investigated (Simões et al., 2015)(**Figure 13**).

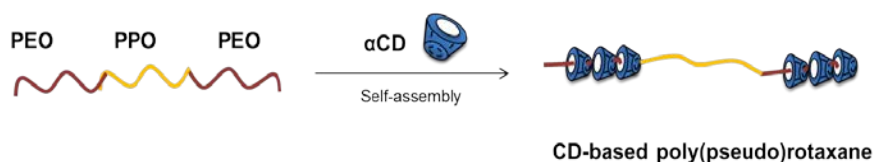


Figure 13. Schematic illustration of poly(pseudo)rotaxane of α -CD and PEO-PPO-PEO triblock copolymers.

These gels display thixotropic behavior, and they undergo gel-to sol transition under shear-stress, behaving as an injectable drug delivery system.

There are different methods of preparation. Zhang et al. (2016) developed a simple method through host-guest inclusion after the addition of polymer micelles into an α -CD aqueous solution led to the formation of a micellar supramolecular hydrogel. Marcos et al. (2016) found that inclusion complex formation between poloxamer (Pluronic[®] P123) and hydroxyethyl cellulose (HEC) with α -CD led to supramolecular hydrogels that can solubilize griseofulvin.

2 Aims

The purpose of this thesis was to develop novel cyclodextrin-based nanocarriers that enhance aqueous drug solubility in the eye structure, increase drug absorption after prolonged contact time at the eye surface and able to permeate into membrane barriers (i.e., cornea and sclera) in order to treat common ocular diseases such as inflammation or fungal keratitis. Then, the suitability of aggregates, micelles, and poly(pseudo)rotaxanes as topical drug delivery systems into the eye was evaluated. The project was divided into three tasks:

1. Investigate the formation of self-assembled drug/ cyclodextrin complex aggregates using a hydrophobic drug as a model, nepafenac, and a mixture of cyclodextrins (HP β -CD/ γ -CD). For this reason, different studies were performed: (1) evaluation of physicochemical properties of nepafenac/cyclodextrin complex, (2) analysis of the effect of specific water-soluble polymers on the solubility of nepafenac/ CD complex and (3) complex characterization in solid-state.

2. Design, in vitro and ex vivo evaluation of eye drops containing these aggregates. Physicochemical and rheological analysis, in vitro mucoadhesive studies, ocular tolerance test, diffusion studies, in vitro cell viability in murine fibroblasts, in vitro anti-inflammatory efficacy on macrophages and ex vivo bovine permeability studies of nine formulations was carried out.

3. Study of self-assembly of amphiphilic polymers with cyclodextrins for ocular delivery of natamycin. For this purpose, Soluplus[®] and Pluronic[®] P103 were selected as surfactants for preparing single and mixed micelles and poly(pseudo)rotaxanes in order to enhance low aqueous solubility and ocular penetration of natamycin. They were analyzed in terms of solubility, particle size, zeta potential, pH, rheological properties, diffusion studies, ocular irritancy, and ex vivo cornea and sclera permeation.

3 Materials and methods

3.1 Materials

Nepafenac (98% purity, MW 254.28 g/mol) was obtained from Fagron (Netherlands) and natamycin (665.73 g/mol) was purchased from AK Scientific (San Francisco, CA, USA).

α -Cyclodextrin (α -CD), β -cyclodextrin (β -CD), γ -cyclodextrin (γ -CD), 2-hydroxypropyl- α -cyclodextrin, DS 3.6 (MW 1180Da) (HP α -CD) and 2-hydroxypropyl- γ -cyclodextrin, DS 4.2 (MW 1540 Da) (HP γ -CD) were obtained from Wacker Chemie (Munich, Germany). 2-Hydroxypropyl- β -cyclodextrin, DS 4.2 (MW 1380 Da) (HP β -CD) was kindly provided by Janssen Pharmaceutica (Beerse, Belgium).

Soluplus[®] (115,000 g/mol) and Pluronic[®] P103 (EO17PO60EO17; 4950 g/mol) were obtained from BASF (Ludwigshafen, Germany). Methylcellulose (MC; MW 14,000 Da; viscosity ~ 15 centipoises) from ICN Biomedicals Inc. (Ohio, USA); sodium alginate from Fagron Iberica (SA; MW 80,000-12,000 Da Zaragoza, Spain); sodium hyaluronate (HA, MW 360,000 Da, glucuronic acid 47.4%) from Guinama (La Pobla de Valbona, Spain). Reagent grade tyloxapol (MW 280.4 g/mol), 87–90 % hydrolyzed poly(vinyl alcohol) (PVA) (average MW 30.000–70.000 Da), hydroxypropylmethyl cellulose (HPMC; MW 26,000 Da, viscosity approx. 100 centipoises), polyvinylpyrrolidone (PVP; average MW 10,000 Da and 40,000 Da) and carboxymethylcellulose (CMC) sodium salt (CMC; MW 90,000 Da; low viscosity), benzalkonium chloride (BAK), ethylenediamine-tetraacetic acid disodium salt dihydrate (EDTA) were purchased from Sigma-Aldrich (St. Louis, MO, USA). Sodium chloride, MgCl₂•6H₂O, and acetonitrile were acquired from Scharlab SL (Barcelona, Spain); NaOH, KH₂PO₄, NaHCO₃, CaCl₂•2H₂O, and NaH₂PO₄•H₂O were provided from Merck (Darmstadt, Germany); KCl from Prolabo (Fontenay-Sous-Bois, France); phosphate-buffered saline (PBS) was purchased from Sigma (St. Louis, MO, USA); ethanol absolute was obtained from Panreac (Barcelona, Spain).

Phosphate buffer pH 6.4 was prepared by mixing 250 mL of solution A (0.2 M 62.5 mL KH₂PO₄) and solution B (0.2 M 16.4 mL NaOH) with water. Carbonate buffer pH 7.2 was prepared by mixing buffer solution A (100 mL; 1.24 g NaCl, 0.071 g KCl, 0.02 g NaH₂PO₄, 0.49 g NaHCO₃) and buffer solution B (100 mL; 0.023 g CaCl₂, 0.031 g MgCl₂).

BALB/3T3 clone A31 mouse fibroblasts (ATCC CCL-163™) and monocytes THP-1 (ATCC TIB-202™) were acquired from the American Type Culture Collection (ATCC, Manassas, VA, USA). Fetal bovine serum (FBS), antibiotic solution (penicillin 10,000 units/mL and streptomycin 10.00 µg/mL), LPS from E.coli, phorbol 12-myristate 13-acetate (PMA), tris hydrochloride and lauryl sulfate sodium salt (SDS) were purchased from Sigma-Aldrich (Saint Louis, MO, USA). DMEM/F12 - Dulbecco's Modified Eagle Medium: Nutrient Mixture F-12 and RPMI 1640 were provided by Gibco (Termofisher, Paisley, UK). Cell Proliferation Reagent WST-1 was acquired from La Roche (Manheim, Germany).

Membrane filters (0.45 µm) were obtained from Phenomenex (Cheshire, United Kingdom). Water was filtered purified using reverse osmosis (resistivity > 18 MΩcm, MilliQ, Millipore®, Spain). All other reagents were analytical grade.

3.2 Quantitative analysis

3.2.1 Nepafenac quantification method

Nepafenac content from nepafenac/ CD aggregates was quantified at 254 nm using a Dionex Ultimate 3000 series system (Germering, Germany) UHPLC (LPG-3400SD pump with a built-in degasser, WPS-3000 autosampler, TCC-3100 column compartment, and CoronaR ultra RS detector) fitted with a C18 column (Phenomenex Kinetex C18, 5 µm, 4.6 × 150 mm) and using the software Chromeleon version 7.2 SR4 (ThermoScientific, Waltham, MA, USA). The mobile phase was acetonitrile and water (50:50) at 1 mL/min, 25 °C and 10 µL as the injection volume. Nepafenac quantification for nepafenac eye drops diffusion studies were carried out in a different research facility. In this case, UV-Vis spectrophotometer (Agilent 8453, Waldbronn, Germany) at 254 nm was used to determine nepafenac content from eye drop formulations using a valid calibration curve. Permeated nepafenac from bovine corneas and scleras were measured at 254 nm using a Jasco HPLC system (AS-4140 autosampler, PU-4180 pump, LC-NetII/ADC interface box, CO-4060 column oven, MD-4010 photodiode array detector), with a C18 column (Waters Symmetry C18, 5 µm, 3.9 × 150 mm) and ChromNAV software. The mobile phase is comprised of acetonitrile: water (50:50) at a flow rate of 1 mL/min and 90 µL for volume injection.

3.2.2 Natamycin quantification method

Natamycin content was determined in the solubility studies and diffusion assays by UV-Vis spectrophotometer (Agilent 8453, Waldbronn, Germany) at 304 nm by use of a previous validated method with standard solutions in ethanol/water (20:80% v/v) mixture. Permeated natamycin was measured at 304 nm (retention time 3.3 min) using high-performance liquid chromatography (HPLC) systems, Jasco (Tokyo, Japan) HPLC (AS-4140 Autosampler, PU-4180 Pump, LC-NetII/ADC Interface Box, CO-4060 Column Oven, MD-4010 Photodiode Array Detector), fitted with a C18 column (Waters Symmetry C18, 5 μ m, 3.9 μ 150 mm) and using ChromNAV software (ver. 2, Jasco, Tokyo, Japan). The mobile phase consisted of acetonitrile: 30 mM of perchloric acid (35:65) at 1 mL/min, 30 °C and 90 μ L as the injection volume.

3.3 Solubility studies

3.3.1 Phase-solubility studies of nepafenac

Phase-solubility studies have been widely proposed by Higuchi & Connors (1965) as one of the most common methods to study complex formation. In this study, phase-solubility analysis of nepafenac with six different cyclodextrins was carried out in triplicate following a heating method in an ultrasonic bath (Jansook et al., 2010, Messner et al., 2011, Loftsson et al., 2012). Then, nepafenac (approximately 5 mg) was added in excess to vials containing known concentrations of α -CD, HP α -CD, γ -CD, HP γ -CD, HP β -CD (up to 15% w/v) and β -CD (up to 1.5% w/v) aqueous solutions. Then, vials were sonicated for 60 min at 60 °C in an ultrasonic bath (Branson 3510 Ultrasonic Cleaner, Marshall Scientific, Hampton, NH, USA). After reaching room temperature, a small amount of drug (approx. 2 mg) was added to each vial to lead to drug precipitation and they were closed and kept under constant agitation (KS 15 A Shaker, EB Edmund Bühler GmbH, Germany) for 7 days until equilibrium was reached. After equilibration, they were filtered through 0.45 μ m membrane filters, diluted with MiliQ water and nepafenac content was analyzed by UHPLC.

Solubility profiles were determined by plotting the equilibrium concentrations of nepafenac vs. CDs concentration. Assuming 1:1 stoichiometric ratio of complexes, the apparent stability constant ($K_{1:1}$) was determined following this equation:

$$K_{1:1} = \frac{\text{Slope}}{S_0(1-\text{Slope})} \quad (1)$$

Additionally, complexation efficiency (CE) was calculated from the ratio of the concentration of the drug/CD complex to free CD (Jambhekar & Breen, 2016):

$$CE = \frac{\text{Slope}}{1-\text{Slope}} = \frac{\left(\frac{\text{Guess}}{\text{CD complex}}\right)}{(\text{CD})} \quad (2)$$

The effect of various excipients (PVP, PVA, CMC and tyloxapol) on the solubility of nepafenac in pure γ -CD and mixed γ -CD/HPB-CD in different ratios was also analyzed by UHPLC method previously validated in Section 3.2.1. All experiments were performed in triplicate.

3.3.2 Solubility of nepafenac eye drops

Nepafenac (18 mg) was added to 6 mL of an aqueous 15% γ -CD/8%HP- β CD (w/v) solution containing different polymers (**Table 4**), 0.1% (w/v) EDTA, 0.02% (w/v) BAK, and 0.04% (w/v) NaCl.

Table 4. Polymers used to prepare nepafenac eye drop formulations and their percentages.

Component (% w/v)	Eye drop formulations								
	A1	A2	A3	A4	A5	A6	A7	A8	A9
PVP	-	-	-	-	1.0	-	-	-	-
PVA	-	-	2.0	-	-	-	-	-	2.0
CMC	-	1.0	1.0	1.0	1.0	1.0	-	1.0	1.0
HPMC	-	-	-	-	0.1	-	-	-	-
MC	-	-	-	-	-	-	-	-	0.1
Tyloxapol	-	-	0.1	-	-	-	-	-	-
HA	0.2	-	-	0.2	-	-	-	0.2	-

Phase-solubility studies were carried out in accordance with the previous method in section 3.3.1, described by Higuchi & Connors (1965). The apparent nepafenac solubility was determined by UV-Vis spectroscopy at 254 nm using a standard calibration curve previously validated.

3.3.3 Solubility tests of natamycin

3.3.3.1 Solubility of natamycin in micelle dispersions

Natamycin in excess (approx. 2 mg) was added to aliquots (approx. 5mL) of each Soluplus and Pluronic P103 dispersion (0.01%, 0.1%, 1%, 2%, 3%, 4%, 5%, and 10% w/v) previously prepared in triplicate in 0.9% NaCl under stirring after addition of Soluplus and Pluronic P103 copolymers. After being continuously agitated (Unitronic, JP Selecta, Barcelona, Spain) for 6 days at 37 °C, dispersions were centrifuged (centrifuge model 5804R, Eppendorf AG, Germany) at 5000× g rpm for 30 min, and supernatants were diluted in ethanol/water (20:80% v/v) mixture. Mixtures of Soluplus (10% w/v) and Pluronic P103 (10% w/v) dispersions were also prepared by mixing them at different volume ratios (1:4, 2:3, 3:2, and 4:1). Natamycin content was determined by UV-Vis spectrophotometer (Agilent 8453, Waldbronn, Germany) at 304 nm using a previously validated method with standard solutions in ethanol/water (20:80% v/v) mixture.

Moreover, data from the solubility study were used to estimate the following parameters (Alvarez-Rivera et al., 2016; Varela-Garcia et al., 2018):

(a) Molar solubilization capacity represents the moles of drug that can be solubilized per mol of copolymer forming micelles:

$$X = S_{\text{tot}} - S_w C_{\text{copol}} - \text{CMC} \quad (3)$$

(b) Micelle–water partition coefficient, is the ratio between the drug concentration in the micelle and the aqueous phase:

$$P = \frac{S_{\text{tot}} - S_w S_w}{S_w} \quad (4)$$

(c) Molar micelle–water partition coefficient, which eliminates the P dependence on the copolymer concentration assigning a default concentration of 1 M:

$$\text{PM} = X (1 - \text{CMC}) S_w \quad (5)$$

(d) Gibbs standard-free energy of solubilization, that was predicted from the molar micelle/water partition coefficient (PM):

$$\Delta G_s = -RT \ln(\text{PM}) \quad (6)$$

(e) The proportion of drug molecules encapsulated in the micelles:

$$m_f = S_{\text{tot}} - S_w S_{\text{tot}} \quad (7)$$

In these equations, S_{tot} is the total solubility of natamycin in the micellar solution, S_w is the solubility of natamycin in water, C_{copol} is the copolymer concentration in each micelle solution, CMC is the critical micelle concentration, and R is the universal constant of gases.

3.3.3.2 Solubility of natamycin in α -CD

Natamycin was added in excess (approx. 8 mg in 10 mL) to solutions of 5% and 10% w/v of α -CD in 0.9% NaCl or pH 6.4 buffer, that were previously prepared. They were kept under magnetic stirring at room temperature for 5 days, centrifuged at 5000x g rpm for 30 min, and then, supernatants were diluted in ethanol/water (20:80% v/v) mixture. Natamycin content was determined by UV-Vis spectrophotometry at 304 nm using a method previously validated.

3.4 Nepafenac/ CD aggregates

3.4.1 Moisture content of CDs

The water content of γ -CD and HP β -CD was analyzed by A&D MX-50 moisture analyzer (A&D Company, Limited, Tokyo, Japan). Briefly, 1 g of solid powdered γ -CD and HP β -CD were poured into different aluminum pans, and then measurements were done in triplicate.

3.4.2 Chemical stability of nepafenac

Chemical stability of nepafenac in an aqueous CD solution containing 1% w/v γ -CD was analyzed after heating in an ultrasonic bath at 60 $^{\circ}$ C (Jansook et al., 2010, Messner et al., 2011, Loftsson & Brewster, 2012, Ogawa et al., 2016). The solution was shaken for 24 hours to make sure that nepafenac was dissolved entirely; then, it was filtered (0.45 μ m membrane filter) and divided into four sealed vials. Vial 1 was selected as a blank (no heated), while vials 2, 3 and 4 were heated in a sonicator at 60 $^{\circ}$ C for 20, 40 and 60 min, respectively. Nepafenac concentrations in vials 2, 3 and 4 were determined by UHPLC.

3.4.3 Preparation of inclusion complexes

Inclusion complexes of γ -CD/ HP β -CD with nepafenac were prepared by the freeze-drying method (Del Valle, 2004; Kicuntod et al., 2018). Aliquot of clear supernatant from phase solubility studies of (A_L -type profile) were selected to confirm the presence of nepafenac/ CD complexes. Briefly, supernatants (approx. 200 μ L) were collected in triplicate, placed in small Eppendorfs and freeze-dried at -55 $^{\circ}$ C for 24 h in a Snijders scientific 2040 Freeze dryer (Snijders Labs, Tilburg, The Netherlands).

3.4.4 Solid state characterization of nepafenac/CD complexes

3.4.4.1 Fourier Transform Infra-Red (FT-IR) Spectroscopy

The FT-IR spectra of pure nepafenac, pure CDs and their freeze-dried complexes were analyzed at room temperature in a FT-IR spectrometer (Thermo Fisher Scientific model Nicolet iS10, Waltham, MA, USA) using an Attenuated Total Reflectance (ATR) technique in the framework region 500–4000 cm^{-1} .

3.4.4.2 Differential Scanning Calorimetry (DSC)

Thermal behavior of pure nepafenac, pure CDs and their freeze-dried complexes were studied by DSC (Model DSC 214 polyma, Netzsch Group, Selb, Germany). Samples (approx. 3–5 mg) were sealed in aluminum pans under nitrogen and heated from 30 to 250 $^{\circ}$ C at a heating rate of 10 $^{\circ}$ C/min. An empty aluminum pan was used as a reference.

3.4.4.3 $^1\text{H-NMR}$ studies

NMR experiments were recorded on Bruker AV-400 NMR spectrometer (Bruker Biospin GmbH, Rheinstetten, Germany) at 500 MHz at room temperature. Pure nepafenac sample was dissolved in deuterated chloroform ($\text{CDCl}_3\text{-d}_6$) while γ -CD, HP β -CD and nepafenac/ CD complexes were dissolved in deuterium oxide (D_2O).

3.4.4.4 Preliminary eye drops studies

Nine preliminary formulations containing 0.5% (w/v) nepafenac, 15% (w/v) γ -CD, 8% (w/v) HP β -CD, 0.1% (w/v) EDTA, 0.02% (w/v) benzalkonium chloride, 0.05% (w/v) sodium chloride and different ratios of polymers were firstly prepared (**Table 5**).

Table 5. The polymer composition of the preliminary eye drop formulations.

Component (% w/v)	Preliminary eye drop formulations								
	F1	F2	F3	F4	F5	F6	F7	F8	F9
PVP	-	-	-	-	1.0	1.0	-	1.0	-
PVA	2.0	-	2.0	2.0	-	-	2.0	-	2.0
CMC	-	1.0	1.0	-	1.0	-	1.0	-	1.0
HPMC	0.1	-	-	-	0.1	-	-	-	-
MC	-	-	-	-	-	0.1	0.1	-	0.1
Tyloxapol	0.1	-	0.1	0.1	-	-	0.1	0.1	-

They were characterized regarding solid drug fraction, particle size, viscosity, osmolality and transmission electron microscope (TEM) analysis.

Nepafenac content in the solid phase was calculated, after sample centrifugation at 13000 x g rpm (MC6 centrifuge, Sarstedt AG, Nümbrecht, Germany) at room temperature for 30 min, following this equation (Sunna et al., 2015):

$$\% \text{ solid drug fraction (SDF)} = \frac{(\text{Total drug-dissolved drug})}{(\text{Total drug content})} \times 100 \quad (8)$$

where the dissolved drug in the supernatant was determined by HPLC.

Size, viscosity and osmolality of aggregates were analyzed by dynamic light scattering using Nanotrak Wave particle size analyzer from Microtrac Inc. (Montgomeryville, PA, USA), Brookfield viscometer (model DV2T) attached to a water bath (model TC-150) with a spindle (CPA-40Z) at 25 °C (Middleborough, MA, USA) and Osmomat 030 Gonotec (Berlin, Germany), respectively. All measurements were carried out in triplicate at room temperature.

Moreover, the morphology of aggregates was investigated by TEM (JEOL, JEM-2100 F, USA). Samples were prepared following the negative staining method previously described by Muankaew (2014).

3.5 Formulations

3.5.1 Optimization of nepafenac eye drops

Best preliminary eye drops formulations, F2, F3, F5 and F9, were selected for further evaluation. In addition, novel CD-based aqueous eye drop formulations containing various high mucoadhesive polymers, sodium hyaluronate and sodium alginate, were evaluated and compared with previous preliminary formulations to deliver nepafenac to the eye to treat inflammation, increase drug concentration in the posterior segment, and reduce the levels of inflammatory mediators. Compositions of these optimized nepafenac eye drop selected for further evaluation were previously described in **Table 1**.

Size of nepafenac formulations A1 to A9, that were previously filtered and diluted with MiliQ water, was calculated by dynamic light scattering using Nanotracs Wave particle size analyzer from Microtrac Inc. (Montgomeryville, PA, USA). Additionally, their zeta potential was assessed using Zetasizer[®] 3000HS (Malvern Instruments, UK). The pH was analyzed by pH meter GLP22 (Crison Instruments, Spain). All measurements were done in triplicate at 25 °C.

3.5.1.1 *In vitro* mucoadhesive studies

The mucoadhesive strength of nepafenac formulations was tested in triplicate using a TA.XT Plus Texture Analyzer (Stable Micro Systems Products, Godalming, UK) at room temperature (Campaña-Seoane et al., 2014 and Akhter et al., 2016). To simulate eye drops instillation, a force of 0.5 N for 60 seconds was applied to bovine corneas that they were placed under the end of the spindle. An aliquot of each formulation (approx. 15 µL) was placed at the bottom in a petri dish. Mucoadhesive resistance was determined as the force needed to separate the formulation from the bovine cornea.

3.5.1.1 *In vitro* cell viability

Cytotoxicity of eye drop formulations was evaluated using murine fibroblasts on BALB/3T3 clone A31 (ATCC[®] CCL-163TM) by WST-1 test. BALB 3T3 cells were cultured in DMEM/F12 (Dulbecco's Modified Eagle Medium) culture medium supplemented with 10% fetal bovine serum (Hyclone) and 1% of penicillin/streptomycin (Gibco). Cells were seeded (100 µL/well) in 96-well plate (1.5 x10⁴ cells/well) and were incubated 4 hours at 37 °C and 5% CO₂ to boost the growth. After 24 hours of culture, WST-1 assay was performed following the manufacturer's instructions. DMEM/F12 medium and

medium with blank formulations were used as controls. All samples (Nevanac 3mg /mL, formulations from A1 to A9 and the control) were diluted 1:50, 1:100 and 1:150 times with medium to be under EC50 value of nepafenac and they were added to the monolayers (Fernandez-Ferreiro et al., 2015). Then, the absorbance was calculated at 450 nm using a Model 680 microplate reader (Bio-Rad, Hercules, CA, USA) and the software Microplate Manager 5.2.1. Cell viability was measured as the percentage of living cells compared to untreated cells (controls).

3.5.1.2 *In vitro* anti-inflammatory activity

THP-1 human monocytes (ATCC TIB-202™) were cultured in RPMI 1640 (Gibco) supplemented with 10% fetal bovine serum (Hyclone), 2-mercaptoethanol (0.05 mM; Gibco), and 1% penicillin-streptomycin (Gibco). They were counted in a Coulter Multisizer3 (Beckman Coulter, Indianapolis, IN, USA) and adjusted to 200,000 cells per mL. Then, phorbol 12-myristate 13-acetate (PMA; Sigma-Aldrich) 200 nM was added to differentiate THP-1 cells into macrophages and they were incubated for 72 hours at 37 °C. Afterward, PMA solution was removed and cell monolayers were washed with Dulbecco's phosphate-buffered saline (DPBS) and trypsinized following standard protocols. Macrophages were seeded into 48-well plates at 4.5×10^4 cells/well, treated with 100 ng/mL of lipopolysaccharides (LPS) from *Escherichia coli* O111: B4 (Sigma-Aldrich) to induce an inflammatory response and incubated for 24 hours at 37° C and 5% CO₂ with the samples. Formulations A2, A3, A5, A8 and A9 were selected for anti-inflammatory efficacy and their blank correspondent formulations (without the drug) were also tested as controls. Cells treated only with LPS and without LPS (unstimulated cells) used as positive control and negative control, respectively. After incubation, cell culture supernatants were collected and stored at -150° C until cytokine assessments.

The secretion of three inflammatory mediators (PEG-2 IL-6 and IL-1ra) was tested. PEG-2 was analyzed using an EIA assay (Arbor Assays) while IL-6 and IL-1ra were analyzed by specific ELISAs (Sigma, St Louis, MO, USA) following the manufacturer's instructions after adequate dilutions.

3.5.2 Natamycin micelles and poly(pseudo)rotaxanes

3.5.2.1 *Micelle preparation and characterization*

Soluplus and Pluronic P103 micelles (0.1%, 0.01%, 1%, 2%, 3%, 4%, 5% w/v) were prepared in triplicate by dispersing under magnetic stirring at room

temperature each copolymer in 0.9% NaCl. Also, Soluplus and Pluronic P103 at 10% (w/v) were prepared in pH 6.4 buffer and 0.9% NaCl aqueous solution and kept under magnetic stirring for 12 h to ensure complete copolymer dispersion. Natamycin-loaded micelles (0.4 mg drug/mL dispersion) were compared with unloaded micelles. Size, polydispersion index (PDI) and zeta potential of the formed micelles were determined in triplicate using a Zetasizer[®] 3000HS (Malvern Instruments, Malvern, UK). The pH of the dispersions was also analyzed by pH meter GLP22 (Crison Instruments, L'Hospitalet de Llobregat, Spain).

Stability against dilution of natamycin-loaded pluronic micelles was analyzed by measuring the absorbance at 304 nm every 30 s for 30 min (UV-Vis spectrophotometer Agilent 8453, Waldbronn, Germany). Samples were poured into quartz cells for a sudden 30-fold or 60-fold dilution. All experiments were carried out in triplicate.

3.5.2.2 Preparation of poly(pseudo)rotaxanes

Polypseudorotaxanes were prepared by mixing copolymer solution and α -CD solution both in pH 6.4 buffer and 0.9% NaCl media. Natamycin (up to 240 μ g/mL) was added to 20% (w/w) Soluplus or Pluronic P103 dissolved dispersion in each media. After natamycin was fully dissolved, they were kept under magnetic stirring at room temperature for 24 h. Then solution containing 20% (w/v) α -CD was prepared in pH 6.4 buffer and 0.9% NaCl. Following, copolymer and α -CD solutions were mixed and the final concentration was 10% (w/w) copolymers, 10% (w/w) α -CD, and 120 μ g/mL natamycin in each medium. Dispersions without CD, containing only the copolymers and natamycin at the same final concentration were also prepared to be compared for similarities. Changes in clarity were studied visually.

3.6 Rheological analysis

Rheological characterization of nepafenac eye drops and natamycin micelles and poly(pseudo)rotaxanes were recorded in a Rheolyst AR-1000N rheometer (TA Instruments, Newcastle, UK) has an AR2500 data analyzer, a Peltier Plate and a cone geometry (6 cm diameter and 2.1°). Evolution of storage (G') and loss (G'') moduli of nepafenac eye drops were recorded at 37 °C and 0.1 Pa, applying angular frequency sweeps from 0.1 to 50 rad/s. Then, after rotational runs at 37 °C for 2 min with shear stress in the range 0.1 to 200 s^{-1} , viscosity and flow curves were carried out. Moreover, the effect of temperature on the storage (G') and loss (G'') moduli of Soluplus and

Pluronic P103 dispersions, with and without α -CD, in pH 6.4 buffer or 0.9% NaCl were conducted at a fixed angular frequency of 5 rad/s and oscillation stress of 0.1 Pa from 20 to 40 °C with a ramp of 2 °C/min. Experiments were performed using 1.5 mL for each formulation. Rheology advantage data analysis software was used to evaluate the data.

3.7 HET-CAM

The Hen's Egg Test on Chorio-Allantoic Membrane (HET-CAM) assay, a valid substitute to animal testing of ocular irritancy, was carried out as preliminary screening for ocular irritancy as previously described (Grimaudo et al., 2018). Briefly, fertilized chicken eggs, kindly provided by The Coren Technological Incubation Center (San Cibrao das Viñas, Spain), were incubated at 37 °C and 60 % RH for 9 days. Eggs were rotated 180° three times per day to ensure the correct development of the embryo. On a ninth day, a cut (about 1 cm in diameter) was made by a rotatory saw (Dremel 300, Breda, The Netherlands) to remove the eggshell. The inner membrane was wet with 0.9% NaCl, and then carefully removed to expose the chorioallantoic membrane (CAM). Defective eggs were discarded. Aliquots of natamycin-loaded Soluplus and Pluronic P103 micelles (200 μ L) and poly(pseudo)rotaxanes (150 μ L) dispersions were placed on the CAM of different eggs. Also, all nepafenac formulations were tested (200 μ L). Each test was performed at least in duplicate. 0.9% NaCl and 0.1 N NaOH solutions were used as negative and positive controls, respectively. Vessels of CAM were monitored for 5 minutes after the addition of each formulation for hemorrhage, vascular lysis, or coagulation. The irritation scored (IS) was calculated by this expression (Alvarez-Rivera et al., 2016):

$$IS = \frac{(301-tH) \times 5}{300} + \frac{(300-tL) \times 7}{300} + \frac{(301-tC) \times 9}{300} \quad (9)$$

where tH, tL and tC are the times at which hemolysis, lysis and coagulation appeared. The damage was categorized using IS as non-irritant ($IS < 1$), a mild irritant ($1 \leq IS < 5$), moderately irritant ($5 \leq IS < 10$), or severe irritant ($IS > 10$).

3.8 In vitro diffusion studies

Nepafenac and natamycin diffusion tests from respective formulations were evaluated in triplicate at 37 °C in vertical Franz diffusion cells under sink

conditions and kept under magnetic stirring at 300 rpm. The donor phase in both natamycin and nepafenac formulations was filled with 1.00 mL of the test formulation. The receptor phase comprised 6.00 mL of medium 2.5% (w/v) γ -CD/HP β -CD ratio (80/20) to ensure sink conditions in the case of nepafenac formulations and 6.00 mL of medium (0.9% NaCl or pH 6.4 buffer) for natamycin formulations. Compartments were separated by cellulose acetate membrane filters (0.45 μ m pore size, 25 mm diameter) that were soaked in the receptor medium one hour before starting the experiment. The surface available for diffusion was 0.786 cm². Samples (1 mL for nepafenac formulations and 0.70 mL for natamycin formulations) were taken from the receptor phase at pre-established times (30, 60, 90, 120, 180, 210, 240, 300 and 360 min) and replaced with fresh medium. In the case of nepafenac formulations, commercial eye drops (Nevanac 3 mg/mL) were also tested. The drug content in the collected samples was quantified from absorbance measurements following validated methods in section 3.2.

Diffusion coefficients (D) were estimated by following the Higuchi equation:

$$\frac{Q}{A} = 2C_0 \left(\frac{Dt}{\pi} \right)^{1/2} \quad (10)$$

where Q is the amount of drug (g) released by time t (min), A is diffusion area (cm²), C₀ is the initial drug concentration in the formulation (g/mL), and D is the diffusion coefficient (cm²/min).

3.9 Ex-vivo cornea and sclera permeability studies

Permeability tests with nepafenac and natamycin formulations were carried out using bovine cornea and sclera following a protocol previously described. The fresh bovine eyes that they were kindly donated by a local slaughterhouse were kept in PBS solution supplemented with antibiotics (penicillin 100 IU/mL and streptomycin 100 μ g/mL) in an ice bath during transport. Corneas and scleras were isolated with a scalpel, washed with PBS and placed on vertical diffusion Franz cells. To balance the ocular tissues, both receptor and donor phases were filled with carbonate buffer pH 7.2 following BCOP protocol, placed inside a water bath at 37 °C and kept under magnetic stirring during 1 h in order. Then, the volume of the entire donor chamber was removed entirely and replaced by the formulations (2 mL). So as to prevent evaporation, chambers were closed with parafilm (0.785 cm² area available for permeation). Samples (1 mL) were taken from the receptor chamber at pre-established times (0.5, 1, 2, 3, 4, 5 and 6 h), and they were substituting the same volume with carbonate buffer each time,

avoiding bubbles from the diffusion cells. All experiments were carried out in triplicate. Nepafenac and natamycin permeated were quantified by HPLC methods summarized in section 3.2.

After 6-h permeation test, formulations were extracted from donor chambers and they were taken for HPLC quantification. Therefore, corneas and scleras previously inspected were removed and placed in tubes with 3 mL of ethanol: water (50:50 v/v) mixture, for 24 hours at 37 °C and applying sonication for 90 minutes in an ultrasound bath at 37 °C. Afterward, tubes were centrifuged (1000 rpm, 5 min, 25 °C), and the supernatant filtered (Acrodisc® Syringe Filter, 0.22µm GHP Minispike, Waters) into small eppendorfs, centrifuged again (14000 rpm, 20 min, 25 °C). Drug extracted from bovine corneas and scleras were filtered and calculated by HPLC.

The apparent permeability coefficient (P_{app}) was calculated from the flux (J) following this equation (Varela-Garcia et al., 2018):

$$P_{app} = \frac{J}{C_0} \quad (11)$$

where J is the flux calculated as the slope (Q/t) of the linear section of the cumulative amount of drug permeated per area in the receptor chamber (Q) versus time (t) and C_0 is the initial concentration of drug in the donor phase.

3.10 Statistical Analysis

Data are presented as mean ± standard deviation (SD) (n=3). Effect of formulation composition on natamycin permeation through the sclera and anti-inflammatory response of nepafenac eye drops was analyzed using ANOVA and multiple range test (Statgraphics Centurion XVI 1.16.1.11, StatPoint Technologies Inc., Warrenton, VA, USA). Differences were considered significant at $p < 0.05$.

4 Results and discussion

With the project being divided into 3 parts, the results of each one will be discussed separately.

4.1 Nepafenac-loaded cyclodextrin/ polymer aggregates

4.1.1 Stability of nepafenac after a heating method

Firstly, the water content of γ -CD and HP β -CD was found 10.70% and 6.22%, respectively. Then, the chemical stability of nepafenac in aqueous CD solutions was studied after heating in an ultrasonic water bath and calculating its concentration by HPLC (**Table 6**).

Table 6. Nepafenac concentrations in an aqueous solution containing 1% (w/v) γ -CD after heating by sonication. Results are expressed as mean \pm SD (n=3).

Sonication	Nepafenac concentration ($\mu\text{g/ml}$)
60 °C 20 min	6.41 \pm 0.08
60 °C 40 min	6.49 \pm 0.07
60 °C 60 min	6.57 \pm 0.08

Results showed no degradation of nepafenac using sonication and this heating method was selected for phase solubility studies of nepafenac in aqueous CD solutions.

4.1.2 Phase-solubility studies

The nepafenac solubility with various CDs in aqueous solutions is summarized in **Table 7**. Some parameters, such as complexation efficiency (CE) and the apparent stability constants ($K_{1:1}$) of the multi-component complexes, were also determined. The phase-solubility analysis of nepafenac in α -CD, β -CD, γ -CD, HP α -CD, HP β -CD and HP γ -CD aqueous solutions are shown in **Figure 14**.

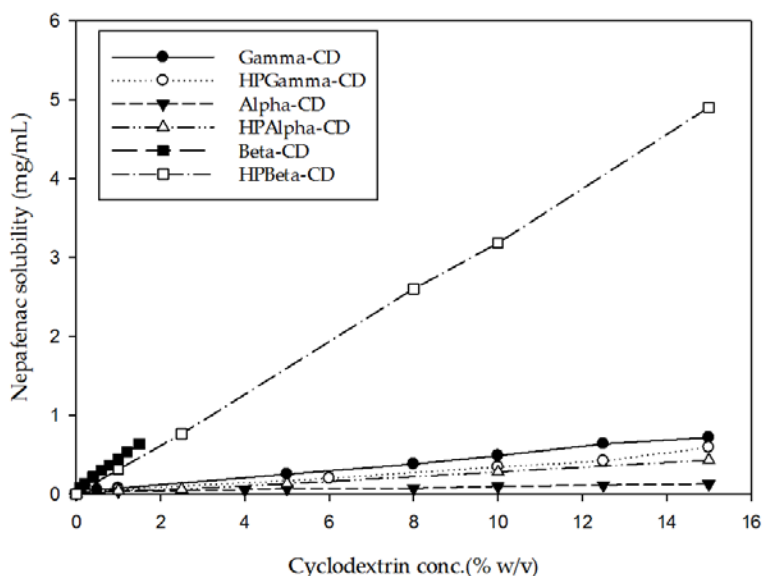


Figure 14. Phase-solubility diagram of nepafenac at 25 °C in various CDs aqueous solutions. Results are expressed as mean ($n=3$).

Table 7. Values of the apparent stability constant ($K_{1:1}$) and complexation efficiency (CE).

Cyclodextrin	Type	Slope	Corr.	$K_{1:1}$ (M^{-1})	CE	Solubility (mg/mL) in the presence of 15%(w/v) CD
γ -CD	A_L^{-a}	0.024	0.998	248	0.024	0.715
HP γ -CD	A_p^{-a}	0.022	0.978	218	0.021	0.590
α -CD	A_L^{-a}	0.029	0.991	289	0.028	0.131

HP α -CD	A _L ^{-a}	0.011	0.984	113	0.011	0.401
β -CD	A _L	0.180	0.998	2230	0.220	- ^b
HP β -CD	A _L ^{-a}	0.198	0.999	2515	0.247	4.460

^a Measured from 0–15% CD;

^b CD was not soluble in water at this concentration.

CDs solubilizing capacity was studied by phase-solubility studies, proposed by Higuchi & Connors (1956). The phase solubility diagram was obtained by plotting the apparent equilibrium concentrations of nepafenac against various CD concentrations. Based on the phase-solubility profiles, all inclusion complexes were soluble (A-type profile). Complexes including γ -CD, β -CD, α -CD, HP β -CD, HP α -CD showed an A_L profile, due to the linear relation between nepafenac solubility and these CD concentrations, suggesting the formation of 1:1 complexes. Nevertheless, HP γ -CD showed an A_P-type profile, indicating an upward trend from linearity.

Among the different CDs investigated, HP β -CD showed the highest CE.

4.1.3 Effect of ternary complexes on nepafenac/ CD complex solubility

Usually, the complexation efficiency of CDs is quite low and can be enhanced by the formation of ternary complexes, i.e., using polymers (Loftsson et al., 1994; Wang et al., 2013; Vieira et al., 2015). One objective of this study was to clarify if the addition of hydrophilic polymers to nepafenac/ CD complex could enhance its solubility. For that, various polymers widely used in the preparation of eye drops, such as PVP, PVA, CMC and tyloxapol (Ludwig, 2005), were tested (**Figure 15**).

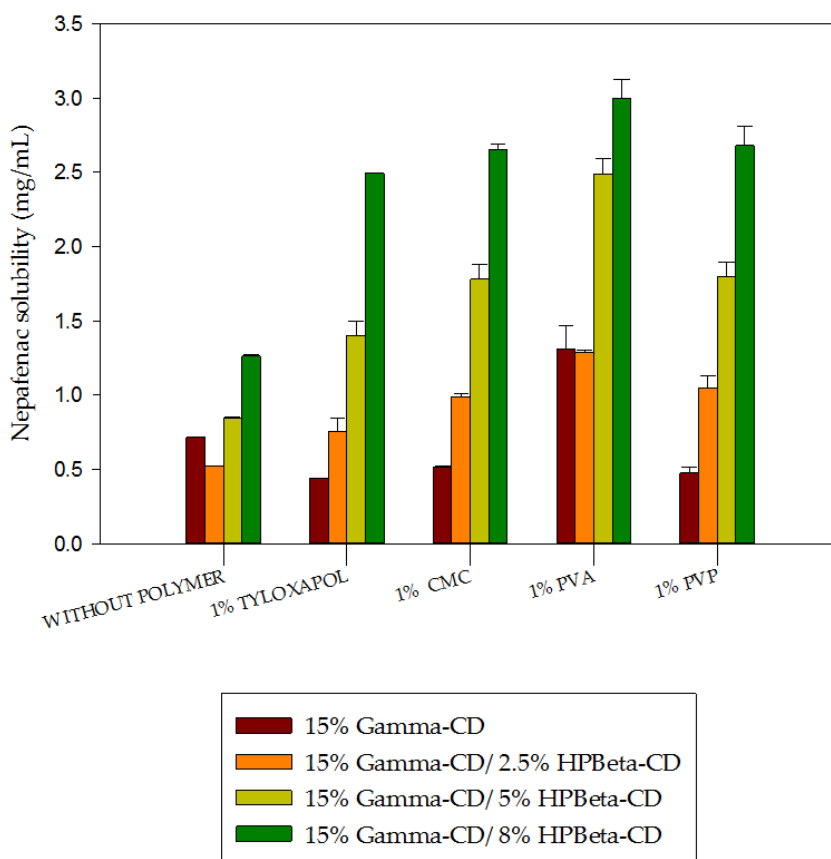


Figure 15. Effect of cyclodextrins and hydrophilic polymers on the apparent solubility of nepafenac.

Addition of 1% (w/v) PVA to 15% γ -CD aqueous solution increased almost three times the apparent solubility of nepafenac. Differently, the addition of 1% (w/v) PVP, CMC and tyloxapol had a slightly negative effect on the apparent solubility of nepafenac, suggesting the displacement of nepafenac by these polymers inside the CD cavity (Nogueiras-Nieto et al., 2012). The addition of 8% (w/v) of HP β -CD to 15% γ -CD aqueous solution led to the highest increase in the apparent solubility of nepafenac, from to (**Figure 15**). This could be attributed to the great solubilizing capacity of HP β -CD that was found about 2.5 mg/mL using 8% HP β -CD. A combination of two cyclodextrins in aqueous solution has been widely investigated. Jóhannsdóttir

et al. (2015) combined α -CD and γ -CD to increase the solubility of Fourier transform infrared (FT-IR) spectroscopy and differential scanning calorimetry (DSC) analysis were used to verify nepafenac/ CD complex formation in solid-state.

4.1.4 Solid state characterization of nepafenac/ CD inclusion complexes

Fourier transform infrared (FT-IR) spectroscopy and differential scanning calorimetry (DSC) analysis were used to verify nepafenac/ CD complex formation in solid-state. **Figure 16** represents the FT-IR spectra of pure nepafenac, γ -CD and HP β -CD, as well as nepafenac/ CD complex prepared by freeze-drying. Bands described pure compounds were compared to the band for the complex.

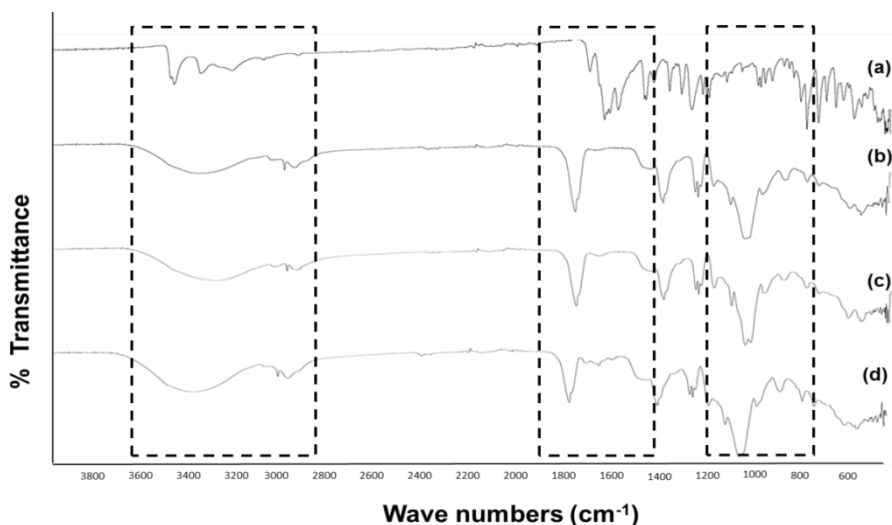


Figure 16. FT-IR spectra of (a) pure nepafenac, (b) pure HP β CD, (c) pure γ -CD and (d) freeze-dried nepafenac/15% γ -CD/8%HP β -CD complex.

In the spectrogram of pure nepafenac (**Figure 16a**), the sharp peak appeared at 1631, 1664, 3500-3300 cm^{-1} representing the stretching vibration of the secondary amide, ketone group and NH_2 , respectively. Another four distinct peaks appeared at 1818, 1968, 3040, and 3080 cm^{-1} , which were associated with the stretching vibration of benzene aromatic. The spectrum of pure γ -CD and HP β -CD (**Figures 16b** and **c**) showed intense absorption bands at 3300, 3410, 1420 and 1330 cm^{-1} relating to OH stretch and at 1079 and 1029 cm^{-1} relating to CO stretch. Nevertheless, in the

spectrum of inclusion complex (**Figure 16d**), the absorption peak at 1631, 1664, 1818 and 1968 cm^{-1} displayed changes in intensity and widths and the absorption peak at 3500-3300 cm^{-1} disappeared, suggesting that nepafenac may be encapsulated into the CDs cavities and formed a new compound.

DSC measurements may provide additional information on complex formation based on the disappearance or shift of molecules because of their incorporation into the CD cavities. The DSC curves for nepafenac, CDs and their complex are shown in **Figure 17**.

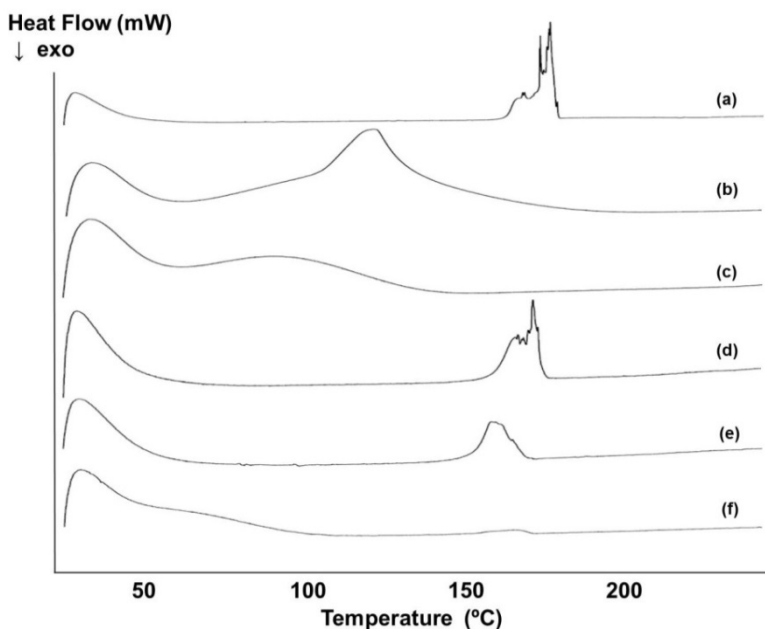


Figure 17. DSC curves of (a) pure nepafenac, (b) pure γ -CD, (c) pure HP β -CD, (d) freeze-dried nepafenac and mixture of 15% γ -CD/ 2.5% HP β -CD complex, (e) freeze-dried of nepafenac/ 15% γ -CD/ 5%HP β -CD complex and (f) freeze-dried nepafenac/ 15% γ -CD/ 8%HP β -CD complex. Exo; exothermic.

The DSC curve of nepafenac revealed a sharp endothermic peak at 178 °C, which correspond to its melting point (**Figure 17a**). DSC curves for γ -CD and HP β -CD (**Figures 17b** and **c**), showed a broad endothermic peak between approximately 100 °C and 150 °C as a result of the dehydration process. Nevertheless, the DSC curve of inclusion complex (**Figures 17d, e, and f**) did not show any sharp endothermic peak at the range of nepafenac melting point, which can presume the interaction between nepafenac and γ -CD/ HP β -CD.

The disappearance of endothermic DSC curve and absorption peaks at some ranges after FT-IR spectroscopy highly suggests the inclusion of nepafenac into the CD cavities.

NMR spectroscopy provides useful information about the complex formed, for example, the position of the guest molecule inside the host CD cavity (Yuan et al., 2012; Goswami & Sarkar, 2018). The formation of inclusion complexes results in chemical shifts ($\Delta\delta$) since proton environments are altered after encapsulation of the guest molecule into the CD cavity. $\Delta\delta$ can be calculated using the following equation:

$$\Delta\delta^* = \delta_{\text{complex}} - \delta_{\text{free}} \quad (12)$$

where δ_{complex} and δ_{free} are chemical shifts between free and bound CD molecules, respectively. Usually, chemical shifts are small since interactions between guest and host are mainly non-covalent bonds.

For the confirmation of the formation of the inclusion complex of nepafenac with γ - and HP β -CD, a one-dimensional $^1\text{H-NMR}$ spectra of nepafenac and each nepafenac/ CD complex were obtained and compared (see **Appendix, Figure A1**). Variation of the chemical shifts between free and bound CDs molecules are shown in **Table 8** and **Table 9**.

Table 8. Variation of $^1\text{H-NMR}$ chemical shift, expressed in ppm, of free γCD alone and nepafenac/ $\gamma\text{-CD}$ complex.

Protons	$\gamma\text{-CD}$	Nepafenac/ $\gamma\text{-CD}$	$\Delta\delta^*$
H1	5.1320	5.1554	+0.0234
H2	3.6754	3.7031	+0.0277
H3	3.9564	3.9782	+0.0218
H4	3.6115	3.6339	+0.0224
H5	3.8712	3.8925	+0.0213
H6	3.8903	3.9146	+0.0243

Table 9. Variation of $^1\text{H-NMR}$ chemical shift, expressed in ppm, of free HP β CD alone and nepafenac/ HP β CD complex.

Protons	HP β -CD	Nepafenac/ HP β CD	$\Delta\delta^*$
H1	5.1207	5.1137	-0.007
H2	3.6686	3.6625	-0.0061
H3	4.0386	4.0046	-0.034
H4	3.5485	3.5468	-0.0017
H5	3.9010	3.7681	-0.1329
H6	3.9487	3.8912	-0.0575
-CH3	1.1952	1.1864	-0.0088

Changes in $^1\text{H-NMR}$ chemical shift ($\Delta\delta$) of γ -CD were higher for H-3 proton than H-5 proton (0.0218 for the H-3 and 0.0213 for H-5 protons, respectively) when nepafenac was present, suggesting that nepafenac may occupy the entire γ -CD cavity (**Table 8**). On the other hand, changes in $\Delta\delta$ of HP β -CD in the presence of nepafenac were more significant for H-5 proton (-0.1329) than the H-3 proton (-0.034), suggesting partial inclusion of nepafenac in the HP β -CD cavity (**Table 9**).

Variation of the $^1\text{HNMR}$ chemical shifts, in ppm, of free nepafenac, nepafenac/ γ -CD complex and nepafenac/ HP β -CD complex were also examined (see **Appendix, Figure A1**). 2D ROESY NMR spectroscopy was carried out to confirm the position of the guest in the complex.

4.2 Nepafenac eye drops

Although the combination of 15% γ -CD and 8% HP β -CD displayed lower solubility than only 8% HP β -CD alone, due to the higher capability of γ -CD to form aggregates, and greater solubilizing capacity showed by HP β -CD, 15% γ -CD and 8% HP β -CD were selected for preliminary studies of nepafenac eye drops (see **Appendix Figure A2 and Table A1**). Then, most promising formulations, A1 to A9, were selected for further evaluations and are widely discussed below.

4.2.1 Solubility of nepafenac eye drops and their characterization

Drug solubilization, zeta potential, and pH of all formulations, **Table 10**, were evaluated.

Table 10. Apparent drug solubility, zeta potential, and pH of nepafenac eye drop suspensions.

Formulation	Apparent drug solubility at 25 °C (mg/mL)	Dissolved drug content (%)	Zeta potential (mV)	pH
A1	1.87 ± 0.03	62.33	-10.9 ± 0.6	6.08 ± 0.23
A2	1.95 ± 0.02	65.00	-10.4 ± 0.3	6.18 ± 0.05
A3	2.23 ± 0.01	74.33	-6.4 ± 0.8	6.09 ± 0.03
A4	1.91 ± 0.02	63.66	-12.1 ± 1.4	6.21 ± 0.09
A5	2.50 ± 0.02	83.33	-7.8 ± 0.9	6.07 ± 0.02
A6	1.89 ± 0.05	63.00	-27.4 ± 1.7	6.13 ± 0.33
A7	1.68 ± 0.01	56.00	-14.4 ± 1.4	6.01 ± 0.23
A8	1.95 ± 0.02	65.00	-14.7 ± 1.2	6.16 ± 0.15
A9	2.61 ± 0.02	87.00	-6.9 ± 1.4	6.08 ± 0.05

The solubility of nepafenac at 25 °C in water has been described in the literature to be 0.0197 mg/mL. Using eye drops media, a mixture of cyclodextrins and water-soluble polymers, the solubility of all formulations increased to 1.68 ± 0.01- 2.61 ± 0.02 mg/mL, depending on the polymers used (from higher to lower solubility enhancement rank order of A9>A5>A3>A2 ~A8>A4>A6>A1>A7). This part of the study aimed to explain if the addition of water-soluble polymers to previous nepafenac eye drops could increase nepafenac solubility and enhance retention time at the eye structure. The highest enhancement in solubility was in formulation A9, which contained CMC, PVA, and MC with an apparent solubility value of 2.61 ± 0.02 mg/mL. Differently, formulation A7, containing SA solely, showed a minor increase, being 1.68 ± 0.01 mg/mL. These results agree with our previous studies, which revealed that formulations containing CMC and PVA led to the highest solubilization of nepafenac (Lorenzo-Veiga et al., 2019).

The zeta potential of all formulations evaluated (**Table 10**) was negative or close to zero, in accordance with the anionic or nonionic nature of the

polymers and surfactants involved. All formulations showed a pH suitable for ocular administration, ranging from 6.01 ± 0.23 to 6.21 ± 0.09 (Shelley et al., 2018). Formulations had a size range between 340 and 5950 nm (**Table 11**) and high polydispersity index, which may be attributed to the continuous formation and destruction of aggregates.

Table 11. Particle size results of aqueous nepafenac eye drop formulations. Formulations were diluted with MiliQ water. Data reported are means of three determinations.

Formulation	Peak summary	
	Size (d. nm)	Intensity (%)
A1	5880.0	73.3
	2619.0	19.9
A2	5880.0	46.9
	4300.0	46.8
	1953.0	6.3
A3	5590.0	96.3
	827.0	3.7
A4	5870.0	100.0
A5	3090.0	53.5
	5950.0	42.0
	481.0	4.5
A6	5575.0	100.0
A7	3380.0	65.1
	5560.0	34.9
A8	4510.0	66.4
	1572.0	33.6

	5510.0	77.1
A9	3250.0	15.3
	340.0	7.6

All formulations exhibited microparticles (approx.5–6 μm), and formulations A3, A5, and A9, which contained PVA and CMC or PVP and CMC, also exhibited a small population of smaller particles (less than 1 μm). The larger size of our formulations compared with Nevanac, which size was reported by Shelley et al. (2018) to be about 2 μm , could be attributed to the different polymers, CDs and eye drop vehicle. Similar size range was reported by Jansook et al. (2015) after the preparation of irbesartan eye drops also containing 15% γ -CD, various polymers and eye drop vehicle.

4.2.2 Rheological analysis

To evaluate their rheological properties, viscosity profiles of formulations A1 to A9 and commercially available nepafenac -based eye drops, Nevanac[®], were firstly performed (Figure 18).

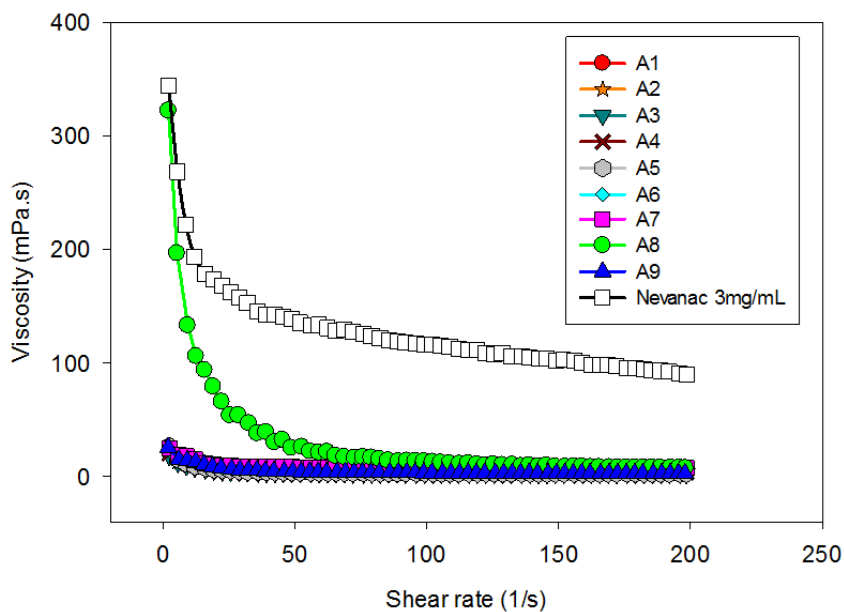


Figure 18. Dependence of viscosity on shear rate conditions of eye drops determined at 37 °C.

All formulations exhibited a pseudoplastic-like behavior with high viscosity values decreasing in the 0.1 to 200 s^{-1} shear rate range, demonstrating features adequate for prolonged residence at the ocular surface, preventing its removal under blinking conditions (Saldias et al., 2015). Regarding viscoelastic behavior, the addition of 1% CMC, 0.2 % HA, and 0.4% SA to a formulation containing nepafenac/ γ -CD/ HP- β CD (formulation A8) caused significant changes in the rheological properties (**Figure 19**).

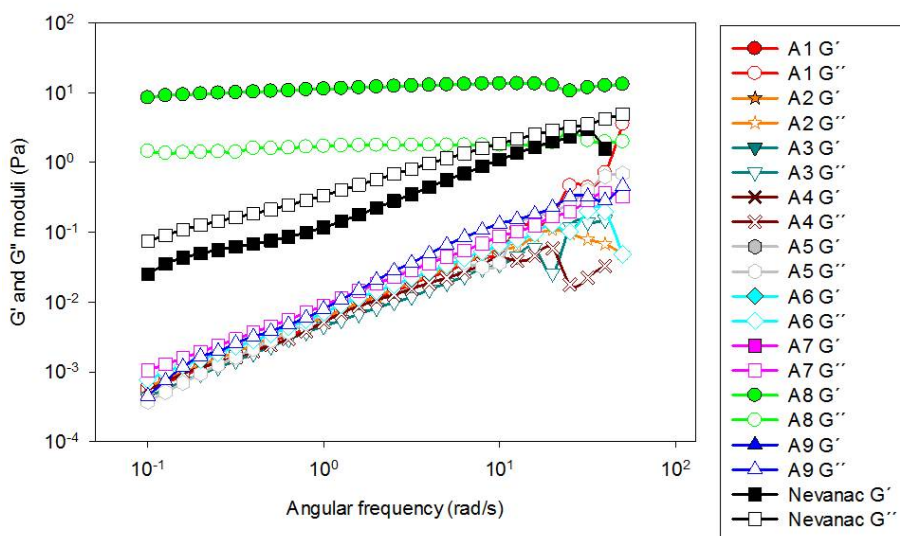


Figure 19. Evolution of storage (G' , solid symbols) and loss (G'' , open symbols) moduli as a function of angular frequency (rad/s).

Formulations A1 to A7 and A9 behaved as very liquid-like systems (values of G' were negligible), confirming that they displayed more viscous than elastic behavior. In contrast, formulation A8, which contained CMC, HA, and SA, behaved as a well-structured gel ($G' \gg G''$) and displayed pseudoplastic behavior while Nevanac behaved as a weak gel (G' and G'' values increased with the angular frequency).

4.2.3 Mucoadhesion studies

Mucoadhesive delivery systems have been suggested as a strategy to enhance drug retention of topical ophthalmic formulations. Polymer–mucin bonds can retain formulations on the surface of the eye, increasing the thickness of the tear film (Greaves & Wilson, 1993). Various in vitro techniques have been used to assess the mucoadhesive properties of

potential ophthalmic formulations (Ivarsson & Wahlgren, 2012). Among them, in vitro tensile test was employed to calculate mucoadhesive strength in relation to the detachment force needed to separate the formulations and ex vivo bovine corneas (Campana-Seoane et al., 2014 and Almeida et al., 2016)(Table 12). It was claimed that the force needed during eye blinking was 0.8 N (Shelley at al., 2018).

Table 12. Mucoadhesive strength of ophthalmic formulations on ex vivo bovine cornea.

Formulation	Mucoadhesive strength (N)
A1	0.39 ± 0.15
A2	0.54 ± 0.13
A3	0.41 ± 0.04
A4	0.56 ± 0.11
A5	0.52 ± 0.02
A6	0.39 ± 0.06
A7	0.36 ± 0.08
A8	0.47 ± 0.02
A9	0.38 ± 0.06
Nevanac 3 mg/mL	0.67 ± 0.03

As mucoadhesion is correlated with viscosity, Nevanac displayed the greatest mucoadhesive strength (0.672 ± 0.03 N), following the rank order of formulation A4 > A2 > A5, all of them containing CMC. Results obtained were in line with other studies reported in the literature using CMC. Brako and co-workers (2018) studied the mucoadhesion of progesterone-loaded nanofibers. They found that the addition of CMC to the fibers also increased their mucoadhesion in both artificial and mucosal membranes.

4.2.4 HET-CAM and cytocompatibility tests

The compatibility of all formulations was evaluated with the chorioallantoic membrane (CAM) of fertilized chicken eggs and BALB/3T3 cells. The Hen's Egg Test – Chorioallantoic Membrane (HET-CAM) test has been considered

as one adequate alternative to test eye irritation in vitro due to the similarity with the Draize test (Scheel et al., 2011). All formulations were tested regarding ocular biocompatibility using the HET-CAM test for the evaluation of potential ocular irritation on the CAM of fertilized eggs. None of the formulations directly placed on the CAM induced hemorrhage, lysis, or coagulation, showing an IS value of 0.0 as well as the negative control (0.9% NaCl)(**Figure 20**). Differently, the positive control (0.1N NaOH) displayed an IS value of 17.

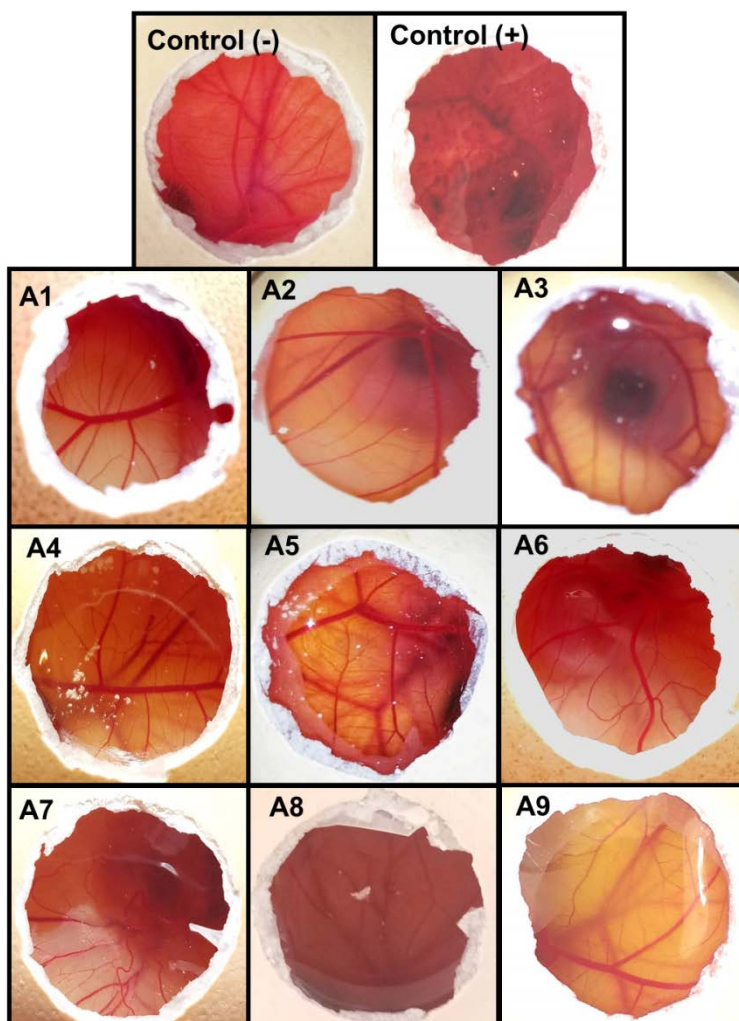


Figure 20. Pictures of the HET-CAM test recorded after 5 min contact with nepafenac formulations. Negative and positive controls refer to 0.9% NaCl and 0.1 N NaOH, respectively.

The percentage of cell survival relative to the negative control of formulations A1 to A9 and Nevanac at three dilutions (1:50, 1:100 and 1:150) is shown in **Figure 21**. All samples tested were diluted with DMEM/F12 medium to be under EC50 (Fernandez-Ferreiro et al., 2015) and they have shown to be not dangerous to BALB 3T3 cells, with cell viability similar to the marketed formulation, Nevanac (**Figure 8**).

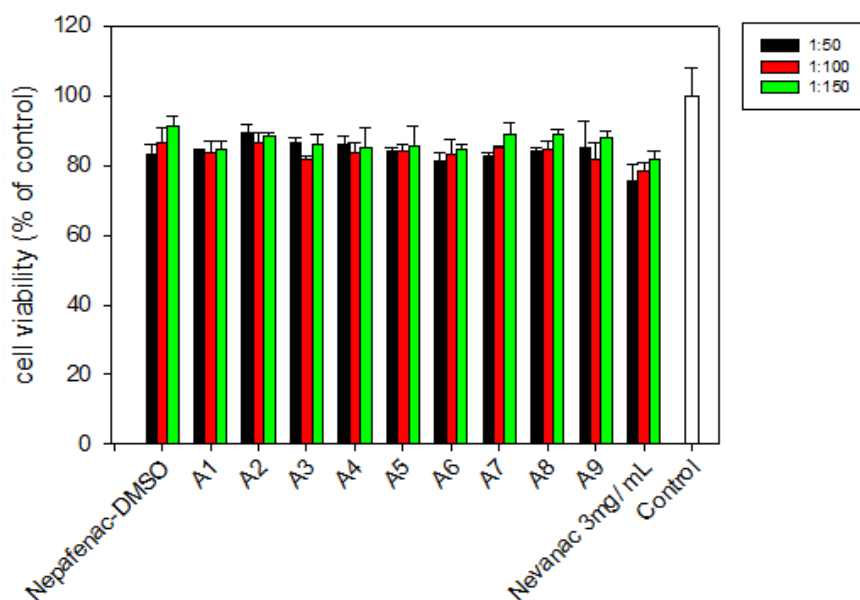


Figure 21. Viability of BALB/3T3 cells after 24 hours of exposure to ophthalmic formulations A1–A9 and Nevanac at various concentrations and control.

Results confirmed that a dilution of 1:100 was correct for the evaluation of the anti-inflammatory activity.

4.2.5 In vitro diffusion studies

Then, in vitro diffusion studies of formulations A1 to A9 and Nevanac were carried out by vertical Frank diffusion cells, using cellulose acetate membranes (0.45 μm pore size, 25 mm diameter) to separate the donor from the receptor compartments under sink conditions and taking samples at pre-established times up to 6 hours (**Figure 22**).

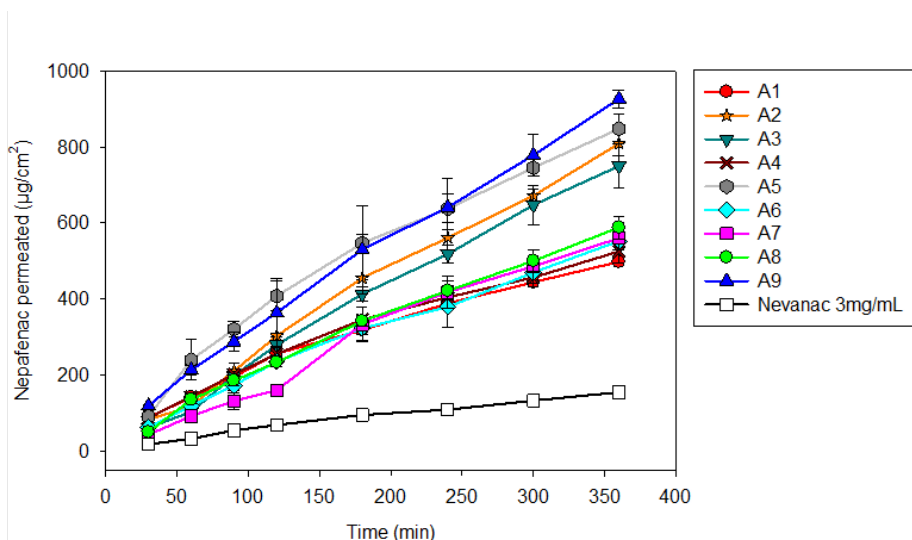


Figure 22. Nepafenac diffusion test through cellulose acetate membrane at 37 °C from eye drop formulations A1 to A9.

The rank order of fastest diffusion was formulation A9 ($926.1 \pm 23.4 \mu\text{g}/\text{cm}^2$) > A5 ($847.8 \pm 39.5 \mu\text{g}/\text{cm}^2$) > A3 ($749.6 \pm 58.4 \mu\text{g}/\text{cm}^2$). These findings are in good agreement with their solubilizing capacity, suggesting that the increase in the apparent drug solubility should favor the diffusion of the drug through cellulose acetate membrane.

4.2.6 Ex vivo corneal and scleral permeability studies

The next step was to evaluate the potential of formulations A1 to A9 to provide therapeutic amounts of nepafenac to the ocular surface. Results from formulations A1 to A9 were compared to those achieved with marketed nepafenac eye drops, Nevanac (3 mg/mL). The ex vivo permeability studies were carried out similarly, using bovine corneas and scleras. Nevanac displayed the lowest amount of nepafenac permeated through bovine cornea ($7.75 \pm 0.26 \mu\text{g}/\text{cm}^2$) and sclera ($19.44 \pm 1.74 \mu\text{g}/\text{cm}^2$) after 6 h compared to formulations A1 to A9 (**Figure 23**). These results are in good agreement with data reported in the literature and occurred due to the low amount of nepafenac that is solubilized in Nevanac 3 mg/mL ($37.87 \mu\text{g}/\text{mL}$) compared to our formulations. Actually, various studies mentioned that the low release rate of Nevanac was because it contains Carbopol 974P, which is a highly cross-linked bioadhesive polymer that enables near-zero or anomalous release rate (Yu et al., 2017, and Shelley et al., 2018).

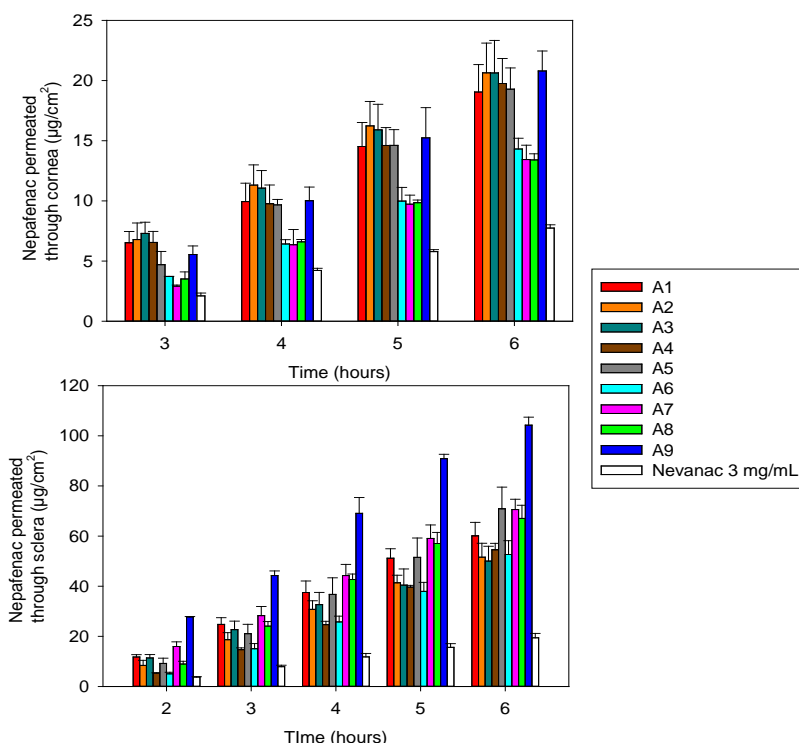


Figure 23. Nepafenac permeated through (A) bovine cornea and (B) sclera measured in the receptor chamber as a function of time.

As expected, all formulations displayed slower permeability through cornea than through sclera (**Figure 23**). They showed a lag time of three hours in the case of cornea and two hours for sclera. Sclera had shown higher permeability than cornea due to its porous structure (Loch et al., 2012).

All formulations tested showed higher permeability rate compared with Nevanac. This is probably due to the presence of cyclodextrins in our formulations and higher fraction of solubilized nepafenac. In fact, various studies have shown that CDs enhance drug penetration through biological barriers consisting of an aqueous exterior and a mucosal membrane. Aktaş and co-workers (2003) reported that eye drops containing pilocarpine/ HPβ-CD complexes caused four times higher transcorneal penetration compared to a formulation without CD. Moreover, similar behavior was also observed by Shelley et al. (2018), when they studied the permeability of nepafenac across porcine cornea compared to cyclodextrin formulations of nepafenac. The highest permeability through both bovine cornea and sclera was achieved by

formulation A9, $20.80 \pm 1.66 \mu\text{g}/\text{cm}^2$ in cornea and $104.24 \pm 3.21 \mu\text{g}/\text{cm}^2$ in sclera, respectively. This could be attributed to their high solubilizing capacity.

Then, after 6 h-test, the amount of nepafenac accumulated at bovine corneal and scleral surfaces and in these tissue was monitored and quantified (**Figure 24**).

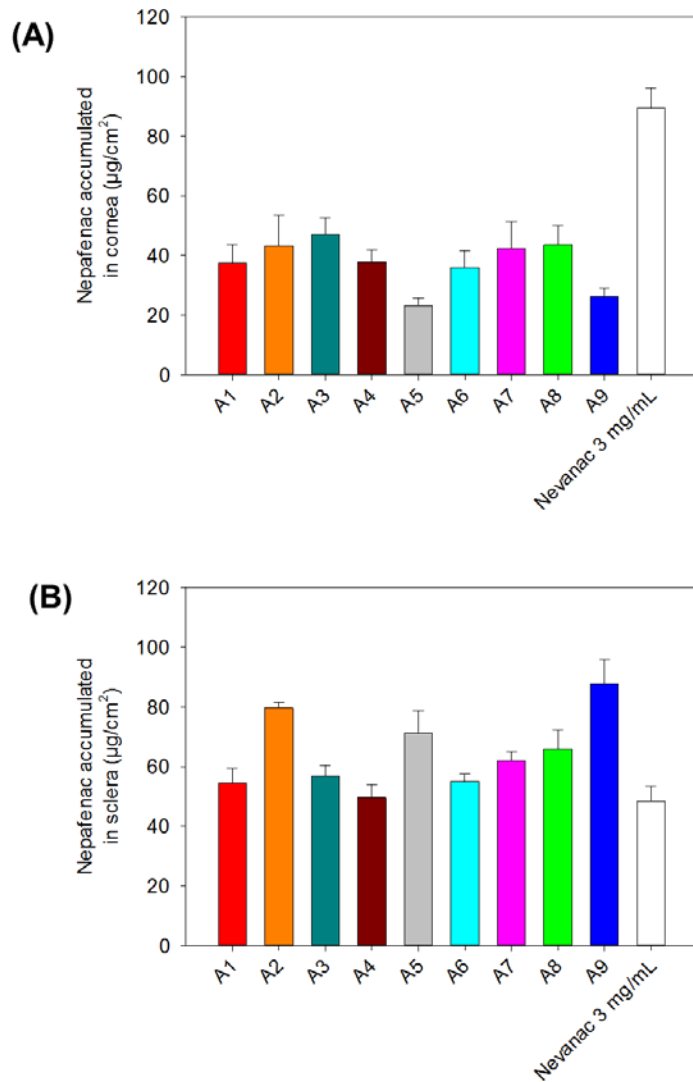


Figure 24. Nepafenac accumulated on the surface and inside **(A)** cornea and **(B)** sclera after 6 hours exposition.

Nevanac showed the highest accumulation in the cornea after 6h exposition ($89.57 \pm 6.66 \mu\text{g}/\text{cm}^2$), which can be associated to the high viscosity of the formulation at the surface. Compared to Nevanac, encapsulation of nepafenac into CDs was advantageous in both terms of total amount of nepafenac accumulated in the sclera and steady-state flux. Formulations A1 to A9 showed higher amounts of drug permeated through sclera were than those recorded for cornea experiments. Since the experiments were carried out using similar surface areas, these differences are clearly related to the higher permeability of sclera, which has a porous structure that allows drug diffusion either as free molecules or after being encapsulated into CD cavities.

Formulation A9 was the most accumulated in the sclera, again due to their highest solubilizing capacity.

To summarize, ex vivo permeability studies carried out in freshly bovine eyes confirmed the capability of our formulations to deliver nepafenac to the posterior segment of the eye via the scleral route.

4.2.7 Anti-inflammatory activity

Finally, Nevanac and the most promising formulations (A2, A3, A5, A8, A9), as well as their blanks, were selected to verify their anti-inflammatory activity and were compared. It is known that cytokines and prostaglandins play essential roles in eye inflammation. Here, the effect of these formulations on secretion levels of two pro-inflammatory mediators (interleukin 6, IL-6, and prostaglandin E2, PGE2) and one anti-inflammatory mediator (interleukin-1 receptor agonist, IL-1Ra) in macrophages after exposition to lipopolysaccharide (LPS) stimulation was investigated (**Figure 25**).

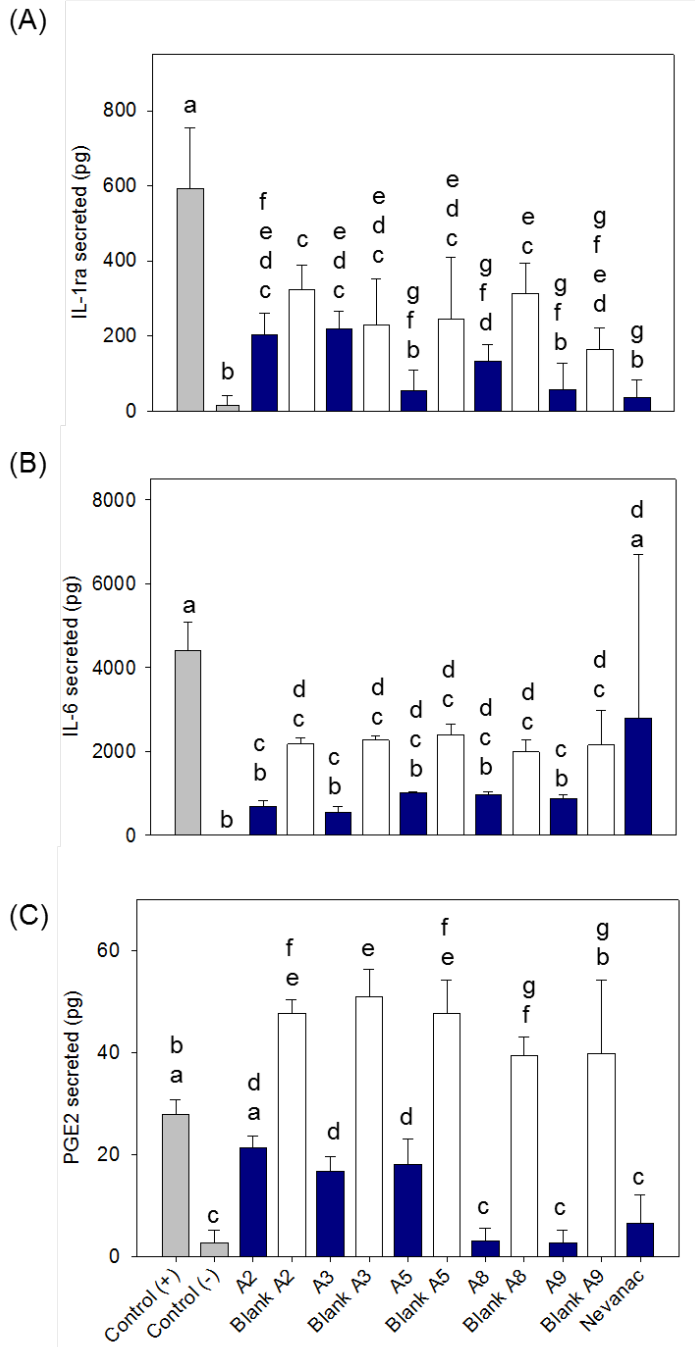


Figure 25. Effect of ophthalmic formulations on levels of (A) IL-1ra, (B) IL-6, and (C) prostaglandin E2 (PGE2) in macrophages. Negative controls refer to unstimulated cells (without lipopolysaccharide (LPS)); positive control refers to cells only stimulated with LPS. Same letters denote statistically homogeneous groups (ANOVA and multiple range test $p < 0.05$; $n = 3$).

Figure 25 compares nepafenac loaded formulations to their corresponding blank systems. Formulations A2, A3, A5, A8 and A9 containing aggregates successfully decreased the secretion of pro-inflammatory molecules (IL-6, PGE2) without altering the secretion of anti-inflammatory markers (IL-1ra), indicating a definite anti-inflammatory effect. Moreover, formulations A8 and A9 exhibited better results as anti-inflammatory systems, reaching IL-6 and PGE2 levels similar to non-LPS stimulated cells and showing superior anti-inflammatory capacity than the commercially available formulation Nevanac. These results are in line with other studies. Kern et al. (2007) found that treatment with nepafenac eye drops (0.3%) led to a remarkable inhibition of PGE2 levels at the retina in patients at an early stage diabetic retinopathy. Calles et al. (2016) measured changes in IL-6 levels after dexamethasone-loaded film exposure using an in vitro model of corneal inflammation and they found that inflamed cells exposed to the dexamethasone films reduced secretion of IL-6 production significantly compared to controls.

4.3 Natamycin micelles and poly(pseudo)rotaxanes

4.3.1 Micelles preparation and natamycin solubilization

Soluplus micelles in 0.9% NaCl aqueous medium were larger (70-90 nm) and more acid (\sim pH 4) than Pluronic P103 (20 nm; \sim pH 6). The zeta potential of both types of copolymer was similar, being slightly negative in all cases (**Table 10**). The concentration of each copolymer selected for this study was above the reported CMC values ($6.60 \cdot 10^{-8}$ M for Soluplus and $1.41 \cdot 10^{-4}$ M for Pluronic P103)(Alvarez-Rivera et al., 2016, Bernabeu et al., 2016, Bodratti & Alexandridis 2018).

Mixtures of 10% (w/v) Soluplus and 10% (w/v) Pluronic dispersions (1:4, 2:3, 3:2 and 4:1% v/v) in 0.9% NaCl showed intermediate pH values and larger micelles increasing Pluronic P103 proportion, suggesting the incorporation of PPO block of Pluronic P103 (EO17PO60EO17) inside Soluplus cores (**Table 13**). Also, Pluronic P103 is more hydrophobic (HLB= 9) (40) than Soluplus (HLB =16) (32). Since some studies reported that natamycin is more stable at pH 4 to 7 (Koontz & Marcy, 2003), formulations

were additionally prepared in buffer pH 6.4 (**Table 13**) to facilitate comparison of micelle properties.

Table 13. The pH, size and zeta potential of unloaded micelles of Soluplus and Pluronic P103 and their mixtures prepared at various volume ratios in 0.9% NaCl and pH 6.4 buffer.

0.9% NaCl				
Copolymer (%w/v)	pH	Diameter (nm)	PDI	Zeta potential (mV)
Soluplus (10 %)	3.34	90.0 ± 1.3	0.168 ± 0.010	-0.40 ± 0.19
Pluronic (10 %)	6.34	20.5 ± 0.6	0.238 ± 0.003	1.03 ± 0.47
Soluplus / Pluronic P103 (1:4)	4.67	129.6 ± 2.9	0.246 ± 0.019	-0.66 ± 0.20
Soluplus / Pluronic P103 (2:3)	3.89	131.0 ± 3.0	0.214 ± 0.011	-0.81 ± 0.08
Soluplus / Pluronic P103 (3:2)	3.70	121.7 ± 1.0	0.190 ± 0.017	-1.49 ± 0.46
Soluplus / Pluronic P103 (4:1)	3.52	110.7 ± 1.8	0.209 ± 0.008	-0.56 ± 0.41
Buffer pH 6.4				
Copolymer (%w/v)	pH	Diameter (nm)	PDI	Zeta potential (mV)
Soluplus (10 %)	6.08	102.8 ± 1.0	0.189 ± 0.018	-0.14 ± 0.36
Pluronic (10 %)	6.36	16.1 ± 0.4	0.226 ± 0.018	1.15 ± 0.28
Soluplus / Pluronic P103 (1:4)	6.49	150.8 ± 4.5	0.217 ± 0.011	0.48 ± 0.06
Soluplus / Pluronic P103 (2:3)	6.47	140.5 ± 0.7	0.176 ± 0.008	-0.02 ± 0.15
Soluplus / Pluronic P103	6.20	127.8 ± 0.9	0.171 ± 0.011	-0.12 ± 0.01

(3:2)				
Soluplus / Pluronic P103 (4:1)	6.48	114.7 ± 2.4	0.170 ± 0.011	-0.18 ± 0.13

The apparent solubility of natamycin in 0.9% NaCl (0% block copolymer) was $43.82 \pm 1.76 \mu\text{g/mL}$, which is consistent with previous values reported in the literature (Cevher et al., 2008). As was expected, increasing the concentration of copolymer in both mediums led to an increase in natamycin apparent solubility confirming the accommodation of natamycin into the nanomicelles (**Figures 26**).

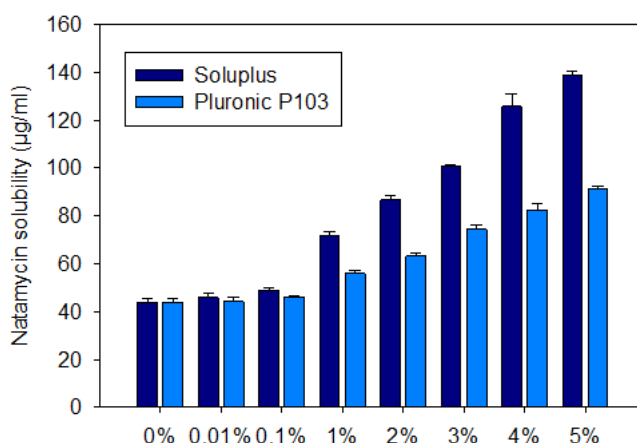


Figure 26. Apparent solubility of natamycin in Soluplus and Pluronic P 103 dispersions (0, 0.01, 0.1, 1, 2, 3, 4 and 5% w/v) prepared in 0.9% NaCl at 25°C.

Soluplus dispersions showed more significant apparent solubility enhancement ($138.6 \pm 1.9 \mu\text{g/mL}$ in Soluplus 5% w/v in 0.9% NaCl at 25°C) due to their large core (Bernabeu et al., 2016). Parameters used to quantify the solubilizing efficiency of Soluplus and Pluronic nanomicelles are summarized in **Tables 14 and 15**. The molar solubilization capacity (χ) was remarkably higher for Soluplus than Pluronic P103 micelles suggesting that more unimers are involved in micelle formation. Natamycin encapsulation occurred spontaneously and was thermodynamically more favorable (more negative ΔG) for Soluplus systems. Regarding the molar fraction of drug encapsulated into the micelle, Soluplus micelles (5% w/v) had approximately

70% of natamycin inside the micelles while Pluronic P103 (5% w/v) had only 50%.

Moreover, micelles stability against dilution was investigated. Only Pluronic P103 nanomicelles could be analyzed since Soluplus nanomicelles absorbed light in the same UV region as the drug and caused noise under the dilution with an aqueous medium (**Figure 27**).

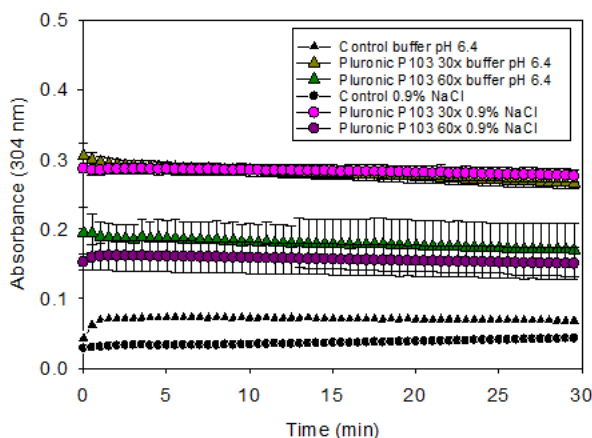


Figure 27. Modification of the absorbance of natamycin-loaded Pluronic P103 10%(w/v) nanomicelle formulations after 30-fold and 60-fold dilution in 0.9% NaCl or pH 6.4 buffer.

Nevertheless, this low Soluplus UV absorption did not interfere with drug solubility quantification in the apparent solubility studies since they disassemble in the ethanol-water medium. As shown in **Figure 27**, the absorbance of Pluronic P103 nanomicelle after strong dilution in 0.9% NaCl solution or pH 6.4 buffer, revealed a small initial decrease followed by a stable recovery due to the rapid rebalancing of the micelle-medium partition equilibrium.

Table 14. Parameters that characterize the capacity of Soluplus dispersions in 0.9% NaCl to solubilize natamycin estimated using Eqs. (3)–(7). (NAT: natamycin; χ : molar solubilization capacity; P: partition coefficient; PM: molar partition coefficient; ΔG : standard-free Gibbs energy of solubilization; mf: the molar fraction of drug encapsulated inside the micelle). *Data from solubility experiments carried out in pH 6.4 buffer.

Copolymer (% w/w)	Soluplus (M)	NAT (M)	NAT ($\mu\text{g/mL}$)	χ	P	PM	ΔG (KJ/mol)	mf
0.1	$0.87 \cdot 10^{-5}$	$0.71 \cdot 10^{-4}$	46.99	0.52	0.07	7869.6	-22227.0	0.06
1	$8.70 \cdot 10^{-5}$	$1.04 \cdot 10^{-4}$	69.31	0.44	0.58	6619.2	-21798.2	0.37
2	$1.74 \cdot 10^{-4}$	$1.26 \cdot 10^{-4}$	84.03	0.35	0.91	5233.1	-21216.1	0.48
3	$2.61 \cdot 10^{-4}$	$1.47 \cdot 10^{-4}$	97.93	0.31	1.23	4700.0	-20949.8	0.55
4	$3.48 \cdot 10^{-4}$	$1.84 \cdot 10^{-4}$	122.51	0.34	1.78	5131.2	-21167.3	0.64
5	$4.35 \cdot 10^{-4}$	$2.03 \cdot 10^{-4}$	135.23	0.31	2.07	4769.5	-20986.2	0.67
10	$8.70 \cdot 10^{-4}$	$2.98 \cdot 10^{-4}$	198.49	0.27	3.51	4038.0	-20573.7	0.78
10 (buffer)*	$8.70 \cdot 10^{-4}$	$3.96 \cdot 10^{-4}$	263.73	0.38	4.99	5743.2	-21446.5	0.83

Table 15. Parameters that characterize the capacity of Pluronic P103 dispersions in 0.9% NaCl to solubilize natamycin estimated using Eqs. (3)–(7). (NAT: natamycin; χ : molar solubilization capacity; P: partition coefficient; PM: molar partition coefficient; ΔG : standard-free Gibbs energy of solubilization; mf: the molar fraction of drug encapsulated inside the micelle). *Data from solubility experiments carried out in pH 6.4 buffer.

Copolymer (% w/w)	Pluronic P103 (M)	NAT(M)	NAT ($\mu\text{g/mL}$)	χ	P	PM	ΔG (KJ/mol)	mf
0.1	$0.20 \cdot 10^{-3}$	$0.70 \cdot 10^{-4}$	46.27	$5.59 \cdot 10^{-2}$	0.05	845.5	-16699.6	0.05
1	$2.02 \cdot 10^{-3}$	$0.84 \cdot 10^{-4}$	56.00	$9.59 \cdot 10^{-3}$	0.27	145.1	-12332.5	0.21
2	$4.04 \cdot 10^{-3}$	$0.95 \cdot 10^{-4}$	63.21	$7.40 \cdot 10^{-3}$	0.44	112.0	-11690.4	0.30
3	$6.06 \cdot 10^{-3}$	$1.12 \cdot 10^{-4}$	74.37	$7.71 \cdot 10^{-3}$	0.69	116.6	-11790.1	0.41
4	$8.08 \cdot 10^{-3}$	$1.24 \cdot 10^{-4}$	82.63	$7.31 \cdot 10^{-3}$	0.88	110.6	-11659.3	0.47
5	$1.01 \cdot 10^{-2}$	$1.37 \cdot 10^{-4}$	91.06	$7.10 \cdot 10^{-3}$	1.07	107.4	-11586.3	0.52

10	$2.02 \cdot 10^{-2}$	$2.16 \cdot 10^{-4}$	143.49	$7.45 \cdot 10^{-3}$	2.27	112.7	-11706.4	0.69
10 (buffer)*	$2.02 \cdot 10^{-2}$	$2.15 \cdot 10^{-4}$	143.39	$7.44 \cdot 10^{-3}$	2.26	112.6	-11704.0	0.69

Then, Soluplus (10% w/v) and Pluronic (10% w/v) were prepared and compared their solubilization capacity with those of the mixed micellar solutions (1:4, 2:3, 3:2, 4:1 vol/vol) in 0.9% NaCl and pH 6.4 buffer (**Figure 28**).

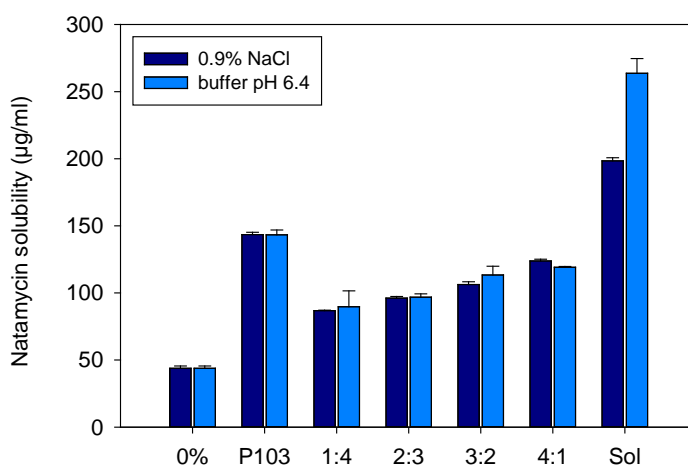


Figure 28. Apparent solubility of natamycin in micelle dispersions of 10% (w/v) of Soluplus and Pluronic P103 and their mixtures (Soluplus: Pluronic P103) prepared at various volume ratios in 0.9% NaCl and pH 6.4 buffer. Total copolymer concentration was 10% w/v in all cases.

As occurred before, Soluplus (10% w/v) micelles showed higher apparent solubility enhancement ($263.7 \pm 10.9 \mu\text{g/mL}$ in pH 6.4 buffer and $198.5 \pm 2.3 \mu\text{g/mL}$ in 0.9% NaCl medium). The apparent solubility of natamycin in the Soluplus/ Pluronic mixtures was in the ranges of 86.8 ± 0.3 to $123.8 \pm 1.3 \mu\text{g/mL}$ in 0.9% NaCl, and 89.7 ± 11.9 to $119.1 \pm 0.6 \mu\text{g/mL}$ in pH 6.4 buffer (Figure 15).

As the Pluronic P103 ratio increases, the solubilizing capacity decreases. The partition coefficients (P) for Soluplus/ Pluronic P103 1:4 and 4:1 (vol/vol) were in the ranges 0.98-1.05 and 1.72-1.82, respectively, which support the

hypothesis that Pluronic P103 takes up the core of Soluplus micelles and reduce the ability to harbor natamycin. Similar behavior was reported by Bernabeu et al. (2016) for mixed systems consisting of Soluplus and D- α -tocopheryl polyethylene glycol 1000 succinate (TPGS). They found that by increasing the ratio in Soluplus, the self-assembly of the Soluplus micelles was more complicated, the micelles became larger, and their ability to host paclitaxel decreased. In our case, as the variety we tested (Pluronic P103) is more hydrophobic than those evaluated in other studies (P105 and F127) (Zhang et al., 2017 and Ke et al., 2017), it could explain more severe effects on the properties of mixed micelles. For the following experiments, only Soluplus/ Pluronic P103 4:1 were tested as they are more similar in size to the pure Soluplus micelles (**Figure 29**).

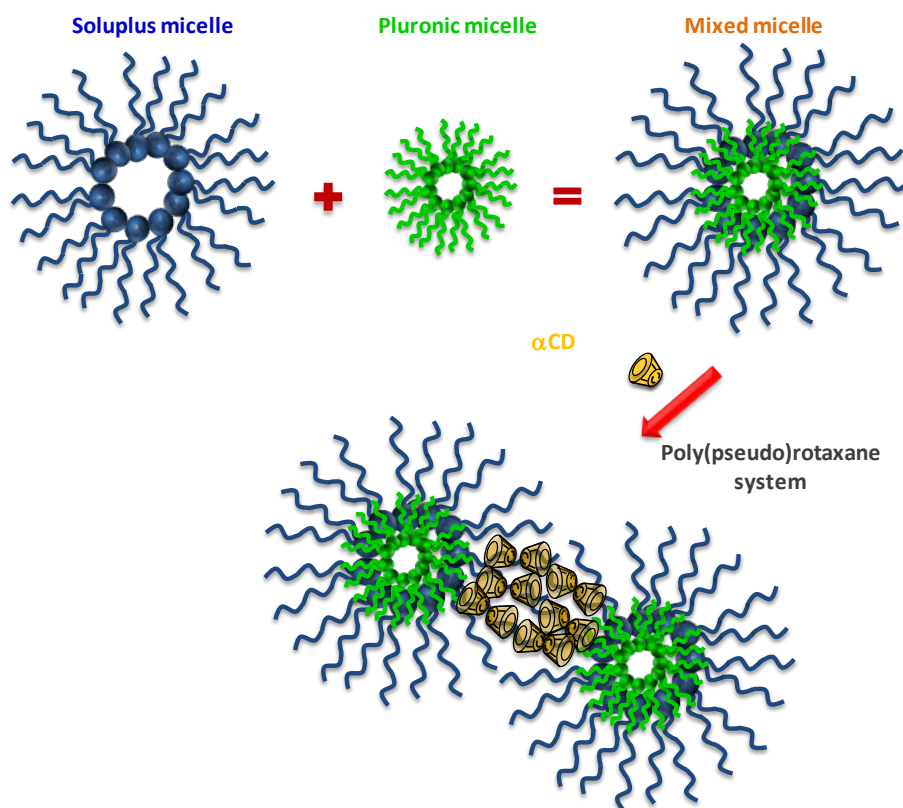


Figure 29. Schematic illustration of single and mixed nanomicelles formed by self-assembly of the amphiphilic block copolymers, and the CD-based poly(pseudo)rotaxanes.

4.3.2 Poly(pseudo)rotaxane formation

The ability of α -CD to form inclusion complexes with natamycin was firstly investigated. Then, the apparent solubility of natamycin in 5-10% (w/v) α -CD aqueous solutions was determined in 0.9% NaCl and pH 6.4 buffer (**Figure 30**).

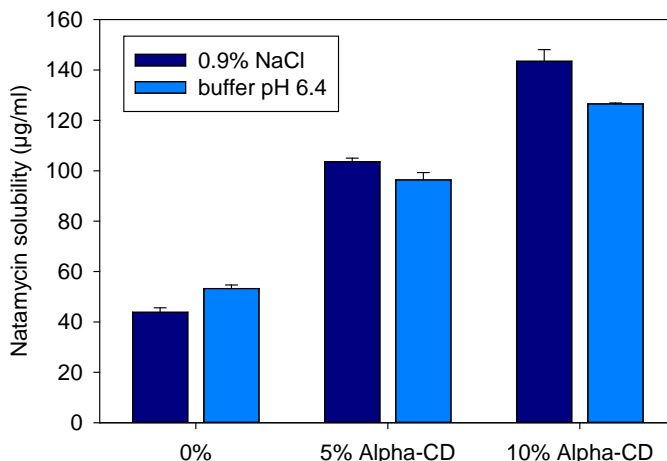


Figure 30. The apparent solubility of natamycin without α -CD and containing 5-10% (w/v) in 0.9% NaCl and pH 6.4 buffer at 25° C.

The apparent solubility of natamycin in 5% and 10% (w/v) α -CD aqueous solutions was 103.7 ± 1.4 µg/mL and 143.5 ± 4.6 µg/mL in 0.9% NaCl medium, and 96.4 ± 2.9 µg/mL and 126.6 ± 0.4 µg/mL in pH 6.4 buffer, respectively, showing results similar to Pluronic P103 micelles at the same concentrations but lower than those obtained from Soluplus micelles.

Based on these studies, 10% Soluplus, 10% Pluronic P103 and binary systems Soluplus 10%/Pluronic P103 10% (4:1 vol/vol) in aqueous 0.9% NaCl medium or pH 6.4 buffer were selected for poly(pseudo)rotaxane formation. Initially, transparent dispersions of Pluronic P103 and opalescent dispersions (Soluplus) were observed (**Figure 31A**). Then, the addition of α -CD solution to a final concentration of 10% and mixing with each copolymer, quickly led to turbid systems, which indicated the formation of poly(pseudo) rotaxane (**Figure 31B**). In each final dispersion of poly(pseudo) rotaxane, a concentration of natamycin of 120 µg/ml had been established, which is 3

times higher than the apparent solubility of the drug in water but less than the solubilization capacity of each component (copolymer/ α -CD) separately.

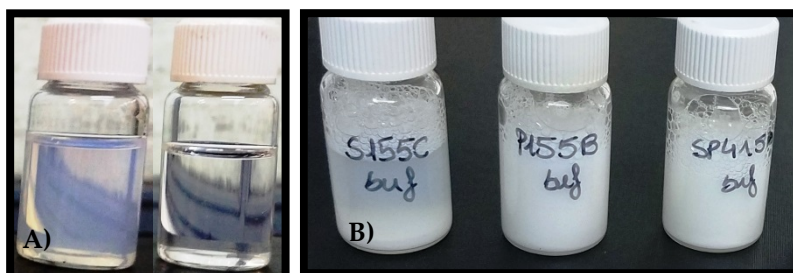


Figure 31. Evolution at 25° C of appearance of (A) Soluplus 10% (left) and Pluronic P103 10% (right) dispersions in 0.9% NaCl; (B) (Poly(pseudo)rotaxane formation after addition of 10 % α CD to Soluplus (left), Soluplus/Pluronic P103 in ratio (4:1) (in the middle) and Pluronic P103 dispersions (right) in pH 6.4 buffer after storage for 12h at room temperature.

4.3.3 Rheological properties

Poly(pseudo)rotaxane formation was also verified by rheological analysis of copolymer dispersions with and without α -CD (**Figure 32**).

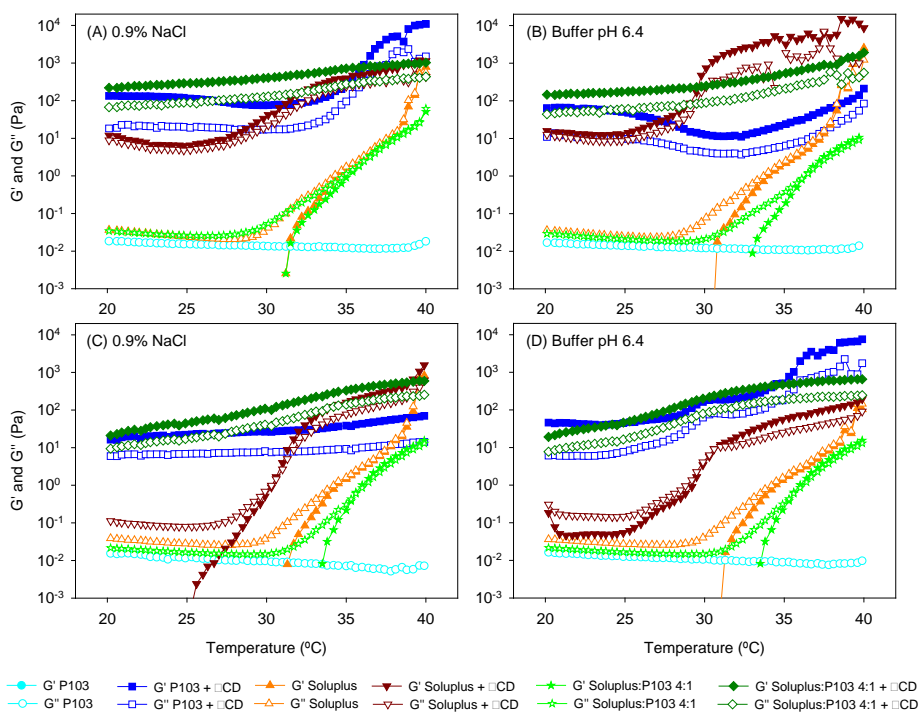


Figure 32. Evolution of the storage (G') and the loss (G'') moduli as a function of the temperature of (A, B) unloaded and (C, D) drug-loaded copolymer dispersions and their mixtures with and without α -CD poly(pseudo)rotaxanes in 0.9% NaCl (left) and pH 6.4 buffer (right). Total copolymer concentration was 10% w/v in all cases.

The addition of 10% (w/v) α -CD to copolymer dispersions produced variations in the rheological properties and sol-gel transition (**Figure 32**). Pluronic P103 10% (w/v) dispersions behaved as free-flowing liquid-like material. The values of storage modulus (G') were negligible and sol-to-gel transitions were not observed (G'' values remained constant in the temperature range tested). The addition of α -CD at 10% increased remarkable both G' and G'' , and G' became even more significant than G'' , due to the formation of supramolecular assemblies (Simões et al., 2015). Pluronic P103-based poly(pseudo)rotaxane system behaved as weak gels in the 20 to 40 °C range and the addition of natamycin did not cause significant changes in their viscoelastic behavior. Whereas Soluplus 10% w/v dispersions showed a sol-to-gel transition (Alvarez-Rivera et al., 2016 and Varela-Garcia et al., 2018), with values of both G' and G'' progressively increased with the temperature after 34 °C, suggesting a poorly-cooperative

hydrophobic-driven transition due to the different hydrophilicity of the blocks in Soluplus. Natamycin-loaded Soluplus and unloaded Soluplus dispersions showed differences suggesting that the addition of natamycin to Soluplus dispersions could alter the ability of Soluplus to form strong complexes with α -CD at 25 °C. Soluplus-based poly(pseudo)rotaxanes behaved as weak gels at 20 °C, with values of both G' and G'' increased above 30 °C. Compared to Soluplus dispersions, Soluplus-based poly(pseudo)rotaxanes showed more significant G' and G'' values at the temperature of the eye surface (37 °C).

To the best of our knowledge, this is the first time that the formation of poly(pseudo)rotaxane of mixed micelles has been investigated. In the case of Soluplus/P103 4:1 dispersions, a shift in the sol-to-gel transition was shown towards higher values (36.1 °C) compared to Soluplus solely dispersion excluding the unloaded system in NaCl 0.9%, which confirms that the self-assembly of Soluplus became distorted as hypothesized before, since Pluronic P103 accommodates in micelle core. After the addition of α -CD to the mixed micelles, the system behaved as a weak gel at 20 °C, and only a slight increase in their viscoelastic behavior was perceived during heating. Interestingly, the presence of natamycin slightly decreased both G' and G'' confirming our hypothesis that Pluronic P103 attenuated the effects of hosting natamycin in Soluplus cores due to the preferential threading of α -CDs along with Pluronic P103 in the mixed micelles. These results are in line with data obtained by (Segredo-Morales et al., 2018) after nuclear magnetic resonance diffusion studies of α -CD Pluronic F127.

4.3.4 HET-CAM assay

Preliminary screening of ocular irritancy of micelle or poly(pseudo)rotaxane dispersions were evaluated using the HET-CAM test (Alvarez-Rivera et al., 2016; McKenzie et al., 2015 and Abdelkader et al., 2012). All formulations were considered as non-irritants since they did not produce hemorrhage, lysis, or coagulation leading to an IS value of 0.0), as well as the negative control (0.9% NaCl) (**Figure 33**). Otherwise, the IS for the positive control (NaOH 0.1N) was 18.58. This behavior is in line with previously reported studies (Alvarez-Rivera et al., 2016 and Taveira et al., 2018).

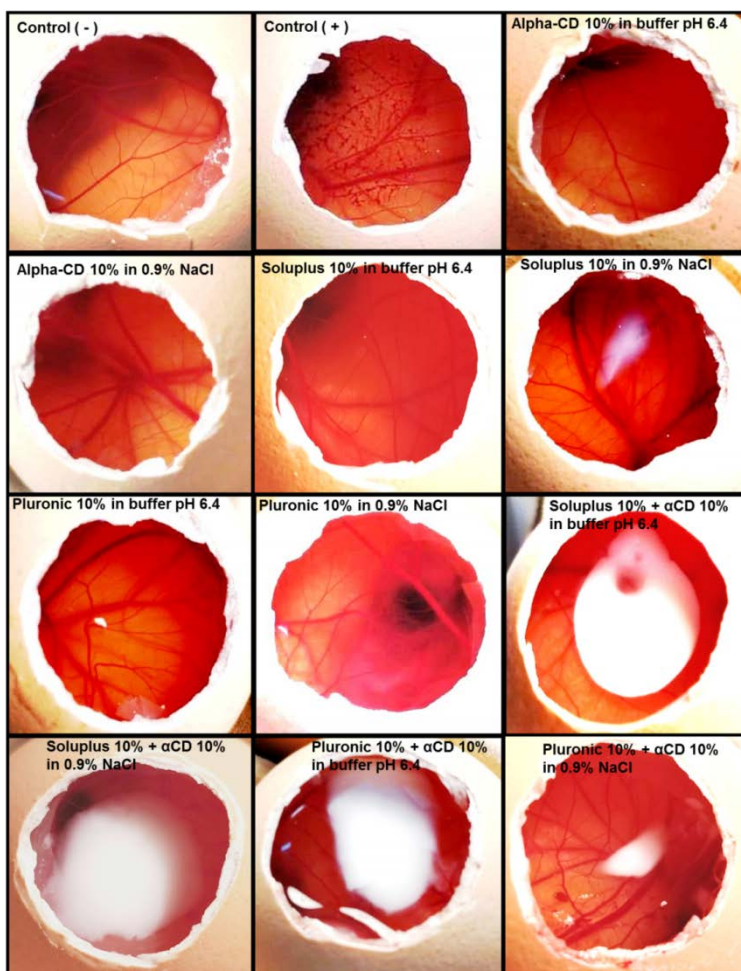


Figure 33. Photographs of HET-CAM tests of Soluplus and Pluronic P103 formulations. Negative and positive controls refer to 0.9% NaCl and 0.1 N NaOH, respectively.

4.3.5 Natamycin diffusion

In vitro natamycin diffusion from micelles and poly(pseudo)rotaxanes prepared in 0.9% NaCl and pH 6.4 buffer was investigated at 37° C under sink conditions using a large pore size membrane (0.45 μm) to calculate the potential of the formulations to control drug release. All dispersions showed sustained diffusion during 6h-test (**Figure 34**); nevertheless, faster diffusion was observed depending on the copolymer and the addition of α -CD.

Regarding micelles, Pluronic P103 10% w/v formulation showed faster diffusion ($46.45 \pm 1.41 \mu\text{g}/\text{cm}^2$ in 0.9% NaCl and $48.25 \pm 0.42 \mu\text{g}/\text{cm}^2$ in buffer pH 6.4 after 6 h), and then mixed micelles ($25.69 \pm 0.50 \mu\text{g}/\text{cm}^2$ in 0.9% NaCl and $42.25 \pm 1.72 \mu\text{g}/\text{cm}^2$ in buffer pH 6.4 after 6 h) and Soluplus micelles ($13.39 \pm 1.04 \mu\text{g}/\text{cm}^2$ in 0.9% NaCl and $20.13 \pm 0.95 \mu\text{g}/\text{cm}^2$ in buffer pH 6.4 after 6 h). The partition coefficient, P, for Soluplus /Pluronic P103 4:1 (vol/vol) was in the 1.72-1.82 range, higher than those recorded for pure Soluplus or Pluronic in separate, suggesting that there were more free drug molecules in the mixed micelles. However, diffusion of Soluplus/ Pluronic P103 4:1 (vol/vol) was slower than from Pluronic micelles, which agreed with the hypothesis that the smaller size and less compact structure of Pluronic P103 micelles and mixed micelles compared to those of Soluplus have an important role in the diffusion rate. However, other factors, for example, copolymer composition and drug-core interactions, may also affect the diffusion kinetics.

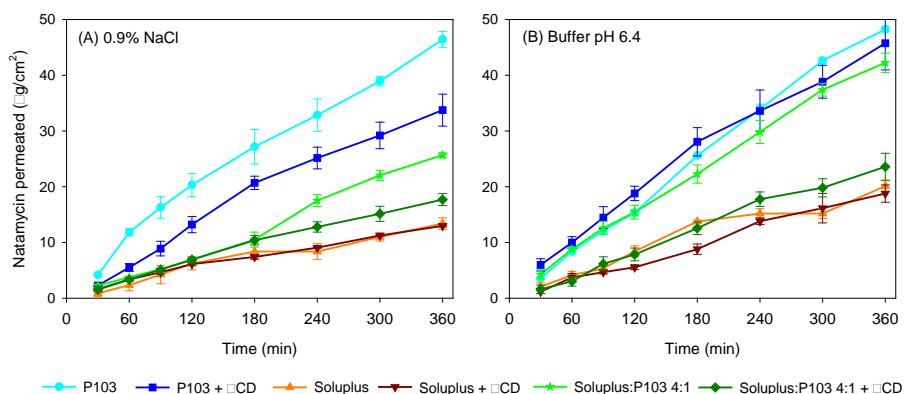


Figure 34. Natamycin diffusion test at 37 °C from Soluplus and Pluronic micelles, Soluplus: Pluronic P103 4:1 vol/vol mixed micelles, and poly(pseudo)rotaxanes in 0.9% NaCl (left) and pH 6.4 buffer (right). Total copolymer concentration was 10% w/v in all cases.

In the case of poly(pseudo)rotaxanes, also Pluronic P103 formulation showed the faster diffusion ($33.76 \pm 2.86 \mu\text{g}/\text{cm}^2$ in 0.9% NaCl and $45.76 \pm 4.79 \mu\text{g}/\text{cm}^2$ in pH 6.4 buffer), right after poly(pseudo)rotaxanes of mixed micelles ($17.71 \pm 1.08 \mu\text{g}/\text{cm}^2$ in 0.9% NaCl and $23.60 \pm 2.42 \mu\text{g}/\text{cm}^2$ in pH 6.4 buffer) and Soluplus-based poly(pseudo)rotaxanes ($12.99 \pm 0.19 \mu\text{g}/\text{cm}^2$ in 0.9% NaCl and $18.78 \pm 1.55 \mu\text{g}/\text{cm}^2$ in pH 6.4 buffer). The slow drug diffusion observed for poly(pseudo)rotaxanes is related to the formation of a more structured network with higher viscosity (Taveira et al., 2018) as detailed in their rheological analysis in section 4.3.3. Minor differences in

drug release between micelles and poly(pseudo)rotaxanes have been shown for carvedilol transdermal formulations, suggesting the increase in macroviscosity in our formulations might not directly lead to higher microviscosity (Alvarez-Lorenzo et al., 1999). Diffusion coefficients (D) of natamycin calculated following Eq.(6) are presented in **Table 16**.

Table 16. Natamycin diffusion coefficients from Soluplus and Pluronic micelles, Soluplus: Pluronic P103 4:1 vol/vol mixed micelles and poly(pseudo)rotaxanes in 0.9% NaCl and pH 6.4 buffer. Total copolymer concentration was 10% w/v. Results are expressed using mean value and, in parenthesis, standard deviation (n = 3).

Formulation	0.9% NaCl		Buffer pH 6.4	
	D x 10 ⁶ (cm ² /min)	R ²	D x 10 ⁶ (cm ² /min)	R ²
Pluronic P103 10%	49.46 (3.99)	0.992	65.14 (0.96)	0.992
Pluronic P103 + α CD 10%	32.66 (4.73)	0.990	50.30 (11.57)	0.990
Soluplus 10%	5.56 (1.62)	0.992	10.58 (0.53)	0.982
Soluplus 10% + α CD 10%	3.72 (0.24)	0.982	9.92 (2.38)	0.992
Soluplus /Pluronic P 103 (4:1)	18.31 (1.24)	0.998	45.68 (4.10)	0.989
Soluplus /Pluronic P 103 (4:1) + α CD 10%	8.21 (1.22)	0.970	16.14 (2.00)	0.996

Correlation coefficients (R^2) fitted to Higuchi's kinetics. Diffusion coefficients (D) were quite similar in formulations prepared in pH 6.4 buffer or 0.9% NaCl. Soluplus micelles displayed lower diffusion coefficients compared to Pluronic micelles, while the addition of α -CD to both Soluplus and Pluronic P103 micelles decreased diffusion coefficients (D). It should be noted that poly(pseudo)rotaxanes made from mixed micelles showed intermediate natamycin diffusion coefficients compared to those of Pluronic P103-based and Soluplus-based poly(pseudo)rotaxane suggesting that preparation of mixed micelles could be a useful approach to adjust drug release from poly(pseudo)rotaxanes.

4.3.6 Ex vivo permeation assay

Bovine corneal and scleral permeability tests were carried out by monitoring the amount of natamycin that diffused from micelles and poly(pseudo)rotaxanes (each formulation loaded with μg) towards fresh bovine cornea and sclera mounted in vertical (Franz) diffusion cells and using carbonate buffer pH 7.2 as the receptor medium (37 °C) as previously described in section 4.2.6 (**Figure 35**). Initial natamycin concentration was set to 120 $\mu\text{g}/\text{mL}$ for all formulations, which was almost 3 times larger than its apparent solubility in water and above the highest minimal inhibitory concentration (MIC90 = 64 $\mu\text{g}/\text{mL}$) reported for some fungi species (Sun et al., 2014).

In the case of cornea permeation test, the amount of natamycin in the receptor chamber was quite low (<0.01 $\mu\text{g}/\text{mL}$) and only quantifiable after 6 hours, suggesting that natamycin was mostly accumulated at the cornea and only a tiny portion of the drug molecules reached the receptor compartment.

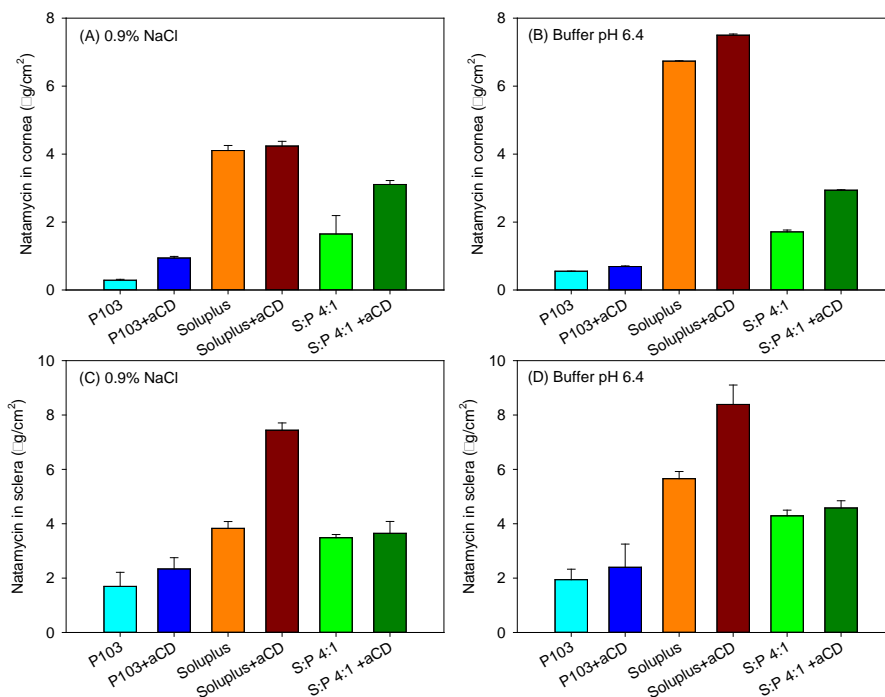


Figure 35. The amount of natamycin accumulated inside bovine cornea (A, B) and sclera (C, D) after addition of Soluplus and Pluronic micelles, Soluplus: Pluronic P103 4:1 vol/vol mixed micelles and their poly(pseudo)rotaxanes in 0.9% NaCl (left) and pH 6.4 buffer (right) after 6

hours experimentation. Total copolymer concentration was 10% w/v in all cases.

Unlike in vitro membranes where the membrane does not suppose a barrier to the diffusion of drug molecules, the cornea is considered an essential barrier to the permeability of any drug, leading in some studies to significant diffusion lag times owing to the flow of drug molecules into the cornea. A transcorneal penetration studies performed by Patil et al. (2017) with ex vivo rabbit eyes using Natacyn[®] (natamycin suspension diluted to 3 mg drug per ml) revealed low transcorneal flux ($0.14 \pm 0.1 \cdot 10^{-6}$ cm/s). Drug encapsulation into micelles and poly(pseudo)rotaxanes results in a rise in the apparent solubility of the drug, favoring the penetration of the drug due to an increase in the concentration gradient of the drug molecules in the tissues. Nevertheless, tissue and size restrictions of the encapsulated molecules may prevent passive diffusion of the drug. α -CD in polypseudorotaxanes could facilitate the entry of natamycin into the cornea; however, in this case, natamycin lipophilicity seems low enough (log P 1.1) to facilitate transcorneal penetration (Natamycin. PubChem). Though, sclera usually exhibits more significant permeability for most drugs compared to cornea due to its sclera larger surface area of absorption (Del Amo et al., 2017 and Loch et al., 2012), for comparative reasons, in the ex vivo studies the area available for diffusion was the same as for the cornea tests.

Accumulation of amounts of natamycin in both cornea and sclera were higher in poly(pseudo)rotaxanes than those accumulated at their corresponding micelles, disregarding the copolymer involved. Soluplus-based poly(pseudo)rotaxanes displayed greater corneal accumulation both in 0.9% NaCl or pH 6.4 buffer ($4.24 \pm 0.13 \mu\text{g}/\text{cm}^2$ and $7.50 \pm 0.03 \mu\text{g}/\text{cm}^2$, respectively)(**Figure 36A and B**). As expected, larger amounts of natamycin were accumulated in sclera (**Figure 36C and D**). Differently to cornea, natamycin was able to permeate through sclera and reached the receptor chamber. Small Pluronic P103 micelles showed faster permeation at the sclera than the larger Soluplus micelles and the mixed micelles (**Figure 36**).

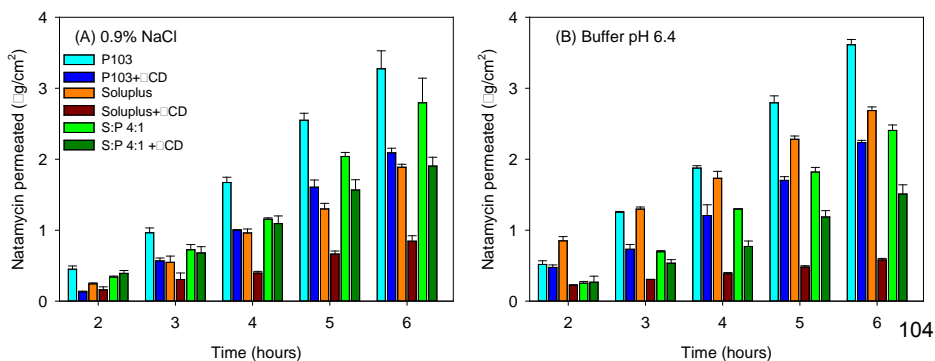


Figure 36. The amount of natamycin permeated through bovine sclera and measured in the receptor chamber as a function of time. Natamycin was formulated in Soluplus and Pluronic micelles, Soluplus: Pluronic P103 4:1 vol/vol mixed micelles, and their poly(pseudo)rotaxanes in 0.9% NaCl (left) and pH 6.4 buffer (right). Total copolymer concentration was 10% w/v in all cases.

Natamycin permeability through bovine sclera showed a lag time of 2 hours. After that, the cumulative amount of natamycin permeated per area showed a linear dependence on time. Permeability coefficient (P_{app}) of natamycin through bovine sclera was determined as the ratio of flux (J) and natamycin concentration in the donor phase and summarized in **Table 17**. In all cases, poly(pseudo)rotaxanes resulted in smaller P_{app} than the corresponding micelles (ANOVA and multiple range test; $F_{5,12df} = 90.73$; $p < 0.001$ in 0.9% NaCl; $F_{5,12df} = 377.62$; $p < 0.001$ in buffer pH 6.4). Soluplus poly(pseudo)rotaxane showed the lowest P_{app} of natamycin, while Pluronic P103 solely micelles showed the highest P_{app} .

Table 17. Transcleral steady-state flux (J) and permeability coefficients (P_{app}) estimated for natamycin formulated in Soluplus and Pluronic micelles, Soluplus: Pluronic P103 4:1 vol/vol mixed micelles, and poly(pseudo)rotaxanes in 0.9% NaCl and pH 6.4 buffer. Total copolymer concentration was 10% w/v. Results are expressed as mean values and, in parenthesis, their standard deviation (n = 3).

Formulation	0.9% NaCl		Buffer pH 6.4	
	J ($\mu\text{g}/(\text{cm}^2 \cdot \text{h})$)	$P_{app} \times 10^6$ (cm/s)	J ($\mu\text{g}/(\text{cm}^2 \cdot \text{h})$)	$P_{app} \times 10^6$ (cm/s)
Pluronic P103 10%	0.724 (0.042)	1.67 (0.09)	0.774 (0.032)	1.79 (0.07)
Pluronic P103 + α CD 10%	0.496 (0.023)	1.15 (0.05)	0.449 (0.012)	1.04 (0.03)
Soluplus 10%	0.403 (0.006)	0.93 (0.01)	0.466 (0.024)	1.08 (0.05)
Soluplus 10% + α CD 10%	0.174 (0.018)	0.40 (0.04)	0.090 (0.008)	0.27 (0.02)
Soluplus /Pluronic P 103 (4:1)	0.623 (0.065)	1.44 (0.15)	0.543 (0.021)	1.26 (0.05)
Soluplus /Pluronic P 103 (4:1) + α CD 10%	0.391 (0.023)	0.91 (0.05)	0.313 (0.016)	0.73 (0.04)

5 Summary and conclusions

This research project was focused on the design of various CD-based nanocarriers at both macro-and nano-scale and evaluation of their suitability as delivery systems for hydrophobic drugs. First, a deep understanding of complex formation and strategies to enhance its solubility and aggregation is essential before designing successful cyclodextrin-based eye drop formulations with the capacity to deliver drugs to the anterior or posterior segment of the eye. Eye drops containing a mixture of γ -CD/ HP β -CD complexes were developed for nepafenac delivery. Furthermore, encapsulation of natamycin into Soluplus and Pluronic P103 nanomicelles and poly(pseudo)rotaxanes was carried out and they have proven to be suitable for controlled release of poorly soluble drugs. Permeability experiments confirmed the capability of CDs to increase drug bioavailability through bovine cornea or sclera with no negative impact on biocompatibility.

The main observations in this dissertation are:

1. Combination of γ -CD and HP β -CD and addition of various hydrophilic polymers (such as PVA, CMC, tyloxapol or PVP) improved nepafenac solubility and aggregates formation. HP β -CD performed best in terms of solubilization, while γ -CD performed best in terms of enhancing aggregate formation. Any synergistic effect on solubility was found using mixtures of γ -CD and HP β -CD. Complex formation was confirmed by phase solubility analysis, DSC, FT-IR and $^1\text{H-NMR}$ studies. DSC studies suggested that as a minimum, 8% (w/v) HP β -CD was needed for complex formation when using 15% (w/v) γ -CD.

2. Nine nepafenac aggregate formulations, containing a mixture of γ -CD/HP β -CD complexes, eye drop vehicle and various hydrophilic polymers, were found suitable for ocular administration. They were non-irritating (HET-CAM assay), cytocompatible with fibroblasts and with suitable features for topical instillation into the eye. The formulation containing CMC, PVA and MC exhibited the highest retention in ex vivo bovine sclera and better in vitro anti-inflammatory efficacy in LPS-stimulated THP-1 human monocytes compared to commercial product Nevanac (3 mg/mL).

3. Soluplus and Pluronic P103 micelles and poly(pseudo)rotaxanes and their corresponding mixtures in ratio 4:1 were able to encapsulate natamycin. Soluplus micelles led to the highest increase at the apparent solubility of natamycin. The addition of α -CD to the copolymer dispersions caused remarkable changes in the rheological properties and sol-gel transition, increasing both G' and G'' values. The increment in the apparent macroviscosity of the poly(pseudo)rotaxanes could be useful to increase its retention at the ocular surface. However, they led to a decrease in drug diffusion, especially in the case of the mixed micelles system.

4. As far as we know, this is the first time that the formation of poly(pseudo)rotaxanes using mixed micelles has been investigated. It is interesting to note that mixed micelles of Soluplus and Pluronic showed a noteworthy increase in the micelle size, suggesting that the PPO block of Pluronic P103 accommodates inside the Soluplus cores, and as a result led to lower solubilization capability compared to Soluplus micelles alone.

5. To summarize, our results suggested that formulations of ternary systems, drug/ CD/ polymers, can be prepared with without complication to lead to aggregates formation. Although further investigations should be completed so as to evaluate its feasibility in vivo, they may signify an alternative to treat ocular diseases at the back of the eye. Moreover, after preparing and having tested single micelles and poly(pseudo)rotaxanes as well as mixed micelles and mixed poly(pseudo)rotaxanes, the poly(pseudo)rotaxanes of mixed micelles were pointed out as suitable tools for the controlled release of poorly soluble drugs since they permit the modification of features disclosed by each copolymer system in a separate way.

References

- Achouri, D., Alhanout, K., Piccerelle, P., & Andrieu, V. (2013). Recent advances in ocular drug delivery. *Drug Dev Ind Pharm*, 39(11), 1599-1617. doi:10.3109/03639045.2012.736515.
- Akhter, S., Anwar, M., Siddiqui, M. A., Ahmad, I., Ahmad, J., Ahmad, M. Z., Bhatnagar, A., Ahmad, F. J. (2016). Improving the topical ocular pharmacokinetics of an immunosuppressant agent with mucoadhesive nanoemulsions: Formulation development, in-vitro and in-vivo studies. *Colloids Surf B Biointerfaces*, 148, 19-29. doi:10.1016/j.colsurfb.2016.08.048.
- Ako-Adounvo, A. M., Nagarwal, R. C., Oliveira, L., Boddu, S. H., Wang, X. S., Dey, S., Karla, P. K. (2014). Recent patents on ophthalmic nanoformulations and therapeutic implications. *Recent Pat Drug Deliv Formul*, 8(3), 193-201. doi:10.2174/1872211308666140926112000.
- Aktaş, Y., Unlü, N., Orhan, M., Irkeç, M., Hincal, A. A. (2003). Influence of hydroxypropyl beta-cyclodextrin on the corneal permeation of pilocarpine. *Drug Dev Ind Pharm*, 29(2), 223-230. doi:10.1081/ddc-120016730.
- Ali, J., Fazil, M., Qumbar, M., Khan, N., Ali, A. (2016). Colloidal drug delivery system: amplify the ocular delivery. *Drug Deliv*, 23(3), 710-726. doi:10.3109/10717544.2014.923065.
- Almeida, H., Amaral, M. H., Lobão, P., Silva, A. C., Lobo, J. M. (2014). Applications of polymeric and lipid nanoparticles in ophthalmic pharmaceutical formulations: present and future considerations. *J Pharm Pharm Sci*, 17(3), 278-293. doi:10.18433/j3dp43.
- Almeida, H., Lobão, P., Frigerio, C., Fonseca, J., Silva, R., Quaresma, P., Lobo, J.M.S. Amaral, M. H. (2016). Development of mucoadhesive and thermosensitive eyedrops to improve the ophthalmic bioavailability of ibuprofen. *J Drug Deliv Sci Tec*, 35, 69-80. doi:https://doi.org/10.1016/j.jddst.2016.04.010.
- Alvarez-Lorenzo, C., Gómez-Amoza, J. L., Martínez-Pacheco, R., Souto, C., Concheiro, A. (1999). Microviscosity of hydroxypropylcellulose gels as a basis for prediction of drug diffusion rates. *Int J Pharm*, 180(1), 91-103. doi:10.1016/s0378-5173(98)00409-8.
- Alvarez-Lorenzo, C., Yañez, F., Barreiro-Iglesias, R., Concheiro, A. (2006). Imprinted soft contact lenses as norfloxacin delivery systems. *J Control Release*, 113(3), 236-244. doi:10.1016/j.jconrel.2006.05.003.

Alvarez-Rivera, F., Fernández-Villanueva, D., Concheiro, A., Alvarez-Lorenzo, C. (2016). α -Lipoic Acid in Soluplus® Polymeric Nanomicelles for Ocular Treatment of Diabetes-Associated Corneal Diseases. *J Pharm Sci*, 105(9), 2855-2863. doi:10.1016/j.xphs.2016.03.006.

Alvarez-Rivera, F., Serro, A. P., Silva, D., Concheiro, A., Alvarez-Lorenzo, C. (2019). Hydrogels for diabetic eyes: Naltrexone loading, release profiles and cornea penetration. *Mater Sci Eng C Mater Biol Appl*, 105, 110092. doi:10.1016/j.msec.2019.110092.

Ambati, J., Canakis, C. S., Miller, J. W., Gragoudas, E. S., Edwards, A., Weissgold, D. J., Kim, I., Delori, F. C., Adamis, A. P. (2000). Diffusion of high molecular weight compounds through sclera. *Invest Ophthalmol Vis Sci*, 41(5), 1181-1185.

Awwad, S., Mohamed Ahmed, A. H. A., Sharma, G., Heng, J. S., Khaw, P. T., Brocchini, S., Lockwood, A. (2017). Principles of pharmacology in the eye. *Br J Pharmacol*, 174(23), 4205-4223. doi:10.1111/bph.14024.

Bachu, R. D., Chowdhury, P., Al-Saedi, Z. H. F., Karla, P. K., Boddu, S. H. S. (2018). Ocular Drug Delivery Barriers-Role of Nanocarriers in the Treatment of Anterior Segment Ocular Diseases. *Pharmaceutics*, 10(1). doi:10.3390/pharmaceutics10010028.

Barar, J., Javadzadeh, A. R., Omid, Y. (2008). Ocular novel drug delivery: impacts of membranes and barriers. *Expert Opin Drug Deliv*, 5(5), 567-581. doi:10.1517/17425247.5.5.567.

Bassi da Silva, J., Ferreira, S. B. S., de Freitas, O., Bruschi, M. L. (2017). A critical review about methodologies for the analysis of mucoadhesive properties of drug delivery systems. *Drug Dev Ind Pharm*, 43(7), 1053-1070. doi:10.1080/03639045.2017.1294600.

Benedetto, D. A., Shah, D. O., Kaufman, H. E. (1975). The instilled fluid dynamics and surface chemistry of polymers in the precocular tear film. *Invest Ophthalmol*, 14(12), 887-902.

Bernabeu, E., Gonzalez, L., Cagel, M., Gergic, E. P., Moretton, M. A., Chiappetta, D. A. (2016). Novel Soluplus®-TPGS mixed micelles for encapsulation of paclitaxel with enhanced in vitro cytotoxicity on breast and ovarian cancer cell lines. *Colloids Surf B Biointerfaces*, 140, 403-411. doi:10.1016/j.colsurfb.2016.01.003.

Bhattacharjee, A., Das, P. J., Adhikari, P., Marbaniang, D., Pal, P., Ray, S., Mazumder, B. (2019). Novel drug delivery systems for ocular therapy: With special reference to liposomal ocular delivery. *Eur J Ophthalmol*, 29(1), 113-126. doi:10.1177/1120672118769776.

Biro, T., Aigner. (2019). Current Approaches to Use Cyclodextrins and Mucoadhesive Polymers in Ocular Drug Delivery—A Mini-Review. *Sci Pharm*, 87, 15. doi:10.3390/scipharm87030015.

Bodratti, A. M., Alexandridis, P. (2018). Formulation of Poloxamers for Drug Delivery. *J Funct Biomater*, 9(1), 11. doi:10.3390/jfb9010011.

Borba, P. A. A., Pinotti, M., de Campos, C. E. M., Pezzini, B. R., Stulzer, H. K. (2016). Sodium alginate as a potential carrier in solid dispersion formulations to enhance dissolution rate and apparent water solubility of BCS II drugs. *Carbohydr Polym*, 137, 350-359. doi:10.1016/j.carbpol.2015.10.070.

Bourne, R. R. A., Flaxman, S. R., Braithwaite, T., Cicinelli, M. V., Das, A., Jonas, J. B., J. B., Keeffe, J., Kempen, J. H., Leasher, J., Limburg, H., Naidoo, K., Pesudovs, K., Resnikoff, S., Silvester, A., Stevens, G. A., Tahhan, N., Wong, T. Y., Taylor, H. R., Vision Loss Expert Group. (2017). Magnitude, temporal trends, and projections of the global prevalence of blindness and distance and near vision impairment: a systematic review and meta-analysis. *Lancet Glob Health*, 5(9), e888-e897. doi:10.1016/s2214-109x(17)30293-0.

Brako, F., Thorogate, R., Mahalingam, S., Raimi-Abraham, B., Craig, D. Q. M., Edirisinghe, M. (2018). Mucoadhesion of Progesterone-Loaded Drug Delivery Nanofiber Constructs. *ACS Appl Mater Interfaces*, 10(16), 13381-13389. doi:10.1021/acsami.8b03329.

Bravo-Osuna, I., Andrés-Guerrero, V., Pastoriza Abal, P., Molina-Martínez, I. T., Herrero-Vanrell, R. (2016). Pharmaceutical microscale and nanoscale approaches for efficient treatment of ocular diseases. *Drug Deliv Transl Res*, 6(6), 686-707. doi:10.1007/s13346-016-0336-5.

Brewster, M. E., Loftsson, T. (2007). Cyclodextrins as pharmaceutical solubilizers. *Adv Drug Deliv Rev*, 59(7), 645-666. doi:10.1016/j.addr.2007.05.012.

Calles, J. A., López-García, A., Vallés, E. M., Palma, S. D., Diebold, Y. (2016). Preliminary characterization of dexamethasone-loaded cross-linked hyaluronic acid films for topical ocular therapy. *Int J Pharm*, 509(1-2), 237-243. doi:10.1016/j.ijpharm.2016.05.054.

Campaña-Seoane, M., Peleteiro, A., Laguna, R., Otero-Espinar, F. J. (2014). Bioadhesive emulsions for control release of progesterone resistant to vaginal fluids clearance. *Int J Pharm*, 477(1-2), 495-505. doi:10.1016/j.ijpharm.2014.10.066.

Cevher, E., Sensoy, D., Zloh, M., Mülazimoğlu, L. (2008). Preparation and characterisation of natamycin: gamma-cyclodextrin inclusion complex and its evaluation in vaginal mucoadhesive formulations. *J Pharm Sci*, 97(10), 4319-4335. doi:10.1002/jps.21312.

Challa, R., Ahuja, A., Ali, J., Khar, R. K. (2005). Cyclodextrins in drug delivery: an updated review. *AAPS PharmSciTech*, 6(2), E329-357. doi:10.1208/pt060243.

Chastain, J. E., Sanders, M. E., Curtis, M. A., Chemuturi, N. V., Gadd, M. E., Kapin, M. A., Markwardt, K. L., Dahlin, D. C. (2016). Distribution of topical ocular nepafenac and its active metabolite amfenac to the posterior segment of the eye. *Exp Eye Res*, 145, 58-67. doi:10.1016/j.exer.2015.10.009.

Chaudhari, P., Ghate, V. M., Lewis, S. A. (2019). Supramolecular cyclodextrin complex: Diversity, safety, and applications in ocular therapeutics. *Exp Eye Res*, 189, 107829. doi:10.1016/j.exer.2019.107829.

Chen, C. W., Yeh, M. K., Shiau, C. Y., Chiang, C. H., Lu, D. W. (2013). Efficient downregulation of VEGF in retinal pigment epithelial cells by integrin ligand-labeled liposome-mediated siRNA delivery. *Int J Nanomedicine*, 8, 2613-2627. doi:10.2147/ijn.s39622.

Cholkar, K., Dasari, S., Pal, D., Mitra, A. (2013). Eye: Anatomy, physiology and barriers to drug delivery. *Ocular Transporters and Receptors: Their Role in Drug Delivery*, 1-36. doi:10.1533/9781908818317.1.

Cholkar, K., Vadlapudi, A. D., Dasari, S., Mitra, A. (2014). *Ocular Drug Delivery* (pp. 219-263).

Chou, T. Y., Hong, B. Y. (2014). Ganciclovir ophthalmic gel 0.15% for the treatment of acute herpetic keratitis: background, effectiveness, tolerability, safety, and future applications. *Ther Clin Risk Manag*, 10, 665-681. doi:10.2147/tcrm.s58242.

Cirri, M., Maestrelli, F., Corti, G., Furlanetto, S., Mura, P. (2006). Simultaneous effect of cyclodextrin complexation, pH, and hydrophilic polymers on naproxen solubilization. *J Pharm Biomed Anal*, 42(1), 126-131. doi:10.1016/j.jpba.2005.11.029.

Conceicao, J., Adeoye, O., Cabral-Marques, H. M., Lobo, J. M. S. (2018). Cyclodextrins as Drug Carriers in Pharmaceutical Technology: The State of the Art. *Curr Pharm Des*, 24(13), 1405-1433. doi:10.2174/1381612824666171218125431.

Connors, K. A. (1997). The Stability of Cyclodextrin Complexes in Solution. *Chem Rev*, 97(5), 1325-1358. doi:10.1021/cr960371r.

Del Amo, E. M., Rimpelä, A. K., Heikkinen, E., Kari, O. K., Ramsay, E., Lajunen, T., Schmitt, M., Pelkonen, L., Bhattacharya, M., Richardson, D., Subrizi, A., Turunen, T., Reinisalo, M., Itkonen, J., Toropainen, E., Casteleijn, M., Kidron, H., Antopolsky, M., Vellonen, K. S., Ruponen, M., Urtti, A. (2017). Pharmacokinetic aspects of retinal drug delivery. *Prog Retin Eye Res*, 57, 134-185. doi:10.1016/j.preteyeres.2016.12.001.

Del Valle, E. M. M. (2004). Cyclodextrins and their uses: a review. *Process Biochem*, 39(9), 1033-1046. doi:[https://doi.org/10.1016/S0032-9592\(03\)00258-9](https://doi.org/10.1016/S0032-9592(03)00258-9).

Dubald, M., Bourgeois, S., Andrieu, V., Fessi, H. (2018). Ophthalmic Drug Delivery Systems for Antibiotherapy-A Review. *Pharmaceutics*, 10(1). doi:10.3390/pharmaceutics10010010.

Dubashynskaya, N., Poshina, D., Raik, S., Urtti, A., Skorik, Y. A. (2019). Polysaccharides in Ocular Drug Delivery. *Pharmaceutics*, 12(1). doi:10.3390/pharmaceutics12010022.

European Patent EP2937076A1. Eye drops containing prostaglandin and tyloxapol. Available from: <https://patents.google.com/patent/EP2937076A1/en>. Accessed: March 2020.

Eye physiology. Available from: <https://www.ncbi.nlm.nih.gov/books/NBK470322/>. Accessed: March 2020.

Fathi, M., Barar, J., Aghanejad, A., Omidi, Y. (2015). Hydrogels for ocular drug delivery and tissue engineering. *Bioimpacts*, 5(4), 159-164. doi:10.15171/bi.2015.31.

Fernández-Ferreiro, A., Santiago-Varela, M., Gil-Martínez, M., Parada, T. G., Pardo, M., González-Barcia, M., Piñeiro-Ces, A., Rodríguez-Ares, M. T., Blanco-Mendez, J., Lamas, M. J., & Otero-Espinar, F. J. (2015). Ocular safety comparison of non-steroidal anti-inflammatory eye drops used in pseudophakic cystoid macular edema prevention. *Int J Pharm*, 495(2), 680-691. doi:10.1016/j.ijpharm.2015.09.058.

Flaxman, S. R., Bourne, R. R. A., Resnikoff, S., Ackland, P., Braithwaite, T., Cicinelli, M. V., Das, A., Jonas, J. B., Keeffe, J., Kempen, J. H., Leasher, J., Limburg, H., Naidoo, K., Pesudovs, K., Silvester, A., Stevens, G. A., Tahhan, N., Wong, T. Y., Taylor, H.R (2017). Global causes of blindness and distance vision impairment 1990-2020: a systematic review and meta-analysis. *Lancet Glob Health*, 5(12), e1221-e1234. doi:10.1016/s2214-109x(17)30393-5.

Fricke, T. R., Tahhan, N., Resnikoff, S., Papas, E., Burnett, A., Ho, S. M., Naduvilath, T., Naidoo, K. S. (2018). Global Prevalence of Presbyopia and Vision Impairment from Uncorrected Presbyopia: Systematic Review, Meta-analysis, and Modelling. *Ophthalmology*, 125(10), 1492-1499. doi:10.1016/j.optha.2018.04.013. Vision Lost Expert Group

Gajra, B., Pandya, S., Vidyasagar, G., Rabari, H., Dedania, R., Rao, S. (2011). Poly vinyl alcohol Hydrogel and its Pharmaceutical and Biomedical Applications: A Review. *Int J Pharm Sci Res*, 4, 20-26.

Gaudana, R., Jwala, J., Boddu, S. H., Mitra, A. K. (2009). Recent perspectives in ocular drug delivery. *Pharm Res*, 26(5), 1197-1216. doi:10.1007/s11095-008-9694-0.

Gaudana, R., Ananthula, H. K., Parenky, A., Mitra, A. K. (2010). Ocular drug delivery. *AAPS J*, 12(3), 348-360. doi:10.1208/s12248-010-9183-3.

Geroski, D. H., Edelhauser, H. F. (2001). Transscleral drug delivery for posterior segment disease. *Adv Drug Deliv Rev*, 52(1), 37-48. doi:10.1016/s0169-409x(01)00193-4.

Gipson, I. K., Argüeso, P. (2003). Role of mucins in the function of the corneal and conjunctival epithelia. *Int Rev Cytol*, 231, 1-49. doi:10.1016/s0074-7696(03)31001-0.

Godínez, L. A., Schwartz, L., Criss, C. M., Kaifer, A. E. (1997). Thermodynamic Studies on the Cyclodextrin Complexation of Aromatic and Aliphatic Guests in Water and Water-Urea Mixtures. Experimental Evidence for the Interaction of Urea with Arene Surfaces. *J Phys Chem B*, 101(17), 3376-3380. doi:10.1021/jp970359i.

Goswami, S., Sarkar, M. (2018). Fluorescence, FTIR and ¹H NMR studies of the inclusion complexes of the painkiller lornoxicam with β-, γ-cyclodextrins and their hydroxy propyl derivatives in aqueous solutions at different pHs and in the solid state. *New J Chem*, 42(18), 15146-15156. doi:10.1039/C8NJ03093F.

Greaves, J. L., Wilson, C. G. (1993). Treatment of diseases of the eye with mucoadhesive delivery systems. *Adv Drug Deliv Rev*, 11(3), 349-383. doi:https://doi.org/10.1016/0169-409X(93)90016-W.

Grimaudo, M. A., Pescina, S., Padula, C., Santi, P., Concheiro, A., Alvarez-Lorenzo, C., Nicoli, S. (2018). Poloxamer 407/TPGS Mixed Micelles as Promising Carriers for Cyclosporine Ocular Delivery. *Mol Pharm*, 15(2), 571-584. doi:10.1021/acs.molpharmaceut.7b00939.

Gupta, H., Aqil, M., Khar, R. K., Ali, A., Bhatnagar, A., Mittal, G. (2015). An alternative in situ gel-formulation of levofloxacin eye drops for prolong ocular retention. *J Pharm Bioallied Sci*, 7(1), 9-14. doi:10.4103/0975-7406.149810.

Guter, M., Breunig, M. (2017). Hyaluronan as a promising excipient for ocular drug delivery. *Eur J Pharm Biopharm*, 113, 34-49. doi:10.1016/j.ejpb.2016.11.035.

Harada, A., Li, J., Kamachi, M. (1993). Preparation and properties of inclusion complexes of polyethylene glycol with .alpha.-cyclodextrin. *Macromolecules*, 26(21), 5698-5703. doi:10.1021/ma00073a026.

Higuchi T, Connors KA (1965) Phase solubility techniques. *Adv. Anal. Chem. Instrum.* 4: 117–122.

Hiratani, H., Alvarez-Lorenzo, C. (2002). Timolol uptake and release by imprinted soft contact lenses made of N,N-diethylacrylamide and methacrylic acid. *J Control Release*, 83(2), 223-230. doi:10.1016/s0168-3659(02)00213-4.

Hoare, T. R., Kohane, D. S. (2008). Hydrogels in drug delivery: Progress and challenges. *Polymer*, 49(8), 1993-2007. doi:https://doi.org/10.1016/j.polymer.2008.01.027.

Huang, W.-C., Cheng, F., Wang, Y.-J., Chen, C.-C., Hu, T.-L., Yin, S.-C., Liu., C.-P., Yu., N.-C., Huang., K.-K., Lin, M.-N. (2019). A corneal-penetrating eye drop formulation for enhanced therapeutic efficacy of soft corticosteroids against anterior uveitis. *J Drug Deliv Sci Tec*, 54, 101341. doi:https://doi.org/10.1016/j.jddst.2019.101341.

Hughes, P. M., Olejnik, O., Chang-Lin, J. E., Wilson, C. G. (2005). Topical and systemic drug delivery to the posterior segments. *Adv Drug Deliv Rev*, 57(14), 2010-2032. doi:10.1016/j.addr.2005.09.004.

Ivarsson, D., Wahlgren, M. (2012). Comparison of in vitro methods of measuring mucoadhesion: ellipsometry, tensile strength and rheological measurements. *Colloids Surf B Biointerfaces*, 92, 353-359. doi:10.1016/j.colsurfb.2011.12.020.

Jacob, S., Nair, A. B. (2018). Cyclodextrin complexes: Perspective from drug delivery and formulation. *Drug Dev Res*, 79(5), 201-217. doi:10.1002/ddr.21452.

Jambhekar, S. S., Breen, P. (2016). Cyclodextrins in pharmaceutical formulations I: structure and physicochemical properties, formation of complexes, and types of complex. *Drug Discov Today*, 21(2), 356-362. doi:10.1016/j.drudis.2015.11.017.

Jansook, P., Loftsson, T. (2009). CDs as solubilizers: effects of excipients and competing drugs. *Int J Pharm*, 379(1), 32-40. doi:10.1016/j.ijpharm.2009.06.005.

Jansook, P., Ritthidej, G. C., Ueda, H., Stefansson, E., Loftsson, T. (2010). γ CD/HPyCD mixtures as solubilizer: solid-state characterization and sample dexamethasone eye drop suspension. *J Pharm Pharm Sci*, 13(3), 336-350.

Jansook, P., Pichayakorn, W., Muankaew, C., Loftsson, T. (2016). Cyclodextrin-ploxamer aggregates as nanocarriers in eye drop formulations: dexamethasone and amphotericin B. *Drug Dev Ind Pharm*, 42(9), 1446-1454. doi:10.3109/03639045.2016.1141932.

Jansook, P., Ogawa, N., Loftsson, T. (2018). Cyclodextrins: structure, physicochemical properties and pharmaceutical applications. *Int J Pharm*, 535(1-2), 272-284. doi:10.1016/j.ijpharm.2017.11.018.

Jiang M., Gan L., Zhu C., Dong Y., Liu J., Gan Y. (2012). Cationic core-shell liponanoparticles for ocular gene delivery. *Biomaterials*, 33:7621–7630. DOI: 10.1016/j.biomaterials.2012.06.079.

Jiang, S., Franco, Y.L., Zhou, Y., Chen, J. (2018). Nanotechnology in retinal drug delivery. *Int J Ophthalmol*, 11(6):1038-44. DOI: 10.18240/ijo.2018.06.23.

Jóhannsdóttir, S., Jansook, P., Stefánsson, E., Loftsson, T. (2015). Development of a cyclodextrin-based aqueous cyclosporin A eye drop formulations. *Int J Pharm*, 493(1-2), 86-95. doi:10.1016/j.ijpharm.2015.07.040.

Jóhannsdóttir, S., Kristinsson, J. K., Fülöp, Z., Ásgrímsdóttir, G., Stefánsson, E., Loftsson, T. (2017). Formulations and toxicologic in vivo studies of aqueous cyclosporin A eye drops with cyclodextrin nanoparticles. *Int J Pharm*, 529(1-2), 486-490. doi:10.1016/j.ijpharm.2017.07.044.

Kadajji, V., Betageri, G. (2011). Water Soluble Polymers for Pharmaceutical Applications. *Polymers*, 3. doi:10.3390/polym3041972.

Kang-Mieler, J. J., Osswald, C. R., Mieler, W. F. (2014). Advances in ocular drug delivery: emphasis on the posterior segment. *Expert Opin Drug Deliv*, 11(10), 1647-1660. doi:10.1517/17425247.2014.935338.

Ke, Z., Zhang, Z., Wu, H., Jia, X., Wang, Y. (2017). Optimization and evaluation of Oridonin-loaded Soluplus(®)-Pluronic P105 mixed micelles for oral administration. *Int J Pharm*, 518(1-2), 193-202. doi:10.1016/j.ijpharm.2016.12.047.

Kern, T. S., Miller, C. M., Du, Y., Zheng, L., Mohr, S., Ball, S. L., Kim, M., Jamison, J. A., Bingaman, D. P. (2007). Topical administration of nepafenac inhibits diabetes-induced retinal microvascular disease and underlying abnormalities of retinal metabolism and physiology. *Diabetes*, 56(2), 373-379. doi:10.2337/db05-1621.

Kesavan, K., Nath, G., Pandit, J. K. (2010). Sodium alginate based mucoadhesive system for gatifloxacin and its in vitro antibacterial activity. *Sci Pharm*, 78(4), 941-957. doi:10.3797/scipharm.1004-24.

Khan, N., Aqil, M., Imam, S. S., Ali, A. (2015). Development and evaluation of a novel in situ gel of sparfloxacin for sustained ocular drug delivery: in vitro and ex vivo characterization. *Pharm Dev Technol*, 20(6), 662-669. doi:10.3109/10837450.2014.910807.

Kharenko, E., Larionova, N., Demina, N. (2009). Mucoadhesive drug delivery systems (Review). *Pharm Chem*, 43, 200-208. doi:10.1007/s11094-009-0271-6.

Kicuntod, J., Sangpheak, K., Mueller, M., Wolschann, P., Viernstein, H., Yanaka, S., Kato, K., Chavasiri, W., Pongsawasdi, P., Kungwan, N.,

Rungrotmongkol, T. (2018). Theoretical and Experimental Studies on Inclusion Complexes of Pinostrobin and β -Cyclodextrins. *Sci Pharm*, 86(1). doi:10.3390/scipharm86010005.

Kim, S. J. (2014). Novel Approaches for Retinal Drug and Gene Delivery. *Transl Vis Sci Technol*, 3(5), 7. doi:10.1167/tvst.3.5.7.

Kim, H., Jeong, H., Han, S., Beack, S., Hwang, B. W., Shin, M., Oh, S. S., Hahn, S. K. (2017). Hyaluronate and its derivatives for customized biomedical applications. *Biomaterials*, 123, 155-171. doi:10.1016/j.biomaterials.2017.01.029.

Kleiter, M., Malarkey, D. E., Ruslander, D. E., Thrall, D. E. (2004). Expression of cyclooxygenase-2 in canine epithelial nasal tumors. *Vet Radiol Ultrasound*, 45(3), 255-260. doi:10.1111/j.1740-8261.2004.04046.x.

Koichiro, M., Masahiro, S., Masayuki, N. (1983). Viscosity B-Coefficients, Apparent Molar Volumes, and Activity Coefficients for α - and γ -Cyclodextrins in Aqueous Solutions. *Bull Chem Soc Jpn*, 56(12), 3556-3560. doi:10.1246/bcsj.56.3556.

Koontz, J. L., Marcy, J. E. (2003). Formation of natamycin:cyclodextrin inclusion complexes and their characterization. *J Agric Food Chem*, 51(24), 7106-7110. doi:10.1021/jf030332y.

Kristl, J., Teskac, K., Milek, M., Mlinaric-Rascan, I. (2008). Surface active stabilizer tyloxapol in colloidal dispersions exerts cytostatic effects and apoptotic dismissal of cells. *Toxicol Appl Pharmacol*, 232(2), 218-225. doi:10.1016/j.taap.2008.06.019.

Kumari, A., Sharma, P. K., Garg, V. K., Garg, G. (2010). Ocular inserts - Advancement in therapy of eye diseases. *J Adv Pharm Technol Res*, 1(3), 291-296. doi:10.4103/0110-5558.72419.

Kuo, J. H., Jan, M. S., Chiu, H. W. (2006). Cytotoxic properties of tyloxapol. *Pharm Res*, 23(7), 1509-1516. doi:10.1007/s11095-006-0281-y.

Law, S. L., Huang, K. J., Chiang, C. H. (2000). Acyclovir-containing liposomes for potential ocular delivery. Corneal penetration and absorption. *J Control Release*, 63(1-2), 135-140. doi:10.1016/s0168-3659(99)00192-3.

Leal, J., Smyth, H. D. C., Ghosh, D. (2017). Physicochemical properties of mucus and their impact on transmucosal drug delivery. *Int J Pharm*, 532(1), 555-572. doi:10.1016/j.ijpharm.2017.09.018.

Liaw, J., Chang, S. F., Hsiao, F. C. (2001). In vivo gene delivery into ocular tissues by eye drops of poly(ethylene oxide)-poly(propylene oxide)-poly(ethylene oxide) (PEO-PPO-PEO) polymeric micelles. *Gene Ther*, 8(13), 999-1004. doi:10.1038/sj.gt.3301485.

Lin, C. P., Boehnke, M. (1999). Influences of methylcellulose on corneal epithelial wound healing. *J Ocul Pharmacol Ther*, 15(1), 59-63. doi:10.1089/jop.1999.15.59.

Liu, Z., Li, J., Nie, S., Liu, H., Ding, P., Pan, W. (2006). Study of an alginate/HPMC-based in situ gelling ophthalmic delivery system for gatifloxacin. *Int J Pharm*, 315(1-2), 12-17. doi:10.1016/j.ijpharm.2006.01.029.

Liu, G., Yuan, Q., Hollett, G., Zhao, W., Kang, Y., Wu, J. (2018). Cyclodextrin-based host-guest supramolecular hydrogel and its application in biomedical fields. *Polym Chem*, 9(25), 3436-3449. doi:10.1039/C8PY00730F.

Loch, C., Zakelj, S., Kristl, A., Nagel, S., Guthoff, R., Weitschies, W., Seidlitz, A. (2012). Determination of permeability coefficients of ophthalmic drugs through different layers of porcine, rabbit and bovine eyes. *Eur J Pharm Sci*, 47(1), 131-138. doi:10.1016/j.ejps.2012.05.007.

Loftsson, T., Frikdriksdóttir, H., Sigurkdardóttir, A. M., Ueda, H. (1994). The effect of water-soluble polymers on drug-cyclodextrin complexation. *Int J Pharm*, 110(2), 169-177. doi:https://doi.org/10.1016/0378-5173(94)90155-4.

Loftsson, T. (2002). Cyclodextrins and the Biopharmaceutics Classification System of Drugs. *J Incl Phenom*, 44, 63-67. doi:10.1023/A:1023088423667.

Loftsson, T., Stefánsson, E. (2002). Cyclodextrins in eye drop formulations: enhanced topical delivery of corticosteroids to the eye. *Acta Ophthalmol Scand*, 80(2), 144-150. doi:10.1034/j.1600-0420.2002.800205.x.

Loftsson, T., Hreinsdóttir, D., Másson, M. (2005). Evaluation of cyclodextrin solubilization of drugs. *Int J Pharm*, 302(1-2), 18-28. doi:10.1016/j.ijpharm.2005.05.042.

Loftsson, T., Duchêne, D. (2007). Cyclodextrins and their pharmaceutical applications. *Int J Pharm*, 329(1-2), 1-11. doi:10.1016/j.ijpharm.2006.10.044.

Loftsson, T. (2012). Drug permeation through biomembranes: cyclodextrins and the unstirred water layer. *Pharmazie*, 67(5), 363-370.

Loftsson, T., Brewster, M. E. (2012a). Cyclodextrins as functional excipients: methods to enhance complexation efficiency. *J Pharm Sci*, 101(9), 3019-3032. doi:10.1002/jps.23077.

Loftsson, T., Jansook, P., Stefánsson, E. (2012b). Topical drug delivery to the eye: dorzolamide. *Acta Ophthalmol*, 90(7), 603-608. doi:10.1111/j.1755-3768.2011.02299.x.

Loftsson, T., Stefánsson, E. (2017). Cyclodextrins and topical drug delivery to the anterior and posterior segments of the eye. *Int J Pharm*, 531(2), 413-423. doi:10.1016/j.ijpharm.2017.04.010.

Lorenzo-Veiga, B., Sigurdsson, H. H., Loftsson, T. (2019). Nepafenac-Loaded Cyclodextrin/Polymer Nanoaggregates: A New Approach to Eye Drop Formulation. *Materials (Basel)*, 12(2). doi:10.3390/ma12020229.

Losa, C., Calvo, P., Castro, E., Vila-Jato, J. L., Alonso, M. J. (1991). Improvement of ocular penetration of amikacin sulphate by association to poly(butylcyanoacrylate) nanoparticles. *J Pharm Pharmacol*, 43(8), 548-552. doi:10.1111/j.2042-7158.1991.tb03534.x.

Losa, C., Marchal-Heussler, L., Orallo, F., Vila Jato, J. L., Alonso, M. J. (1993). Design of new formulations for topical ocular administration: polymeric nanocapsules containing metipranolol. *Pharm Res*, 10(1), 80-87. doi:10.1023/a:1018977130559.

Ludwig, A. (2005). The use of mucoadhesive polymers in ocular drug delivery. *Adv Drug Deliv Rev*, 57(11), 1595-1639. doi:10.1016/j.addr.2005.07.005.

Macha, S., Hughes, P., Mitra, A. (2003). Overview of Ocular Drug Delivery (pp. 1-12).

Maharjan, P., Cho, K. H., Maharjan, A., Shin, M. C., Moon, C., & Min, K. A. (2019). Pharmaceutical challenges and perspectives in developing ophthalmic drug formulations. *J Pharm Investig*, 49(2), 215-228. doi:10.1007/s40005-018-0404-6.

Malhotra, A., Minja, F. J., Crum, A., Burrowes, D. (2011). Ocular anatomy and cross-sectional imaging of the eye. *Semin Ultrasound CT MR*, 32(1), 2-13. doi:10.1053/j.sult.2010.10.009.

Marcos, X., Pérez-Casas, S., Llovo, J., Concheiro, A., Alvarez-Lorenzo, C. (2016). Poloxamer-hydroxyethyl cellulose- α -cyclodextrin supramolecular gels for sustained release of griseofulvin. *Int J Pharm*, 500(1-2), 11-19. doi:10.1016/j.ijpharm.2016.01.015.

Másson, M., Loftsson, T., Másson, G., Stefánsson, E. (1999). Cyclodextrins as permeation enhancers: some theoretical evaluations and in vitro testing. *J Control Release*, 59(1), 107-118. doi:10.1016/s0168-3659(98)00182-5.

McKenzie, B., Kay, G., Matthews, K. H., Knott, R. M., Cairns, D. (2015). The hen's egg chorioallantoic membrane (HET-CAM) test to predict the ophthalmic irritation potential of a cysteamine-containing gel: Quantification using Photoshop(R) and ImageJ. *Int J Pharm*, 490(1-2), 1-8. doi:10.1016/j.ijpharm.2015.05.023.

Messner, M., Kurkov, S. V., Jansook, P., Loftsson, T. (2010). Self-assembled cyclodextrin aggregates and nanoparticles. *Int J Pharm*, 387(1-2), 199-208. doi:10.1016/j.ijpharm.2009.11.035.

Messner, M., Kurkov, S. V., Flavià-Piera, R., Brewster, M. E., Loftsson, T. (2011). Self-assembly of cyclodextrins: the effect of the guest molecule. *Int J Pharm*, 408(1-2), 235-247. doi:10.1016/j.ijpharm.2011.02.008.

Moiseev, R. V., Morrison, P. W. J., Steele, F., Khutoryanskiy, V. V. (2019). Penetration Enhancers in Ocular Drug Delivery. *Pharmaceutics*, 11(7). doi:10.3390/pharmaceutics11070321.

Muankaew, C., Jansook, P., Stefánsson, E., Loftsson, T. (2014). Effect of γ -cyclodextrin on solubilization and complexation of irbesartan: influence of pH and excipients. *Int J Pharm*, 474(1-2), 80-90. doi:10.1016/j.ijpharm.2014.08.013.

Muankaew, C., Loftsson, T. (2018). Cyclodextrin-Based Formulations: A Non-Invasive Platform for Targeted Drug Delivery. *Basic Clin Pharmacol Toxicol*, 122(1), 46-55. doi:10.1111/bcpt.12917.

Mura, P. (2015). Analytical techniques for characterization of cyclodextrin complexes in the solid state: A review. *J Pharm Biomed Anal*, 113, 226-238. doi:10.1016/j.jpba.2015.01.058.

Musumeci, T., Bucolo, C., Carbone, C., Pignatello, R., Drago, F., Puglisi, G. (2013). Polymeric nanoparticles augment the ocular hypotensive effect of melatonin in rabbits. *Int J Pharm*, 440(2):135-40. DOI: 10.1016/j.ijpharm.2012.10.014.

Natamycin. PubChem. Available from: <https://pubchem.ncbi.nlm.nih.gov/compound/natamycin#section=Solubility>. Accessed: March 2020.

Natarajan, J. V., Darwitan, A., Barathi, V. A., Ang, M., Htoon, H. M., Boey, Tam, K. C., Wong, T. T., Venkatraman, S. S. (2014). Sustained drug release in nanomedicine: a long-acting nanocarrier-based formulation for glaucoma. *ACS Nano*, 8(1), 419-429. doi:10.1021/nn4046024.

Nogueiras-Nieto, L., Sobarzo-Sánchez, E., Gómez-Amoza, J. L., & Otero-Espinar, F. J. (2012). Competitive displacement of drugs from cyclodextrin inclusion complex by polypseudorotaxane formation with poloxamer: Implications in drug solubilization and delivery. *Eur J Pharm Sci*, 80(3), 585-595. doi:https://doi.org/10.1016/j.ejpb.2011.12.001.

Novack, G. D., Robin, A. L. (2016). Ocular pharmacology. *J Clin Pharmacol*, 56(5), 517-527. doi:10.1002/jcph.634.

Ogawa, N., Furuishi, T., Nagase, H., Endo, T., Takahashi, C., Yamamoto, Kawashima, Y., Loftsson, T., Kobayashi, M., Ueda, H. (2016). Interaction of fentanyl with various cyclodextrins in aqueous solutions. *J Pharm Pharmacol*, 68(5), 588-597. doi:10.1111/jphp.12437.

Patel, A., Cholkar, K., Agrahari, V., Mitra, A. K. (2013). Ocular drug delivery systems: An overview. *World J Pharmacol*, 2(2), 47-64. doi:10.5497/wjp.v2.i2.47.

Patil, A., Lakhani, P., Majumdar, S. (2017). Current perspectives on natamycin in ocular fungal infections. *J Drug Deliv Sci Tec*, 41, 206-212. doi:https://doi.org/10.1016/j.jddst.2017.07.015.

Pepić, I., Hafner, A., Lovrić, J., Pirkić, B., Filipović-Grcić, J. (2010). A nonionic surfactant/chitosan micelle system in an innovative eye drop formulation. *J Pharm Sci*, 99(10), 4317-4325. doi:10.1002/jps.22137.

Pignatello, R., Bucolo, C., Ferrara, P., Maltese, A., Puleo, A., Puglisi, G. (2002). Eudragit RS100 nanosuspensions for the ophthalmic controlled delivery of ibuprofen. *Eur J Pharm Sci*, 16(1-2), 53-61. doi:10.1016/s0928-0987(02)00057-x.

Popielec, A., Loftsson, T. (2017). Effects of cyclodextrins on the chemical stability of drugs. *Int J Pharm*, 531(2), 532-542. doi:10.1016/j.ijpharm.2017.06.009.

Rabinovich-Guilatt, L., Couvreur, P., Lambert, G., Dubernet, C. (2004). Cationic vectors in ocular drug delivery. *J Drug Target*, 12(9-10), 623-633. doi:10.1080/10611860400015910.

Raghava, S., Hammond, M., Kompella, U. B. (2004). Periocular routes for retinal drug delivery. *Expert Opin Drug Deliv*, 1(1), 99-114. doi:10.1517/17425247.1.1.99.

Rajala, A., Wang, Y., Zhu, Y., Ranjo-Bishop, M., Ma, J. X., Mao, C., Rajala, R. V. (2014). Nanoparticle-assisted targeted delivery of eye-specific genes to eyes significantly improves the vision of blind mice in vivo. *Nano Lett*, 14(9), 5257-5263. doi:10.1021/nl502275s.

Rodell, C. B., Mealy, J. E., Burdick, J. A. (2015). Supramolecular Guest-Host Interactions for the Preparation of Biomedical Materials. *Bioconjug Chem*, 26(12), 2279-2289. doi:10.1021/acs.bioconjchem.5b00483.

Rodrigues, G. A., Lutz, D., Shen, J., Yuan, X., Shen, H., Cunningham, J., Rivers, H. M. (2018). Topical Drug Delivery to the Posterior Segment of the Eye: Addressing the Challenge of Preclinical to Clinical Translation. *Pharm Res*, 35(12), 245. doi:10.1007/s11095-018-2519-x.

Ryzhakov, A., Do Thi, T., Stappaerts, J., Bertoletti, L., Kimpe, K., AR, S. C., Saokham, P., Van den Mooter, G., Augustijns, P., Somsen, G. W., Kurkov, S., Inghelbrecht, S., Arien, A., Jimidar, M. I., Schrijnemakers, K., Loftsson, T. (2016). Self-Assembly of Cyclodextrins and Their Complexes in Aqueous Solutions. *J Pharm Sci*, 105(9), 2556-2569. doi:10.1016/j.xphs.2016.01.019.

Saarinen-Savolainen, P., Järvinen, T., Araki-Sasaki, K., Watanabe, H., Urtti, A. (1998). Evaluation of cytotoxicity of various ophthalmic drugs, eye drop excipients and cyclodextrins in an immortalized human corneal epithelial cell line. *Pharm Res*, 15(8), 1275-1280. doi:10.1023/a:1011956327987.

Sahoo, S. K., Dilnawaz, F., Krishnakumar, S. (2008). Nanotechnology in ocular drug delivery. *Drug Discov Today*, 13(3-4), 144-151. doi:10.1016/j.drudis.2007.10.021.

Saldias, C., Velasquez, L., Quezada, C., Leiva, A. (2015). Physicochemical assessment of dextran-g-poly (varepsilon-caprolactone) micellar nanoaggregates as drug nanocarriers. *Carbohydr Polym*, 117, 458-467. doi:10.1016/j.carbpol.2014.09.035.

Salzillo, R., Schiraldi, C., Corsuto, L., D'Agostino, A., Filosa, R., De Rosa, M., La Gatta, A. (2016). Optimization of hyaluronan-based eye drop formulations. *Carbohydr Polym*, 153, 275-283. doi:10.1016/j.carbpol.2016.07.106.

Scheel, J., Kleber, M., Kreutz, J., Lehringer, E., Mehling, A., Reisinger, K., Steiling, W. (2011). Eye irritation potential: usefulness of the HET-CAM under the Globally Harmonized System of classification and labeling of chemicals (GHS). *Regul Toxicol Pharmacol*, 59(3), 471-492. doi:10.1016/j.yrtph.2011.02.003.

Segredo-Morales, E., Martin-Pastor, M., Salas, A., Évora, C., Concheiro, A., Alvarez-Lorenzo, C., Delgado, A. (2018). Mobility of Water and Polymer Species and Rheological Properties of Supramolecular Polypseudorotaxane Gels Suitable for Bone Regeneration. *Bioconjug Chem*, 29(2), 503-516. doi:10.1021/acs.bioconjchem.7b00823.

Sensoy, D., Cevher, E., Sarici, A., Yilmaz, M., Ozdamar, A., Bergişadi, N. (2009). Bioadhesive sulfacetamide sodium microspheres: evaluation of their effectiveness in the treatment of bacterial keratitis caused by *Staphylococcus aureus* and *Pseudomonas aeruginosa* in a rabbit model. *Eur J Pharm Biopharm*, 72(3), 487-495. doi:10.1016/j.ejpb.2009.02.006.

Shah, S. S., Denham, L. V., Elison, J. R., Bhattacharjee, P. S., Clement, C., Huq, T., Hill, J. M. (2010). Drug delivery to the posterior segment of the eye for pharmacologic therapy. *Expert Rev Ophthalmol*, 5(1), 75-93. doi:10.1586/eop.09.70.

Shaikh, R., Raj Singh, T. R., Garland, M. J., Woolfson, A. D., Donnelly, R. F. (2011). Mucoadhesive drug delivery systems. *J Pharm Bioallied Sci*, 3(1), 89-100. doi:10.4103/0975-7406.76478.

Shelley, H., Rodriguez-Galarza, R. M., Duran, S. H., Abarca, E. M., Babu, R. J. (2018). In Situ Gel Formulation for Enhanced Ocular Delivery of

Nepafenac. *J Pharm Sci*, 107(12), 3089-3097. doi:10.1016/j.xphs.2018.08.013.

Simões, S. M., Rey-Rico, A., Concheiro, A., Alvarez-Lorenzo, C. (2015). Supramolecular cyclodextrin-based drug nanocarriers. *Chem Commun (Camb)*, 51(29), 6275-6289. doi:10.1039/c4cc10388b.

Souza, J., Maia, K., Patricio, P., Fernandes-Cunha, G., da Silva, M., Jensen, C. E. D., Silva, G. (2016). Ocular inserts based on chitosan and brimonidine tartrate: Development, characterization and biocompatibility. *J Drug Deliv Sci Tec*, 32, 21-30. doi:10.1016/j.jddst.2016.01.008.

Sridhar, M. S. (2018). Anatomy of cornea and ocular surface. *Indian J Ophthalmol*, 66(2), 190-194. doi:10.4103/ijo.IJO_646_17.

Srinivasarao, D. A., Lohiya, G., Katti, D. S. (2019). Fundamentals, challenges, and nanomedicine-based solutions for ocular diseases. *Wiley Interdiscip Rev Nanomed Nanobiotechnol*, 11(4), e1548. doi:10.1002/wnan.1548.

Stella, V. J., Rao, V. M., Zannou, E. A., Zia, V. V. (1999). Mechanisms of drug release from cyclodextrin complexes. *Adv Drug Deliv Rev*, 36(1), 3-16. doi:10.1016/s0169-409x(98)00052-0.

Szekalska, M., Puciłowska, A., Szymańska, E., Ciosek, P., Winnicka, K. (2016). Alginate: Current Use and Future Perspectives in Pharmaceutical and Biomedical Applications. *Int J Polym Sci*, 2016, 1-17. doi:10.1155/2016/7697031.

Takahashi, Y., Watanabe, A., Matsuda, H., Nakamura, Y., Nakano, T., Asamoto, K., Ikeda, H., Kakizaki, H. (2013). Anatomy of secretory glands in the eyelid and conjunctiva: a photographic review. *Ophthalmic Plast Reconstr Surg*, 29(3), 215-219. doi:10.1097/IOP.0b013e3182833dee.

Taveira, S. F., Varela-Garcia, A., Dos Santos Souza, B., Marreto, R. N., Martin-Pastor, M., Concheiro, A., Alvarez-Lorenzo, C. (2018). Cyclodextrin-based poly(pseudo)rotaxanes for transdermal delivery of carvedilol. *Carbohydr Polym*, 200, 278-288. doi:10.1016/j.carbpol.2018.08.017.

The concept of ocular inserts as drug delivery systems: An overview. Available from <https://pdfs.semanticscholar.org/f6b2/605ee988f061e3a215a9c6826cf7a92ae864.pdf>. Accessed: March 2020.

Thevi, T., Basri, M., Reddy, S. (2012). Prevalence of eye diseases and visual impairment among the rural population - a case study of temerloh hospital. *Malays Fam Physician*, 7(1), 6-10.

Tighsazzadeh, M., Mitchell, J. C., Boateng, J. S. (2019). Development and evaluation of performance characteristics of timolol-loaded composite ocular

films as potential delivery platforms for treatment of glaucoma. *Int J Pharm*, 566, 111-125. doi:10.1016/j.ijpharm.2019.05.059.

Tyagi, P., Barros, M., Stansbury, J. W., Kompella, U. B. (2013). Light-activated, in situ forming gel for sustained suprachoroidal delivery of bevacizumab. *Mol Pharm*, 10(8), 2858-2867. doi:10.1021/mp300716t.

Vaishya, R. D., Khurana, V., Patel, S., Mitra, A. K. (2014). Controlled ocular drug delivery with nanomicelles. *Wiley Interdiscip Rev Nanomed Nanobiotechnol*, 6(5), 422-437. doi:10.1002/wnan.1272.

Varela-Garcia, A., Concheiro, A., Alvarez-Lorenzo, C. (2018). Soluplus micelles for acyclovir ocular delivery: Formulation and cornea and sclera permeability. *Int J Pharm*, 552(1-2), 39-47. doi:10.1016/j.ijpharm.2018.09.053.

Varma, R., Vajaranant, T. S., Burkemper, B., Wu, S., Torres, M., Hsu, C., houdhury, F., McKean-Cowdin, R. (2016). Visual Impairment and Blindness in Adults in the United States: Demographic and Geographic Variations From 2015 to 2050. *JAMA Ophthalmol*, 134(7), 802-809. doi:10.1001/jamaophthalmol.2016.1284.

Velagaleti, P. R., Anglade, E., Khan, I. J., Gilger, B. C., Mitra, A. K. (2010). Topical delivery of hydrophobic drugs using a novel mixed nanomicellar technology to treat diseases of the anterior & posterior segments of the eye. *Drug Deliv Technol*, 10, 42-47.

Wang, D., Li, H., Gu, J., Guo, T., Yang, S., Guo, Z., Zhang, J. (2013). Ternary system of dihydroartemisinin with hydroxypropyl- β -cyclodextrin and lecithin: Simultaneous enhancement of drug solubility and stability in aqueous solutions. *J Pharm Biomed Anal*, 83, 141-148. doi:https://doi.org/10.1016/j.jpba.2013.05.001.

Weng, Y., Liu, J., Jin, S., Guo, W., Liang, X., Hu, Z. (2017). Nanotechnology-based strategies for treatment of ocular disease. *Acta Pharm Sin B*, 7(3), 281-291. doi:10.1016/j.apsb.2016.09.001.

Winkler, J., Wirbelauer, C., Frank, V., Laqua, H. (2001). Quantitative distribution of glycosaminoglycans in young and senile (cataractous) anterior lens capsules. *Exp Eye Res*, 72(3), 311-318. doi:10.1006/exer.2000.0952.

Xu, J., Li, X., Sun, F., Cao, P. (2010). PVA hydrogels containing beta-cyclodextrin for enhanced loading and sustained release of ocular therapeutics. *J Biomater Sci Polym Ed*, 21(8-9), 1023-1038. doi:10.1163/156856209x463690.

Xu, Q., Boylan, N. J., Suk, J. S., Wang, Y. Y., Nance, E. A., Yang, J. C., McDonnell, P. J., Cone, R. A., Duh, E. J., Hanes, J. (2013). Nanoparticle diffusion in, and microrheology of, the bovine vitreous ex vivo. *J Control Release*, 167(1), 76-84. doi:10.1016/j.jconrel.2013.01.018.

Yu, S., Tan, G., Liu, D., Yang, X., & Pan, W. (2017). Nanostructured lipid carrier (NLC)-based novel hydrogels as potential carriers for nepafenac applied after cataract surgery for the treatment of inflammation: design, characterization and in vitro cellular inhibition and uptake studies. *RSC Advances*, 7(27), 16668-16677. doi:10.1039/C7RA00552K.

Yuan, C., Jin, Z., Xu, X. (2012). Inclusion complex of astaxanthin with hydroxypropyl-beta-cyclodextrin: UV, FTIR, ¹H NMR and molecular modeling studies. *Carbohydr Polym*, 89(2), 492-496. doi:10.1016/j.carbpol.2012.03.033.

Yuan, X., Marcano, D. C., Shin, C. S., Hua, X., Isenhardt, L. C., Pflugfelder, S. C., Acharya, G. (2015). Ocular drug delivery nanowafer with enhanced therapeutic efficacy. *ACS Nano*, 9(2), 1749-1758. doi:10.1021/nn506599f.

Zhang, J., Wang, S. (2009). Topical use of coenzyme Q10-loaded liposomes coated with trimethyl chitosan: tolerance, precorneal retention and anti-cataract effect. *Int J Pharm*, 372(1-2), 66-75. doi:10.1016/j.ijpharm.2009.01.001.

Zhang, J., Ma, P. X. (2013). Cyclodextrin-based supramolecular systems for drug delivery: recent progress and future perspective. *Adv Drug Deliv Rev*, 65(9), 1215-1233. doi:10.1016/j.addr.2013.05.001.

Zhang, Z., He, Z., Liang, R., Ma, Y., Huang, W., Jiang, R., Shi, S., Chen, H., & Li, X. (2016). Fabrication of a Micellar Supramolecular Hydrogel for Ocular Drug Delivery. *Biomacromolecules*, 17(3), 798-807. doi:10.1021/acs.biomac.5b01526.

Zhang, Z., Cui, C., Wei, F., Lv, H. (2017). Improved solubility and oral bioavailability of apigenin via Soluplus/Pluronic F127 binary mixed micelles system. *Drug Dev Ind Pharm*, 43(8), 1276-1282. doi:10.1080/03639045.2017.1313857.

Paper I

Article

Nepafenac-Loaded Cyclodextrin/Polymer Nanoaggregates: A New Approach to Eye Drop Formulation

Blanca Lorenzo-Veiga, Hakon Hrafn Sigurdsson *  and Thorsteinn Loftsson 

Faculty of Pharmaceutical Sciences, University of Iceland, Hofsvallagata 53, IS-107 Reykjavik, Iceland; blv3@hi.is (B.L.-V.); thorstlo@hi.is (T.L.)

* Correspondence: hhs@hi.is; Tel.: +354-525-5821

Received: 7 December 2018; Accepted: 7 January 2019; Published: 11 January 2019



Abstract: The topical administration route is commonly used for targeting therapeutics to the eye; however, improving the bioavailability of drugs applied directly to the eye remains a challenge. Different strategies have been studied to address this challenge. One of them is the use of aggregates that are formed easily by self-assembly of cyclodextrin (CD)/drug complexes in aqueous solution. The aim of this study was to design a new eye drop formulation based on aggregates formed between CD/drug complexes. For this purpose, the physicochemical properties of the aggregates associated with six CDs and selected water-soluble polymers were analysed. Complex formation was studied using differential scanning calorimetry (DSC), Fourier-transform infrared spectroscopy (FT-IR) and ^1H nuclear magnetic resonance spectroscopy ($^1\text{H-NMR}$). Results showed that HP β CD performed best in terms of solubilization, while γ CD performed best in terms of enhancing nanoaggregate formation. Formation of inclusion complexes was confirmed by DSC, FT-IR and $^1\text{H-NMR}$ studies. A mixture of 15% (*w/v*) γ CD and 8% (*w/v*) HP β CD was selected for formulation studies. It was concluded that formulations with aggregate sizes less than 1 μm and viscosity around 10–19 centipoises can be easily prepared using a mixture of CDs. Formulations containing polymeric drug/CD nanoaggregates represent an interesting strategy for enhanced topical delivery of nepafenac.

Keywords: cyclodextrin; nepafenac; polymer; complexation; aggregate; self-assemble; ocular drug delivery

1. Introduction

Nepafenac (2-amino-3-benzoylbenzeneacetamide) is a potent non-steroidal anti-inflammatory drug (NSAID) used to treat the pain and inflammation associated with cataract surgery. It is currently available as a 0.1% ophthalmic suspension. However, in powdered form, nepafenac is known to have low water solubility and low tissue permeability and is classified as a class IV compound by the Biopharmaceutical Classification System [1–4]. Thus, developing a new eye drop formulation of nepafenac with improved bioavailability is of considerable interest.

Improving the bioavailability of a drug applied topically to the eye remains a challenge [5–7]. Different strategies to improve bioavailability include the use of penetration enhancers [8], viscosity modifiers [9], carrier systems or external forces such as electrical currents or ultrasounds and drug/cyclodextrin (CD) complexation [10–13].

CDs are cyclic oligosaccharides of α -D-glucopyranose that contain a hydrophobic central cavity and have a hydrophilic outer surface. The natural CDs, α , β and γ , are composed of six, seven or eight D-glucopyranose units linked by α 1, 4 glycosidic bonds (see Supplementary Information, Figure S1). CDs have been widely explored in polymer chemistry because of their ability to form complexes with

hydrophilic polymers, monomers and drugs. Chemically crosslinked or grafted with polymer, CDs have been proposed for use in smart drug delivery systems in many studies [10,11,14–18].

Native or non-substituted CDs and their hydroxy-propyl derivatives have been used as pharmaceutical excipients to increase drug solubility, improve chemical stability, reduce toxicity and transport molecules to specific sites [19–23]. Importantly, drug/CD complexation increases the aqueous solubility of poorly soluble drugs without altering their properties [24]; as a result, CDs have been used in over 40 marketed products to date. Nevertheless, solubility enhancement via drug/CD complexation has certain limitations such as the high molecular weight of the CDs, toxicity issues and high costs [25–27].

The addition of a second solubilizing agent to a drug/CD complex to form a ternary system has been reported as an interesting strategy [21,28–33]. For example, the incorporation of salts [34], co-solvents [35], amino acids [36] or hydrophilic polymers [37–39] in the complexation media can improve the solubility of the drug and make the formulation more cost effective by allowing use of lower concentrations of CDs. Mennini et al. [31] studied the effect of an amino acid, L-arginine, in enhancing the complexation and solubilizing abilities of randomly-methylated- β CD (Rame β CD) toward oxaprozin. They found that complexation with Rame β CD and simultaneous salt formation with L-arginine was a successful strategy for improving the solubility and dissolution properties of oxaprozin. Soliman et al. [40] explored the effect of different hydrophilic polymers including polyethylene glycol (PEG-4000), chitosan, polyvinyl pyrrolidone (PVP K-30), hydroxypropylmethyl cellulose (HPMC) and hydroxyethyl cellulose (HEC), on avanafil/ β -CD inclusion complexes. They confirmed that the addition of 7% PVP K-30 to avanafil/ β -CD inclusion complexes improved complex stability. Also, they found that using higher concentrations of some of these polymers (PVP K-30 or PEG-4000) led to a decrease in avanafil solubility, suggesting that they can displace the drug from the CD cavity at high concentrations. The use of supramolecular structures formed between CDs and amphiphilic copolymers, known as poly(pseudo)rotaxanes, have been extensively investigated [11,41,42].

Eye drop formulations designed by our group containing CDs have been shown to deliver lipophilic drugs effectively both to the anterior and posterior segment of the eye, despite the various ocular barriers that make delivering new drug formulations to the eye a challenge [43–46]. The aim of this study was to formulate a new aqueous-based anti-inflammatory eye drop containing nepafenac, CD and polymer. For this purpose, different studies were performed: (1) to evaluate the physicochemical characteristics of the nepafenac/CD complex, (2) to study the influence of selected hydrophilic polymers on the solubility of the nepafenac/CD complex, (3) to investigate the possible synergistic effect of using a mixture of γ CD and HP β CD on complex solubility and (4) to characterize the solid-state inclusion complex.

2. Materials and Methods

2.1. Materials

Nepafenac was purchased from Sigma-Aldrich (St. Louis, MO, USA). α -Cyclodextrin (α CD), β -cyclodextrin (β CD) and γ -cyclodextrin (γ CD) were obtained from Wacker Chemie (Munich, Germany). 2-Hydroxypropyl- α -cyclodextrin (HP α CD), 2-hydroxypropyl- β -cyclodextrin (HP β CD) and 2-hydroxypropyl- γ -cyclodextrin (HP γ CD) were kindly donated by Janssen Pharmaceutica (Beerse, Belgium).

Polyvinylpyrrolidone (PVP) (average MW 10.000 kDa), 87–90% hydrolysed poly(vinyl alcohol) (PVA) (average MW 30.000–70.000 kDa), carboxymethylcellulose (CMC) sodium salt (low viscosity), hydroxypropylmethylcellulose (HPMC; viscosity approx. 100 centipoises) and reagent grade tyloxapol were obtained from Sigma-Aldrich (St. Louis, MO, USA). Methyl cellulose (MC; viscosity approx. 15 centipoises) was purchased from ICN Biomedicals Inc. (Solon, OH, USA). Membrane filters (0.45 μ m) were purchased from Phenomenex (Cheshire, UK).

All other chemicals used were of analytical reagent grade purity. Milli-Q (Millipore, Billerica, MA, USA) water was used for the preparation of all solutions.

2.2. Moisture Content of CDs

A small amount (1 g) of solid powdered γ CD and HP β CD were placed in separate aluminium pans and their water content measured using an A&D MX-50 moisture analyser (A&D company, Limited, Tokyo, Japan). Measurements were made in triplicate. The water content of γ CD and HP β CD was 10.70% and 6.22%, respectively.

2.3. Chemical Stability of Nepafenac

The chemical stability of nepafenac was determined in aqueous solution containing 1% *w/v* γ CD following heating by sonication [47–50]. The solution was shaken for 24 h until the drug was completely dissolved and then passed through a 0.45 μ m membrane filter. The solution was then divided between four sealed vials. Vial 1 was used as a blank. Vials 2, 3 and 4 were heated in a sonicator at 60 °C for 20, 40 and 60 min, respectively. Drug concentrations were determined by HPLC.

2.4. Quantitative Analysis

The HPLC assay was performed using a reverse-phase ultra-high-performance liquid chromatography (UHPLC) Ultimate 3000 series system (Dionex Softron GmbH, Germering, Germany) consisting of a LPG-3400SD pump (Dionex, Germering, Germany) with a built-in degasser, WPS-3000 autosampler (Dionex, Germering, Germany), TCC-3100 column compartment (Dionex, Germering, Germany) and CoronaR ultra RS detector (Dionex, Germering, Germany). During the stationary phase, a Phenomenex Kinetex C18 column (150 \times 4.6 mm, 5 μ m) with matching HPLC Security Guard (Phenomenex, Cheshire, UK) was used. The mobile phase used a mixture of acetonitrile and water (50:50). The flow rate was 1 mL/min, the column oven temperature was \pm 25 °C and the detection wave length was set to 254 nm. The retention time for nepafenac under these conditions was 2.3 min.

Peak area and other variables were analysed using the software Chromeleon version 7.2 SR4 (ThermoScientific, Waltham, MA, USA).

2.5. Phase Solubility Studies

The solubility of nepafenac in combination with different cyclodextrin concentrations was determined following heating by sonication [47,49,50]. The schematic representation of this method is shown in Figure 1. Firstly, an excess amount of nepafenac (approximately 5 mg) was added to aqueous solutions containing known concentrations of CDs (ranging up to 15% (*w/v*) for α CD, γ CD, HP α CD, HP β CD, HP γ CD and 1.5% (*w/v*) for β CD) in pure water. The drug suspensions were saturated with nepafenac and heated in a sonicator in sealed vials at 60 °C for 60 min, before being allowed to cool to room temperature. Then, a small amount of solid nepafenac (approximately 2 mg) was added to each suspension to produce drug precipitation. Vials were resealed and placed in a shaker under constant agitation for 7 days. After reaching equilibrium, suspensions were filtered using 0.45 μ m membrane filters, before being diluted in pure water and analysed by UHPLC. Determinations were made in triplicate.

The most frequent method to study the formation of complexes is through the phase solubility studies proposed by Higuchi and Connor. In them, we can distinguish different solubility profiles (type A and B) depending on the effect of the cyclodextrin on the solubilization of the drug [51].

The apparent stability constant ($K_{1:1}$) according to the hypothesis of a 1:1 stoichiometric ratio of complexes was calculated using the following equation:

$$K_{1:1} = \frac{\text{slope}}{S_0(1 - \text{slope})} \quad (1)$$

In addition, complexation efficiency (CE) was calculated. This factor can be calculated either from the slope of the phase solubility profile or from the ratio of the concentration of the drug/CD complex to free CD [52]:

$$CE = \frac{\text{slope}}{(1 - \text{slope})} = \frac{[\text{Guess / CD complex}]}{[\text{CD}]} \quad (2)$$

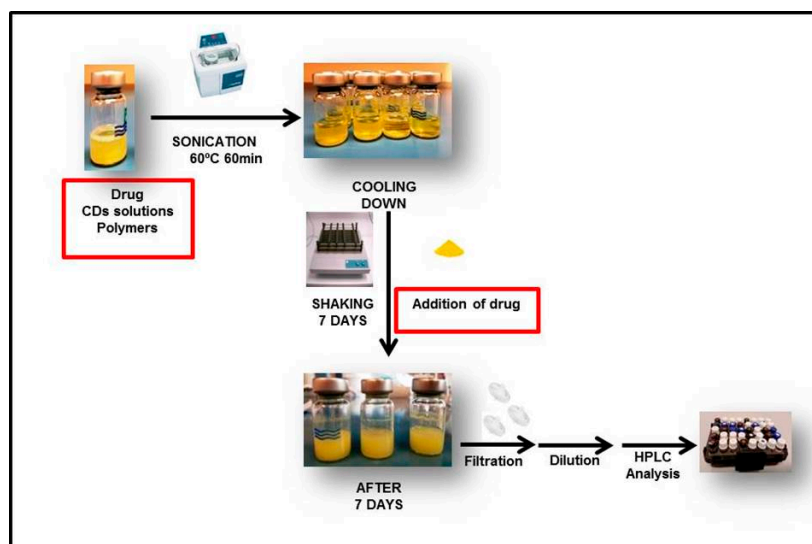


Figure 1. Schematic representation describing the steps involved in the formation of drug/CD inclusion complexes in phase solubility studies.

2.6. Complex Characterization in Solid State

2.6.1. Preparation of Inclusion Complexes

Samples were prepared using a freeze drying method [53,54]. Clear supernatant solutions from phase solubility studies of γ CD and HP β CD that had shown AL-type profiles were used to confirm the presence of nepafenac/CDs complexes. 200 μ L was collected from each vial, placed in small Eppendorfs and freeze-dried at -55 $^{\circ}$ C for 24 h in a Snijders scientific 2040 Freeze dryer (Snijders Labs, Tilburg, The Netherlands).

2.6.2. Fourier Transform Infra-Red (FT-IR) Spectroscopy

The FT-IR spectra of pure nepafenac, pure CDs and their freeze-dried complexes were measured with a FT-IR spectrometer (Thermo Fisher Scientific model Nicolet iS10, Waltham, MA, USA) using an Attenuated Total Reflectance (ATR) technique. Data were obtained in the range of 500–4000 cm^{-1} . Analyses were performed at room temperature.

2.6.3. Differential Scanning Calorimetry (DSC)

DSC curves were recorded on Netzsch DSC 214 polyma (Netzsch Group, Selb, Germany). Samples (approximately 3–5 mg) were heated at the rate of 10 $^{\circ}$ C/min in sealed aluminium pans under nitrogen. The temperature ranged from 30 to 250 $^{\circ}$ C. An empty aluminium pan was used as a reference.

2.7. Structure of Inclusion Complexes Combining Nepafenac with γ CD and HP β CD

$^1\text{H-NMR}$ spectrums were analysed to study inclusion complexes. Experiments were carried out at 500 MHz in a Bruker AVANCE 400 instrument (Bruker Biospin GmbH, Rheinstetten, Germany). Deuterated chloroform ($\text{CDCl}_3\text{-d}_6$) was used to dissolve nepafenac and deuterium oxide (D_2O) to dissolve nepafenac/CD complexes, γ CD and HP β CD.

2.8. Influence of Water-Soluble Polymers on Solubility of Complexes and Effect of Mixtures of γ CD and HP β CD

PVP, PVA, CMC and tyloxapol were selected as polymers. The polymer was firstly dissolved in pure water and then added to aqueous solutions containing CD to a final concentration of 1% *w/v*. The solubility of nepafenac was analysed by UHPLC method previously validated in Section 2.4. Effect of cyclodextrins and excipients on osmolality, viscosity and size of binary and ternary systems with nepafenac were also analysed (see Supplementary Information, Table S1). All samples were prepared in triplicate.

2.9. Preparation and Characterization of 0.5% (*w/v*) Nepafenac Eye Drops

Nine formulations were prepared (Table 1) and all of them contained: 0.5% (*w/v*) nepafenac, 15% (*w/v*) γ CD, 8% (*w/v*) HP β CD, 0.1% (*w/v*) EDTA, 0.02% (*w/v*) benzalkonium chloride, 0.05% (*w/v*) sodium chloride and different ratios of polymers as outlined in Table 1.

Table 1. Polymer composition of the nine eye drop formulations.

Formulations	PVP (% <i>w/v</i>)	PVA (% <i>w/v</i>)	CMC (% <i>w/v</i>)	HPMC (% <i>w/v</i>)	MC (% <i>w/v</i>)	Tyloxapol (% <i>w/v</i>)
F1	-	2.0	-	0.1	-	0.1
F2	-	-	1.0	-	-	-
F3	-	2.0	1.0	-	-	0.1
F4	-	2.0	-	-	-	0.1
F5	1.0	-	1.0	0.1	-	-
F6	1.0	-	-	-	0.1	-
F7	-	2.0	1.0	-	0.1	0.1
F8	1.0	-	-	-	-	0.1
F9	-	2.0	1.0	-	0.1	-

PVP, polyvinylpyrrolidone; PVA, hydrolysed poly(vinyl alcohol); CMC, carboxymethylcellulose; HPMC, hydroxypropylmethylcellulose; MC, methyl cellulose.

2.9.1. Solid Drug Fraction

The formulation (6 mL) being tested was centrifuged at 13,000 rpm (MC6 centrifuge, Sarstedt AG, Nümbrecht, Germany) at room temperature (22–23 °C) for 30 min and the supernatant was analysed by HPLC. The drug content in solid phase was calculated as:

$$\% \text{ solid drug fraction (SDF)} = \frac{(\text{total drug} - \text{dissolved drug})}{\text{Total drug content}} \times 100 \quad (3)$$

2.9.2. Dynamic Light Scattering

The particle sizes within the eye drop formulations were characterized by dynamic light scattering using a Nanotrak Wave particle size analyser from Microtrac Inc. (Montgomeryville, PA, USA). Measurements were in triplicate as described previously.

2.9.3. Physicochemical Properties

The viscosity of the eye drop formulations was measured using a Brookfield viscometer (model DV2T) attached to a Brookfield water bath (model TC-150) with a spindle (CPA-40Z) operating at 25 °C (Middleborough, MA, USA). Each formulation was measured in triplicate. The osmolality of the formulations was determined using an Osmomat 030 Gonotec (Berlin, Germany) freezing point osmometer.

2.9.4. Transmission Electron Microscope (TEM) Analysis

The morphology of nepafenac-loaded CD/polymer nanoaggregates was studied visually by TEM. Samples were prepared using 4% of uranyl acetate as negative staining agent. Firstly, 3 μ L of each sample was loaded into a coated grid in a parafilm[®] located inside a petri dish and left to dry for

30 min at 37–40 °C. After centrifugation of uranyl acetate at 10,000 rpm for 5 min, a drop of 26 µL of the dye was transferred to another petri dish containing a parafilm[®] flip-loaded grid onto uranyl acetate and left for 5 min. Finally, the excess of dye was removed and the grid dried with filter paper and left at room temperature during 12 h. Finally, the samples were analysed using a Model JEM 1400 TEM (JEOL, Tokyo, Japan).

3. Results and Discussion

3.1. Stability of Nepafenac in Autoclave and Sonicator

The chemical stability of nepafenac in CD aqueous solutions after heating in sonicator was studied (Table 2). From the results, can be seen that nepafenac/CD complexes could be prepared using sonication as a heating method for the phase-solubility studies since it was safe, ease to use and no degradation of nepafenac was observed.

Table 2. Nepafenac concentrations in aqueous solution containing 1% *w/v* γ CD after heating by sonication. Results are expressed as mean \pm SD (n = 3).

Sonication	Mean (\pm SD) Nepafenac Concentration (μ g/mL)
60 °C 20 min	6.41 \pm 0.08
60 °C 40 min	6.49 \pm 0.07
60 °C 60 min	6.57 \pm 0.08

3.2. Phase-Solubility Studies

The solubility of nepafenac in water in the presence of the different CD forms can be seen in Table 3. Phase-solubility profiles of nepafenac in aqueous CD solutions containing α CD, β CD, γ CD, HP α CD, HP β CD and HP γ CD are shown in Figure 2. Based on the phase-solubility profiles, the solubility of nepafenac increases with increasing CD concentration in the aqueous media.

Table 3. Values of the apparent stability constant ($K_{1:1}$) and complexation efficiency (CE).

Cyclodextrin	Type	Slope	Corr.	$K_{1:1}$ (M^{-1})	CE	Solubility (mg/mL) in the Presence of 15% (<i>w/v</i>) CD
γ CD	A_L^a	0.024	0.998	248	0.024	0.715
HP γ CD	A_P^a	0.022	0.978	218	0.021	0.590
α CD	A_L^a	0.029	0.991	289	0.028	0.131
HP α CD	A_L^a	0.011	0.984	113	0.011	0.401
β CD	A_L	0.180	0.998	2230	0.220	^b
HP β CD	A_L^a	0.198	0.999	2515	0.247	4.460

Corr., Correlation; HP, 2-hydroxypropyl; ^a Measured from 0–15% CD; ^b β CD was not soluble in water at this concentration.

According to the Higuchi–Connors classification system, inclusion complexes for all CDs studied were soluble. Complexes including γ CD, β CD, α CD, HP β CD, HP α CD showed an A_L profile, indicating that the solubility of the drug increased linearly with increasing CD concentration. However, HP γ CD showed an A_P -type profile, indicating a positive deviation from linearity. The presence of an A_L profile with a slope less than 1, suggested that a 1:1 nepafenac/CD complex has been formed.

Among the different CDs investigated, the highest CE was found for HP β CD. Challa et al. [55] have previously recommended the CDs γ CD, HP β CD and SBE β CD for use in ocular drug delivery. Moreover, studies on CD toxicity in a human cornea epithelial cell line by Saarinen-Savolainen et al. [56] revealed that γ CD had the least cytotoxic profile, followed jointly by HP β CD and SBE β CD, then DM β CD and finally α CD. Johannsdottir et al. [45] demonstrated that γ CD also had the highest capacity compared with α CD for forming nanoparticles in aqueous solution that were able to solubilize hydrophobic drugs. Based on the phase solubility profiles obtained in our study and the safety profile and capacity of CDs to form nanoparticles reported in previous studies, mixtures of γ CD and HP β CD were selected for further study.

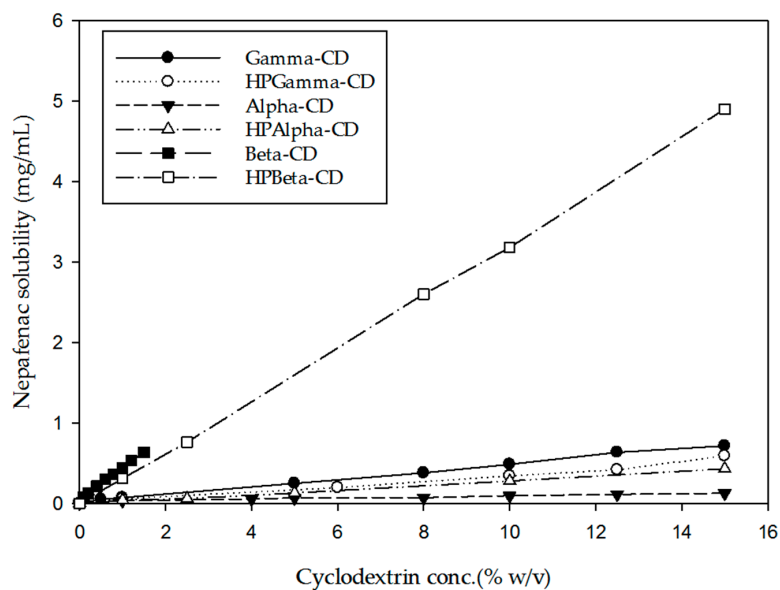


Figure 2. Phase-solubility profile of nepafenac in aqueous solution in combination with different CDs. Results are expressed as mean (n = 3).

3.3. Influence of Adding Water-Soluble Polymers on the Solubility of Nepafenac/CD Complexes and Impact of Mixing γ CD and HP β CD

The impact of adding PVP, PVA, CMC and tyloxapol on the solubility of nepafenac in pure γ CD and mixed γ CD/HP β CD solutions is shown in Figure 3. Tyloxapol is a non-ionic polymer with surfactant properties. PVA, PVP and CMC are also polymers known as “viscosity modifiers”. All of them are widely used in the preparation of eye drops.

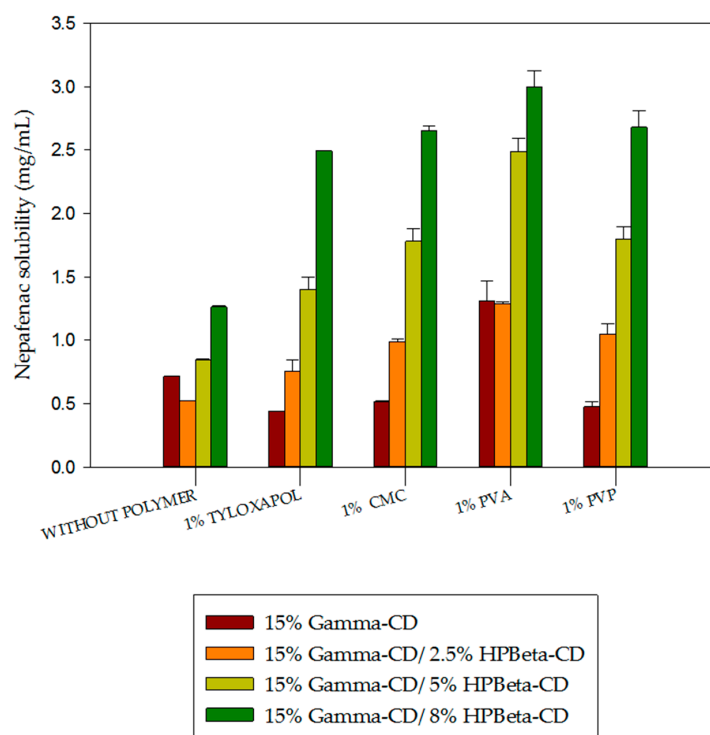


Figure 3. Impact of cyclodextrins and excipients on the solubility of binary and ternary complexes including nepafenac.

In Figure 3, results showed that the addition of 1% PVP, CMC and tyloxapol had a slightly negative effect on nepafenac/ γ CD complex solubility. However, nepafenac/ γ CD complex solubility was almost tripled following the addition of 1% PVA. PVA was also associated with higher solubility than other polymers when added to nepafenac/CD complexes containing a mixture of γ CD and HP β CD. No synergistic effect was found by combining 15% γ CD with 2.5% HP β CD (the solubility of nepafenac in pure 2.5% HP β CD is 0.85 mg/mL—see Figure 2). However, when we carried out the solid state characterization of the complex, its formation was easily achieved using higher amounts of HP β CD, such as 8%. The impact of mixing CDs on solubility was previously investigated by Jansook et al. [57]. This group studied the synergistic effect between γ CD and HP γ CD using a variety of drugs, including dexamethasone [58]. They found that synergistic-type effects only occurred when a drug with a B-type profile was combined with γ CD and HP γ CD. This may explain why no synergistic effect was found when combining the A-type profile drug nepafenac with γ CD or HP β CD.

3.4. Solid State Characterization of Nepafenac/CD Inclusion Complexes

3.4.1. FT-IR Spectra

Fourier transform infra-red (FT-IR) spectroscopy was applied to confirm the presence of guest and host molecules in the inclusion complex. The FT-IR spectra of pure nepafenac, γ CD and HP β CD, as well as nepafenac/CD complexes prepared by freeze-drying are shown in Figure 4. Bands representing pure compounds were compared to the band for the complex. The disappearance or change in position of peaks indicates the formation of complexes.

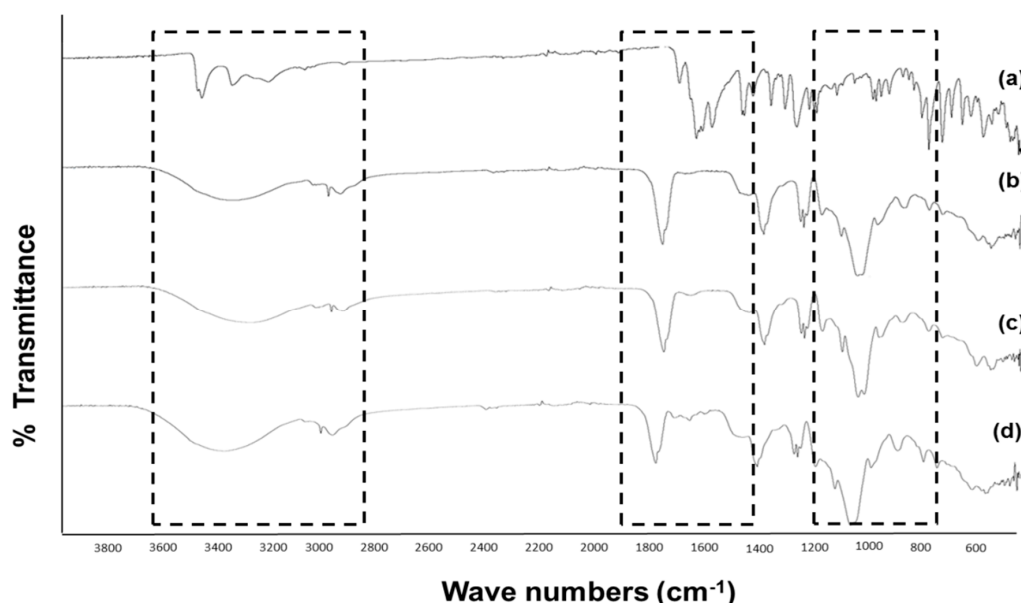


Figure 4. Comparison of FT-IR spectra of: (a) pure nepafenac, (b) pure HP β CD, (c) pure γ CD and (d) freeze-dried nepafenac/15% γ CD/8%HP β CD complex.

For pure nepafenac, characteristic absorption peaks appeared at 1631 cm^{-1} (attributed to C=O stretch absorption of the secondary amide group), 1664 cm^{-1} (attributed to C=O stretch absorption of the ketone group), $3500\text{--}3300\text{ cm}^{-1}$ (attributed to NH_2 stretch absorption) and 3080 , 3040 , 1968 and 1818 cm^{-1} (attributed to benzene aromatic stretching) (Figure 4a). For pure γ CD and HP β CD (Figure 4b,c, respectively), the characteristic absorption bands relating to OH stretch were observed at 3300 , 3410 , 1420 and 1330 cm^{-1} , while the absorption bands relating to CO stretch were seen at 1079 and 1029 cm^{-1} . In the case of freeze-dried nepafenac/ γ CD/HP β CD complex (Figure 4d), the NH_2 stretch and benzene aromatic stretch absorption bands were less intense than for pure

nepafenac, suggesting that this part of the nepafenac compound may be encapsulated within the complex containing both CDs.

3.4.2. DSC

DSC measurements were used to obtain information about the thermal stability and phase transition of all components. This thermal method confirmed the solid-state interaction between nepafenac and both CDs since their DSC curves (Figure 5d–f) showed shifting to lower temperatures than the melting point of nepafenac (Figure 5a). The DSC curves for nepafenac, CDs and their complexes are presented in Figure 5.

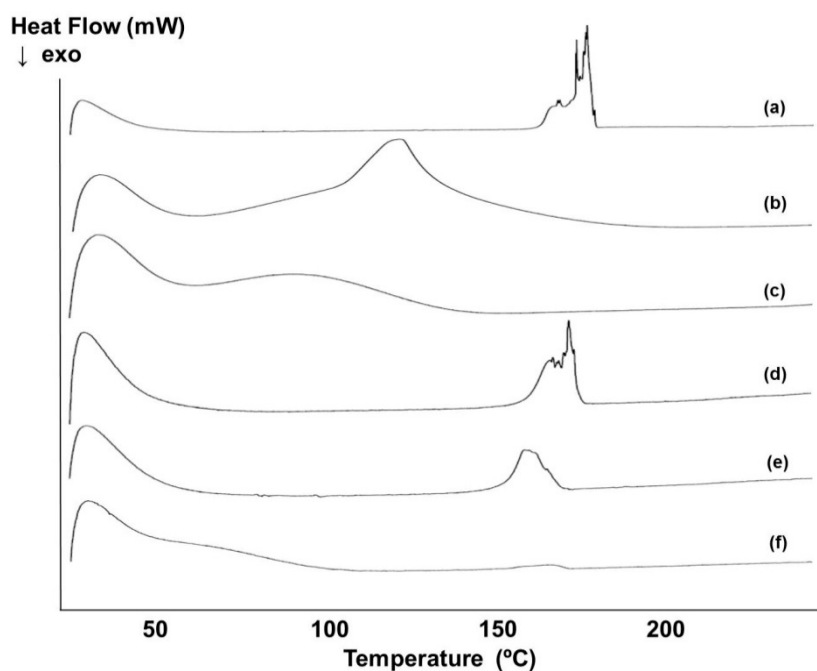


Figure 5. Differential scanning calorimetry (DSC) curves for: (a) pure nepafenac, (b) pure γ CD, (c) pure HP β CD, (d) freeze-dried nepafenac and mixture of 15% γ CD/2.5%HP β CD complex, (e) freeze-dried of nepafenac/15% γ CD/5%HP β CD complex and (f) freeze-dried nepafenac/15% γ CD/8%HP β CD complex. Exo; exothermic.

The DSC curve for pure nepafenac showed a sharp endothermic peak at 178 °C, corresponding to the melting point of the drug (Figure 5a). DSC curves for γ CD and HP β CD showed a wide endothermal effect between approximately 30 °C and 150 °C (Figure 5b,c), as a result of the dehydration process. For the freeze-dried ternary complex (nepafenac/15% γ CD/2.5%HP β CD) (Figure 5d), the intensity of the endothermic peak was reduced and also shifted to lower temperatures compared with nepafenac. A similar pattern was seen for the nepafenac/15% γ CD/5%HP β CD complex relative to the 15% γ CD/2.5%HP β CD complex, with both a decrease in the intensity of the endothermic peak and a shift to a lower temperature range. This noticeable decrease in intensity of the endothermic peak and shift to a lower temperature is indicative of a loss of nepafenac crystalline structure and the formation of a solid dispersion. Moreover, for the nepafenac/15% γ CD/8%HP β CD complex, the endothermic peak corresponding to the melting point of the drug vanished. This may be due to the formation of solid-state nepafenac /CD inclusion complexes.

3.5. Structure of Nepafenac/ γ CD/HP β CD Inclusion Complexes

1 H-NMR spectroscopy has become the most important method for structural elucidation of organic compounds in solution state [59]. These studies provide useful information on the characteristics of guest/host CD inclusion complexes, including the orientation of the guest molecule

inside the hydrophobic cavity of the CD host molecule [60,61]. The formation of inclusion complexes lead to chemical shifts ($\Delta\delta$) in the ^1H -NMR spectra of the guest molecule; $\Delta\delta$ can be calculated using the following equation:

$$\Delta\delta^* = \delta_{\text{complex}} - \delta_{\text{free}} \quad (4)$$

where δ_{complex} and δ_{free} are chemical shifts between free and bound CD molecules, respectively. Chemical shifts are shown in ppm.

^1H -NMR spectroscopy has proven useful in the study of the formation of CD inclusion complexes with many compounds [62,63]. In γCD , there are six protons: the H-3 and H-5 protons are located inside the cavity, whereas the others (H-1, H-2, H-4 and H-6) are located on the exterior of the CD molecule (Figure 6). In the case of HP βCD , there is an additional methyl group [64]. In order to confirm the formation of the inclusion complex of nepafenac with γ - and HP β -CD, a one-dimensional ^1H NMR study was performed (see Supplementary Information, Figure S2). The difference in the chemical shifts between free and bound CDs molecules are shown in Tables 4 and 5.

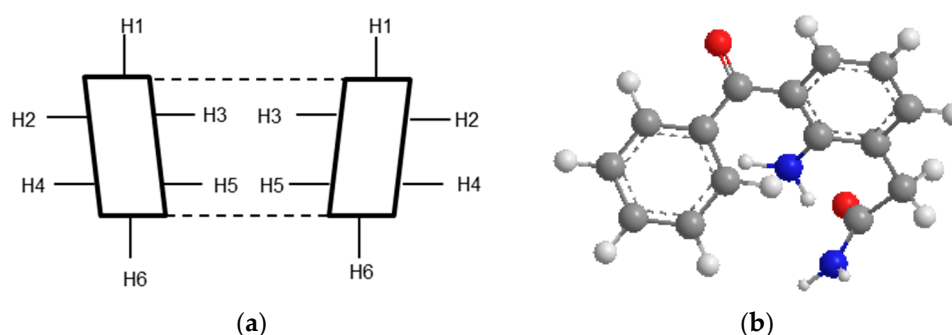


Figure 6. Cross-section of CD molecule (a) and nepafenac 3D structure (b).

Table 4. H-NMR Chemical shift corresponding to free γCD alone and in the presence of nepafenac.

Protons	γCD	Nepafenac/ γCD	$\Delta\delta^*$
H1	5.1320	5.1554	+0.0234
H2	3.6754	3.7031	+0.0277
H3	3.9564	3.9782	+0.0218
H4	3.6115	3.6339	+0.0224
H5	3.8712	3.8925	+0.0213
H6	3.8903	3.9146	+0.0243

$$\Delta\delta^* = \delta_{\text{complex}} - \delta_{\text{free}}$$

Table 5. H-NMR Chemical shift corresponding to free HP βCD alone and in the presence of nepafenac.

Protons	HP βCD	Nepafenac/HP βCD	$\Delta\delta^*$
H1	5.1207	5.1137	−0.007
H2	3.6686	3.6625	−0.0061
H3	4.0386	4.0046	−0.034
H4	3.5485	3.5468	−0.0017
H5	3.9010	3.7681	−0.1329
H6	3.9487	3.8912	−0.0575
−CH3	1.1952	1.1864	−0.0088

$$\Delta\delta^* = \delta_{\text{complex}} - \delta_{\text{free}}$$

The changes in $\Delta\delta$ of γCD in the presence of nepafenac for the H-3 (+0.0218) and H-5 (+0.0213) protons were downfield (Table 4). Moreover, the $\Delta\delta$ of the H-3 proton was higher than that for the H-5 proton. These results showed that the guest molecule, nepafenac, occupies the entire volume of the cavity inside γCD .

As shown in Table 5, changes in $\Delta\delta$ for the H-3 (-0.034) and H-5 (-0.1329) proton of HP β CD were upfield, indicating the formation of an inclusion complex. Also, $\Delta\delta^*$ of the H-5 proton was higher than $\Delta\delta^*$ of the H-3 proton, suggesting partial inclusion of nepafenac in the HP β CD cavity [64,65].

2D correlation spectroscopy was conducted to confirm the location of the guest in the complex. Chemical shifts corresponding to free nepafenac alone and in the presence of γ CD or HP β CD were also examined (See Supplementary Information, Table S2).

3.6. Characterization of Formulation of 0.5% (*w/v*) Nepafenac Eye Drops

As shown in Table 6, the formulations with the largest drug solubilization capacity—F3, F4 and F1—had the highest recorded solid drug fraction values (63.6%, 62.4% and 61.3%, respectively). Several parameters can affect the viscosity of eye drops, such as the addition of surfactants, ions and also particle size. The formulations with the highest viscosity levels were F2, F3 and F5, with values between 14 and 19 centipoises (cP), making them suitable for use as eye drops. The formulations F8 and F1 had viscosity levels of approximately 4 cP and so were not considered for the formulation of eye drops due to low viscosity. The addition of 1% (*w/v*) CMC in formulations F2, F3, F5 and F7 led to higher viscosity and osmolality values than observed for the formulations that did not contain this polymer. Aggregates were between 208 and 581 nm in diameter for all formulations, with the exception of F1 and F8 which had diameters of 98 and 17 nm, respectively.

Table 6. Characteristics of 0.5% (*w/v*) eye drop formulations including solubility of nepafenac, proportion of solid drug fraction, osmolality, viscosity and aggregate size.

Formulations	Solubility of Nepafenac (mg/mL)	Solid Drug Fraction (%)	Osmolality (mOsm/kg)	Viscosity (cP)	Size (nm)	
					Diameter (nm)	Vol (%)
F1 (2% PVA, 0.1 HPMC, 0.1% tyloxapol)	3.063 \pm 0.108	61.26	198 \pm 2	3.62 \pm 0.03	98	58.1
					424	41.9
F2 (1% CMC)	2.516 \pm 0.014	50.32	338 \pm 13	18.92 \pm 2.16	212	55.4
					135	28.9
					427	13.7
					18	2
F3 (2% PVA, 1% CMC, 0.1% tyloxapol)	3.180 \pm 0.066	63.60	410 \pm 10	13.95 \pm 0.36	247	88.5
					3.0	11.5
F4 (2% PVA, 0.1% tyloxapol)	3.119 \pm 0.010	62.38	200 \pm 2	4.17 \pm 0.11	581	29
					241	28.8
					1127	23.4
					106	18.8
F5 (1% PVP, 1% CMC, 0.1% HPMC)	2.656 \pm 0.074	53.12	400 \pm 8	15.31 \pm 0.88	310	50.1
					170	27.5
					13	22.4
F6 (1% PVP, 0.1% MC)	2.384 \pm 0.172	47.08	186 \pm 5	4.89 \pm 0.31	350	77.4
					21	22.6
F7 (2% PVA, 1% CMC, 0.1% MC, 0.1% tyloxapol)	2.817 \pm 0.015	56.34	390 \pm 4	10.15 \pm 0.47	208	89.4
					644	9.1
					54	1.5
F8 (1% PVP, 0.1% tyloxapol)	1.685 \pm 0.054	33.70	193 \pm 2	3.83 \pm 0.16	17	74.5
					781	22.5
					1.0	3
F9 (2% PVA, 1% CMC, 0.1% MC)	2.422 \pm 0.056	48.44	392 \pm 7	13.56 \pm 0.92	208	97.7
					28	2.3

The best results in terms of solubility, size and viscosity were obtained for formulation F3 which contains 2% (*w/v*) PVA, 1% (*w/v*) CMC and 0.1% (*w/v*) tyloxapol. In all cases, more sodium chloride (NaCl) should be added to reach normal osmolality values of about 300 mOsm/kg [45].

TEM Analysis

Formulations F2, F3 and F5 were selected for morphology characterization by TEM (Figure 7).

In all formulations, aggregate particles were spherical or irregularly shaped. In the case of F2 (Figure 7a), aggregates were detected with varying sizes up to 500 nm. Smaller aggregates were found in F3 (Figure 7b) and F5 (Figure 7c), ranging in size between 200 and 300 nm. Size data obtained by TEM confirmed results regarding the size distribution of these nanoaggregates obtained through dynamic light scattering.

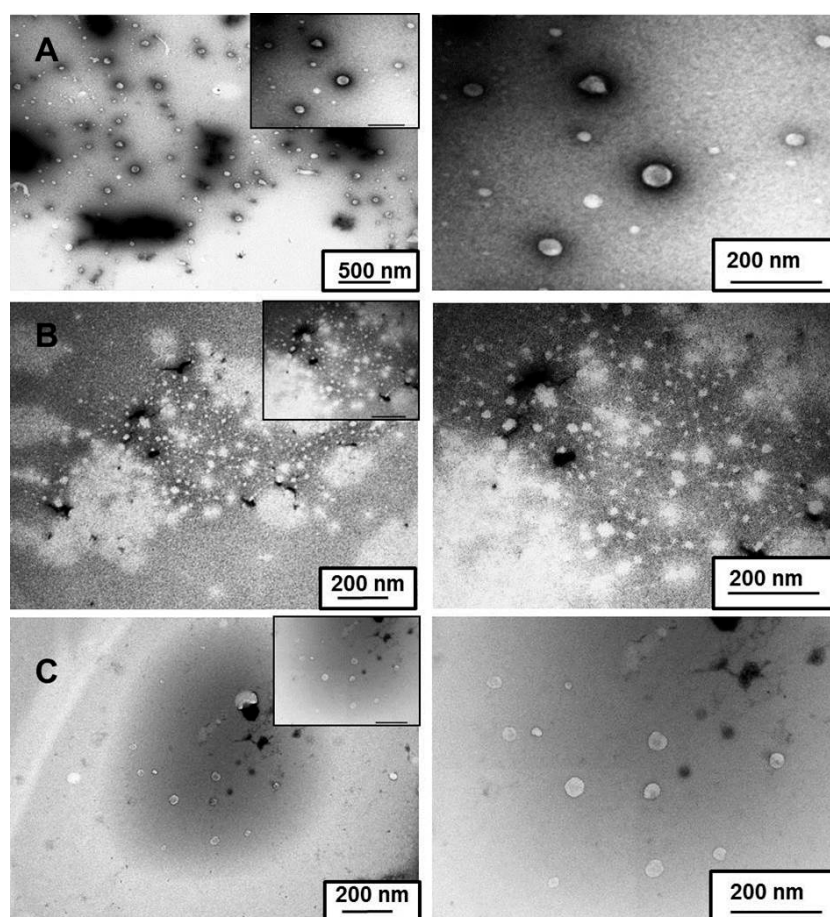


Figure 7. Transmission electron microscope (TEM) images of (a) F2 magnified by 15 k (left) and 60 k (right), (b) F3 magnified by 30 k (left) and 60 k (right) and (c) F5 magnified by 30 k (left) and 60 k (right).

4. Conclusions

This study was the first to investigate the strategy of adding hydrophilic polymers to nepafenac drug/CD complexes that included two different CDs in order to improve drug solubility and promote nanoaggregate formation. Results show that HP β CD performed best in terms of solubilization, while γ CD performed best in terms of enhancing nanoaggregate formation. The mean size of these aggregates was found in the range of 220–322 nm. Formation of inclusion complexes was confirmed by DSC, FT-IR and $^1\text{H-NMR}$ studies. DSC studies suggested that at least 8% (*w/v*) HP β CD was needed for optimal complex formation when used with 15% (*w/v*) γ CD. No synergistic effect on solubility was found using mixtures of γ CD and HP β CD. Addition of hydrophilic polymers, in particular CMC, PVA and tyloxapol, to formulations containing CDs led to higher nepafenac solubility. Overall, results of this study on the solubility and aggregate formation associated with various CDs in polymer solutions indicates that formulations of polymeric drug/CD nanoaggregates can be formed easily and represent a promising new approach to the formulation of nepafenac eye drops.

Supplementary Materials: The following are available online at <http://www.mdpi.com/1996-1944/12/2/229/s1>, Figure S1: Chemical structure of (a) natural cyclodextrins (α -, β - and γ -CDs) and (b) their hydroxyl-propyl derivatives (HP α -, HP β - and HP γ -CDs), Figure S2: H-NMR spectra of (a) HP β CD alone (top) and their complex (bottom) and (b) γ CD alone (top) and their complex (bottom), Table S1: Effect of cyclodextrins and excipients on osmolality, viscosity and size of binary and ternary systems with nepafenac, Table S2: Chemical shift corresponding to free nepafenac alone and in the presence of γ CD or HP β CD.

Author Contributions: Conceptualization, all authors; Methodology, all authors; Formal analysis, B.L.-V.; Resources, T.L. and B.L.-V.; Data Curation, B.L.-V.; Writing—Original Draft Preparation, B.L.-V.; Writing—Review and Editing, H.H.S.; Supervision, H.H.S and T.L.; Project Administration, H.H.S and T.L.; Funding Acquisition, T.L.

Funding: This research received no external funding.

Conflicts of Interest: The authors declare no conflicts of interest.

References

1. Achiron, A.; Karmona, L.; Mimouni, M.; Gershoni, A.; Dzhannov, Y.; Gur, Z.; Burgansky, Z. Comparison of the Tolerability of Diclofenac and Nepafenac. *J. Ocul. Pharmacol. Ther.* **2016**, *32*, 601–605. [[CrossRef](#)] [[PubMed](#)]
2. Caldwell, M.; Reilly, C. Effects of topical nepafenac on corneal epithelial healing time and postoperative pain after PRK: A bilateral, prospective, randomized, masked trial. *J. Refract. Surg.* **2008**, *24*, 377–382. [[PubMed](#)]
3. Lane, S.S.; Modi, S.S.; Lehmann, R.P.; Holland, E.J. Nepafenac ophthalmic suspension 0.1% for the prevention and treatment of ocular inflammation associated with cataract surgery. *J. Cataract Refract. Surg.* **2007**, *33*, 53–58. [[CrossRef](#)] [[PubMed](#)]
4. Margulis, A.V.; Houben, E.; Hallas, J.; Overbeek, J.A.; Pottegård, A.; Torp-Pedersen, T.; Perez-Gutthann, S.; Arana, A. Ophthalmic nepafenac use in the Netherlands and Denmark. *Acta Ophthalmol.* **2017**, *95*, 509–517. [[CrossRef](#)] [[PubMed](#)]
5. Ikuta, Y.; Aoyagi, S.; Tanaka, Y.; Sato, K.; Inada, S.; Koseki, Y.; Onodera, T.; Oikawa, H.; Kasai, H. Creation of nano eye-drops and effective drug delivery to the interior of the eye. *Sci. Rep.* **2017**, *7*, 44229. [[CrossRef](#)] [[PubMed](#)]
6. Urtti, A. Challenges and obstacles of ocular pharmacokinetics and drug delivery. *Adv. Drug Deliv. Rev.* **2006**, *58*, 1131–1135. [[CrossRef](#)] [[PubMed](#)]
7. Wang, Y.; Xu, X.; Gu, Y.; Cheng, Y.; Cao, F. Recent advance of nanoparticle-based topical drug delivery to the posterior segment of the eye. *Expert Opin. Drug Deliv.* **2018**, *15*, 687–701. [[CrossRef](#)] [[PubMed](#)]
8. Achouri, D.; Alhanout, K.; Piccerelle, P.; Andrieu, V. Recent advances in ocular drug delivery. *Drug Dev. Ind. Pharm.* **2013**, *39*, 1599–1617. [[CrossRef](#)] [[PubMed](#)]
9. Ludwig, A. The use of mucoadhesive polymers in ocular drug delivery. *Adv. Drug Deliv. Rev.* **2005**, *57*, 1595–1639. [[CrossRef](#)] [[PubMed](#)]
10. Shelley, H.; Babu, R.J. Role of Cyclodextrins in Nanoparticle-Based Drug Delivery Systems. *J. Pharm. Sci.* **2018**, *107*, 1741–1753. [[CrossRef](#)]
11. Simões, S.M.N.; Rey-Rico, A.; Concheiro, A.; Alvarez-Lorenzo, C. Supramolecular cyclodextrin-based drug nanocarriers. *Chem. Commun.* **2015**, *51*, 6275–6289. [[CrossRef](#)] [[PubMed](#)]
12. Varan, G.; Varan, C.; Erdogor, N.; Hincal, A.A.; Bilensoy, E. Amphiphilic cyclodextrin nanoparticles. *Int. J. Pharm.* **2017**, *531*, 457–469. [[CrossRef](#)] [[PubMed](#)]
13. Moya-Ortega, M.D.; Alvarez-Lorenzo, C.; Concheiro, A.; Loftsson, T. Cyclodextrin-based nanogels for pharmaceutical and biomedical applications. *Int. J. Pharm.* **2012**, *428*, 152–163. [[CrossRef](#)]
14. De Souza, V.C.; Barros, C.H.N.; Tasic, L.; Gimenez, I.F.; Teixeira Camargo, Z. Synthesis of cyclodextrin polymers containing glutamic acid and their use for the synthesis of Ag nanoparticles. *Carbohydr. Polym.* **2018**, *202*, 11–19. [[CrossRef](#)] [[PubMed](#)]
15. Gidwani, B.; Vyas, A. Synthesis, characterization and application of Epichlorohydrin- β -cyclodextrin polymer. *Colloids Surf. B Biointerfaces* **2014**, *114*, 130–137. [[CrossRef](#)] [[PubMed](#)]
16. Lim, L.M.; Tran, T.T.; Long Wong, J.J.; Wang, D.; Cheow, W.S.; Hadinoto, K. Amorphous ternary nanoparticle complex of curcumin-chitosan-hypromellose exhibiting built-in solubility enhancement and physical stability of curcumin. *Colloids Surf. B Biointerfaces* **2018**, *167*, 483–491. [[CrossRef](#)] [[PubMed](#)]
17. Xiao, P.; Dudal, Y.; Corvini, P.F.X.; Shahgaldian, P. Polymeric cyclodextrin-based nanoparticles: Synthesis, characterization and sorption properties of three selected pharmaceutically active ingredients. *Polym. Chem.* **2011**, *2*, 120–125. [[CrossRef](#)]

18. Zhou, J.; Ritter, H. Cyclodextrin functionalized polymers as drug delivery systems. *Polym. Chem.* **2010**, *1*, 1552–1559. [[CrossRef](#)]
19. Sapte, S.; Pore, Y. Inclusion complexes of cefuroxime axetil with beta-cyclodextrin: Physicochemical characterization, molecular modeling and effect of l-arginine on complexation. *J. Pharm. Anal.* **2016**, *6*, 300–306. [[CrossRef](#)]
20. Schwarz, D.H.; Engelke, A.; Wenz, G. Solubilizing steroidal drugs by beta-cyclodextrin derivatives. *Int. J. Pharm.* **2017**, *531*, 559–567. [[CrossRef](#)]
21. Szabó, Z.I.; Deme, R.; Mucsi, Z.; Rusu, A.; Mare, A.D.; Fiser, B.; Toma, F.; Sipos, E.; Tóth, G. Equilibrium, structural and antibacterial characterization of moxifloxacin- β -cyclodextrin complex. *J. Mol. Struct.* **2018**, *1166*, 228–236. [[CrossRef](#)]
22. Vaidya, B.; Parvathaneni, V.; Kulkarni, N.S.; Shukla, S.K.; Damon, J.K.; Sarode, A.; Kanabar, D.; Garcia, J.V.; Mitragotri, S.; Muth, A.; et al. Cyclodextrin modified erlotinib loaded PLGA nanoparticles for improved therapeutic efficacy against non-small cell lung cancer. *Int. J. Biol. Macromol.* **2019**, *122*, 338–347. [[CrossRef](#)]
23. Vaidya, B.; Shukla, S.K.; Kolluru, S.; Huen, M.; Mulla, N.; Mehra, N.; Kanabar, D.; Palakurthi, S.; Ayehunie, S.; Muth, A.; et al. Nintedanib-cyclodextrin complex to improve bio-activity and intestinal permeability. *Carbohydr. Polym.* **2019**, *204*, 68–77. [[CrossRef](#)] [[PubMed](#)]
24. Ryzhakov, A.; Do Thi, T.; Stappaerts, J.; Bertolotti, L.; Kimpe, K.; Couto, A.R.S.; Saokham, P.; Van den Mooter, G.; Augustijns, P.; Somsen, G.W.; et al. Self-Assembly of Cyclodextrins and Their Complexes in Aqueous Solutions. *J. Pharm. Sci.* **2016**, *105*, 2556–2569. [[CrossRef](#)] [[PubMed](#)]
25. Gidwani, B.; Vyas, A. A Comprehensive Review on Cyclodextrin-Based Carriers for Delivery of Chemotherapeutic Cytotoxic Anticancer Drugs. *BioMed Res. Int.* **2015**, *2015*, 198268. [[CrossRef](#)] [[PubMed](#)]
26. Jambhekar, S.S.; Breen, P. Cyclodextrins in pharmaceutical formulations I: Structure and physicochemical properties, formation of complexes and types of complex. *Drug Discov. Today* **2016**, *21*, 356–362. [[CrossRef](#)] [[PubMed](#)]
27. Monteil, M.; Lecouvey, M.; Landy, D.; Ruellan, S.; Mallard, I. Cyclodextrins: A promising drug delivery vehicle for bisphosphonate. *Carbohydr. Polym.* **2017**, *156*, 285–293. [[CrossRef](#)] [[PubMed](#)]
28. Aloisio, C.; de Oliveira, A.G.; Longhi, M. Solubility and release modulation effect of sulfamerazine ternary complexes with cyclodextrins and meglumine. *J. Pharm. Biomed. Anal.* **2014**, *100*, 64–73. [[CrossRef](#)]
29. Higashi, K.; Ideura, S.; Waraya, H.; Moribe, K.; Yamamoto, K. Structural evaluation of crystalline ternary gamma-cyclodextrin complex. *J. Pharm. Sci.* **2011**, *100*, 325–333. [[CrossRef](#)]
30. Inoue, Y.; Iohara, D.; Sekiya, N.; Yamamoto, M.; Ishida, H.; Sakiyama, Y.; Hirayama, F.; Arima, H.; Uekama, K. Ternary inclusion complex formation and stabilization of limaprost, a prostaglandin E1 derivative, in the presence of alpha- and beta-cyclodextrins in the solid state. *Int. J. Pharm.* **2016**, *509*, 338–347. [[CrossRef](#)]
31. Mennini, N.; Maestrelli, F.; Cirri, M.; Mura, P. Analysis of physicochemical properties of ternary systems of oxaprozin with randomly methylated- β -cyclodextrin and l-arginine aimed to improve the drug solubility. *J. Pharm. Biomed. Anal.* **2016**, *129*, 350–358. [[CrossRef](#)] [[PubMed](#)]
32. Palma, S.D.; Tartara, L.I.; Quinteros, D.; Allemandi, D.A.; Longhi, M.R.; Granero, G.E. An efficient ternary complex of acetazolamide with HP- β -CD and TEA for topical ocular administration. *J. Control. Release* **2009**, *138*, 24–31. [[CrossRef](#)]
33. Wang, D.; Li, H.; Gu, J.; Guo, T.; Yang, S.; Guo, Z.; Zhang, X.; Zhu, W.; Zhang, J. Ternary system of dihydroartemisinin with hydroxypropyl-beta-cyclodextrin and lecithin: Simultaneous enhancement of drug solubility and stability in aqueous solutions. *J. Pharm. Biomed. Anal.* **2013**, *83*, 141–148. [[CrossRef](#)] [[PubMed](#)]
34. Terekhova, I.; Chibunova, E.; Kumeev, R.; Kruchinin, S.; Fedotova, M.; Kozbiał, M.; Wszelaka-Rylik, M.; Gierycz, P. Specific and nonspecific effects of biologically active inorganic salts on inclusion complex formation of cyclodextrins with aromatic carboxylic acids. *Chem. Eng. Sci.* **2015**, *122*, 97–103. [[CrossRef](#)]
35. De Medeiros, A.S.; Zoppi, A.; Barbosa, E.G.; Oliveira, J.I.; Fernandes-Pedrosa, M.F.; Longhi, M.R.; da Silva-Júnior, A.A. Supramolecular aggregates of oligosaccharides with co-solvents in ternary systems for the solubilizing approach of triamcinolone. *Carbohydr. Polym.* **2016**, *151*, 1040–1051. [[CrossRef](#)]
36. Jadhav, P.; Petkar, B.; Pore, Y.; Kulkarni, A.; Burade, K. Physicochemical and molecular modeling studies of cefixime-l-arginine-cyclodextrin ternary inclusion compounds. *Carbohydr. Polym.* **2013**, *98*, 1317–1325.
37. Bera, H.; Chekuri, S.; Sarkar, S.; Kumar, S.; Muvva, N.B.; Mothe, S.; Nadimpalli, J. Novel pimozone- β -cyclodextrin-polyvinylpyrrolidone inclusion complexes for Tourette syndrome treatment. *J. Mol. Liq.* **2016**, *215*, 135–143. [[CrossRef](#)]

38. Davis, M.T.; Potter, C.B.; Mohammadpour, M.; Albadarin, A.B.; Walker, G.M. Design of spray dried ternary solid dispersions comprising itraconazole, soluplus and HPMCP: Effect of constituent compositions. *Int. J. Pharm.* **2017**, *519*, 365–372. [[CrossRef](#)]
39. Patel, P.; Agrawal, Y.K.; Sarvaiya, J. Cyclodextrin based ternary system of modafinil: Effect of trimethyl chitosan and polyvinylpyrrolidone as complexing agents. *Int. J. Biol. Macromol.* **2016**, *84*, 182–188. [[CrossRef](#)]
40. Soliman, K.A.; Ibrahim, H.K.; Ghorab, M.M. Effect of different polymers on avanafil-beta-cyclodextrin inclusion complex: In vitro and in vivo evaluation. *Int. J. Pharm.* **2016**, *512*, 168–177. [[CrossRef](#)]
41. Nogueiras-Nieto, L.; Sobarzo-Sanchez, E.; Gomez-Amoza, J.L.; Otero-Espinar, F.J. Competitive displacement of drugs from cyclodextrin inclusion complex by polypseudorotaxane formation with poloxamer: Implications in drug solubilization and delivery. *Eur. J. Pharm. Biopharm.* **2012**, *80*, 585–595. [[CrossRef](#)]
42. Taveira, S.F.; Varela-Garcia, A.; dos Santos Souza, B.; Marreto, R.N.; Martin-Pastor, M.; Concheiro, A.; Alvarez-Lorenzo, C. Cyclodextrin-based poly(pseudo)rotaxanes for transdermal delivery of carvedilol. *Carbohydr. Polym.* **2018**, *200*, 278–288. [[CrossRef](#)]
43. Jansook, P.; Muankaew, C.; Stefansson, E.; Loftsson, T. Development of eye drops containing antihypertensive drugs: Formulation of aqueous irbesartan/ γ CD eye drops. *Pharm. Dev. Technol.* **2015**, *20*, 626–632. [[CrossRef](#)]
44. Jansook, P.; Pichayakorn, W.; Muankaew, C.; Loftsson, T. Cyclodextrin-poloxamer aggregates as nanocarriers in eye drop formulations: Dexamethasone and amphotericin B. *Drug Dev. Ind. Pharm.* **2016**, *42*, 1446–1454. [[CrossRef](#)]
45. Johannsdottir, S.; Jansook, P.; Stefansson, E.; Loftsson, T. Development of a cyclodextrin-based aqueous cyclosporin A eye drop formulations. *Int. J. Pharm.* **2015**, *493*, 86–95. [[CrossRef](#)]
46. Muankaew, C.; Jansook, P.; Sigurdsson, H.H.; Loftsson, T. Cyclodextrin-based telmisartan ophthalmic suspension: Formulation development for water-insoluble drugs. *Int. J. Pharm.* **2016**, *507*, 21–31. [[CrossRef](#)] [[PubMed](#)]
47. Loftsson, T.; Brewster, M.E. Cyclodextrins as functional excipients: Methods to enhance complexation efficiency. *J. Pharm. Sci.* **2012**, *101*, 3019–3032. [[CrossRef](#)]
48. Ogawa, N.; Furuishi, T.; Nagase, H.; Endo, T.; Takahashi, C.; Yamamoto, H.; Kawashima, Y.; Loftsson, T.; Kobayashi, M.; Ueda, H. Interaction of fentanyl with various cyclodextrins in aqueous solutions. *J. Pharm. Pharm.* **2016**, *68*, 588–597. [[CrossRef](#)]
49. Jansook, P.; Kurkov, S.V.; Loftsson, T. Cyclodextrins as solubilizers: Formation of complex aggregates. *J. Pharm. Sci.* **2010**, *99*, 719–729. [[CrossRef](#)]
50. Messner, M.; Kurkov, S.V.; Maraver Palazon, M.; Alvarez Fernandez, B.; Brewster, M.E.; Loftsson, T. Self-assembly of cyclodextrin complexes: Effect of temperature, agitation and media composition on aggregation. *Int. J. Pharm.* **2011**, *419*, 322–328. [[CrossRef](#)]
51. Higuchi, T.; Connors, K.A. Advances in Analytical Chemistry and Instrumentation. *Adv. Anal. Chem. Instrum.* **1965**, *4*, 117–212.
52. Jambhekar, S.S.; Breen, P. Cyclodextrins in pharmaceutical formulations II: Solubilization, binding constant and complexation efficiency. *Drug Discov. Today* **2016**, *21*, 363–368. [[CrossRef](#)] [[PubMed](#)]
53. Del Valle, E.M.M. Cyclodextrins and their uses: A review. *Process Biochem.* **2004**, *39*, 1033–1046. [[CrossRef](#)]
54. Kicuntod, J.; Sangpheak, K.; Mueller, M.; Wolschann, P.; Viernstein, H.; Yanaka, S.; Kato, K.; Chavasiri, W.; Pongsawasdi, P.; Kungwan, N.; et al. Theoretical and Experimental Studies on Inclusion Complexes of Pinostrobin and beta-Cyclodextrins. *Sci. Pharm.* **2018**, *86*, 5. [[CrossRef](#)] [[PubMed](#)]
55. Challa, R.; Ahuja, A.; Ali, J.; Khar, R.K. Cyclodextrins in drug delivery: An updated review. *AAPS PharmSciTech* **2005**, *6*, E329–E357. [[CrossRef](#)] [[PubMed](#)]
56. Saarinen-Savolainen, P.; Jarvinen, T.; Araki-Sasaki, K.; Watanabe, H.; Urtti, A. Evaluation of cytotoxicity of various ophthalmic drugs, eye drop excipients and cyclodextrins in an immortalized human corneal epithelial cell line. *Pharm. Res.* **1998**, *15*, 1275–1280. [[CrossRef](#)] [[PubMed](#)]
57. Jansook, P.; Ritthidej, G.C.; Ueda, H.; Stefansson, E.; Loftsson, T. γ CD/HPyCD mixtures as solubilizer: Solid-state characterization and sample dexamethasone eye drop suspension. *J. Pharm. Pharm.* **2010**, *13*, 336–350. [[CrossRef](#)]
58. Jansook, P.; Loftsson, T. CDs as solubilizers: Effects of excipients and competing drugs. *Int. J. Pharm.* **2009**, *379*, 32–40. [[CrossRef](#)] [[PubMed](#)]
59. Schneider, H.J.; Hacket, F.; Rudiger, V.; Ikeda, H. NMR Studies of Cyclodextrins and Cyclodextrin Complexes. *Chem. Rev.* **1998**, *98*, 1755–1786. [[CrossRef](#)] [[PubMed](#)]

60. Goswami, S.; Sarkar, M. Fluorescence, FTIR and ^1H NMR studies of the inclusion complexes of the painkiller lornoxicam with β -, γ -cyclodextrins and their hydroxypropyl derivatives in aqueous solutions at different pHs and in the solid state. *New J. Chem.* **2018**, *42*, 15146–15156. [[CrossRef](#)]
61. Yuan, C.; Jin, Z.; Xu, X. Inclusion complex of astaxanthin with hydroxypropyl-beta-cyclodextrin: UV, FTIR, ^1H NMR and molecular modeling studies. *Carbohydr. Polym.* **2012**, *89*, 492–496. [[CrossRef](#)] [[PubMed](#)]
62. Corti, G.; Cirri, M.; Maestrelli, F.; Mennini, N.; Mura, P. Sustained-release matrix tablets of metformin hydrochloride in combination with triacetyl- β -cyclodextrin. *Eur. J. Pharm. Biopharm.* **2008**, *68*, 303–309. [[CrossRef](#)] [[PubMed](#)]
63. Tang, P.; Li, S.; Wang, L.; Yang, H.; Yan, J.; Li, H. Inclusion complexes of chlorzoxazone with beta- and hydroxypropyl-beta-cyclodextrin: Characterization, dissolution and cytotoxicity. *Carbohydr. Polym.* **2015**, *131*, 297–305. [[CrossRef](#)] [[PubMed](#)]
64. He, J.; Zheng, Z.P.; Zhu, Q.; Guo, F.; Chen, J. Encapsulation Mechanism of Oxyresveratrol by beta-Cyclodextrin and Hydroxypropyl-beta-Cyclodextrin and Computational Analysis. *Molecules* **2017**, *22*, 1801. [[CrossRef](#)] [[PubMed](#)]
65. Rekharsky, M.V.; Goldberg, R.N.; Schwarz, F.P.; Tewari, Y.B.; Ross, P.D.; Yamashoji, Y.; Inoue, Y. Thermodynamic and Nuclear Magnetic Resonance Study of the Interactions of α - and β -Cyclodextrin with Model Substances: Phenethylamine, Ephedrines and Related Substances. *J. Am. Chem. Soc.* **1995**, *117*, 8830–8840. [[CrossRef](#)]



© 2019 by the authors. Licensee MDPI, Basel, Switzerland. This article is an open access article distributed under the terms and conditions of the Creative Commons Attribution (CC BY) license (<http://creativecommons.org/licenses/by/4.0/>).

Paper II



Article

In Vitro and Ex Vivo Evaluation of Nepafenac-Based Cyclodextrin Microparticles for Treatment of Eye Inflammation

Blanca Lorenzo-Veiga ¹, Patricia Diaz-Rodriguez ^{2,3}, Carmen Alvarez-Lorenzo ³, Thorsteinn Loftsson ¹ and Hakon Hrafn Sigurdsson ^{1,*}

¹ Faculty of Pharmaceutical Sciences, University of Iceland, Hofsvallagata 53, IS-107 Reykjavik, Iceland; blv3@hi.is (B.L.-V.); thorstlo@hi.is (T.L.)

² Departamento de Ingeniería Química y Tecnología Farmacéutica, Facultad de Ciencias de la Salud, Universidad de la Laguna (ULL), Campus de Anchieta, 38200 La Laguna (Tenerife), Spain; pdiarodr@ull.edu.es

³ Departamento de Farmacología, Farmacia y Tecnología Farmacéutica, R+D Pharma Group (GI-1645), Facultad de Farmacia and Health Research Institute of Santiago de Compostela (IDIS), Universidade de Santiago de Compostela, 15782 Santiago de Compostela, Spain; carmen.alvarez.lorenzo@usc.es

* Correspondence: hhs@hi.is

Received: 6 March 2020; Accepted: 7 April 2020; Published: 9 April 2020



Abstract: The aim of this study was to design and evaluate novel cyclodextrin (CD)-based aggregate formulations to efficiently deliver nepafenac topically to the eye structure, to treat inflammation and increase nepafenac levels in the posterior segment, thus attenuating the response of inflammatory mediators. The physicochemical properties of nine aggregate formulations containing nepafenac/ γ -CD/hydroxypropyl- β (HP β)-CD complexes as well as their rheological properties, mucoadhesion, ocular irritancy, corneal and scleral permeability, and anti-inflammatory activity were investigated in detail. The results were compared with a commercially available nepafenac suspension, Nevanac[®] 3 mg/mL. All formulations showed microparticles, neutral pH, and negative zeta potential (−6 to −27 mV). They were non-irritating and nontoxic and showed high permeation through bovine sclera. Formulations containing carboxymethyl cellulose (CMC) showed greater anti-inflammatory activity, even higher than the commercial formulation, Nevanac[®] 0.3%. The optimized formulations represent an opportunity for topical instillation of drugs to the posterior segment of the eye.

Keywords: eye drop; cyclodextrin; nepafenac; HET-CAM; ex vivo permeation studies; ocular inflammation

1. Introduction

Inflammation of the eye and surrounding tissues is among the ocular pathologies with the highest incidence in ophthalmology, which, deprived of the appropriate treatment, can lead to visual loss [1]. The main symptoms include eye redness, eye pain, itchiness, blurred vision, swelling, and visual distortions [2]. The most common causes of ocular inflammation at the posterior segment of the eye are related to eye disorders such as glaucoma, macular edema, cataract surgery intervention, scleritis, posterior uveitis, and diabetic retinopathy [3,4]. Other causes that affect the anterior segment of the eye include conjunctivitis, ocular infections, anterior and intermediate uveitis, dry eye syndrome, keratitis, use of contact lenses, and trauma [5]. Although inflammation can be triggered by a variety of etiological causes, the symptoms are similar, as they induce similar immunological response [6,7].

Treating inflammation at the posterior segment classically involves ophthalmic steroids as well as nonsteroidal anti-inflammatory drugs (NSAIDs) [8,9]. The repetitive use of traditional corticosteroids

such as fluocinolone, dexamethasone, prednisolone, or fluorometholone can lead to undesirable side effects, such as high intraocular pressure, risk of infection, cataract formation, or macular edema [10]. Ophthalmic NSAIDs approved by the US Food and Drug Administration (FDA) used for the treatment of ocular inflammation and pain include diclofenac 0.1%, ketorolac 0.6%, and bromfenac 0.09% solutions, and nepafenac 0.1% and 0.3% suspensions [11,12]. The use of topical NSAID formulations can lead to cornea infiltrations, cornea melting, or keratitis [13]. Nepafenac is an NSAID prescribed prophylactically as well as post cataract surgery. It is currently approved for treatment of pain and inflammation after cataract surgery and commercialized as an eye drop suspension, Nevanac[®], in two doses, 1 mg/mL three times per day and 3 mg/mL once per day [14]. The side effects include increased intraocular pressure, decreased visual acuity, and sticky eyes [15]. Sahu et al. [16] analyzed the effects of three topical NSAIDs (ketorolac 0.4%, nepafenac 0.1%, and bromfenac 0.09%) on inflammation after surgery. Their results showed that nepafenac was significantly more effective than the others at reducing anterior chamber redness. Moreover, Modi et al. [17] demonstrated the convenience of instilling nepafenac 0.3% once a day compared to Nevanac[®] 0.1% three times a day, as they both showed the same efficacy.

Unlike other NSAIDs, nepafenac is a prodrug. After topical ocular treatment, it penetrates the cornea and is transformed by ocular tissue hydrolases into its active metabolite, amfenac (Figure 1), an inhibitor of cyclooxygenase-1 and -2 (COX-1, COX-2) [18,19]. The expression of cyclooxygenase enzyme has been widely studied [19,20]. The activation of COX-1 and COX-2 is involved in prostaglandin production, and therefore in the inflammation process in the eye. Because of eye inflammation, changes to the blood–ocular barrier, ocular angiogenesis, and vascular permeability can occur. Inhibition of COX activity blocks the formation of proinflammatory mediators, including prostaglandins, reducing edema and inflammation [21,22].



Figure 1. Structures of (a) nepafenac and (b) amfenac.

Treating the posterior segment in eye diseases by means of topical instillation is still a challenge, due to the different biological membranes and physical boundaries of the eye that restrict drug passage and penetration [23–25]. Newly biodegradable nanoparticulated drug systems have been proposed as promising alternatives in the treatment of retinal diseases [26–28]. Tahara et al. [29] prepared poly(lactide-co-glycolide) (PLGA) nanoparticles of three corticosteroids (dexamethasone, hydrocortisone acetate and prednisolone acetate) suspended in gels for the treatment of macular edema and studied their ex vivo permeation using rabbit eyes. These polymeric nanoparticles were able to sustain drug delivery to the retina after episcleral administration. Furthermore, Balguri et al. [30] designed chitosan-based solid lipid nanoparticles that were able to deliver indomethacin to the cornea and sclera. Additionally, conventional eye drops are not able to maintain therapeutic concentrations in the ocular tissues due to short contact time and fast elimination [31–33]. To overcome these problems, cyclodextrin (CD) nanoparticles have been proposed as one of the best options for topical eye drop instillation of both small-molecule drugs and biomolecules to the eye [34]. An aqueous-based eye drop formulation of 0.2% (w/v) cyclosporine A with 12.5% (w/v) alpha-cyclodextrin (α -CD), various amounts of gamma-cyclodextrin (γ -CD), and 1.4% (w/v) hydrolyzed poly(vinyl alcohol) (PVA) was shown to be well tolerated in rabbits [35,36]. Furthermore, some CD-based eye drop formulations are already commercialized (Clorocil[®], Voltaren[®], Vitaseptol[®], and Indocid[®]) [37]. Combinations of polymers and cyclodextrins have been reported as a strategy to enhance drug permeation in ocular tissues [38–40].

Recently, we found that the addition of one or more polymers to nepafenac/ γ -CD/hydroxypropyl- β (HP β)-CD complexes (Table 1) leads to the enhancement of its solubility in water, offering an alternative to current nepafenac eye drops [41], and therefore their efficacy should be further evaluated. The polymer compositions of preliminary eye drop suspensions are summarized in Table 1.

Table 1. Preliminary nepafenac aggregate formulations. All contain a mixture of 15% (w/v) γ -CD and 8% (w/v) HP β -CD in aqueous solution [41].

Formulations
F2 = 1.0% (w/v) CMC
F3 = 2.0% (w/v) PVA + 1.0% (w/v) CMC + 0.1% (w/v) Tyloxapol
F5 = 1.0% (w/v) PVP + 1.0% (w/v) CMC + 0.1% (w/v) HPMC
F9 = 2.0% (w/v) PVA + 1.0% (w/v) CMC + 0.1% (w/v) MC

CD, cyclodextrin; HP β , hydroxypropyl- β ; CMC, carboxymethylcellulose; HPMC, hydroxypropylmethylcellulose; MC, methyl cellulose; PVA, hydrolyzed poly(vinyl alcohol); PVP, polyvinylpyrrolidone.

This study was aimed at the development and evaluation of novel CD-based aqueous eye drop formulations containing mucoadhesive polymers (sodium hyaluronate and sodium alginate) and comparing their effectiveness with previous formulations developed to efficiently deliver nepafenac to the eye in order to treat inflammation, increase drug concentration in the posterior segment, and reduce the expression of inflammatory mediators. All aggregate formulations were evaluated for in vitro diffusion studies, rheological and mucoadhesive properties, in vitro anti-inflammatory activity, and ex vivo corneal and scleral permeability studies. They were compared with a commercial Nevanac[®] 3 mg/mL suspension. To the best of our knowledge, this is the first time that formulations containing γ -CD/HP β -CD nanoparticles have been evaluated in vitro and ex vivo.

2. Materials and Methods

2.1. Materials

Nepafenac (98% purity, MW 254.28 g/mol) was acquired from Fagron (Rotterdam, Netherlands); γ -cyclodextrin (γ -CD) was provided by Wacker Chemie (Munich, Germany); 2-hydroxypropyl- β -cyclodextrin, DS 0.62 (HP β -CD; MW 1380 Da) was kindly donated by Janssen Pharmaceutica (Beerse, Belgium). Methyl cellulose (MC; MW 14,000 Da; viscosity ~15 cPs) was from ICN Biomedicals Inc. (Solon, OH, USA); sodium alginate (SA; MW 80,000–12,000 Da) was from Fagron Iberica (Zaragoza, Spain); sodium hyaluronate (HA; MW 360,000 Da, glucuronic acid 47.4%) was from Guinama (La Pobra de Valbona, Spain).

Benzalkonium chloride (BAK), ethylenediamine-tetraacetic acid disodium salt dihydrate (EDTA), reagent-grade tyloxapol (MW 280.4 g/mol), 87%–90% hydrolyzed poly(vinyl alcohol) (PVA) (average MW 30,000–70,000 Da), hydroxypropyl methylcellulose (HPMC; MW 26,000 Da, viscosity ~100 cPs), polyvinylpyrrolidone (PVP; average MW 40,000 Da), and carboxymethylcellulose (CMC) sodium salt (MW 90,000 Da; low viscosity) were purchased from Sigma-Aldrich (St. Louis, MO, USA). Membrane filters (0.45 μ m) were obtained from Phenomenex (Cheshire, UK). Water was purified using reverse osmosis (resistivity > 18 M Ω cm; Milli-Q, Millipore[®], Madrid, Spain). All other reagents were analytical grade.

Carbonate buffer, pH 7.2, was prepared by mixing buffer solution A (100 mL; 1.24 g NaCl, 0.071 g KCl, 0.02 g NaH₂PO₄, 0.49 g NaHCO₃) and buffer solution B (100 mL; 0.023 g CaC₁₂, 0.031 g MgC₁₂).

BALB/3T3 clone A31 mouse fibroblasts (ATCC CCL-163TM) and THP-1 monocytes (ATCC TIB-202TM) were purchased from the American Type Culture Collection (ATCC, Manassas, VA, USA). Fetal bovine serum (FBS), antibiotic solution (penicillin 10,000 units/mL and streptomycin 10.00 μ g/mL), lipopolysaccharides (LPS) from E. coli, phorbol 12-myristate 13-acetate (PMA), tris hydrochloride, and lauryl sulfate sodium salt (SDS) were acquired from Sigma-Aldrich (St. Louis, MO, USA). Dulbecco's Modified Eagle's Medium with Ham's F-12 Nutrient Mixture (DMEM/F12) and RPMI 1640 were

supplied by Gibco (Thermo Fisher, Paisley, UK). WST-1 Cell Proliferation Reagent was purchased from La Roche (Manheim, Germany).

2.2. Nepafenac Eye Drop Preparation

Nepafenac (18 mg) was added to 6 mL of an aqueous 15% γ -CD/8%HP- β CD (w/v) solution containing different polymers (Table 2), 0.1% (w/v) EDTA, 0.02% (w/v) BAK, and 0.04% (w/v) NaCl.

Table 2. Polymers used to prepare nepafenac eye drop formulations and their percentages.

Component (% w/v)	Eye Drop Formulations								
	A1	A2	A3	A4	A5	A6	A7	A8	A9
PVP	–	–	–	–	1.0	–	–	–	–
PVA	–	–	2.0	–	–	–	–	–	2.0
CMC	–	1.0	1.0	1.0	1.0	1.0	–	1.0	1.0
HPMC	–	–	–	–	0.1	–	–	–	–
MC	–	–	–	–	–	–	–	–	0.1
Tyloxapol	–	–	0.1	–	–	–	–	–	–
HA	0.2	–	–	0.2	–	–	–	0.2	–
SA	–	–	–	–	–	0.4	0.4	0.4	–

CMC, carboxymethylcellulose; HPMC, hydroxypropylmethylcellulose; MC, methyl cellulose; PVA, poly(vinyl alcohol); PVP, polyvinylpyrrolidone; HA, sodium hyaluronate; SA, sodium alginate.

Subsequently, suspensions were placed in an ultrasonic water bath (Branson 3510 Ultrasonic Cleaner, Marshall Scientific, Hampton, NH, USA) at 60 °C for 60 min. They were cooled down to room temperature and kept in a shaker (Unitronic, JP Selecta, Spain) under constant agitation for 7 days at 37 °C. After this, suspensions were filtered (Acrodisc[®] Syringe Filter, 0.22 μ m; GHP Minispikes, Waters) and centrifuged at 4000 rpm for 15 min at 25 °C (centrifuge model 5804R, Eppendorf AG, Germany), and supernatant was diluted with Milli-Q water. The apparent nepafenac solubility was determined by UV-Vis spectroscopy at 254 nm using a standard calibration curve previously validated in triplicate in the range 3–25 μ g/mL.

2.3. Physicochemical Characterization

2.3.1. Particle Size Analysis

Particle size and size distribution of formulations A1 to A9 and Nevanac was measured by dynamic light scattering (DLS) using a Nanotracs Wave particle analyzer (Microtrac, York, PA, USA). Samples that were previously filtered were diluted with Milli-Q water, and measurements were carried out at 25 °C with a 780 nm laser and 180° scattering angle. Each measurement was done in triplicate.

2.3.2. Zeta Potential and pH

Zeta potential of formulations A1 to A9 was recorded using a Zetasizer[®] 3000HS. pH was measured with a GLP22 pH meter (Crisson Instruments, Barcelona, Spain). All measurements were done in triplicate at 25 °C.

2.3.3. Rheological Analysis

Rheological characterization of formulations was carried out using a Rheolyst AR-1000N rheometer (TA Instruments, Newcastle, UK) equipped with an AR2500 data analyzer, a Peltier plate, and a cone (6 cm diameter, 2.1°). First, storage (G') and loss (G'') moduli were recorded at 37 °C and 0.1 Pa applying angular frequency sweeps from 0.1 to 50 rad/s. Viscosity and flow curves were performed under rotational runs at 37 °C for 2 min with shear stress in the range 0.1 to 200 s^{-1} . Data analysis was

carried out using Rheology Advantage data analysis software. Experiments were performed using 1.5 mL for each formulation.

2.3.4. In Vitro Mucoadhesive Studies

Mucoadhesion strength was evaluated in triplicate using a TA.XT Plus Texture analyzer (Stable Micro Systems Products, Godalming, UK) following methods previously described by Akhter et al. [42] and Campaña-Seoane et al. [43] with some modifications. Bovine corneas were placed beneath double-sided tape at the end of the probe. To simulate the eye drop application, 15 μ L of each formulation was placed at the bottom of a Petri dish. Mucoadhesion strength was determined as the detachment force needed to separate the formulation from the cornea after applying a force of 0.5 N for 60 seconds.

2.4. Ocular Tolerance Test (HET-CAM assay)

The ocular irritation test was carried out as previously reported [44]. Briefly, 200 μ L of each formulation was tested, at least in duplicate, on chorioallantoic membranes (Hen's Egg Test-Chorioallantoic Membrane, HET-CAM) of chicken eggs after 10 days of incubation at 37 °C and 60% RH. The time and severity of injuries after the addition of each formulation was recorded. The irritation score (IS) was calculated as follows (34):

$$IS = \frac{(301 - tH) \times 5}{300} + \frac{(301 - tL) \times 7}{300} + \frac{(301 - tC) \times 9}{300} \quad (1)$$

where tH, tL, and tC are the time (in seconds) needed for the appearance of hemolysis, lysis, and coagulation, respectively. Depending on IS values, formulations were classified as non-irritating ($IS < 1$), mildly irritating ($1 \leq IS < 5$), moderately irritating ($5 \leq IS < 10$), or severely irritating ($IS > 10$).

2.5. In Vitro Cell Viability

The cytocompatibility of cyclodextrin formulations was evaluated on BALB/3T3 clone A31 (ATCC[®] CCL-163TM) murine fibroblasts using the WST-1 test. BALB 3T3 cells were cultured in DMEM/F12 culture medium (Corning) supplemented with 10% fetal bovine serum (Hyclone) and 1% penicillin/streptomycin (Gibco). They were seeded in a 96-well plate at 1.5×10^4 cells/well. To allow complete cell attachment, cells were incubated 4 h at 37 °C and 5% CO₂. Aliquots of A1 to A9 formulations, Nevanac 3 mg/mL suspension, and control (DMEM/F12) were diluted 1:50, 1:100, and 1:150 times, respectively, with complete cell culture medium to be below the IC₅₀ of nepafenac, to ensure that nepafenac was not in cytotoxic concentrations, and added to cell monolayers [45]. DMEM/F12 medium was used as control. After 24 hours of incubation with the formulations, WST-1 reagent (Roche) was added and the assay was carried out according to the manufacturer's instructions. The absorbance was measured at 450 nm using a Model 680 microplate reader from Bio-Rad (Hercules, CA, USA) and Microplate Manager software (Version 5.2.1, BioRad, CA, USA).

2.6. Diffusion Assays

Nepafenac diffusion tests from eye drop formulations were performed in triplicate in vertical Franz diffusion cells fitted with cellulose acetate membrane filters (0.45 μ m pore size, 25 mm diameter). Membrane filters were soaked in the receptor medium for 1 hour before starting the experiment. The donor phase consisted of aliquots of 1.00 mL of the test formulation. The receptor phase was 6.00 mL of 2.5% (w/v) γ -CD/HP β -CD ratio (80/20) aqueous medium to ensure sink conditions, and kept at 37 °C and under magnetic stirring at 300 rpm. The diffusion area was 0.786 cm². Samples (1 mL) were taken from the receptor phase at 30, 60, 90, 120, 180, 210, 240, 300, and 360 min and replaced with fresh medium. Commercial eye drops, Nevanac 3 mg/mL, were also tested. Nepafenac content

was determined by UV-VIS spectrophotometry at 254 nm using a method previously validated with standard solutions in the range of 3–25 µg/mL.

Diffusion coefficients (D) were estimated from the Higuchi equation:

$$\frac{Q}{A} = 2C_0 \left(\frac{Dt}{\pi} \right)^{\frac{1}{2}} \quad (2)$$

where Q is the amount of nepafenac (g) released by time t (min), A is the diffusion area (cm²), C₀ is the initial concentration of nepafenac in the formulation (g/mL), and D is the diffusion coefficient (cm²/min).

2.7. Ex Vivo Corneal and Scleral Permeability

Ex vivo corneal and scleral permeability studies of selected nepafenac formulations were carried out using fresh bovine eyes from a local slaughterhouse. The eyes were kept in phosphate-buffered saline (PBS) solution with antibiotics previously added (penicillin 100 IU/mL and streptomycin 100 µg/mL) and maintained in an ice bath during transport. Corneas and scleras were isolated, washed with PBS, and placed on vertical diffusion Franz cells. Both receptor and donor phases were filled with carbonate buffer, pH 7.2, following the bovine corneal opacity and permeability (BCOP) protocol, placed in a bath at 37 °C, and kept under magnetic stirring for 1 h in order to balance ocular tissues. After this, the buffer in the donor chamber was completely removed and replaced by the formulations (2 mL). Chambers were covered with parafilm to prevent evaporation (0.785 cm² area available for permeation). Samples (1 mL) were removed from the receptor chamber at 0.5, 1, 2, 3, 4, 5, and 6 h, replacing the same volume with carbonate buffer each time, and taking care to remove bubbles from the diffusion cells. All experiments were carried out in triplicate.

Permeated nepafenac was quantified at 254 nm using a Jasco HPLC system (AS-4140 autosampler, PU-4180 pump, LC-NetII/ADC interface box, CO-4060 column oven, MD-4010 photodiode array detector), with a C18 column (Waters Symmetry C18, 5 µm, 3.9 × 150 mm) and ChromNAV software. The mobile phase consisted of acetonitrile: water (50:50) at a flow rate of 1 mL/min and 90 µL for injection volume and retention time of 1.9 min.

After a 6 h permeation test, aliquots of the donor chambers were taken for HPLC analysis. Previously injected corneas and scleras were excised and nepafenac content was extracted in tubes with 3 mL of ethanol/water (50:50 v/v) mixture for 24 h at 37 °C, and sonication was applied for 90 min in an ultrasound bath at 37 °C. Afterwards, tubes were centrifuged (1000 rpm, 5 min, 25 °C), and the supernatant was filtered (Acrodisc[®] syringe filter, 0.22 µm GHP Minispike, Waters) into small Eppendorfs, centrifuged again (14,000 rpm, 20 min, 25 °C), and filtered to be measured by HPLC.

The apparent permeability coefficient (P_{app}) was calculated from the flux (J) according to Equation (3):

$$P_{app} = \frac{J}{C_0} \quad (3)$$

where J is the flux, calculated as the slope (Q/t) of the linear section of the amount of drug in the receptor chamber (Q) versus time (t), and C₀ is the initial concentration of nepafenac in the donor phase. Each experiment was performed in triplicate and the results are reported as mean values ± standard deviation (SD).

2.8. Human Monocytes

2.8.1. Differentiation into Macrophages

THP-1 human monocytes (ATCC TIB-202[™]) were cultured in RPMI 1640 (Gibco) supplemented with 10% fetal bovine serum (Hyclone), 2-mercaptoethanol (0.05 mM; Gibco), and 1% penicillin-streptomycin (Gibco). Phorbol 12-myristate 13-acetate (PMA; Sigma-Aldrich) 200 nM was used to promote the differentiation of THP-1 monocytes into macrophages [46]. Previously,

monocytes had been counted in a Coulter Multisizer3 (Beckman Coulter, Indianapolis, IN, USA) and cell density was adjusted to 200,000 cells per mL. Then, PMA 200 nM was added to differentiate THP-1 cells into macrophages and they were incubated for 72 h at 37 °C.

2.8.2. Anti-inflammatory Activity

After macrophage differentiation, PMA solution was removed and cell monolayers were washed with Dulbecco's phosphate buffered saline (DPBS) and trypsinized following standard protocols. Cells were seeded into 48-well plates at 4.5×10^4 cells/well. To induce an inflammatory response, macrophages were treated with 100 ng/mL of lipopolysaccharides (LPS) from *Escherichia coli* O111:B4 (St. Louis, MO, USA, Sigma-Aldrich) and incubated at the same time for 24 h at 37 °C and 5% CO₂ with the samples. Cells treated with only LPS served as positive controls, while unstimulated cells (without LPS) were used as negative controls. Formulations A2, A3, A5, A8, and A9 were selected for anti-inflammatory efficacy, and their corresponding blank formulations (without the drug) were also tested as controls.

After incubation, cell culture supernatants were collected and stored at −150 °C until cytokine assessment. The secretion of 3 inflammatory mediators, PEG-2, IL-6, and IL-1ra, was analyzed. The concentration of PEG-2 was studied using an EIA assay (Arbor Assays), while IL-6 and IL-1ra were analyzed by specific ELISAs (Sigma, St. Louis, MO, USA) after adequate dilution following the manufacturer's instructions.

2.9. Statistical Analysis

Data are presented as mean \pm standard deviation (SD). The effect of formulation composition on anti-inflammatory response was analyzed using ANOVA and multiple range test (Statgraphics Centurion XVI 1.16.1.11, StatPoint Technologies Inc., Warrenton, VA, USA). Differences were considered significant at $p < 0.05$.

3. Results and Discussion

3.1. Solubility of Nepafenac Eye Drops and Their Characterization

The apparent solubility, zeta potential, and pH of the designed formulations of nepafenac are summarized in Table 3.

Table 3. Apparent drug solubility, zeta potential, and pH of nepafenac eye drop suspensions.

Formulation	Apparent Drug Solubility at 25 °C (mg/mL)	Dissolved Drug Content (%)	Zeta Potential (mV)	pH
A1	1.87 \pm 0.03	62.33	−10.9 \pm 0.6	6.08 \pm 0.23
A2	1.95 \pm 0.02	65.00	−10.4 \pm 0.3	6.18 \pm 0.05
A3	2.23 \pm 0.01	74.33	−6.4 \pm 0.8	6.09 \pm 0.03
A4	1.91 \pm 0.02	63.66	−12.1 \pm 1.4	6.21 \pm 0.09
A5	2.50 \pm 0.02	83.33	−7.8 \pm 0.9	6.07 \pm 0.02
A6	1.89 \pm 0.05	63.00	−27.4 \pm 1.7	6.13 \pm 0.33
A7	1.68 \pm 0.01	56.00	−14.4 \pm 1.4	6.01 \pm 0.23
A8	1.95 \pm 0.02	65.00	−14.7 \pm 1.2	6.16 \pm 0.15
A9	2.61 \pm 0.02	87.00	−6.9 \pm 1.4	6.08 \pm 0.05

In the formation of ternary complexes, drug-CD-polymer has been widely explored to enhance solubility and dissolution of poorly soluble drugs [47,48]. One aim of this study was to elucidate if the addition of hydrophilic polymers to nepafenac/CD complex could enhance its solubility as well as increase the residence time at the ocular tissues. For that, different polymers and concentrations were tested. As shown in Table 3, the apparent solubility of nepafenac was increased in all formulations compared to aqueous solubility, which has been reported to be 0.0197 mg/mL at 25 °C in water [49].

The addition of SA displayed the lowest solubility enhancement (formulation A7, 1.68 ± 0.01 mg/mL) while the combination of SA with CM or CMC and HA led to higher complex solubility (1.89 ± 0.05 and 2.61 ± 0.02 mg/mL, respectively). These differences are due to the increase of cyclodextrin complexing-power for nepafenac. Regarding formulations containing CMC, formulation A9 (CMC, PVA, and MC), A5 (CMC, PVP, and HPMC), and A3 (CMC, PVA, and tyloxapol) exhibited the highest solubility, 2.61, 2.50, and 2.23 mg/mL, respectively. These results support our previous preliminary studies, which showed that formulations containing CMC and/or PVA led to the highest solubilization of nepafenac.

All formulations showed negative zeta potential, in good agreement with the anionic or nonionic nature of the polymers and surfactants involved. Formulation A6 showed the highest absolute value of zeta potential, -27.4 ± 1.7 mV. Although a high absolute value of zeta potential is related to the high stability of nanoaggregates, other factors such as ionic strength, pH, or amount of encapsulated drug can influence aggregation behavior [50].

Moreover, all pH values were about 6.08–6.21, i.e., in a range adequate for ocular administration [51]. Particle size and size distribution were also evaluated by DLS (Table 4).

Table 4. Particle size results of diluted aqueous nepafenac eye drops. Data reported are means of three determinations.

Formulation	Peak Summary	
	Size (d. nm)	Intensity (%)
A1	5880.0	73.3
	2619.0	19.9
A2	5880.0	46.9
	4300.0	46.8
	1953.0	6.3
A3	5590.0	96.3
	827.0	3.7
A4	5870.0	100.0
A5	3090.0	53.5
	5950.0	42.0
	481.0	4.5
A6	5575.0	100.0
A7	3380.0	65.1
	5560.0	34.9
A8	4510.0	66.4
	1572.0	33.6
A9	5510.0	77.1
	3250.0	15.3
	340.0	7.6

All formulations tested presented microparticles (approx. 5–6 μm), and formulations A3, A5, and A9, which contained PVA and CMC or PVP and CMC, displayed also small portion of smaller particles (less than 1 μm). Compared to the particle size of Nevanac reported by Shelley et al. [51], the increase in particle size of our formulations could be attributed to the different polymers used. In fact, a similar size range was reported by Jansook and co-workers [52] after the preparation of irbersartan eye drops also containing 15% γ -CD. Moreover, all formulations showed a high polydispersity index, which may be due to the nanoaggregates forming and disrupting continuously.

3.2. Rheological Characterization

Short precorneal residence time limits the ocular bioavailability of drugs formulated as conventional topical eye drops. One strategy to prolong precorneal residence relies on the addition of polymers that can increase viscosity and therefore drug retention in the ocular sac [53]. Viscosity profiles of formulations A1 to A9 and Nevanac are displayed in Figure 2.

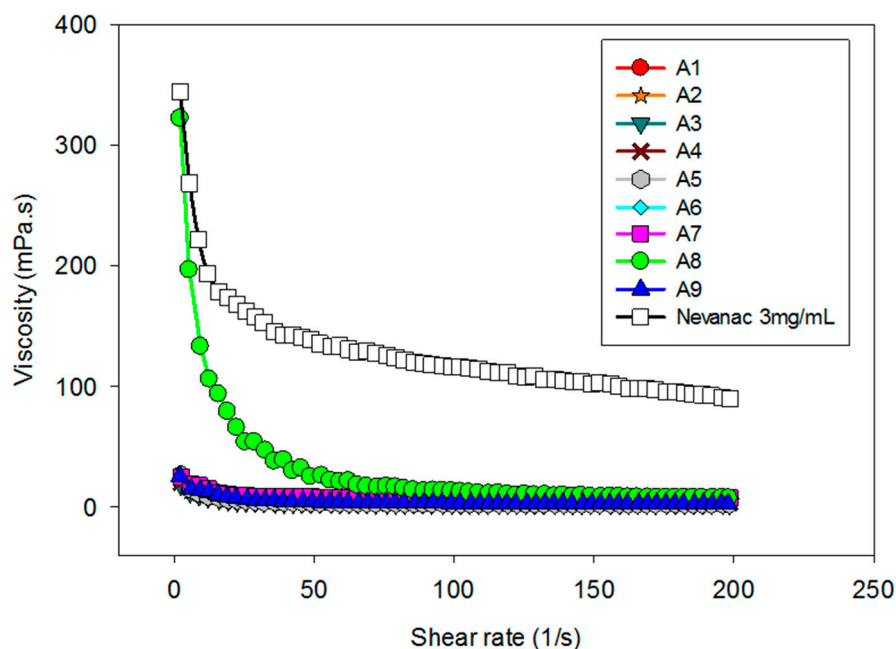


Figure 2. Dependence of viscosity on shear rate conditions of eye drops measured at 37 °C.

It is known that upon application of mechanical force such as eye blinking, viscosity of the natural tear film decreases in a pronounced manner. Eye drops should ideally display pseudoplastic behavior to prevent their removal under blinking conditions [50]. As shown in Figure 2, at 37 °C, all formulations showed pseudoplastic behavior, high viscosity during interblinking (shear rate 0.03 s^{-1}), and low viscosity during blinking (shear rate $4250\text{--}28,500 \text{ s}^{-1}$), which is appropriate for eye drop formulations [51]. Regarding viscosity, Nevanac showed the highest viscosity at 37 °C.

Viscoelastic behavior at 37 °C was also analyzed (Figure 3), recording the dependence of storage (G') and loss (G'') moduli as a function of angular frequency (rad/s).

Regarding viscoelastic behavior, adding 1% CMC, 0.2% HA, and 0.4% SA to aggregate formulations containing nepafenac/ γ -CD/HP- β CD modified the rheological properties of the formulations (Figure 3). Formulations A1 to A7 and A9 performed as very liquid-like systems, and the values of G' were negligible, showing that they had more viscous than elastic behavior. Alternatively, formulation A8, which contained CMC, HA, and SA, behaved as a well-structured gel ($G' \gg G''$) and also displayed pseudoplastic behavior. In the case of Nevanac, G' and G'' values increased with the angular frequency, which is typical of weak gels.

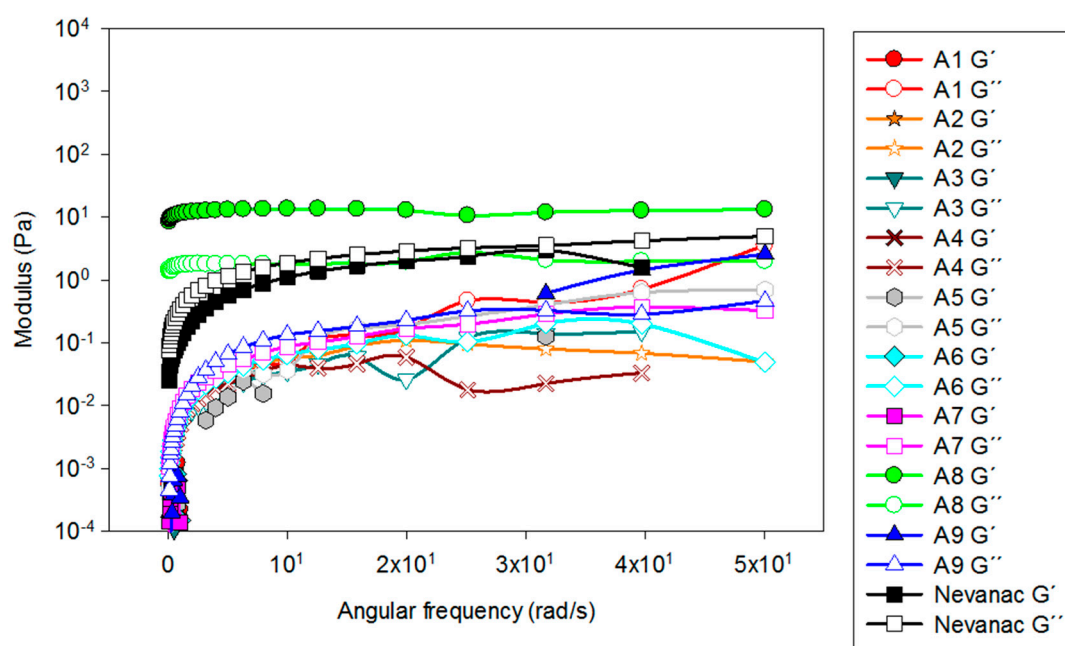


Figure 3. Evolution of storage (G' , solid symbols) and loss (G'' , open symbols) moduli as a function of angular frequency (rad/s).

3.3. Mucoadhesion Studies

It is known that after topical instillation to the eye, precorneal factors and the reflex mechanism of the eye lead to rapid drug elimination, and only a small fraction of the drug is available at the ocular surface. Treatment of eye diseases with mucoadhesive delivery systems has been proposed as a strategy to enhance the drug retention of topical ophthalmic formulations. Polymer–mucin bonds can be used to trap formulations on the surface of the eye, thus increasing the thickness of the tear film [54]. Several *in vitro* techniques have been reported to study mucoadhesion [55]. The *in vitro* tensile test is widely used to assess mucoadhesive strength in terms of the detachment force needed to separate two surfaces [43,56]. The mucoadhesion strength of the formulations is summarized in Table 5.

Table 5. Mucoadhesive strength of ophthalmic formulations on *ex vivo* bovine cornea.

Formulation	Mucoadhesive Strength (N)
A1	0.39 ± 0.15
A2	0.54 ± 0.13
A3	0.41 ± 0.04
A4	0.56 ± 0.11
A5	0.52 ± 0.02
A6	0.39 ± 0.06
A7	0.36 ± 0.08
A8	0.47 ± 0.02
A9	0.38 ± 0.06
Nevanac 3 mg/mL	0.67 ± 0.03

Nevanac displayed the highest mucoadhesive strength (0.672 ± 0.03 N), followed by formulation A4, which contained CMC and HA; A2, which contained CMC; and A5, with PVP, HPMC, and CMC.

Cellulose derivatives such as CMC and HPMC and sodium hyaluronate have been extensively used as mucoadhesive polymers. Brako and co-workers [57] studied the mucoadhesion of progesterone-loaded nanofibers, and found that the addition of CMC to the fibers also increased their mucoadhesion in both artificial and mucosal membranes. Lee et al. [58] found equivalent efficacy in patients with dry eye syndrome treated with HA or CMC eye drops. Mayol et al. [59] designed

poloxamer/hyaluronic acid in situ forming hydrogel for drug delivery, showing good mucoadhesion behavior with sustained drug release.

As mucoadhesion is correlated with viscosity [60], these results agree with the viscosity values shown previously. It was reported that the force needed during eye blinking was 0.8 N [50].

3.4. Ocular Irritancy Test (HET-CAM)

The Hen's Egg Test-Chorioallantoic Membrane (HET-CAM) test is based on the detection of vascular damage in the chorioallantoic membrane, which is an analog for ocular conjunctiva [61]. Different alternatives to the Draize rabbit eye test have been proposed to elucidate the toxicity of potential eye irritants [62,63]. HET-CAM has been described as one of the most suitable alternatives to test eye irritation in vitro since it was found to have good correlation with the Draize test [64]. The HET-CAM assay confirmed that the formulations were not irritants as negative controls (IS = 0) (Figure 4); the IS for the positive control was around 17.

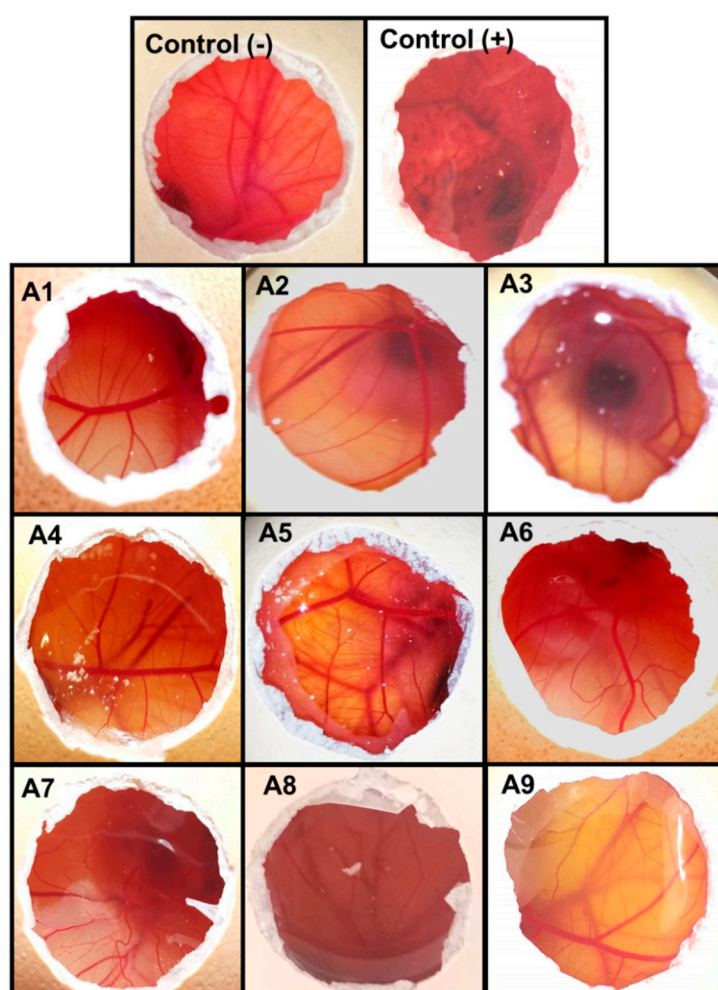


Figure 4. Pictures of Hen's Egg Test-Chorioallantoic Membrane (HET-CAM) test recorded after five minutes of contact with nepafenac formulations. Negative and positive controls refer to 0.9% NaCl and 0.1 N NaOH, respectively.

3.5. Cell Viability

The percentage of cell survival relative to the negative control of fibroblasts treated with formulations A1 to A9 and Nevanac at three dilutions is shown in Figure 5.

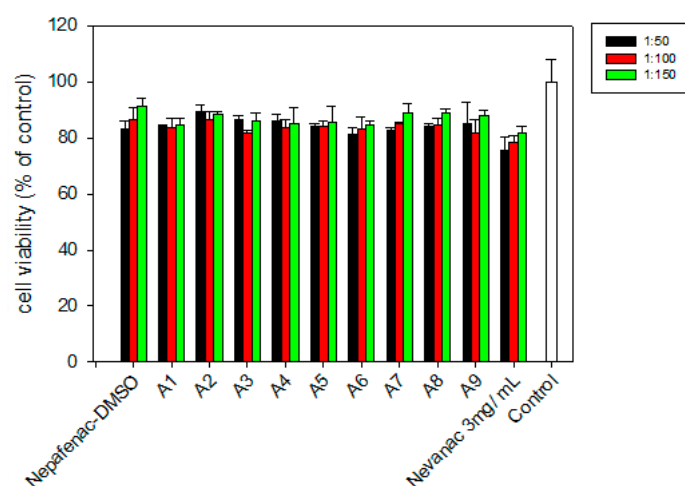


Figure 5. Viability of BALB/3T3 cells after 24 hours of exposure to ophthalmic formulations A1–A9 and Nevanac at various concentrations and control.

Nepafenac was diluted with DMEM/F12 medium to obtain final concentrations of nepafenac of 0.236 mM, 0.118 mM, and 0.0787 mM, since EC50 was reported to be 0.0875 mM [45]. All formulations were also diluted with DMEM/F12 medium according to these concentrations.

All samples tested were shown to not be harmful to BALB 3T3 cells, with cell viability similar to that exhibited by the marketed formulation, Nevanac. Results confirmed that a dilution of 1:100 was adequate for further assessment of anti-inflammatory activity.

3.6. In Vitro Diffusion Studies

Nepafenac diffusion from aggregate formulations and marketed suspension was first evaluated in vitro under sink conditions for six hours. A cellulose acetate membrane (0.45 μm pore size, 25 mm diameter) was used to separate the donor from the receptor compartments (Figure 6).

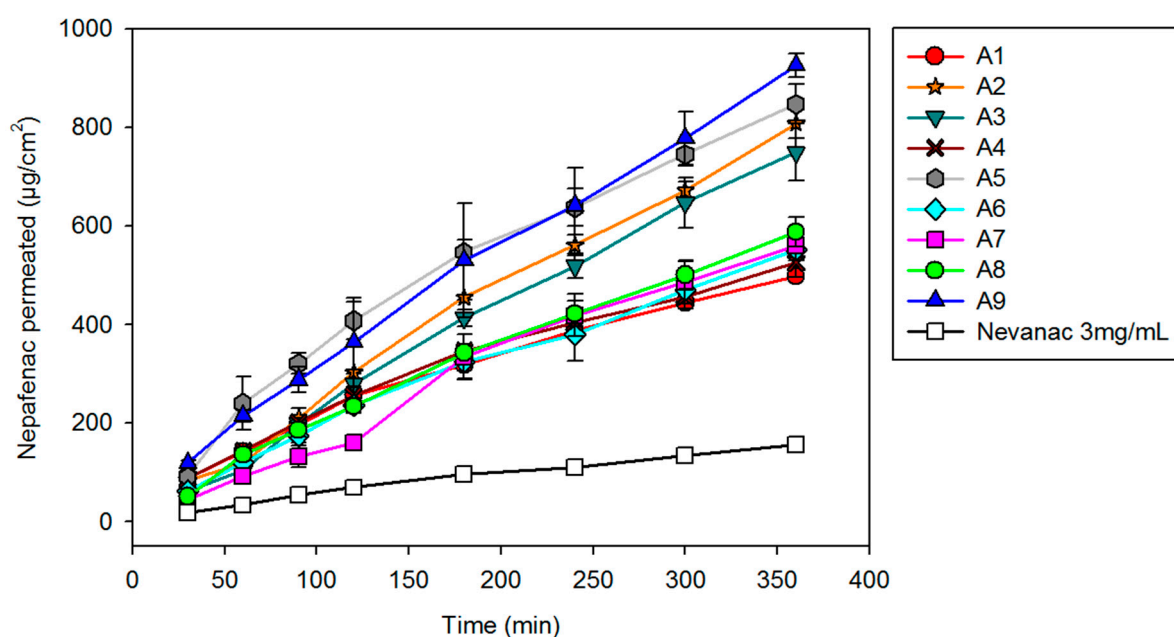


Figure 6. Nepafenac diffusion test through cellulose acetate membrane at 37 °C from eye drop formulations A1 to A9.

Formulation A9 showed the fastest diffusion ($926.1 \pm 23.4 \mu\text{g}/\text{cm}^2$), followed by formulation A5 ($847.8 \pm 39.5 \mu\text{g}/\text{cm}^2$), A2 ($808.9 \pm 31.6 \mu\text{g}/\text{cm}^2$), and A3 ($749.6 \pm 58.4 \mu\text{g}/\text{cm}^2$). The increased diffusion compared to Nevanac is due to a higher fraction of solubilized nepafenac. Since diffusion depends on concentration gradient and formulations A2, A3, A5, and A9 are the ones that showed the greatest solubilizing capacity of the drug.

3.7. Ex Vivo Corneal and Scleral Permeability Studies

The amount of permeated nepafenac from selected formulations through bovine cornea and sclera over six hours is shown in Figure 7.

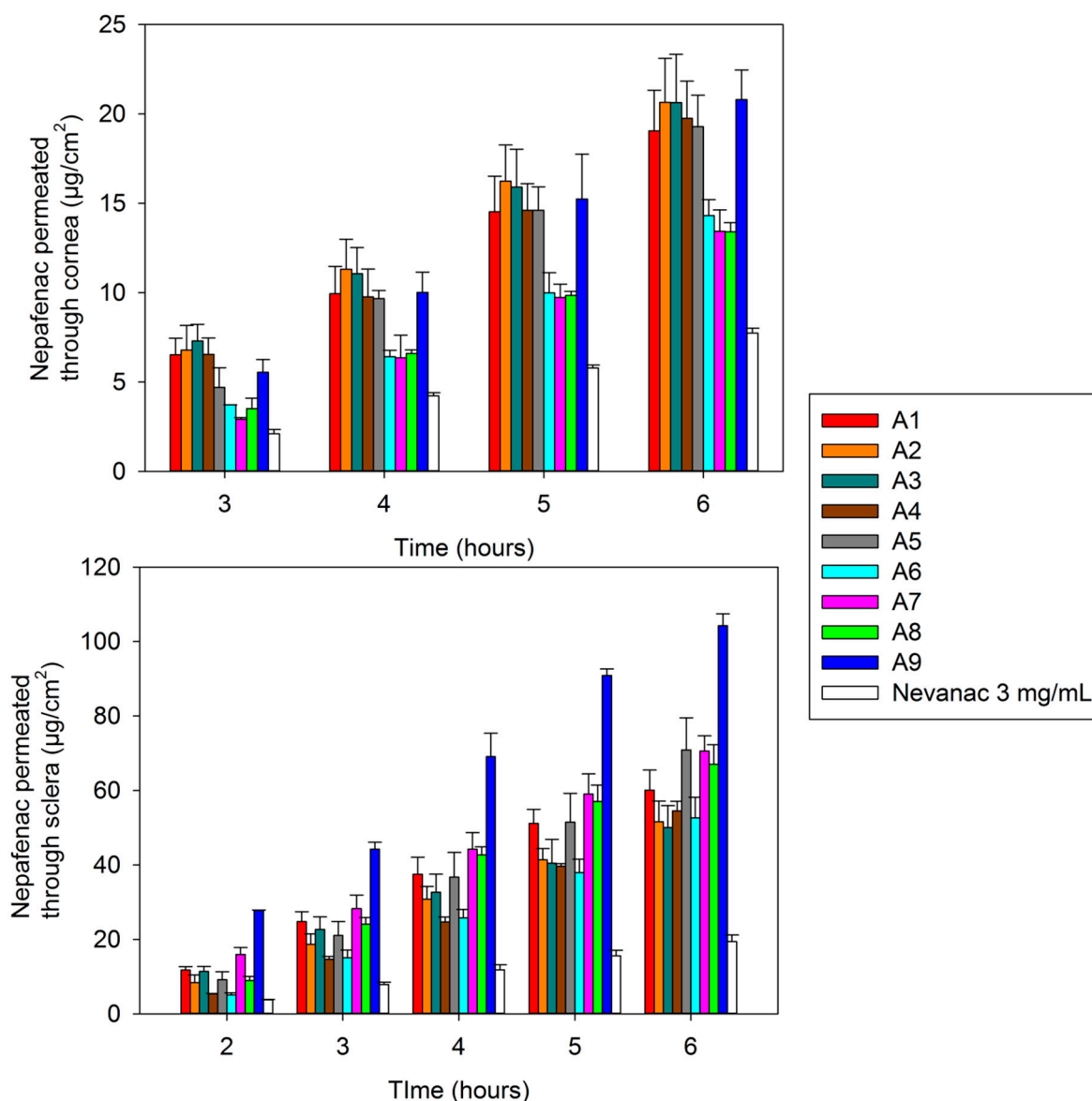


Figure 7. Amount of nepafenac permeated through bovine cornea (**top**) and sclera (**bottom**) measured in the receptor chamber as a function of time.

The transcorneal and transscleral permeation profile of nepafenac aggregate formulations was compared with that of the marketed formulation. Nevanac showed the lowest amount of nepafenac permeated through bovine cornea and sclera after six hours compared to nepafenac suspensions, $7.75 \pm 0.26 \mu\text{g}/\text{cm}^2$ in cornea and $19.44 \pm 1.74 \mu\text{g}/\text{cm}^2$ in sclera (Figure 7). These findings are in line with

those reported in the literature and they could be attributed to the low amount of nepafenac that is solubilized in Nevanac 3 mg/mL (37.87 $\mu\text{g/mL}$) compared to nepafenac suspension. In fact, various studies using Nevanac and nepafenac-loaded lipid nanoparticles [65] or in situ gels [51] suggested that the low release rate of Nevanac was because it contains Carbopol 974P, which is a highly cross-linked bioadhesive polymer that enables near zero or anomalous release rate.

All formulations tested showed higher permeability rate compared with Nevanac. This could be attributed to the presence of cyclodextrins in our formulations and a higher fraction of solubilized nepafenac. Numerous studies have shown that CDs enhance drug penetration through biological barriers consisting of an aqueous exterior and a mucosal membrane. Aktaş and co-workers [66] reported that eye drops containing pilocarpine/HP β -CD complexes demonstrated a four-fold increase in transcorneal penetration compared to a drug formulation without CD. This behavior was also observed by Shelley et al. [51], when they studied the permeability of nepafenac across porcine cornea compared to cyclodextrin formulations of nepafenac. The highest permeability through both bovine cornea and sclera was achieved by formulation A9, 20.80 \pm 1.66 $\mu\text{g/cm}^2$ in cornea and 104.24 \pm 3.21 $\mu\text{g/cm}^2$ in sclera, respectively. The amount of nepafenac accumulated at bovine corneal and scleral surfaces and in the tissue after six hours is displayed in Figure 8.

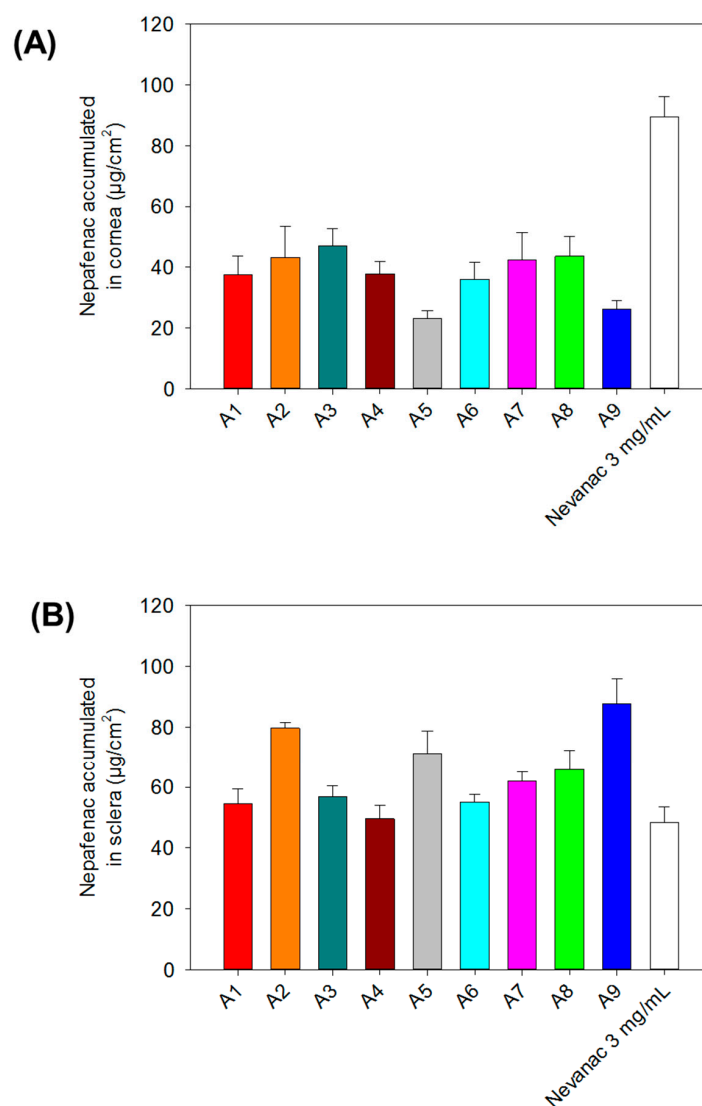


Figure 8. Nepafenac accumulated on the surface and inside (A) cornea and (B) sclera after six hours of exposure.

After six hours, Nevanac accumulated the most onto the surface and inside the bovine cornea ($89.57 \pm 6.66 \mu\text{g}/\text{cm}^2$), which can be attributed to the high viscosity of the formulation at the ocular surface. On the other hand, in sclera higher accumulation was found for formulations A9 ($87.76 \pm 8.08 \mu\text{g}/\text{cm}^2$), A8 ($65.84 \pm 6.34 \mu\text{g}/\text{cm}^2$), A5 ($71.07 \pm 7.64 \mu\text{g}/\text{cm}^2$), and A2 ($79.64 \pm 1.90 \mu\text{g}/\text{cm}^2$). These differences between corneal and scleral accumulation are probably due to aggregate formation. Furthermore, consistent with some reports, sclera demonstrated higher permeability compared to cornea [67]. During the recent years, the efficacy of drug delivery to the posterior segment of the eye after topical application of aqueous cyclodextrin-based eye drops has been demonstrated. Loftsson and Stefansson [34] developed eye drops containing dexamethasone/ γ -CD complexes to deliver dexamethasone to the posterior segment of the eye to treat diabetic macular edema (DME), which was tested in vivo in rabbits and clinically in patients. They found that the results in DME patients treated with CD eye drops were clinically similar to those after intravitreal corticosteroid injection.

In summary, results of ex vivo sclera accumulation confirmed the potential of our formulations to deliver nepafenac to the posterior segment of the eye via the scleral route.

3.8. Anti-Inflammatory Activity

Cytokines and other mediators, such as prostaglandins, play important roles in eye inflammation. Anti-inflammatory drugs used for the treatment of dry eye have been reported to upregulate the production of interleukin 1 (IL-1) receptor antagonist (IL-1ra), among other anti-inflammatory molecules, at the ocular surface [68]. Alternatively, increased levels of IL-6 and prostaglandin E2 (PGE2) have been reported to be involved in dry eye, glaucoma, corneal pathologies, retinal angiogenesis, and diabetic retinopathy progression [69,70]. In this study, we examined the secretion of two pro-inflammatory mediators, IL-6 and PGE2, and one anti-inflammatory mediator, IL-1ra, by macrophages subjected to lipopolysaccharide (LPS) stimulation and treated with the selected formulations to determinate their anti-inflammatory activity (Figure 9).

Figure 9A compares nepafenac loaded formulations to their corresponding blank systems. No significant effect on the secretion of IL-1ra was observed for the developed formulations. The incorporation of nepafenac did not stimulate secretion of this anti-inflammatory molecule. However, a significant reduction in IL-1ra secretion (b-g, ANOVA and multiple range test $p < 0.05$; $n = 3$) was observed for all formulations compared to the positive control. In the case of IL-6 (Figure 9B), all formulations caused a significant decrease in IL-6 secretion compared to the positive control, reaching levels similar to negative controls (nonstimulated cells) in the case of nepafenac loaded formulations. However, this effect was not observed on Nevanac treated cells. In the case of PGE2 secretion (Figure 9C), Nevanac and nepafenac loaded formulations A3, A5, A8, and A9 significantly reduced the secretion levels of PGE2 compared to the positive controls. Interestingly, A8, A9, and Nevanac treated cells reached levels similar to the negative controls. On the other hand, treatment with loaded A2 and A3 significantly decreased secretion of PGE2 compared to their corresponding blank formulations. In summary, formulations tested A2, A3, A5, A8 and A9 showed a clear in vitro anti-inflammatory effect, reducing the secretion levels of pro-inflammatory molecules (IL-6 and PGE2), without modifying the secretion of anti-inflammatory markers, IL-1ra. In the case of Nevanac, only a reduction in the secretion of PGE2 was observed, which was similar to those detected in formulations A8 and A9. Moreover, formulations A8 and A9 showed the best performance, reaching IL-6 and PGE2 levels similar to non-LPS stimulated cells and superior anti-inflammatory capacity than the commercially available formulation.

Several studies have measured the concentration of inflammatory mediators after treatment with anti-inflammatory drugs to assess their therapeutic activity. Kern et al. [71] analyzed the effect of nepafenac eye drops (0.3%) on PGE2 production in the retina at an early stage of diabetic retinopathy. They found that treatment with nepafenac led to a significant inhibition of PGE2 secretion in the retina. Calles et al. [72] studied the in vitro therapeutic efficacy of dexamethasone-loaded films by measuring changes in IL-6 levels after film exposure using an in vitro model of corneal inflammation. They found

that inflamed cells exposed to the dexamethasone films had significantly reduced IL-6 production compared to the controls. In agreement with previously published results, our study points out the effectiveness of formulations loaded with nepafenac, a COX inhibitor, to decrease the secretion of PGE2, improving the performance compared to the commercially available formulation Nevanac. Formulations A8 and A9, containing CDs, CMC, PVA, and MC, showed the most promising data as anti-inflammatory systems.

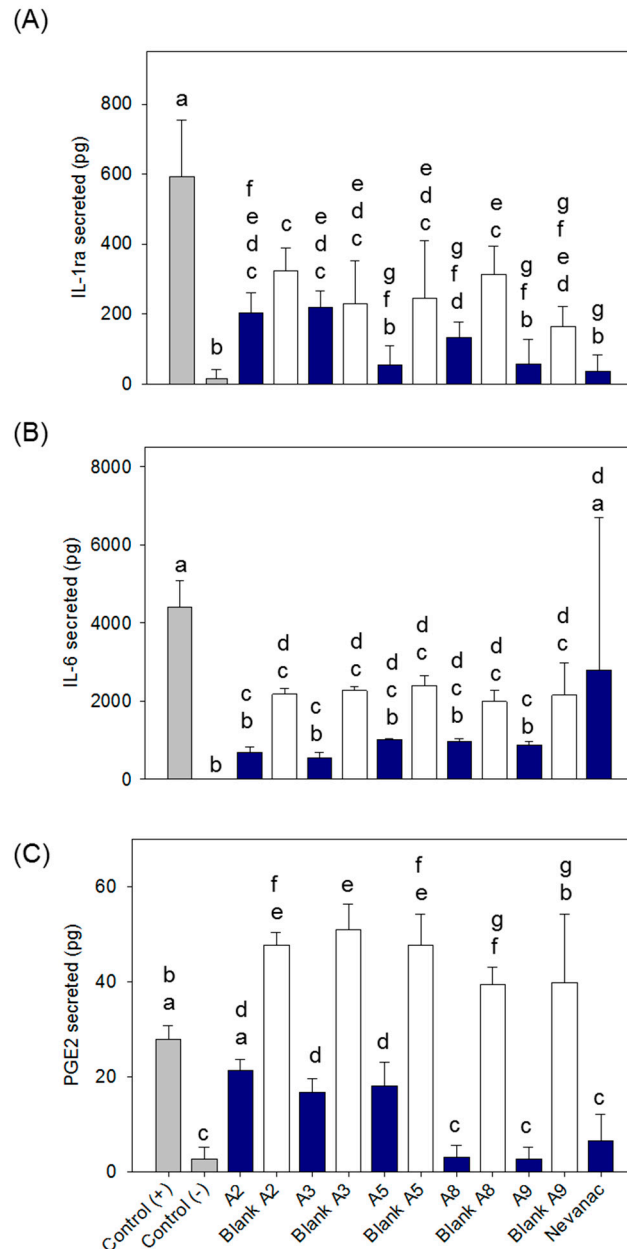


Figure 9. Effect of ophthalmic formulations on the secretion levels of (A) interleukin-1 receptor agonist (IL-1ra), (B) IL-6, and (C) prostaglandin E2 (PGE2) in macrophages. Negative controls refer to unstimulated cells (without lipopolysaccharide (LPS)); positive control refers to cells only stimulated with LPS. Same letters denote statistically homogeneous groups (ANOVA and multiple range test $p < 0.05$; $n = 3$).

4. Conclusions

In summary, we successfully developed cyclodextrin-based aggregate formulations capable of delivering nepafenac to the posterior segment of the eye via the sclera to treat inflammation. All suspensions were found to be nonirritating and biocompatible after HET-CAM assay and in vitro cell viability assay in murine fibroblasts. The optimal eye drop formulation, A9, containing CMC, PVA, and MC, showed high drug solubilizing capacity, high sclera retention, and a higher reduction of the inflammatory response compared to a marketed formulation, Nevanac[®] 3 mg/mL. This provides an alternative for the topical delivery of hydrophobic drugs such as nepafenac used to treat ocular diseases at the back of the eye. In the meantime, further studies should be conducted to assess its feasibility in vivo.

Author Contributions: Conceptualization, H.H.S and C.A.-L.; methodology, B.L.-V., P.D.-R., H.H.S., and C.A.-L.; validation, B.L.-V., P.D.-R., H.H.S., and C.A.-L.; resources, T.L., H.H.S. and C.A.-L.; writing—original draft preparation, B.L.-V., writing—review and editing, P.D.-R., H.H.S., and C.A.-L.; supervision, H.H.S. and C.A.-L. All authors have read and agreed to the published version of the manuscript.

Funding: This research was funded by MINECO (SAF2017-83118-R), Agencia Estatal de Investigación (AEI) Spain, Xunta de Galicia (ED431C 2016/008), and FEDER (Spain). B.L.-V. acknowledges an Erasmus+ traineeship (IS-SM2018-81075).

Acknowledgments: The authors acknowledge M. Vivero-Lopez, A. Lopez-Ulloa, and A. Varela-García for help with HET-CAM assay and ex vivo bovine experiments.

Conflicts of Interest: The authors declare no conflict of interest.

References

- Callegan, M.; Gregory-Ksander, M.; Willcox, M.; Lightman, S. Ocular inflammation and infection. *Int. J. Inflamm.* **2012**, *2012*, 2. [[CrossRef](#)] [[PubMed](#)]
- Red Eye. Available online: <https://www.nhs.uk/conditions/red-eye/> (accessed on 28 August 2019).
- Rodrigues, E.B.; Farah, M.E.; Bottos, J.M.; Bom Aggio, F. Nonsteroidal anti-inflammatory drugs in the treatment of retinal diseases. *Dev. Ophthalmol.* **2016**, *55*, 212–220. [[CrossRef](#)] [[PubMed](#)]
- Hoffman, R.S.; Braga-Mele, R.; Donaldson, K.; Emerick, G.; Henderson, B.; Kahook, M.; Mamalis, N.; Miller, K.M.; Realini, T.; Shorstein, N.H.; et al. Cataract surgery and nonsteroidal antiinflammatory drugs. *J. Cataract Refract. Surg.* **2016**, *42*, 1368–1379. [[CrossRef](#)] [[PubMed](#)]
- Janagam, D.R.; Wu, L.; Lowe, T.L. Nanoparticles for drug delivery to the anterior segment of the eye. *Adv. Drug Deliv. Rev.* **2017**, *122*, 31–64. [[CrossRef](#)]
- Egwuagu, C.E.; Sun, L.; Kim, S.H.; Dambuza, I.M. Ocular inflammatory diseases: Molecular pathogenesis and immunotherapy. *Curr. Mol. Med.* **2015**, *15*, 517–528. [[CrossRef](#)]
- Arango Duque, G.; Descoteaux, A. Macrophage cytokines: Involvement in immunity and infectious diseases. *Front. Immunol.* **2014**, *5*, 491. [[CrossRef](#)]
- Kessel, L.; Tendal, B.; Jorgensen, K.J.; Erngaard, D.; Flesner, P.; Andresen, J.L.; Hjortdal, J. Post-cataract prevention of inflammation and macular edema by steroid and nonsteroidal anti-inflammatory eye drops: A systematic review. *Ophthalmology* **2014**, *121*, 1915–1924. [[CrossRef](#)]
- Miller, K.; Fortun, J.A. Diabetic macular edema: Current understanding, pharmacologic treatment options, and developing therapies. *Asia Pac. J. Ophthalmol.* **2018**, *7*, 28–35. [[CrossRef](#)]
- Comstock, T.L.; Decory, H.H. Advances in corticosteroid therapy for ocular inflammation: Loteprednol etabonate. *Int. J. Inflamm.* **2012**, *2012*, 789623. [[CrossRef](#)]
- Rao, R.; Kumar, R.; Sarwal, A.; Sinha, V.R. Ocular Inflammation and NSAIDs: An Overview with Selective and Non-Selective cox Inhibitors. 2016. Available online: <https://pdfs.semanticscholar.org/97ac/e3cb72c3af14ac8c72d0e397cb930b9f0bac.pdf> (accessed on 28 August 2019).
- Gaynes, B.I.; Onyekwuluje, A. Topical ophthalmic NSAIDs: A discussion with focus on nepafenac ophthalmic suspension. *Clin. Ophthalmol.* **2008**, *2*, 355–368. [[CrossRef](#)]
- Guo, S.; Patel, S.; Baumrind, B.; Johnson, K.; Levinsohn, D.; Marcus, E.; Tannen, B.; Roy, M.; Bhagat, N.; Zarbin, M. Management of pseudophakic cystoid macular edema. *Surv. Ophthalmol.* **2015**, *60*, 123–137. [[CrossRef](#)] [[PubMed](#)]

14. EMA. Nepafenac. Available online: https://www.ema.europa.eu/en/documents/overview/nevanac-epar-summary-public_en.pdf (accessed on 3 June 2019).
15. Paulsamy, M.; Ponnusamy, C.; Palanisami, M.; Nackeeran, G.; Paramasivam, S.; Sugumaran, A.; Kandasamy, R.; Natesan, S.; Palanichamy, R. Nepafenac loaded silica nanoparticles dispersed in-situ gel systems: Development and characterization. *Int. J. Biol. Macromol.* **2018**, *110*, 336–345. [[CrossRef](#)] [[PubMed](#)]
16. Sahu, S.; Ram, J.; Bansal, R.; Pandav, S.S.; Gupta, A. Effect of topical ketorolac 0.4%, nepafenac 0.1%, and bromfenac 0.09% on postoperative inflammation using laser flare photometry in patients having phacoemulsification. *J. Cataract Refract. Surg.* **2015**, *41*, 2043–2048. [[CrossRef](#)] [[PubMed](#)]
17. Modi, S.S.; Lehmann, R.P.; Walters, T.R.; Fong, R.; Christie, W.C.; Roel, L.; Nethery, D.; Sager, D.; Tsozbatzoglou, A.; Philipson, B.; et al. Once-daily nepafenac ophthalmic suspension 0.3% to prevent and treat ocular inflammation and pain after cataract surgery: Phase 3 study. *J. Cataract Refract. Surg.* **2014**, *40*, 203–211. [[CrossRef](#)]
18. Chastain, J.E.; Sanders, M.E.; Curtis, M.A.; Chemuturi, N.V.; Gadd, M.E.; Kapin, M.A.; Markwardt, K.L.; Dahlin, D.C. Distribution of topical ocular nepafenac and its active metabolite amfenac to the posterior segment of the eye. *Exp. Eye Res.* **2016**, *145*, 58–67. [[CrossRef](#)]
19. Kawahara, A.; Utsunomiya, T.; Kato, Y.; Takayanagi, Y. Comparison of effect of nepafenac and diclofenac ophthalmic solutions on cornea, tear film, and ocular surface after cataract surgery: The results of a randomized trial. *Clin. Ophthalmol.* **2016**, *10*, 385–391. [[CrossRef](#)]
20. Kleiter, M.; Malarkey, D.E.; Ruslander, D.E.; Thrall, D.E. Expression of cyclooxygenase-2 in canine epithelial nasal tumors. *Vet. Radiol. Ultrasound. Off. J. Am. Coll. Vet. Radiol. Int. Vet. Radiol. Assoc.* **2004**, *45*, 255–260. [[CrossRef](#)]
21. Kirkby, N.S.; Chan, M.V.; Zaiss, A.K.; Garcia-Vaz, E.; Jiao, J.; Berglund, L.M.; Verdu, E.F.; Ahmetaj-Shala, B.; Wallace, J.L.; Herschman, H.R.; et al. Systematic study of constitutive cyclooxygenase-2 expression: Role of NF- κ B and NFAT transcriptional pathways. *Proc. Natl. Acad. Sci. USA* **2016**, *113*, 434–439. [[CrossRef](#)]
22. Ozcimen, M.; Sakarya, Y.; Goktas, S.; Sakarya, R.; Yener, H.I.; Bukus, A.; Demir, L.S. Effect of nepafenac eye drops on pain associated with pterygium surgery. *Eye Contact Lens* **2015**, *41*, 187–189. [[CrossRef](#)]
23. Kim, S.J. Novel approaches for retinal drug and gene delivery. *Transl. Vis. Sci. Technol.* **2014**, *3*, 7. [[CrossRef](#)]
24. Shah, S.S.; Denham, L.V.; Elison, J.R.; Bhattacharjee, P.S.; Clement, C.; Huq, T.; Hill, J.M. Drug delivery to the posterior segment of the eye for pharmacologic therapy. *Expert Rev. Ophthalmol.* **2010**, *5*, 75–93. [[CrossRef](#)] [[PubMed](#)]
25. Jiang, S.; Franco, Y.L.; Zhou, Y.; Chen, J. Nanotechnology in retinal drug delivery. *Int. J. Ophthalmol.* **2018**, *11*, 1038–1044. [[CrossRef](#)] [[PubMed](#)]
26. Fu, T.; Yi, J.; Lv, S.; Zhang, B. Ocular amphotericin B delivery by chitosan-modified nanostructured lipid carriers for fungal keratitis-targeted therapy. *J. Liposome Res.* **2017**, *27*, 228–233. [[CrossRef](#)] [[PubMed](#)]
27. Alvarez-Trabado, J.; Diebold, Y.; Sanchez, A. Designing lipid nanoparticles for topical ocular drug delivery. *Int. J. Pharm.* **2017**, *532*, 204–217. [[CrossRef](#)] [[PubMed](#)]
28. Kalam, M.A. Development of chitosan nanoparticles coated with hyaluronic acid for topical ocular delivery of dexamethasone. *Int. J. Biol. Macromol.* **2016**, *89*, 127–136. [[CrossRef](#)] [[PubMed](#)]
29. Tahara, K.; Karasawa, K.; Onodera, R.; Takeuchi, H. Feasibility of drug delivery to the eye's posterior segment by topical instillation of PLGA nanoparticles. *Asian J. Pharm. Sci.* **2017**, *12*, 394–399. [[CrossRef](#)]
30. Balguri, S.P.; Adelli, G.R.; Majumdar, S. Topical ophthalmic lipid nanoparticle formulations (SLN, NLC) of indomethacin for delivery to the posterior segment ocular tissues. *Eur. J. Pharm. Biopharm.* **2016**, *109*, 224–235. [[CrossRef](#)]
31. Subrizi, A.; Del Amo, E.M.; Korzhikov-Vlakh, V.; Tennikova, T.; Ruponen, M.; Urtti, A. Design principles of ocular drug delivery systems: Importance of drug payload, release rate, and material properties. *Drug Discov. Today* **2019**, *24*, 1446–1457. [[CrossRef](#)]
32. Srinivasarao, D.A.; Lohiya, G.; Katti, D.S. Fundamentals, challenges, and nanomedicine-based solutions for ocular diseases. *Wiley Interdiscip. Rev. Nanomed. Nanobiotechnol.* **2019**, *11*, e1548. [[CrossRef](#)]
33. Weng, Y.; Liu, J.; Jin, S.; Guo, W.; Liang, X.; Hu, Z. Nanotechnology-based strategies for treatment of ocular disease. *Acta Pharm. Sin. B* **2017**, *7*, 281–291. [[CrossRef](#)]
34. Loftsson, T.; Stefansson, E. Cyclodextrins and topical drug delivery to the anterior and posterior segments of the eye. *Int. J. Pharm.* **2017**, *531*, 413–423. [[CrossRef](#)] [[PubMed](#)]

35. Johannsdottir, S.; Jansook, P.; Stefansson, E.; Loftsson, T. Development of a cyclodextrin-based aqueous cyclosporin a eye drop formulations. *Int. J. Pharm.* **2015**, *493*, 86–95. [CrossRef] [PubMed]
36. Johannsdottir, S.; Kristinsson, J.K.; Fulop, Z.; Asgrimsdottir, G.; Stefansson, E.; Loftsson, T. Formulations and toxicologic in vivo studies of aqueous cyclosporin a eye drops with cyclodextrin nanoparticles. *Int. J. Pharm.* **2017**, *529*, 486–490. [CrossRef] [PubMed]
37. Cyclolab. Available online: https://cyclolab.hu/userfiles/CD%20NEWS2018January_.pdf (accessed on 11 June 2019).
38. Tsai, C.H.; Wang, P.Y.; Lin, I.C.; Huang, H.; Liu, G.S.; Tseng, C.L. Ocular drug delivery: Role of degradable polymeric nanocarriers for ophthalmic application. *Int. J. Mol. Sci.* **2018**, *19*, 2830. [CrossRef] [PubMed]
39. Ludwig, A. The use of mucoadhesive polymers in ocular drug delivery. *Adv. Drug Deliv. Rev.* **2005**, *57*, 1595–1639. [CrossRef]
40. Khare, A.; Grove, K.; Pawar, P.; Singh, I. Mucoadhesive polymers for enhancing retention in ocular drug delivery. In *Progress in Adhesion and Adhesives*; Wiley-Scrivener: Beverly, MA, USA, 2015; Volume 13, pp. 451–484. [CrossRef]
41. Lorenzo-Veiga, B.; Sigurdsson, H.H.; Loftsson, T. Nepafenac-loaded cyclodextrin/polymer nanoaggregates: A new approach to eye drop formulation. *Materials* **2019**, *12*, 229. [CrossRef]
42. Akhter, S.; Anwar, M.; Siddiqui, M.A.; Ahmad, I.; Ahmad, J.; Ahmad, M.Z.; Bhatnagar, A.; Ahmad, F.J. Improving the topical ocular pharmacokinetics of an immunosuppressant agent with mucoadhesive nanoemulsions: Formulation development, in-vitro and in-vivo studies. *Colloids Surf. B Biointerfaces* **2016**, *148*, 19–29. [CrossRef]
43. Campana-Seoane, M.; Peleteiro, A.; Laguna, R.; Otero-Espinar, F.J. Bioadhesive emulsions for control release of progesterone resistant to vaginal fluids clearance. *Int. J. Pharm.* **2014**, *477*, 495–505. [CrossRef]
44. Alvarez-Rivera, F.; Fernandez-Villanueva, D.; Concheiro, A.; Alvarez-Lorenzo, C. Alpha-lipoic acid in soluplus(r) polymeric nanomicelles for ocular treatment of diabetes-associated corneal diseases. *J. Pharm. Sci.* **2016**, *105*, 2855–2863. [CrossRef]
45. Fernandez-Ferreiro, A.; Santiago-Varela, M.; Gil-Martinez, M.; Parada, T.G.; Pardo, M.; Gonzalez-Barcia, M.; Piñeiro-Ces, A.; Rodríguez-Ares, M.T.; Blanco-Mendez, J.; Lamas, M.J.; et al. Ocular safety comparison of non-steroidal anti-inflammatory eye drops used in pseudophakic cystoid macular edema prevention. *Int. J. Pharm.* **2015**, *495*, 680–691. [CrossRef]
46. Chanput, W.; Mes, J.J.; Wichers, H.J. THP-1 cell line: An in vitro cell model for immune modulation approach. *Int. Immunopharmacol.* **2014**, *23*, 37–45. [CrossRef] [PubMed]
47. Hirlekar, R.S.; Sonawane, S.N.; Kadam, V.J. Studies on the effect of water-soluble polymers on drug-cyclodextrin complex solubility. *AAPS PharmSciTech.* **2009**, *10*, 858–863. [CrossRef] [PubMed]
48. Patel, A.R.; Vavia, P.R. Effect of hydrophilic polymer on solubilization of fenofibrate by cyclodextrin complexation. *J. Incl. Phenom. Macrocycl. Chem.* **2006**, *56*, 247–251. [CrossRef]
49. Nepafenac. Available online: <https://www.drugbank.ca/drugs/DB06802> (accessed on 28 August 2019).
50. Saldias, C.; Velasquez, L.; Quezada, C.; Leiva, A. Physicochemical assessment of dextran-g-poly (varepsilon-caprolactone) micellar nanoaggregates as drug nanocarriers. *Carbohydr. Polym.* **2015**, *117*, 458–467. [CrossRef] [PubMed]
51. Shelley, H.; Rodriguez-Galarza, R.M.; Duran, S.H.; Abarca, E.M.; Babu, R.J. In situ gel formulation for enhanced ocular delivery of nepafenac. *J. Pharm. Sci.* **2018**, *107*, 3089–3097. [CrossRef]
52. Jansook, P.; Muankaew, C.; Stefansson, E.; Loftsson, T. Development of eye drops containing antihypertensive drugs: Formulation of aqueous irbesartan/gammaCD eye drops. *Pharm. Dev. Technol.* **2015**, *20*, 626–632. [CrossRef]
53. Irimia, T.; Ghica, M.V.; Popa, L.; Anuța, V.; Arsene, A.L.; Dinu-Pîrvu, C.E. Strategies for improving ocular drug bioavailability and corneal wound healing with chitosan-based delivery systems. *Polym (Basel)* **2018**, *10*, 1221. [CrossRef]
54. Greaves, J.L.; Wilson, C.G. Treatment of diseases of the eye with mucoadhesive delivery systems. *Adv. Drug Deliv. Rev.* **1993**, *11*, 349–383. [CrossRef]
55. Ivarsson, D.; Wahlgren, M. Comparison of in vitro methods of measuring mucoadhesion: Ellipsometry, tensile strength and rheological measurements. *Colloids Surf. B Biointerfaces* **2012**, *92*, 353–359. [CrossRef]

56. Almeida, H.; Lobão, P.; Frigerio, C.; Fonseca, J.; Silva, R.; Quaresma, P.; Lobo, J.M.S.; Amaral, M.H. Development of mucoadhesive and thermosensitive eyedrops to improve the ophthalmic bioavailability of ibuprofen. *J. Drug Deliv. Sci. Technol.* **2016**, *35*, 69–80. [[CrossRef](#)]
57. Brako, F.; Thorogate, R.; Mahalingam, S.; Raimi-Abraham, B.; Craig, D.Q.M.; Edirisinghe, M. Mucoadhesion of progesterone-loaded drug delivery nanofiber constructs. *ACS Appl. Mater. Interfaces* **2018**, *10*, 13381–13389. [[CrossRef](#)] [[PubMed](#)]
58. Lee, J.H.; Ahn, H.S.; Kim, E.K.; Kim, T.I. Efficacy of sodium hyaluronate and carboxymethylcellulose in treating mild to moderate dry eye disease. *Cornea* **2011**, *30*, 175–179. [[CrossRef](#)] [[PubMed](#)]
59. Mayol, L.; Quaglia, F.; Borzacchiello, A.; Ambrosio, L.; La Rotonda, M.I. A novel poloxamers/hyaluronic acid in situ forming hydrogel for drug delivery: Rheological, mucoadhesive and in vitro release properties. *Eur. J. Pharm. Biopharm.* **2008**, *70*, 199–206. [[CrossRef](#)] [[PubMed](#)]
60. Cook, S.L.; Woods, S.; Methven, L.; Parker, J.K.; Khutoryanskiy, V.V. Mucoadhesive polysaccharides modulate sodium retention, release and taste perception. *Food Chem.* **2018**, *240*, 482–489. [[CrossRef](#)] [[PubMed](#)]
61. McKenzie, B.; Kay, G.; Matthews, K.H.; Knott, R.M.; Cairns, D. The hen's egg chorioallantoic membrane (HET-CAM) test to predict the ophthalmic irritation potential of a cysteamine-containing gel: Quantification using Photoshop(R) and ImageJ. *Int. J. Pharm.* **2015**, *490*, 1–8. [[CrossRef](#)] [[PubMed](#)]
62. Yun, J.W.; Hailian, Q.; Na, Y.; Kang, B.C.; Yoon, J.H.; Cho, E.Y.; Lee, M.; Kim, D.; Bae, S.; Seok, S.H.; et al. Exploration and comparison of in vitro eye irritation tests with the ISO standard in vivo rabbit test for the evaluation of the ocular irritancy of contact lenses. *Toxicol. Vitro.* **2016**, *37*, 79–87. [[CrossRef](#)]
63. Hayashi, K.; Mori, T.; Abo, T.; Koike, M.; Takahashi, Y.; Sakaguchi, H.; Nishiyama, N. A tiered approach combining the short time exposure (STE) test and the bovine corneal opacity and permeability (BCOP) assay for predicting eye irritation potential of chemicals. *J. Toxicol. Sci.* **2012**, *37*, 269–280. [[CrossRef](#)]
64. Scheel, J.; Kleber, M.; Kreutz, J.; Lehringer, E.; Mehling, A.; Reisinger, K.; Steiling, W. Eye irritation potential: Usefulness of the HET-CAM under the globally harmonized system of classification and labeling of chemicals (GHS). *Regul. Toxicol. Pharmacol. RTP* **2011**, *59*, 471–492. [[CrossRef](#)]
65. Yu, S.; Tan, G.; Liu, D.; Yang, X.; Pan, W. Nanostructured lipid carrier (NLC)-based novel hydrogels as potential carriers for nepafenac applied after cataract surgery for the treatment of inflammation: Design, characterization and in vitro cellular inhibition and uptake studies. *RSC Adv.* **2017**, *7*, 16668–16677. [[CrossRef](#)]
66. Aktaş, Y.; Ünlü, N.; Orhan, M.; İrkeç, M.; Atilla Hıncal, A. Influence of Hydroxypropyl β -Cyclodextrin on the Corneal Permeation of Pilocarpine. *Drug Dev. Ind. Pharm.* **2003**, *29*, 223–230. [[CrossRef](#)]
67. Loch, C.; Zakelj, S.; Kristl, A.; Nagel, S.; Guthoff, R.; Weitschies, W.; Seidlitz, A. Determination of permeability coefficients of ophthalmic drugs through different layers of porcine, rabbit and bovine eyes. *Eur. J. Pharm. Sci.* **2012**, *47*, 131–138. [[CrossRef](#)] [[PubMed](#)]
68. Amparo, F.; Dastjerdi, M.H.; Okanobo, A.; Ferrari, G.; Smaga, L.; Hamrah, P.; Jurkunus, U.; Schaumberg, D.A.; Dana, R. Topical interleukin 1 receptor antagonist for treatment of dry eye disease: A randomized clinical trial. *JAMA Ophthalmol.* **2013**, *131*, 715–723. [[CrossRef](#)] [[PubMed](#)]
69. Ghasemi, H. Roles of IL-6 in Ocular Inflammation: A Review. *Ocul. Immunol. Inflamm.* **2018**, *26*, 37–50. [[CrossRef](#)] [[PubMed](#)]
70. Doucette, L.P.; Walter, M.A. Prostaglandins in the eye: Function, expression, and roles in glaucoma. *Ophthalmic Genet* **2017**, *38*, 108–116. [[CrossRef](#)] [[PubMed](#)]
71. Kern, T.S.; Miller, C.M.; Du, Y.; Zheng, L.; Mohr, S.; Ball, S.L.; Kim, M.; Jamison, J.A.; Bingaman, D.P. Topical Administration of Nepafenac Inhibits Diabetes-Induced Retinal Microvascular Disease and Underlying Abnormalities of Retinal Metabolism and Physiology. *Diabetes* **2007**, *56*, 373. [[CrossRef](#)]
72. Calles, J.A.; López-García, A.; Vallés, E.M.; Palma, S.D.; Diebold, Y. Preliminary characterization of dexamethasone-loaded cross-linked hyaluronic acid films for topical ocular therapy. *Int. J. Pharm.* **2016**, *509*, 237–243. [[CrossRef](#)]



Paper III

Article

Cyclodextrin–Amphiphilic Copolymer Supramolecular Assemblies for the Ocular Delivery of Natamycin

Blanca Lorenzo-Veiga ¹, Hakon Hrafn Sigurdsson ¹, Thorsteinn Loftsson ¹ and Carmen Alvarez-Lorenzo ^{2,*}

¹ Faculty of Pharmaceutical Sciences, University of Iceland, Hofsvallagata 53, IS-107 Reykjavik, Iceland; blv3@hi.is (B.L.-V.); hhs@hi.is (H.H.S.); thorstlo@hi.is (T.L.)

² Departamento de Farmacología, Farmacia y Tecnología Farmacéutica, R+D Pharma Group (GI-1645), Facultad de Farmacia and Health Research Institute of Santiago de Compostela (IDIS), Universidade de Santiago de Compostela, 15782 Santiago de Compostela, Spain

* Correspondence: carmen.alvarez.lorenzo@usc.es; Tel.: +34-881-815-239

Received: 19 April 2019; Accepted: 8 May 2019; Published: 15 May 2019



Abstract: Natamycin is the only drug approved for fungal keratitis treatment, but its low water solubility and low ocular penetration limit its efficacy. The purpose of this study was to overcome these limitations by encapsulating the drug in single or mixed micelles and poly(pseudo)rotaxanes. Soluplus and Pluronic P103 dispersions were prepared in 0.9% NaCl and pH 6.4 buffer, with or without α -cyclodextrin (α CD; 10% *w/v*), and characterized through particle size, zeta potential, solubilization efficiency, rheological properties, ocular tolerance, in vitro drug diffusion, and ex vivo permeation studies. Soluplus micelles (90–103 nm) and mixed micelles (150–110 nm) were larger than Pluronic P103 ones (16–20 nm), but all showed zeta potentials close to zero. Soluplus, Pluronic P103, and their mixed micelles increased natamycin solubility up to 6.00-fold, 3.27-fold, and 2.77-fold, respectively. Soluplus dispersions and poly(pseudo)rotaxanes exhibited in situ gelling capability, and they transformed into weak gels above 30 °C. All the formulations were non-irritant according to Hen’s Egg Test on the Chorioallantoic Membrane (HET-CAM) assay. Poly(pseudo)rotaxanes facilitated drug accumulation into the cornea and sclera, but led to lower natamycin permeability through the sclera than the corresponding micelles. Poly(pseudo)rotaxanes made from mixed micelles showed intermediate natamycin diffusion coefficients and permeability values between those of Pluronic P103-based and Soluplus-based poly(pseudo)rotaxanes. Therefore, the preparation of mixed micelles may be a useful tool to regulate drug release and enhance ocular permeability.

Keywords: block copolymers; cyclodextrins; ocular drug delivery; fungal keratitis; natamycin; mixed micelles; poly(pseudo)rotaxane; solubility; HET-CAM assay; ocular permeability

1. Introduction

Fungal keratitis or keratomycosis is a globally distributed ocular infection that can lead to visual impairment, and in the worse cases, blindness. In general, this cornea disease is caused by *Aspergillus* and *Fusarium* spp. in subtropical and tropical regions and by *Candida* spp. in high temperate areas [1,2]. The use of contact lenses, recent ocular trauma, surgery, or treatment with ocular steroids has been identified as risk factors in the development of this infection [3–5].

There are three classes of antifungals for the treatment of keratomycosis: polyenes, triazoles, and echinocandins [6]. Natamycin belongs to the group of polyene antifungal antibiotics, and is the only drug approved for the topical ophthalmic treatment of fungal keratitis in the form of suspension eye drops (Figure 1A) [7,8]. Voriconazole has shown higher ocular penetration capacity, but better results have still been reported for patients treated with natamycin. Natamycin suspension is only approved

for topical administration [5,7,9]. Other drugs such as amphotericin B, itraconazole, ketoconazole, or fluconazole can be administered by other routes for systemic treatment.

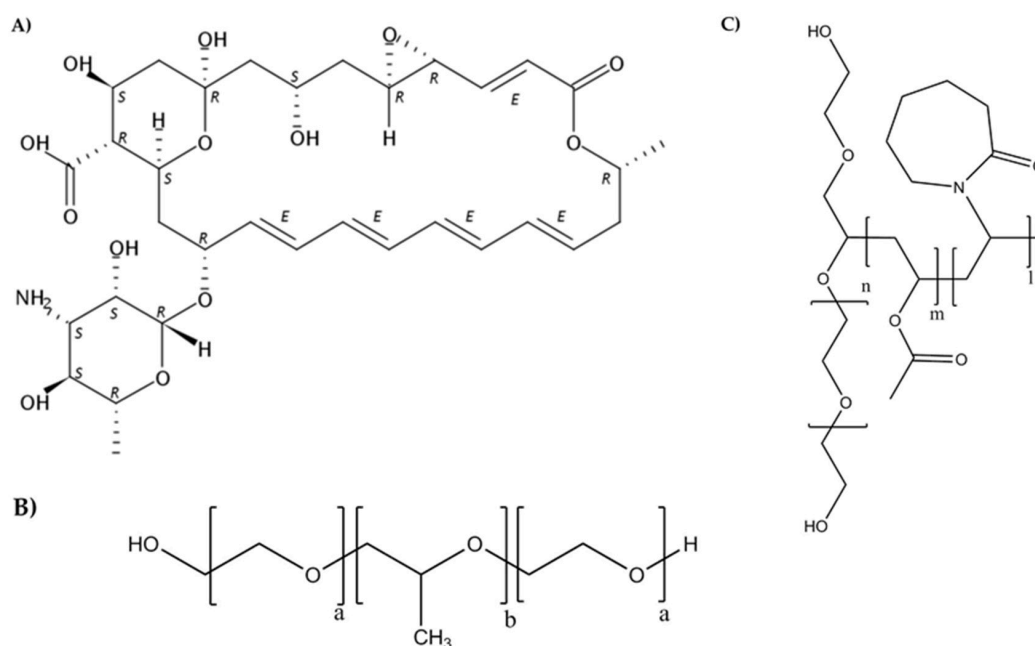


Figure 1. Chemical structures of natamycin (A), Pluronic[®] (B), and Soluplus[®] (C).

The safety of polyene drugs, such as natamycin, relies on their selective interaction with ergosterol at the fungi wall, avoiding interactions with human cholesterol-containing membranes [10]. Thus, a variety of strategies have been explored to increase natamycin solubility (~50 mg/L in water [11]), stability [12], precorneal residence time, and corneal permeability. Several types of delivery systems such as nanoparticles [13–15], hydrogels [16,17], and drug/cyclodextrin complexes [11,18–20] have been proposed. Janga et al. [16] designed ion-sensitive in situ gels of natamycin bilosomes for efficient ocular delivery. Bhatta et al. [13] developed lecithin/chitosan nanoparticles to prolong the ocular penetration of natamycin at reduced dose and dosing frequency. Also, Chandasana et al. [14] developed poly-D-glucosamine functionalized polycaprolactone nanoparticles for prolonged drug release. Phan et al. [19] analyzed the release of natamycin loaded-poly(D,L-lactide)-dextran nanoparticles with the purpose of developing drug-eluting contact lenses. Koontz et al. [18] studied the complex formation between natamycin and β -cyclodextrin (β CD), hydroxypropyl- β -cyclodextrin (HP β CD), and γ -cyclodextrin (γ CD). They managed to increase drug apparent solubility 16-fold, 73-fold, and 152-fold, respectively, although using quite high CD concentrations.

Despite the growing interest in polymeric nanomicelles as ocular drug carriers, only one reference to their use as natamycin nanocarriers was found. In that previous paper by Loh et al. [21], an in situ gelling derivative of Pluronic was evaluated for sustained release, but the solubilizing capability and ocular application were not considered. Compared to other ophthalmic nanocarriers, polymeric nanomicelles (typical diameter 10–100 nm) require simpler preparation and exhibit mucoadhesion to the ocular surface, better penetration, enhanced stability, and larger cargo capacity [22–26]. Linear triblock poly(ethylene oxide)(PEO)–poly(propylene oxide)(PPO)–poly(ethylene oxide)(PEO) copolymers known as poloxamers or Pluronic[®] (Figure 1B) are versatile components of nanomicelles with the extra capabilities of inhibiting P-glucoprotein efflux pumps at the eye surface [27] and undergoing sol-gel transitions upon heating [23,28]. Lately, Soluplus[®], a poly(vinyl caprolactam)–poly(vinyl acetate)–poly(ethylene glycol) graft copolymer with amphiphilic properties (PCL-PVAc-PEG) (Figure 1C), is gaining increasing attention. Nanomicelles prepared with Soluplus[®] are highly stable against dilution due to its low critical micelle concentration (CMC) value [29–31], and may also undergo in situ gelling on the ocular surface. Enhanced penetration into ocular structures has been demonstrated

for α -lipoic acid [25] and acyclovir [32] encapsulated in Soluplus nanomicelles. The combination of Pluronic and Soluplus has recently been proposed for the oral route, since Soluplus may reinforce the physical stability and drug-loading capacity of Pluronics bearing short PPO blocks [33,34].

The combination of amphiphilic copolymers and cyclodextrins has also been shown to prolong drug permeation at the application site [28,35]. In particular, α -cyclodextrin (α CD) can thread on some block polymers, for example, PEO, and reinforce the hydrophobic interactions among the components through crystalline-like associations among the threaded CDs [36] notably increasing the viscoelastic properties of the system. Such reinforcement is reversible, and thus, under a small amount of pressure, the interactions between α CD molecules are broken, increasing the fluidity of the system. At rest, the bonds between the α CD molecules are regenerated, restoring the gel structure [37].

This work is based on the hypothesis that Soluplus and Pluronic P103 can solubilize natamycin in their micelles, and can also interact with α CD forming poly(pseudo)rotaxanes that are able to tune the rheological properties of the dispersions (Figure S1, Supplementary Material). To the best of our knowledge, poly(pseudo)rotaxanes of mixed micelles have not been investigated before. It can be assumed that the different composition and architecture of Soluplus and Pluronic P103 in terms of PEG location may strongly determine the properties of the poly(pseudo)rotaxanes formed by each of them and the mixed micelles. The aim of this study was to ascertain the potential of these nanomicelles and poly(pseudo)rotaxanes as nanocarriers for the ocular delivery of natamycin. To address these statements, sets of dispersions were prepared combining Soluplus and Pluronic P103 with α CD, and they were characterized in terms of particle size, zeta potential, polydispersity index, drug solubility, appearance, rheological properties, in vitro drug diffusion, ocular tolerance, and ex vivo permeation.

2. Materials and Methods

2.1. Materials

Natamycin (665.73 g/mol) was obtained from AK Scientific (San Francisco, CA, USA). Soluplus[®] (115,000 g/mol) and Pluronic[®] P103 (EO₁₇PO₆₀EO₁₇; 4950 g/mol) were provided from BASF (Ludwigshafen, Germany). Sodium chloride, MgCl₂·6H₂O, and acetonitrile were provided from Scharlab SL (Barcelona, Spain); NaOH, KH₂PO₄, NaHCO₃, CaCl₂·2H₂O and NaH₂PO₄·H₂O were provided from Merck (Darmstadt, Germany); KCl from Prolabo (Fontenay-Sous-Bois, France); phosphate-buffered saline (PBS) was provided from Sigma (St. Louis, MO, USA); penicillin and streptomycin were provided from Gibco (Grand Island, NY, USA), and ethanol absolute was provided from Panreac (Barcelona, Spain). α -Cyclodextrin (α CD) was obtained from Wacker Chemie (Munich, Germany).

Phosphate buffer pH 6.4 was prepared by mixing 250 mL of solution A (0.2 M 62.5 mL KH₂PO₄) and solution B (0.2 M 16.4 mL NaOH) with water. Carbonate buffer pH 7.2 was prepared by mixing buffer solution A (100 mL; 1.24 g NaCl, 0.071 g KCl, 0.02 g NaH₂PO₄, 0.49 g NaHCO₃) and buffer solution B (100 mL; 0.023 g CaCl₂, 0.031 g MgCl₂).

2.2. Micelles Preparation and Characterization

Micelles were formed by dispersing Soluplus and Pluronic P103 in different concentrations (0.1%, 0.01%, 1%, 2%, 3%, 4%, 5% *w/v*) in 0.9% NaCl. Also, Soluplus and Pluronic P103 at 10% (*w/v*) were prepared in pH 6.4 buffer and 0.9% NaCl aq solution. They were kept under magnetic stirring for 12 h. Micelles containing natamycin (0.4 mg drug/mL dispersion) were prepared to compare with unloaded micelles.

Size, zeta potential, and polydispersion index (PDI) were measured using Zetasizer[®] 3000HS (Malvern Instruments, Malvern, UK). The pH was recorded using pH meter GLP22 (Crison Instruments, L'Hospitalet de Llobregat, Spain). Micelle stability against dilution was recorded for dispersions of Pluronic P103 containing natamycin, which were poured into quartz cells that contained either 0.9%

NaCl or pH 6.4 buffer for a sudden 30-fold or 60-fold dilution. The absorbance was recorded at 304 nm every 30 s for 30 min (UV-Vis spectrophotometer Agilent 8453, Waldbronn, Germany). All experiments were carried out in triplicate.

2.3. Solubility of Natamycin in Micelle Dispersions

Soluplus and Pluronic P103 dispersions were prepared by adding the required amount of polymer (0.01%, 0.1%, 1%, 2%, 3%, 4%, 5%, and 10% *w/v*) in 0.9% NaCl under stirring. Mixtures were obtained by mixing Soluplus (10% *w/v*) and Pluronic P103 (10% *w/v*) dispersions at various volume ratios (1:4, 2:3, 3:2, and 4:1). Aliquots (5 mL) of each dispersion were placed in test tubes, and natamycin was added in excess (~2 mg). All the dispersions were prepared in triplicate and kept under constant agitation (Unitronic, JP Selecta, Barcelona, Spain) for 6 days at 37 °C. After that, they were centrifuged (centrifuge model 5804R, Eppendorf AG, Germany) at 5000× *g* rpm for 30 min, and supernatants were diluted in ethanol/water (20:80% *v/v*) mixture. Natamycin content was determined by UV-Vis spectrophotometer (Agilent 8453, Waldbronn, Germany) at 304 nm using a previously validated method with standard solutions ranging from 2.0 to 20.0 µg/mL. Also, the pH was measured.

In addition, data from the solubility study were used to calculate the following parameters (25, 32):

(a) Molar solubilization capacity (moles of drug that can be solubilized per mol of copolymer forming micelles):

$$X = \frac{S_{tot} - S_w}{C_{copol} - CMC} \quad (1)$$

(b) Micelle–water partition coefficient (ratio between the drug concentration in the micelle and the aqueous phase):

$$P = \frac{S_{tot} - S_w}{S_w} \quad (2)$$

(c) Molar micelle–water partition coefficient that eliminates the *P* dependence on the copolymer concentration, assigning a default concentration of 1 M:

$$PM = \frac{X \cdot (1 - CMC)}{S_w} \quad (3)$$

(d) Gibbs standard-free energy of solubilization, which was estimated from the molar micelle/water partition coefficient (*PM*):

$$\Delta G_s = -RT \cdot \ln(PM) \quad (4)$$

(e) The proportion of drug molecules encapsulated in the micelles:

$$m_f = \frac{S_{tot} - S_w}{S_{tot}} \quad (5)$$

In these equations, S_{tot} represents the total solubility of natamycin in the micellar solution, S_w is the natamycin solubility in water, C_{copol} is the copolymer concentration in each micelle solution, CMC is the critical micelle concentration, and R is the universal constant of gases.

2.4. Solubility of Natamycin in α CD

Solutions of α CD (5% and 10% *w/v*) in pH 6.4 buffer or 0.9% NaCl were prepared. Natamycin was added in excess (approximately 8 mg in 10 mL), and they were kept under magnetic stirring at room temperature for 5 days. After that, they were centrifuged (as above) at 5000× *g* rpm for 30 min, and supernatants were diluted in ethanol/water (20:80% *v/v*) mixture. Natamycin content was determined by UV-Vis spectrophotometry at 304 nm. The apparent solubility of natamycin in pH 6.4 buffer and 0.9% NaCl without CDs was similarly measured.

2.5. Preparation of Poly(pseudo)rotaxanes

Polypseudorotaxanes were prepared mixing solution A (copolymers) and solution B (α CD) in pH 6.4 buffer and 0.9% NaCl media. For solution A, 20% (*w/w*) Soluplus or Pluronic P103 were prepared in each media. Once dissolved, natamycin (up to 240 μ g/mL) was added to each copolymer dispersion, and the systems were kept under magnetic stirring at room temperature for 24 h. For solution B, 20% (*w/v*) α CD was prepared. Solutions A and B were mixed, and the final concentration was 10% (*w/w*) copolymers, 10% (*w/w*) α CD, and 120 μ g/mL natamycin in each medium. Dispersions containing only the copolymers and natamycin at the same final concentration were also prepared for comparison. Changes in turbidity were examined by visual inspection.

2.6. Rheological Characterization

The influence of temperature on the storage (G') and loss (G'') moduli of Soluplus and Pluronic P103 dispersions, with and without α CD, in pH 6.4 buffer or 0.9% NaCl were recorded in a Rheolyst AR-1000 N rheometer (TA Instruments, UK) equipped with an AR2500 data analyzer, a Peltier plate, and cone geometry (6 cm diameter, 2.1°). Studies were performed at a fixed angular frequency of 5 rad/s and an oscillation stress of 0.1 Pa from 20 to 40 °C with a ramp of 2 °C/min.

2.7. Diffusion Assays

Natamycin diffusion tests from Soluplus and Pluronic dispersions and poly(pseudo)rotaxanes were performed in triplicate in vertical Franz diffusion cells fitted with cellulose acetate membrane filters (0.45-mm pore size, 25-mm diameter). Aliquots of 1.00 mL of the test formulation at 37 °C were placed in the donor compartment. The receptor phase contained 6.00 mL of medium (0.9% NaCl or pH 6.4 buffer) thermostated at 37 °C and kept under magnetic stirring. The area available for diffusion was 0.786 cm². Samples (0.70 mL) were taken from the receptor phase at 30, 60, 90, 120, 180, 210, 240, 300 and 360 min, and replaced immediately with fresh medium. Natamycin concentration was determined by UV-Vis spectrophotometry.

Diffusion coefficients were estimated by following the Higuchi equation:

$$\frac{Q}{A} = 2C_0 \left(\frac{Dt}{\pi} \right)^{\frac{1}{2}} \quad (6)$$

where Q is the amount of natamycin (g) released by time t (min), A is the diffusion area (cm²), C_0 is the initial concentration of natamycin in the formulation (g/mL), and D is the diffusion coefficient (cm²/min). The average size and zeta potential of the formulation tested in this assay were also characterized.

2.8. Ocular Tolerance Test (HET-CAM Test)

Fertile chicken eggs were kindly donated by The Coren Technological Incubation Center (San Cibrao das Viñas, Spain) and incubated at 37 °C and 60% RH. Eggs were manually rotated 180° three times per day to ensure the correct development of the embryo. After 9 days of incubation, a circular cut (about 1 cm in diameter) was made on the eggshell using a rotatory saw. The inner membrane was wet with 0.9% NaCl, and then carefully removed to expose the chorioallantoic membrane (CAM). Any defective egg was discarded. Aliquots of natamycin-loaded Soluplus and Pluronic P103 micelles (200 μ L) and poly(pseudo)rotaxanes (150 μ L) dispersions were placed on the CAM of different eggs. Negative and positive controls were 0.9% NaCl and 0.1 N NaOH solutions, respectively. The development of hemorrhage (tH , bleeding from the vessels), vascular lysis (tL , blood vessel disintegration), or coagulation (tC , intravascular and extravascular protein denaturation) of CAM vessels was monitored for 300 s. Then, the irritation score (IS) was calculated as follows [25]:

$$IS = \frac{(301 - tH) \times 5}{300} + \frac{(301 - tL) \times 7}{300} + \frac{(301 - tC) \times 9}{300} \quad (7)$$

The damage was classified by means of *IS* as non-irritant ($IS < 1$), mild irritant ($1 \leq IS < 5$), moderately irritant ($5 \leq IS < 10$), or severe irritant ($IS > 10$). Each test was performed at least in duplicate.

2.9. Ex-Vivo Corneal and Sclera Permeability Study

Bovine eyes were collected immediately after sacrifice from a local slaughterhouse and transported immersed in PBS solution containing antibiotics (penicillin 100 IU/mL and streptomycin 100 µg/mL) and maintained in an ice bath. Next, corneas and scleras were isolated, rinsed with PBS, and placed on vertical diffusion Franz cells between the donor and receptor compartments. Both compartments were filled with carbonate buffer pH 7.2. The receptors were kept immersed inside a bath at 37 °C, and gentle magnetic stirring was applied for 1 h in order to balance ocular tissues. Then, the buffer at the donor chamber was completely removed and replaced by the formulations (2 mL) prepared as described above either in pH 6.4 buffer or 0.9% NaCl. The donor compartments were covered with parafilm (0.785 cm² area available for permeation). Samples (1 mL) were taken from the receptor compartment at 0.5, 1, 2, 3, 4, 5 and 6 h, and the same volume was replaced with fresh medium, taking care to remove bubbles from the diffusion cells. All the experiments were carried out in triplicate.

Natamycin permeated was quantified using a Jasco (Tokyo, Japan) HPLC (AS-4140 Autosampler, PU-4180 Pump, LC-NetII/ADC Interface Box, CO-4060 Column Oven, MD-4010 Photodiode Array Detector), fitted with a C18 column (Waters Symmetry C18, 5 µm, 3.9 × 150 mm) and operated using ChromNAV software (ver. 2, Jasco, Tokyo, Japan). The mobile phase was acetonitrile: 30 mM of perchlorid acid (35:65) at 1 mL/min and 30 °C. The injection volume was 90 µL, and natamycin was quantified at 304 nm (retention time 3.3 min). Standard solutions of natamycin (0.01–1 µg/mL) in ethanol/water (20:80) were prepared.

After a 6-h permeation test, drug concentration in the donors was quantified. All the corneas and scleras were visually inspected after the 6-h test to verify that none of them had cracks or modified their appearance. Corneas and scleras were soaked in ethanol:water (50:50 *v/v*; 3 mL) medium at 37 °C during 24 h. Then, they were sonicated during 99 min at 37 °C, centrifuged (1000 rpm, 5 min, 25 °C), and the supernatant was filtered (Acrodisc[®] Syringe Filter, 0.22 µm GHP Minispikes, Waters), centrifuged again (14,000× *g* rpm, 20 min, 25 °C), and filtered to be measured in HPLC.

The apparent permeability coefficient (P_{app}) was calculated from the flux (J) according to Equation (8) [32]:

$$P_{app} = \frac{J}{C_0} \quad (8)$$

where J is the flux calculated as the slope (Q/t) of the linear section of the amount of drug in the receptor chamber (Q) versus time (t), and C_0 is the initial concentration of natamycin in the donor phase. Each experiment was performed in triplicate, and the results were reported as the mean values ± standard deviation (SD).

2.10. Statistical Analysis

The effects of formulation composition on natamycin permeation through sclera were analyzed using ANOVA and a multiple range test (Statgraphics Centurion XVI 1.15, StatPoint Technologies Inc., Warrenton VA, USA).

3. Results and Discussion

3.1. Micelles Preparation and Natamycin Solubilization

The first experiments carried out in 0.9% NaCl aqueous medium revealed that Soluplus micelles were larger (70–90 nm) and conferred more acidic environment (~pH 4) than those of Pluronic P103 (20 nm; ~pH 6) (Table 1 and Table S1 in Supplementary Material). The zeta potential was slightly negative in all the cases. The reported CMCs for Soluplus and Pluronic P103 are 0.00076% *w/v*

(i.e., 6.60×10^{-8} M) [25,38] and 0.070% *w/v* (1.41×10^{-4} M) [39], which is in good agreement with our results.

Table 1. The pH, size, and zeta potential of unloaded micelles of Soluplus and Pluronic P103 and their mixtures prepared at various volume ratios in 0.9% NaCl and pH 6.4 buffer.

0.9% NaCl				
Copolymer (% <i>w/v</i>)	pH	Diameter (nm)	PDI	Zeta Potential (mV)
Soluplus (10%)	3.34	90.0 ± 1.3	0.168 ± 0.010	−0.40 ± 0.19
Pluronic (10%)	6.34	20.5 ± 0.6	0.238 ± 0.003	1.03 ± 0.47
Soluplus/Pluronic P103 (1:4)	4.67	129.6 ± 2.9	0.246 ± 0.019	−0.66 ± 0.20
Soluplus/Pluronic P103 (2:3)	3.89	131.0 ± 3.0	0.214 ± 0.011	−0.81 ± 0.08
Soluplus/Pluronic P103 (3:2)	3.70	121.7 ± 1.0	0.190 ± 0.017	−1.49 ± 0.46
Soluplus/Pluronic P103 (4:1)	3.52	110.7 ± 1.8	0.209 ± 0.008	−0.56 ± 0.41
Buffer pH 6.4				
Copolymer (% <i>w/v</i>)	pH	Diameter (nm)	PDI	Zeta Potential (mV)
Soluplus (10%)	6.08	102.8 ± 1.0	0.189 ± 0.018	−0.14 ± 0.36
Pluronic (10%)	6.36	16.1 ± 0.4	0.226 ± 0.018	1.15 ± 0.28
Soluplus/Pluronic P103 (1:4)	6.49	150.8 ± 4.5	0.217 ± 0.011	0.48 ± 0.06
Soluplus/Pluronic P103 (2:3)	6.47	140.5 ± 0.7	0.176 ± 0.008	−0.02 ± 0.15
Soluplus/Pluronic P103 (3:2)	6.20	127.8 ± 0.9	0.171 ± 0.011	−0.12 ± 0.01
Soluplus/Pluronic P103 (4:1)	6.48	114.7 ± 2.4	0.170 ± 0.011	−0.18 ± 0.13

Mixtures of 10% (*w/v*) Soluplus and 10% (*w/v*) Pluronic dispersions prepared at various volume ratios (1:4, 2:3, 3:2, and 4:1) in 0.9% NaCl led to intermediate pH values and significantly larger micelles (Table 1). Studies performed by Koontz et al. [18] revealed that natamycin is more stable at pH ranging from 4 to 7. Thus, for the sake of comparison of the micelle properties avoiding changes in pH, the micelles and their mixtures were also prepared in pH 6.4 buffer (Table 1). Once again, a remarkable increase in the micelle size was observed as the Pluronic P103 proportion increased in the mixed micelles, which suggests that the large PPO block of Pluronic P103 (EO₁₇PO₆₀EO₁₇) accommodates inside the Soluplus cores. Commonly, an increase in micelle size is associated with the expansion of the core, and it should be noted that Pluronic P103 is notably more hydrophobic (HLB = 9) [40] than Soluplus (HLB = 16) [32].

The apparent solubility of natamycin in 0.9% NaCl (0% block copolymer) was 43.82 ± 1.76 µg/mL, which agrees well with the values previously reported [11]. As expected, increasing the concentration of copolymer in the medium resulted in increased natamycin apparent solubility, confirming natamycin incorporation into the nanomicelles (Figures 2 and 3).

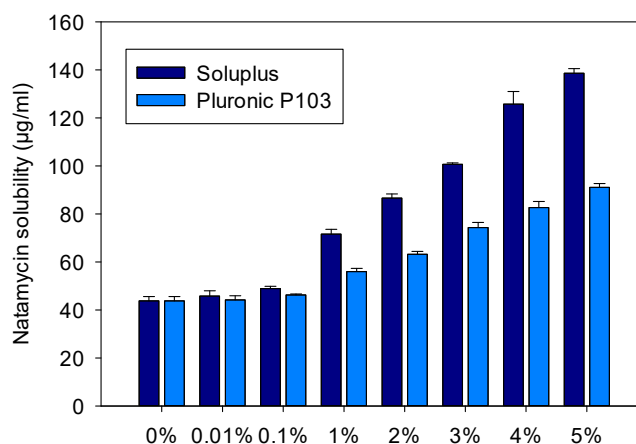


Figure 2. Apparent solubility of natamycin in Soluplus and Pluronic P 103 dispersions (0%, 0.01%, 0.1%, 1%, 2%, 3%, 4%, and 5% *w/v*) prepared in 0.9% NaCl at 25 °C.

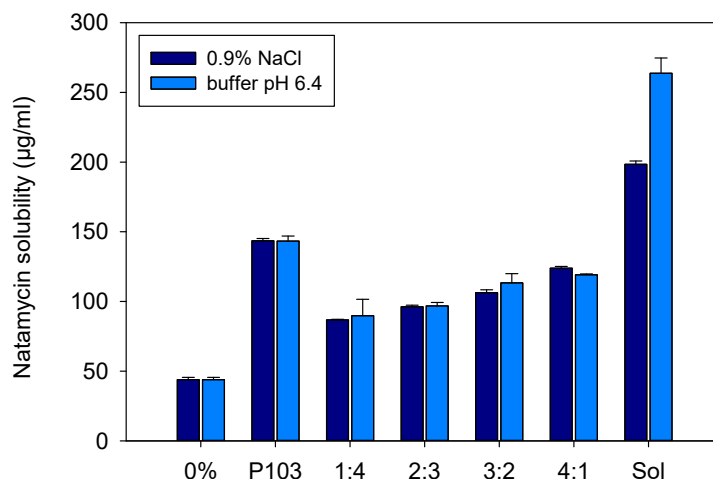


Figure 3. Apparent solubility of natamycin in micelle dispersions of 10% (*w/v*) of Soluplus and Pluronic P103 and their mixtures (Soluplus:Pluronic P103) prepared at various volume ratios in 0.9% NaCl and pH 6.4 buffer. Total copolymer concentration was 10% *w/v* in all cases.

The increase in apparent solubility was evident for both copolymers at concentrations equals to or above 1%, but the increase was significantly greater for the Soluplus dispersions. The apparent solubility of natamycin reached $138.6 \pm 1.9 \mu\text{g/mL}$ in Soluplus 5% *w/v* in 0.9% NaCl at 25 °C. The high solubilizing capability of Soluplus has been associated to its large core, which in turn leads to greater micelles [38]. Parameters related to micelle solubilizing efficiency are summarized in Tables 2 and 3. The molar solubilization capability, χ , was nearly two orders of magnitude greater for Soluplus compared to Pluronic P103. The χ value decreased with increasing copolymer concentration, which indicates that more unimers are involved in micelle formation. The encapsulation of natamycin occurred spontaneously for both micelle types, but the thermodynamics (i.e., standard-free Gibbs energy of solubilization) were more favorable for Soluplus systems. For a fixed concentration of 5% *w/v* copolymer, ca. 70% drug molecules were encapsulated into the Soluplus micelles, while only 50% were encapsulated in the case of Pluronic P103. The stability of the micelles against dilution could be only verified for the Pluronic nanomicelles (Figure S2 in the Supplementary Material), since the Soluplus nanomicelles absorbed light in the same UV region as the drug. This low Soluplus UV absorption did not interfere with drug solubility quantification in the apparent solubility studies as the micelles disassemble in the ethanol–water medium, but it caused noise under the dilution with aqueous medium of the stability test. In the case of Pluronic P103, after strong dilution in either 0.9% NaCl solution or pH 6.4 buffer, the absorbance showed a minor initial decrease followed by a complete and stable recovery, which indicates rapid rebalancing of the micelle–medium partition equilibrium.

Table 2. Capability of Soluplus dispersions in 0.9% NaCl to solubilize natamycin, estimated using Equations (1)–(5). (NAT: natamycin; χ : molar solubilization capacity; P: partition coefficient; PM: molar partition coefficient; ΔG : standard-free Gibbs energy of solubilization; mf: molar fraction of drug encapsulated inside the micelle). * Data from solubility experiments carried out in pH 6.4 buffer.

Copolymer (% <i>w/w</i>)	Soluplus (M)	NAT (M)	NAT ($\mu\text{g/mL}$)	χ	P	PM	ΔG (KJ/mol)	mf
0.1	0.87×10^{-5}	0.71×10^{-4}	46.99	0.52	0.07	7869.6	−22,227.0	0.06
1	8.70×10^{-5}	1.04×10^{-4}	69.31	0.44	0.58	6619.2	−21,798.2	0.37
2	1.74×10^{-4}	1.26×10^{-4}	84.03	0.35	0.91	5233.1	−21,216.1	0.48
3	2.61×10^{-4}	1.47×10^{-4}	97.93	0.31	1.23	4700.0	−20,949.8	0.55
4	3.48×10^{-4}	1.84×10^{-4}	122.51	0.34	1.78	5131.2	−21,167.3	0.64
5	4.35×10^{-4}	2.03×10^{-4}	135.23	0.31	2.07	4769.5	−20,986.2	0.67
10	8.70×10^{-4}	2.98×10^{-4}	198.49	0.27	3.51	4038.0	−20,573.7	0.78
10 (buffer) *	8.70×10^{-4}	3.96×10^{-4}	263.73	0.38	4.99	5743.2	−21,446.5	0.83

Table 3. Capability of Pluronic P103 dispersions in 0.9% NaCl to solubilize natamycin, estimated using Equations (1)–(5). (NAT: natamycin; χ : molar solubilization capacity; P: partition coefficient; PM: molar partition coefficient; ΔG : standard-free Gibbs energy of solubilization; mf: molar fraction of drug encapsulated inside the micelle). * Data from solubility experiments carried out in pH 6.4 buffer.

Copolymer (% w/w)	Pluronic P103 (M)	NAT (M)	NAT ($\mu\text{g/mL}$)	χ	P	PM	ΔG (KJ/mol)	mf
0.1	0.20×10^{-3}	0.70×10^{-4}	46.27	5.59×10^{-2}	0.05	845.5	-16,699.6	0.05
1	2.02×10^{-3}	0.84×10^{-4}	56.00	9.59×10^{-3}	0.27	145.1	-12,332.5	0.21
2	4.04×10^{-3}	0.95×10^{-4}	63.21	7.40×10^{-3}	0.44	112.0	-11,690.4	0.30
3	6.06×10^{-3}	1.12×10^{-4}	74.37	7.71×10^{-3}	0.69	116.6	-11,790.1	0.41
4	8.08×10^{-3}	1.24×10^{-4}	82.63	7.31×10^{-3}	0.88	110.6	-11,659.3	0.47
5	1.01×10^{-2}	1.37×10^{-4}	91.06	7.10×10^{-3}	1.07	107.4	-11,586.3	0.52
10	2.02×10^{-2}	2.16×10^{-4}	143.49	7.45×10^{-3}	2.27	112.7	-11,706.4	0.69
10 (buffer) *	2.02×10^{-2}	2.15×10^{-4}	143.39	7.44×10^{-3}	2.26	112.6	-11,704.0	0.69

Soluplus and Pluronic concentrations were increased to 10% *w/v*, and their solubilization capability was compared to that of the mixed micellar solutions (1:4, 2:3, 3:2, 4:1 *v/v*) prepared in 0.9% NaCl and pH 6.4 buffer (Figure 3). Once again, the Soluplus (10% *w/v*) micelles dispersion showed greater apparent solubility enhancement, especially in pH 6.4 buffer ($263.7 \pm 10.9 \mu\text{g/mL}$) compared to 0.9% NaCl medium ($198.5 \pm 2.3 \mu\text{g/mL}$). The apparent solubility of natamycin in the Soluplus /Pluronic mixtures ranged from 86.8 ± 0.3 to $123.8 \pm 1.3 \mu\text{g/mL}$ in 0.9% NaCl, and from 89.7 ± 11.9 to $119.1 \pm 0.6 \mu\text{g/mL}$ in pH 6.4 buffer. The higher the content in P103, the lower the solubilization capability. The partition coefficients P for Soluplus/Pluronic P103 1:4 and 4:1 (*v/v*) were in the ranges 0.98 to 1.05 and 1.72 to 1.82, respectively. This finding correlates with the increase in size observed for the mixed micelles, which suggests that Pluronic P103 occupies the core of Soluplus micelles and alters the inner hydrophobic interactions, which in turn hinders the accommodation of natamycin. Similar behavior was observed by Bernabeu et al. [38] for mixed systems formed with Soluplus and D- α -tocopheryl polyethylene-glycol 1000 succinate (TPGS). The incorporation of TPGS into Soluplus micelles made the self-assembly of Soluplus molecules more difficult, increased the size of the micelles, and notably decreased their capability to host paclitaxel. These detrimental effects attenuated as the Soluplus ratio increased. It should be noted that compared to previous reports on Soluplus/Pluronic mixed micelles, the variety that we tested (Pluronic P103) is more hydrophobic than those evaluated before (P105 and F127) [33,34], which may explain the stronger effects on the properties of the mixed micelles. For subsequent studies, only the mixed micelles with the largest ratio in Soluplus (i.e., 4:1), and thus with the size more similar to pure Soluplus micelles were considered.

3.2. Poly(pseudo)rotaxane Formation

Previous to the preparation of the poly(pseudo)rotaxanes, the capability of αCD to form an inclusion complex with natamycin, which is more soluble than free natamycin, was verified. The information available on the use of αCD to solubilize ocular antifungal drugs is so far very limited [41]. The apparent solubility of natamycin in aqueous 5% and 10% (*w/v*) αCD solutions was determined to be $103.7 \pm 1.4 \mu\text{g/mL}$ and $143.5 \pm 4.6 \mu\text{g/mL}$ in 0.9% NaCl medium, and $96.4 \pm 2.9 \mu\text{g/mL}$ and $126.6 \pm 0.4 \mu\text{g/mL}$ in pH 6.4 buffer, respectively (Figure S3 in the Supplementary Material). These values indicate an efficient encapsulation of the drug in αCD cavities, achieving apparent solubility values similar to those obtained for Pluronic P103 micellar dispersions at the same concentrations, although lower than those provided by Soluplus. A further increase in αCD concentration was not tested due to safety concerns [42].

Based on these preliminary data, 10% Soluplus, 10% Pluronic P103, and binary systems containing Soluplus 10%/Pluronic P103 10% (4:1 *v/v*) in aqueous pH 6.4 buffer were selected for poly(pseudo)rotaxane formation. Each dispersion was prepared at double concentration and then mixed in vortex for a few minutes. Natamycin concentration was set at $120 \mu\text{g/mL}$, which is three-fold

greater than the apparent drug solubility in water, but still below the solubilizing capability of each separate component (copolymer/ α CD). The addition of α CD solution up to a final concentration of 10% caused remarkable changes in gel appearance and rheological properties. The initial transparent (Pluronic P103) or opalescent (Soluplus) dispersions rapidly transformed into whitish systems, which indicated poly(pseudo)rotaxane formation. All these changes occurred both in 0.9% NaCl or pH 6.4 buffer (Figure 4).

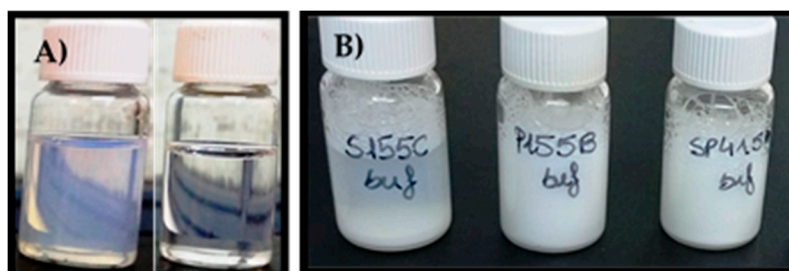


Figure 4. Appearance of (A) Soluplus 10% (left) and Pluronic P103 10% (right) dispersions in 0.9% NaCl; (B) Poly(pseudo)rotaxane formation after the addition of 10% α CD to Soluplus (left), Soluplus/Pluronic P103 in ratio (4:1) (in the middle), and Pluronic P103 dispersions (right) in pH 6.4 buffer after storage for 12 h at room temperature.

Poly(pseudo)rotaxane formation was also confirmed by recording the viscoelastic behavior of the copolymer dispersions with and without α CD (Figure 5). Pluronic P103 10% *w/v* dispersions were performed as a liquid-like material with negligible storage modulus (G'). Moreover, G'' values remained constant in the temperature range evaluated; namely, a sol-to-gel transition was not observed. The addition of α CD caused a remarkable increase in both G' and G'' ; the G' values became larger than the G'' ones. The poly(pseudo)rotaxane system behaved as weak gels in the 20 to 40 °C range. α CD has been reported to be able to rapidly thread along PEO blocks, decreasing their hydrophilicity and favoring the stacking of the PEO blocks through channel-type interactions between the threaded α CDs [37]. This stacking reinforces the tie junctions among the poloxamer molecules, which in the absence of α CDs are only driven by the PPO–PPO hydrophobic interactions. The presence of natamycin caused minor changes in the viscoelastic performance of the Pluronic P103-based poly(pseudo)rotaxanes.

Differently, Soluplus 10% *w/v* dispersions exhibited a peculiar dependence on temperature. In agreement with previous reports (25, 32), G' values were above 1 Pa at approximately 34 °C, and then rose in parallel with those of G'' . Thus, instead of showing a sudden sol-to-gel transition, the values of both G' and G'' progressively increased with the temperature. This behavior indicates a poorly cooperative hydrophobic-driven transition, which was probably due to the particular configuration of the Soluplus copolymer with three blocks of different hydrophilicity. The addition of α CD to unloaded Soluplus dispersion caused a remarkable increase in both moduli. As in the case of Pluronic P103, the Soluplus-based poly(pseudo)rotaxanes performed as weak gels already at 20 °C, but showed a further increase in G' and G'' values at temperatures above 30 °C. The drug-loaded dispersions behaved quite differently. They maintained low G' and G'' values at room temperature and exhibited a sol-to-gel transition at 30.5 °C, which is a transition temperature that is significantly lower than that recorded in the absence of α CD. Differences between unloaded and natamycin-loaded Soluplus dispersions suggest that the hosting of natamycin in the Soluplus micelles alter the copolymer capability to form strong complexes with α CD at room temperature. Nevertheless, at the temperature of the eye surface, the values of G' and G'' are at least one order of magnitude larger for the poly(pseudo)rotaxanes compared to the Soluplus micelle dispersions.

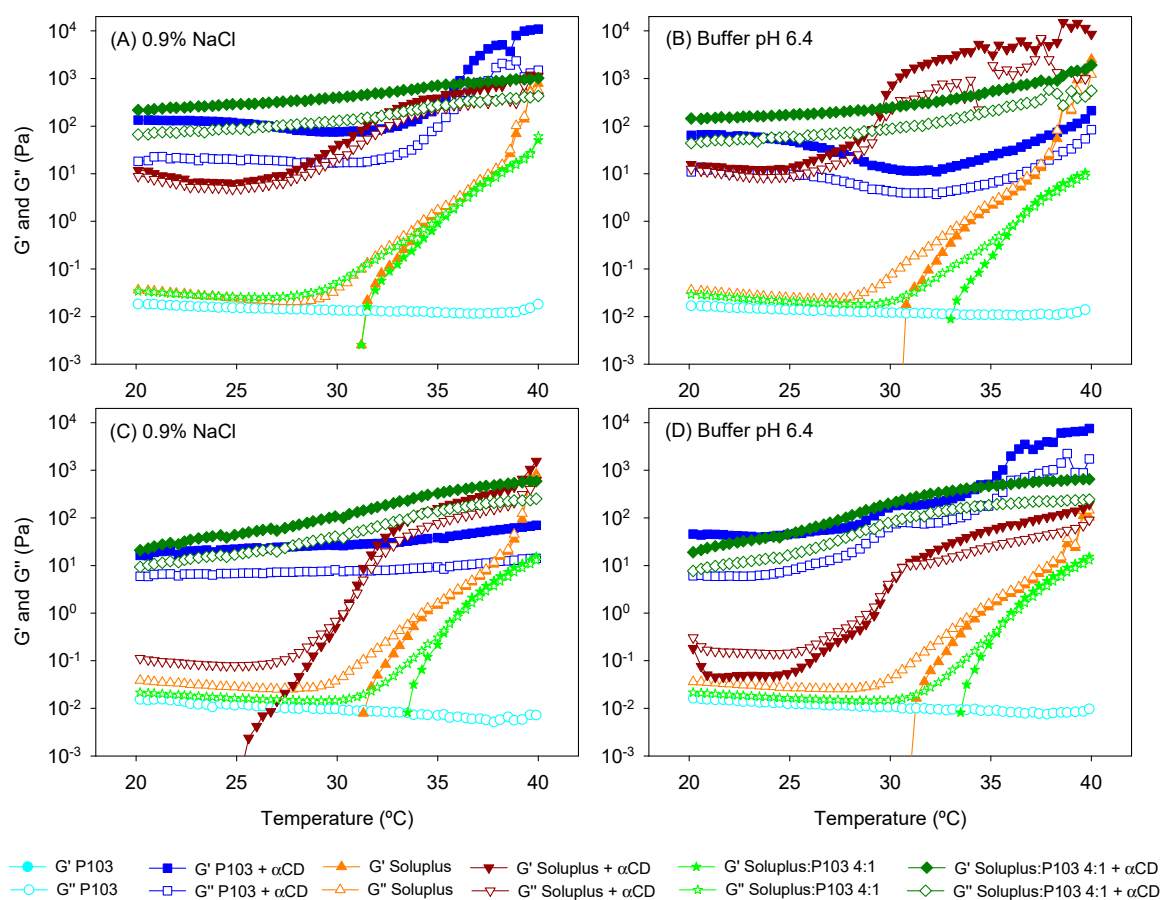


Figure 5. Evolution of the storage (G') and the loss (G'') moduli as a function of temperature of (A,B) unloaded and (C,D) drug-loaded copolymer dispersions and their mixtures with and without α -cyclodextrin (α CD) (poly(pseudo)rotaxanes) in 0.9% NaCl (left) and pH 6.4 buffer (right). Total copolymer concentration was 10% w/v in all cases.

To the best of our knowledge, the poly(pseudo)rotaxane formation of mixed micelles has not been previously investigated. Soluplus/P103 4:1 dispersions showed a shift in the sol-to-gel transition toward higher values (36.1 °C) compared to Soluplus solely dispersion, except for the unloaded system in NaCl 0.9%. This finding agrees well with the distortion of the self-assembly process of Soluplus as Pluronic P103 accommodates in the micelle core (as hypothesized from the increase in micelle size). The addition of α CD to the mixed micelles remarkably increased the viscoelastic parameters. The system performed as a weak gel already at 20 °C, and only a slight increase in G' and G'' was observed during heating. Interestingly, the presence of natamycin only caused a minor decrease in both G' and G'' , which means that Pluronic P103 attenuated the effects of hosting natamycin in Soluplus cores probably because of a preferential interaction of α CD molecules with the PEO blocks of Pluronic P103. It has been previously observed by means of nuclear magnetic resonance diffusion studies that the threading of α CD along PEO moieties of Pluronic F127 causes a remarkable decrease in α CD mobility [43], which is typical of strong complex formation. The decrease in the mobility of α CDs due to the formation of a transient complex with Soluplus was less marked [35], which supports our hypothesis of a preferential threading of α CDs along Pluronic P103 in the mixed micelles.

3.3. HET-CAM Assay

The preliminary screening of potential irritancy of the formulations was performed using the Hen's Egg Test on the Chorioallantoic Membrane (HET-CAM), which is an alternative to Draize rabbit eye test [25,44,45]. The HET-CAM test revealed that no micelle or poly(pseudo)rotaxane dispersions

caused hemorrhage, lysis, or coagulation at the time of study (t_H , t_L , and t_C values $\gg 301$ s) (Figure S4 in Supplementary Material). The IS was 0.0 for all the formulations, as occurred with the negative control (0.9% NaCl). Therefore, they can be considered as non-irritants. Differently, the IS for the positive control (NaOH 0.1N) was 18.58. This behavior is consistent with previously reported studies [25,35].

3.4. Natamycin Diffusion

Natamycin diffusion from micelles, mixed micelles, and poly(pseudo)rotaxanes prepared in 0.9% NaCl and pH 6.4 buffer was first evaluated in vitro (under sink conditions) using a membrane with a large (0.45 mm) pore size in order to quantify the capability of the formulations to control drug release. All the dispersions showed sustained diffusion (Figure 6), but differences were observed depending on the copolymer and the addition of α CD. In the case of micelles, the Pluronic P103 10% w/v formulation provided the fastest diffusion ($46.45 \pm 1.41 \mu\text{g}/\text{cm}^2$ in 0.9% NaCl and $48.25 \pm 0.42 \mu\text{g}/\text{cm}^2$ in buffer pH 6.4 after 6 h), followed by mixed micelles ($25.69 \pm 0.50 \mu\text{g}/\text{cm}^2$ in 0.9% NaCl and $42.25 \pm 1.72 \mu\text{g}/\text{cm}^2$ in buffer pH 6.4 after 6 h) and Soluplus micelles ($13.39 \pm 1.04 \mu\text{g}/\text{cm}^2$ in 0.9% NaCl and $20.13 \pm 0.95 \mu\text{g}/\text{cm}^2$ in buffer pH 6.4 after 6 h). This finding is in agreement with the smaller size of Pluronic P103 micelles and the less compact structure of these micelles and also of the mixed micelles compared to those of Soluplus. The partition coefficient, P , for Soluplus/Pluronic P103 4:1 (v/v) was in the 1.72 to 1.82 range. These values are lower than those recorded for pure Soluplus or Pluronic in separate. This means that there were more free drug molecules in the mixed micelles. Nevertheless, the diffusion was slower than that from Pluronic micelles, which supported the hypothesis that the smaller size of Pluronic micelles plays a relevant role in the diffusion rate, although other factors such as copolymer composition and drug–core interactions may also affect the diffusion kinetics.

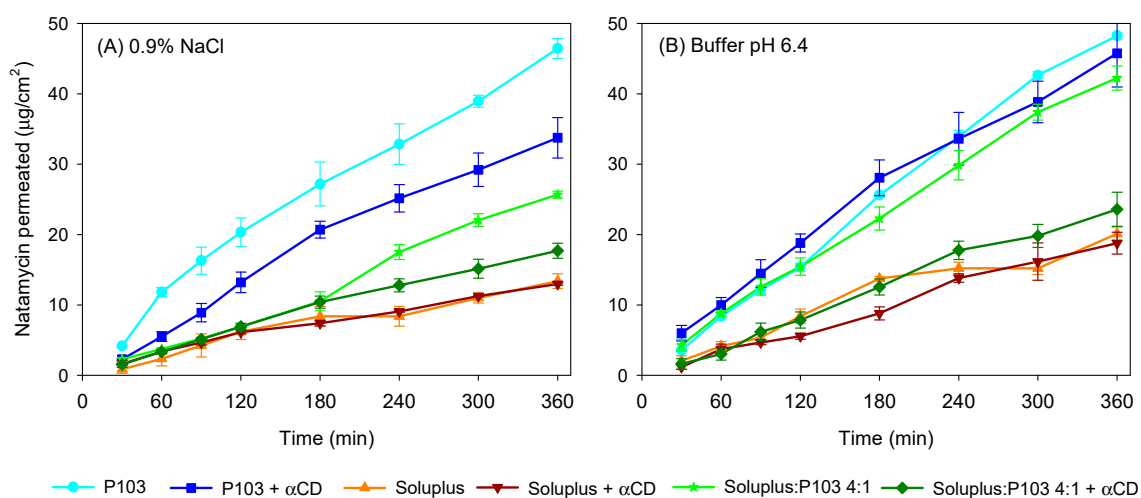


Figure 6. Natamycin diffusion test at 37 °C from Soluplus and Pluronic micelles, Soluplus:Pluronic P103 4:1 v/v mixed micelles, and poly(pseudo)rotaxanes in 0.9% NaCl (A) and pH 6.4 buffer (B). Total copolymer concentration was 10% w/v in all cases.

Regarding poly(pseudo)rotaxanes, the highest amount of natamycin that had diffused after 6 h corresponded to Pluronic P103 formulation ($33.76 \pm 2.86 \mu\text{g}/\text{cm}^2$ in 0.9% NaCl and $45.76 \pm 4.79 \mu\text{g}/\text{cm}^2$ in pH 6.4 buffer), followed by poly(pseudo)rotaxanes of mixed micelles ($17.71 \pm 1.08 \mu\text{g}/\text{cm}^2$ in 0.9% NaCl and $23.60 \pm 2.42 \mu\text{g}/\text{cm}^2$ in pH 6.4 buffer) and Soluplus-based poly(pseudo)rotaxanes ($12.99 \pm 0.19 \mu\text{g}/\text{cm}^2$ in 0.9% NaCl and $18.78 \pm 1.55 \mu\text{g}/\text{cm}^2$ in pH 6.4 buffer). Soluplus poly(pseudo)rotaxanes showed the slowest diffusion rate. The delay in drug diffusion observed for poly(pseudo)rotaxanes is related to the formation of a more structured network with higher viscosity [35], as recorded in the rheometry study. Nevertheless, the increase in macroviscosity might not directly translate to higher microviscosity [46]. Indeed, in the case of Soluplus, it has been previously shown for carvedilol transdermal formulations

that the differences in drug release between micelles and poly(pseudo)rotaxanes are minor [35]. The diffusion coefficients (D) of natamycin calculated applying Equation (6) are shown in Table 4.

Correlation coefficients (R^2) confirmed that the Higuchi's kinetics fitted well. Small differences in drug diffusion coefficients were obtained when the formulations were prepared and tested in pH 6.4 buffer compared to 0.9% NaCl. Diffusion coefficients were almost one order of magnitude lower for Soluplus micelles compared to Pluronic micelles, and for both formulations, the addition of α CD caused a small decrease in the diffusion coefficients. The poly(pseudo)rotaxanes made from mixed micelles showed natamycin diffusion coefficients intermediate between those of Pluronic P103-based and Soluplus-based poly(pseudo)rotaxanes. Therefore, the preparation of mixed micelles may be a useful tool to regulate drug release from poly(pseudo)rotaxanes.

Table 4. Natamycin diffusion coefficients from Soluplus and Pluronic micelles, Soluplus:Pluronic P103 4:1 v/v mixed micelles, and poly(pseudo)rotaxanes in 0.9% NaCl and pH 6.4 buffer. Total copolymer concentration was 10% w/v. Mean values and, in parenthesis, standard deviation (n = 3).

Formulation	0.9% NaCl		Buffer pH 6.4	
	D $\times 10^6$ (cm ² /min)	R ²	D $\times 10^6$ (cm ² /min)	R ²
Pluronic P103 10%	49.46 (3.99)	0.992	65.14 (0.96)	0.992
Pluronic P103 + α CD 10%	32.66 (4.73)	0.990	50.30 (11.57)	0.990
Soluplus 10%	5.56 (1.62)	0.992	10.58 (0.53)	0.982
Soluplus 10% + α CD 10%	3.72 (0.24)	0.982	9.92 (2.38)	0.992
Soluplus/Pluronic P 103 (4:1)	18.31 (1.24)	0.998	45.68 (4.10)	0.989
Soluplus/Pluronic P 103 (4:1) + α CD 10%	8.21 (1.22)	0.970	16.14 (2.00)	0.996

3.5. Ex Vivo Permeation Assay

Bovine cornea and sclera were isolated from fresh eyes and mounted in vertical (Franz) diffusion cells using carbonate buffer pH 7.2 as the receptor medium (37 °C). Natamycin that permeated through ocular tissues to the receptor chamber was monitored for 6 h. In the case of cornea permeation tests, the levels of drug in the receptor compartment were below the quantification limit (0.01 μ g/mL) during the first five hours. At 6 h, only the micelle formulations gave measurable natamycin amounts, and the amounts permeated ranged between 0.13–0.26 μ g/cm², disregarding the copolymer involved. In spite of this low ability to cross the cornea, natamycin accumulated in the cornea tissue at the relevant amount (Figure 7A,B). Interestingly, for each copolymer tested, the poly(pseudo)rotaxanes provided higher amounts of drug accumulated than the corresponding micelles. Soluplus-based poly(pseudo)rotaxanes displayed the highest corneal accumulation, disregarding whether the formulations were prepared in 0.9% NaCl or pH 6.4 buffer (4.24 \pm 0.13 μ g/cm² and 7.50 \pm 0.03 μ g/cm², respectively).

Compared to the in vitro tests in which the membrane is not an effective barrier to drug diffusion, the compact layered structure of the cornea is a quite challenging barrier for any drug, and some studies have shown important diffusion lag times due to the difficult movement of the drugs into the cornea. Indeed, transcorneal penetration studies carried out using ex vivo rabbits' eyes with Natacyn[®] (suspension diluted to 3 mg drug per mL) revealed quite low transcorneal flux (0.14 \pm 0.1 $\times 10^{-6}$ cm/s) [15]. Our formulations had all the same initial concentration in natamycin (120 μ g/mL), which was ca. 3 times larger than the apparent solubility in water and above the highest minimal inhibitory concentration (MIC₉₀ = 64 μ g/mL) reported for clinically relevant fungi species [47]. The increase in apparent drug solubility once encapsulated in the micelles and poly(pseudo)rotaxanes should lead to an increase in drug gradient concentration on the tissue surface, which should favor drug penetration. Nevertheless, the larger size of encapsulating species and restrictions imposed by the tissue itself may hinder passive drug diffusion. In this sense, the presence of α CD in the polypseudorotaxanes may facilitate the mobility of natamycin in the aqueous layer in contact with the cornea, and may also facilitate the entrance in the first hydrophilic layer [48,49], disregarding the apparent macroviscosity of the formulations. To cross the cornea, the drug is expected to abandon the

micelles/CDs. Nevertheless, free drug permeation through the cornea depends on the drug lipophilicity and, in the particular case of natamycin, the LogP is about 1.1 [50], which seems to be quite low for facilitating the transcorneal penetration.

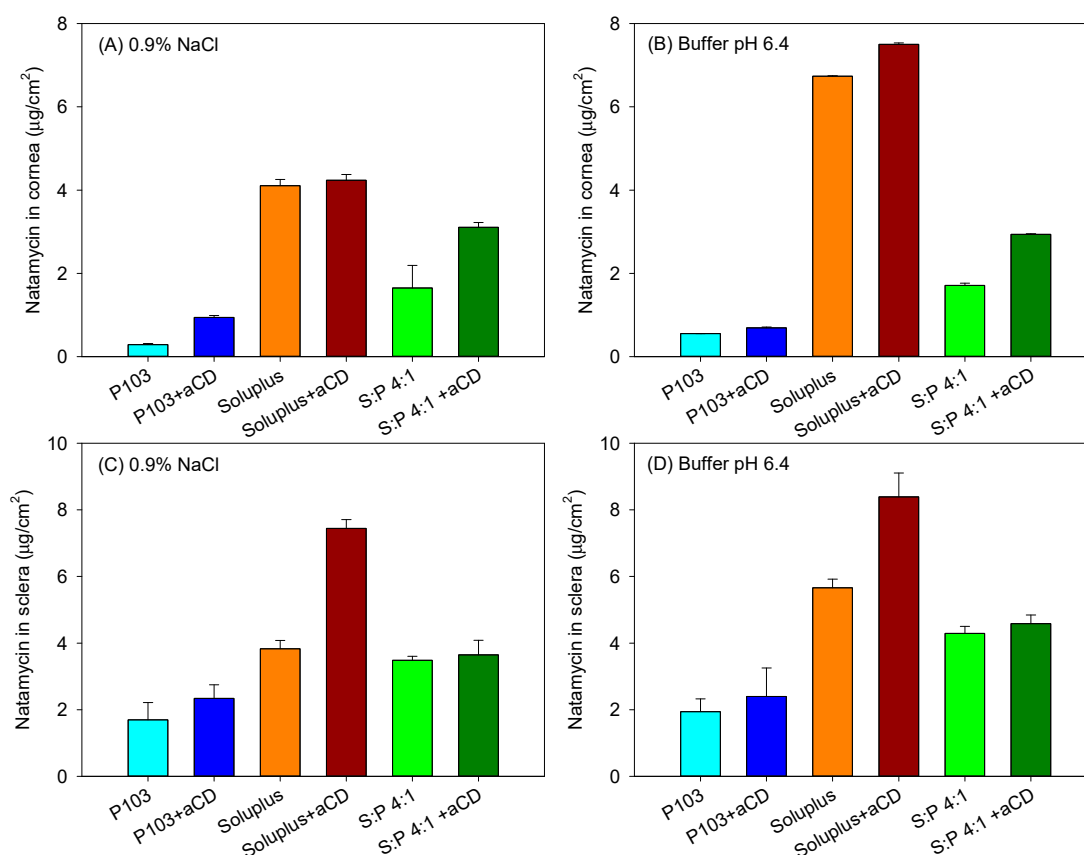


Figure 7. Amount of natamycin accumulated inside bovine cornea (A,B) and sclera (C,D) after 6 h in contact with Soluplus and Pluronic micelles, Soluplus:Pluronic P103 4:1 *v/v* mixed micelles, and their poly(pseudo)rotaxanes in 0.9% NaCl (left) and pH 6.4 buffer (right). Total copolymer concentration was 10% *w/v* in all cases.

Sclera usually exhibits larger permeability for most drugs compared to the cornea due to its larger pores, which even allow the penetration of nanoparticles with sizes in between 20–200 nm [51]. Although *in vivo*, the surface area of absorption in the sclera is larger than that in the cornea [52], for comparative purposes in the *ex vivo* studies, the area available for diffusion was the same as that for the cornea tests. Larger amounts of natamycin accumulated in the sclera (Figure 7C,D), and once again, the poly(pseudo)rotaxanes seemed to facilitate the accumulation. Differently to the cornea, natamycin was able to permeate through sclera toward the receptor chamber. After a lag time of approximately 1 h, natamycin concentration steadily increased in the receptor medium (Figure 8). The amounts permeated were larger for the micelles than for the poly(pseudo)rotaxanes, and ordered inversely to the size of the carrier. Namely, the small Pluronic P103 micelles permeated faster than the larger Soluplus micelles and the mixed micelles.

The amount of natamycin permeated per surface area showed a linear dependence on time. The permeability coefficient (P_{app}) of natamycin across bovine sclera was calculated as the ratio of flux (J) and the concentration of natamycin in the donor phase (Table 5). In all the cases, the poly(pseudo)rotaxanes led to a smaller apparent permeability coefficient than the corresponding micelles (ANOVA and multiple range test; $F_{5,12df} = 90.73$; $p < 0.001$ in 0.9% NaCl; $F_{5,12df} = 377.62$; $p < 0.001$ in buffer pH 6.4). The smallest permeability coefficient was for Soluplus poly(pseudo)rotaxane, while the highest P_{app} corresponded to Pluronic P103 solely micelles.

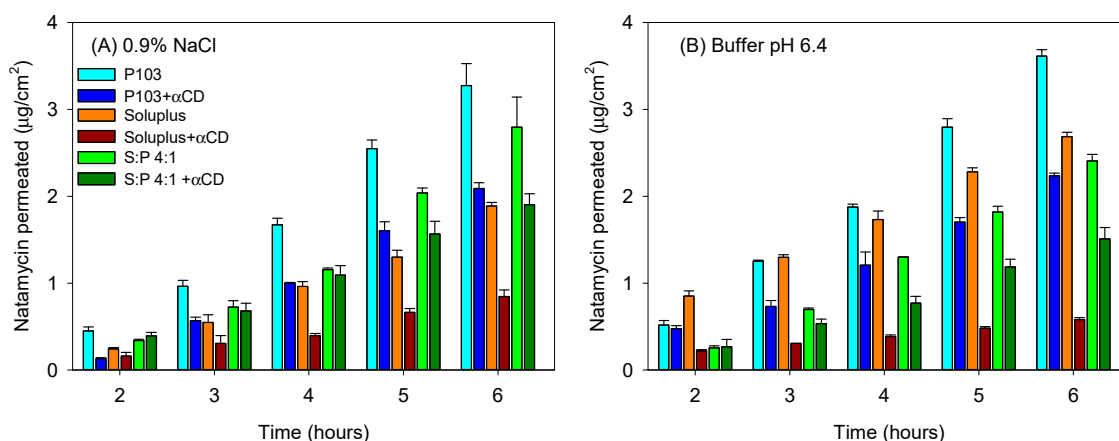


Figure 8. Amount of natamycin permeated through bovine sclera and measured in the receptor chamber as a function of time. Natamycin was formulated in Soluplus and Pluronic micelles, Soluplus:Pluronic P103 4:1 *v/v* mixed micelles, and their poly(pseudo)rotaxanes in 0.9% NaCl (A) and pH 6.4 buffer (B). Total copolymer concentration was 10% *w/v* in all cases.

Table 5. Transcleral steady state flux (*J*) and permeability coefficients (P_{app}) recorded for natamycin formulated in Soluplus and Pluronic micelles, Soluplus:Pluronic P103 4:1 *v/v* mixed micelles, and poly(pseudo)rotaxanes in 0.9% NaCl and pH 6.4 buffer. Total copolymer concentration was 10% *w/v*. Mean values and, in parenthesis, standard deviation (*n* = 3).

Formulation	0.9% NaCl		Buffer pH 6.4	
	<i>J</i> (µg/(cm ² ·h))	$P_{app} \times 10^6$ (cm/s)	<i>J</i> (µg/(cm ² ·h))	$P_{app} \times 10^6$ (cm/s)
Pluronic P103 10%	0.724 (0.042)	1.67 (0.09)	0.774 (0.032)	1.79 (0.07)
Pluronic P103 + αCD 10%	0.496 (0.023)	1.15 (0.05)	0.449 (0.012)	1.04 (0.03)
Soluplus 10%	0.403 (0.006)	0.93 (0.01)	0.466 (0.024)	1.08 (0.05)
Soluplus 10% + αCD 10%	0.174 (0.018)	0.40 (0.04)	0.090 (0.008)	0.27 (0.02)
Soluplus/Pluronic P 103 (4:1)	0.623 (0.065)	1.44 (0.15)	0.543 (0.021)	1.26 (0.05)
Soluplus/Pluronic P 103 (4:1) + αCD 10%	0.391 (0.023)	0.91 (0.05)	0.313 (0.016)	0.73 (0.04)

4. Conclusions

Soluplus and Pluronic P103 micelles as well as αCD can encapsulate natamycin, although the capability of Soluplus micelles to increase the drug apparent solubility is significantly greater. To the best of our knowledge, the formation of poly(pseudo)rotaxanes using mixed micelles has not been previously reported. Interestingly, mixed micelles of Soluplus and Pluronic show a remarkable increase in the micelle size, which suggests that the large PPO block of Pluronic P103 accommodates inside the Soluplus cores. As a consequence, the drug solubilization capability of mixed micelles is lower than that of Soluplus micelles alone. The addition of αCD to the dispersions of micelles caused a remarkable increase in both G' and G'' , and this increase was reinforced by the temperature-responsiveness of the copolymers. The increase in the apparent macroviscosity of the poly(pseudo)rotaxanes on the ocular surface conditions may be useful for prolonging their permanence. Relevantly, the increase in the macroviscosity of the poly(pseudo)rotaxanes causes a decrease in drug diffusion, especially in the case of the mixed micelles system. Overall, mixed micelles and their poly(pseudo)rotaxanes allow for tuning the features that each copolymer system exhibits separately, i.e., mixing Soluplus and Pluronic leads to intermediate natamycin diffusion, cornea and sclera accumulation, and sclera permeability coefficients, without detrimental effects on biocompatibility. Therefore, the poly(pseudo)rotaxanes of mixed micelles are identified as technological tools that are suitable for the controlled release of poorly soluble drugs.

Supplementary Materials: The following are available online at <http://www.mdpi.com/2079-4991/9/5/745/s1>, Table S1: Properties of non-loaded Soluplus and Pluronic P103 micelle dispersions in 0.9% NaCl at 25 °C. Figure S1: Structure of single and mixed nanomicelles formed by self-assembly of the amphiphilic block copolymers, and of

the CD-based poly(pseudo)rotaxanes. Figure S2: Evolution of the absorbance of natamycin-loaded Pluronic P103 (10%) nanomicelle formulations before and after 30-fold and 60-fold dilution. Figure S3: The apparent solubility of natamycin without α CD and containing 5–10% (*w/v*) in 0.9% NaCl and buffer pH 6.4 at 25 °C. Figure S4: Pictures of HET-CAM tests of Soluplus and Pluronic P103 formulations and controls.

Author Contributions: Conceptualization, T.L. and C.A.-L.; methodology, B.L.-V., H.H.S., and C.A.-L.; validation, B.L.-V., H.H.S. and C.A.-L.; resources, T.L. and C.A.-L.; writing—original draft preparation, B.L.-V., writing—review and editing, T.L., H.H.S., and C.A.-L.; supervision, C.A.-L. and H.H.S.

Funding: This research was funded by MINECO [SAF2017-83118-R], Agencia Estatal de Investigación (AEI) Spain, Xunta de Galicia (Grupo de Referencia Competitiva ED431C 2016/008; Agrupación Estratégica en Materiales-AEMAT ED431E 2018/08), and FEDER (Spain). B.L.-V. acknowledges an Erasmus+ traineeship (IS-SM2018-81075).

Acknowledgments: The authors acknowledge F. Alvarez-Rivera, A. Varela-García and M. Vivero-Lopez for help with the bovine cornea experiments.

Conflicts of Interest: The authors declare no conflict of interest.

References

1. Chang, H.Y.; Chodosh, J. Diagnostic and therapeutic considerations in fungal keratitis. *Int. Ophthalmol. Clin.* **2011**, *51*, 33–42. [[CrossRef](#)] [[PubMed](#)]
2. Mahmoudi, S.; Masoomi, A.; Ahmadikia, K.; Tabatabaei, S.A.; Soleimani, M.; Rezaie, S.; Ghahvechian, H.; Banafsheafshan, A. Fungal keratitis: An overview of clinical and laboratory aspects. *Mycoses* **2018**, *61*, 916–930. [[CrossRef](#)] [[PubMed](#)]
3. Dart, J.K.; Stapleton, F.; Minassian, D. Contact lenses and other risk factors in microbial keratitis. *Lancet* **1991**, *338*, 650–653. [[CrossRef](#)]
4. Green, M.; Apel, A.; Stapleton, F. Risk factors and causative organisms in microbial keratitis. *Cornea* **2008**, *27*, 22–27. [[CrossRef](#)]
5. Austin, A.; Lietman, T.; Rose-Nussbaumer, J. Update on the management of infectious keratitis. *Ophthalmology* **2017**, *124*, 1678–1689. [[CrossRef](#)]
6. Qiu, S.; Zhao, G.Q.; Lin, J.; Wang, X.; Hu, L.T.; Du, Z.D.; Wang, Q.; Zhu, C.C. Natamycin in the treatment of fungal keratitis: A systematic review and Meta-analysis. *Int. J. Ophthalmol.* **2015**, *8*, 597–602. [[CrossRef](#)]
7. Patil, A.; Lakhani, P.; Majumdar, S. Current perspectives on natamycin in ocular fungal infections. *J. Drug Deliv. Sci. Technol.* **2017**, *41*, 206–212. [[CrossRef](#)]
8. Arora, R.; Gupta, D.; Goyal, J.; Kaur, R. Voriconazole versus natamycin as primary treatment in fungal corneal ulcers. *Clin. Exp. Ophthalmol.* **2011**, *39*, 434–440. [[CrossRef](#)]
9. O'Day, D.M.; Head, W.S.; Robinson, R.D.; Clanton, J.A. Corneal penetration of topical amphotericin B and natamycin. *Curr. Eye Res.* **1986**, *5*, 877–882. [[CrossRef](#)]
10. Segura, T.; Puga, A.M.; Burillo, G.; Llovo, J.; Brackman, G.; Coenye, T.; Concheiro, A.; Alvarez-Lorenzo, C. Materials with fungi-bioinspired surface for efficient binding and fungi-sensitive release of antifungal agents. *Biomacromolecules* **2014**, *15*, 1860–1870. [[CrossRef](#)]
11. Cevher, E.; Sensoy, D.; Zloh, M.; Mulazimoglu, L. Preparation and characterisation of natamycin: Gamma-cyclodextrin inclusion complex and its evaluation in vaginal mucoadhesive formulations. *J. Pharm. Sci.* **2008**, *97*, 4319–4335. [[CrossRef](#)]
12. Saeed Nihad, A.H.; Salami, M. Study of storage conditions effect (light-heat) on natamycin content and stability in some dairy products (cheese-yoghurt). *Clin. Pharmacol. Biopharm.* **2017**, *6*, 177. [[CrossRef](#)]
13. Bhatta, R.S.; Chandasana, H.; Chhonker, Y.S.; Rath, C.; Kumar, D.; Mitra, K.; Shukla, P.K. Mucoadhesive nanoparticles for prolonged ocular delivery of natamycin: In vitro and pharmacokinetics studies. *Int. J. Pharm.* **2012**, *432*, 105–112. [[CrossRef](#)] [[PubMed](#)]
14. Chandasana, H.; Prasad, Y.D.; Chhonker, Y.S.; Chaitanya, T.K.; Mishra, N.N.; Mitra, K.; Shukla, P.K.; Bhatta, R.S. Corneal targeted nanoparticles for sustained natamycin delivery and their PK/PD indices: An approach to reduce dose and dosing frequency. *Int. J. Pharm.* **2014**, *477*, 317–325. [[CrossRef](#)] [[PubMed](#)]
15. Patil, A.; Lakhani, P.; Taskar, P.; Wu, K.W.; Sweeney, C.; Avula, B.; Wang, Y.H.; Khan, I.A.; Majumdar, S. Formulation development, optimization, and in vitro-in vivo characterization of natamycin-loaded PEGylated nano-lipid carriers for ocular applications. *J. Pharm. Sci.* **2018**, *107*, 2160–2171. [[CrossRef](#)]

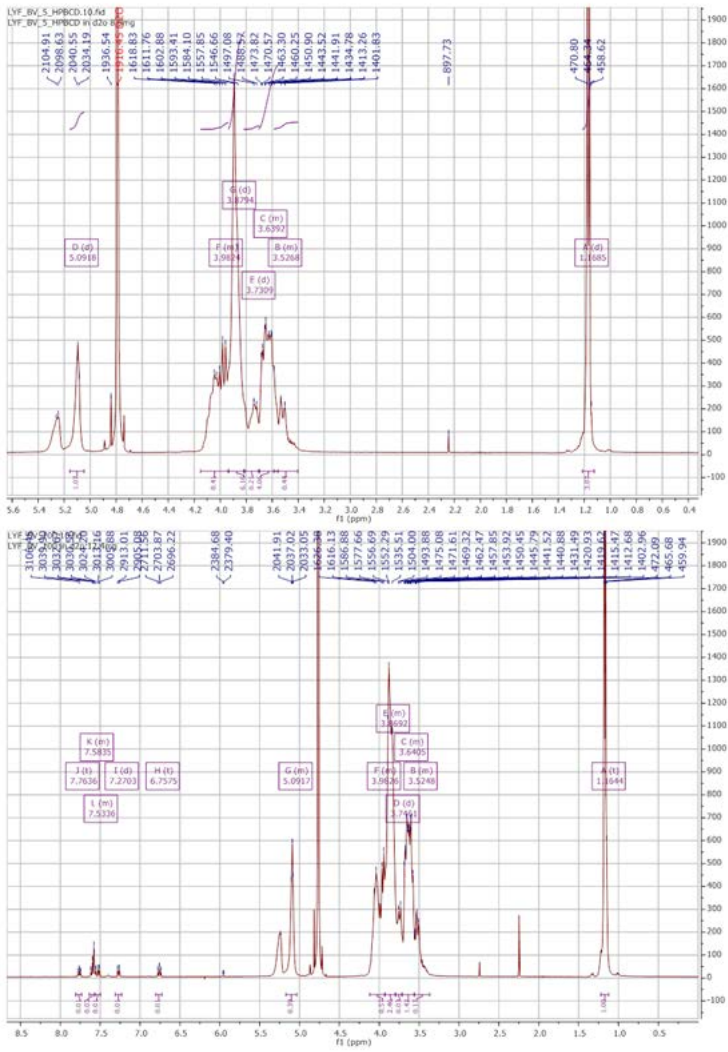
16. Janga, K.Y.; Tatke, A.; Balguri, S.P.; Lamichanne, S.P.; Ibrahim, M.M.; Maria, D.N.; Jablonski, M.M.; Majumdar, S. Ion-sensitive in situ hydrogels of natamycin bilosomes for enhanced and prolonged ocular pharmacotherapy: In vitro permeability, cytotoxicity and in vivo evaluation. *Artif. Cells Nanomed. Biotechnol.* **2018**, *1–12*. [[CrossRef](#)]
17. Phan, C.M.; Subbaraman, L.N.; Jones, L. In vitro uptake and release of natamycin from conventional and silicone hydrogel contact lens materials. *Eye Contact Lens* **2013**, *39*, 162–168. [[CrossRef](#)]
18. Koontz, J.L.; Marcy, J.E. Formation of natamycin:cyclodextrin inclusion complexes and their characterization. *J. Agric. Food Chem.* **2003**, *51*, 7106–7110. [[CrossRef](#)]
19. Phan, C.M.; Subbaraman, L.N.; Jones, L. In vitro drug release of natamycin from beta-cyclodextrin and 2-hydroxypropyl-beta-cyclodextrin-functionalized contact lens materials. *J. Biomater. Sci. Polym. Ed.* **2014**, *25*, 1907–1919. [[CrossRef](#)] [[PubMed](#)]
20. Loftsson, T.; Stefansson, E. Cyclodextrins and topical drug delivery to the anterior and posterior segments of the eye. *Int. J. Pharm.* **2017**, *531*, 413–423. [[CrossRef](#)] [[PubMed](#)]
21. Loh, X.J.; Gan, H.X.; Wang, H.; Tan, S.J.E.; Neoh, K.Y.; Tan, S.S.J.; Diong, H.F.; Kim, J.J.; Lee, W.L.S.; Fang, X.; et al. New thermogelling poly(ether carbonate urethane)s based on Pluronic F127 and poly(polytetrahydrofuran carbonate). *J. Appl. Polym. Sci.* **2014**, *131*, 39924. [[CrossRef](#)]
22. Cagel, M.; Tesan, F.C.; Bernabeu, E.; Salgueiro, M.J.; Zubillaga, M.B.; Moreton, M.A.; Chiappetta, D.A. Polymeric mixed micelles as nanomedicines: Achievements and perspectives. *Eur. J. Pharm. Biopharm.* **2017**, *113*, 211–228. [[CrossRef](#)]
23. Mandal, A.; Bisht, R.; Rupenthal, I.D.; Mitra, A.K. Polymeric micelles for ocular drug delivery: From structural frameworks to recent preclinical studies. *J. Control. Release* **2017**, *248*, 96–116. [[CrossRef](#)]
24. Chiappetta, D.A.; Sosnik, A. Poly(ethylene oxide)-poly(propylene oxide) block copolymer micelles as drug delivery agents: Improved hydrosolubility, stability and bioavailability of drugs. *Eur. J. Pharm. Biopharm.* **2007**, *66*, 303–317. [[CrossRef](#)]
25. Alvarez-Rivera, F.; Fernandez-Villanueva, D.; Concheiro, A.; Alvarez-Lorenzo, C. alpha-Lipoic acid in Soluplus((R)) polymeric nanomicelles for ocular treatment of diabetes-associated corneal diseases. *J. Pharm. Sci.* **2016**, *105*, 2855–2863. [[CrossRef](#)]
26. Simoes, S.M.; Figueiras, A.R.; Veiga, F.; Concheiro, A.; Alvarez-Lorenzo, C. Polymeric micelles for oral drug administration enabling locoregional and systemic treatments. *Expert Opin. Drug Deliv.* **2015**, *12*, 297–318. [[CrossRef](#)]
27. Dey, S.; Patel, J.; Anand, B.S.; Jain-Vakkalagadda, B.; Kaliki, P.; Pal, D.; Ganapathy, V.; Mitra, A.K. Molecular evidence and functional expression of P-glycoprotein (MDR1) in human and rabbit cornea and corneal epithelial cell lines. *Investig. Ophthalmol. Vis. Sci.* **2003**, *44*, 2909–2918. [[CrossRef](#)]
28. Marcos, X.; Perez-Casas, S.; Llovo, J.; Concheiro, A.; Alvarez-Lorenzo, C. Poloxamer-hydroxyethyl cellulose-alpha-cyclodextrin supramolecular gels for sustained release of griseofulvin. *Int. J. Pharm.* **2016**, *500*, 11–19. [[CrossRef](#)]
29. Dian, L.; Yu, E.; Chen, X.; Wen, X.; Zhang, Z.; Qin, L.; Wang, Q.; Li, G.; Wu, C. Enhancing oral bioavailability of quercetin using novel soluplus polymeric micelles. *Nanoscale Res. Lett.* **2014**, *9*, 2406. [[CrossRef](#)]
30. Jin, X.; Zhou, B.; Xue, L.; San, W. Soluplus((R)) micelles as a potential drug delivery system for reversal of resistant tumor. *Biomed. Pharmacother.* **2015**, *69*, 388–395. [[CrossRef](#)]
31. Takahashi, C.; Saito, S.; Suda, A.; Ogawa, N.; Kawashima, Y.; Yamamoto, H. Antibacterial activities of polymeric poly(dl-lactide-co-glycolide) nanoparticles and Soluplus® micelles against *Staphylococcus epidermidis* biofilm and their characterization. *RSC Adv.* **2015**, *5*, 71709–71717. [[CrossRef](#)]
32. Varela-Garcia, A.; Concheiro, A.; Alvarez-Lorenzo, C. Soluplus micelles for acyclovir ocular delivery: Formulation and cornea and sclera permeability. *Int. J. Pharm.* **2018**, *552*, 39–47. [[CrossRef](#)] [[PubMed](#)]
33. Zhang, Z.H.; Cui, C.C.; Wei, F.; Lv, H.X. Improved solubility and oral bioavailability of apigenin via Soluplus/Pluronic F127 binary mixed micelles system. *Drug Dev. Ind. Pharm.* **2017**, *43*, 1276–1282. [[CrossRef](#)] [[PubMed](#)]
34. Ke, Z.C.; Zhang, Z.H.; Wu, H.; Jia, X.B.; Wang, Y.J.E. Optimization and evaluation of Oridonin-loaded Soluplus (R)-Pluronic P105 mixed micelles for oral administration. *Int. J. Pharm.* **2017**, *518*, 193–202. [[CrossRef](#)] [[PubMed](#)]
35. Taveira, S.F.; Varela-Garcia, A.; Dos Santos Souza, B.; Marreto, R.N.; Martin-Pastor, M.; Concheiro, A.; Alvarez-Lorenzo, C. Cyclodextrin-based poly(pseudo)rotaxanes for transdermal delivery of carvedilol. *Carbohydr. Polym.* **2018**, *200*, 278–288. [[CrossRef](#)] [[PubMed](#)]

36. Puig-Rigall, J.; Serra-Gomez, R.; Stead, I.; Grillo, I.; Dreiss, C.A.; Gonzalez-Gaitano, G. Pseudo-polyrotaxanes of cyclodextrins with direct and reverse x-shaped block copolymers: A kinetic and structural study. *Macromolecules* **2019**, *52*, 1458–1468. [CrossRef]
37. Simoes, S.M.N.; Veiga, F.; Torres-Labandeira, J.J.; Ribeiro, A.C.F.; Concheiro, A.; Alvarez-Lorenzo, C. Syringeable self-assembled cyclodextrin gels for drug delivery. *Curr. Top. Med. Chem.* **2014**, *14*, 494–509. [CrossRef]
38. Bernabeu, E.; Gonzalez, L.; Cagel, M.; Gergic, E.P.; Moreton, M.A.; Chiappetta, D.A. Novel Soluplus®—TPGS mixed micelles for encapsulation of paclitaxel with enhanced in vitro cytotoxicity on breast and ovarian cancer cell lines. *Colloids Surf. B Biointerfaces* **2016**, *140*, 403–411. [CrossRef]
39. Bodratti, A.M.; Alexandridis, P. Formulation of poloxamers for drug delivery. *J. Funct. Biomater.* **2018**, *9*, 11. [CrossRef]
40. Kadama, Y.; Bharatiya, B.; Hassan, P.A.; Verma, G.; Aswal, V.K.; Bahadur, P. Effect of an amphiphilic diol (Surfynol®) on the micellar characteristics of PEO–PPO–PEO block copolymers in aqueous solutions. *Colloids Surf. A Physicochem. Eng. Asp.* **2010**, *363*, 110–118. [CrossRef]
41. Díaz-Tomé, V.; Luaces-Rodríguez, A.; Silva-Rodríguez, J.; Blanco-Dorado, S.; García-Quintanilla, L.; Llovo-Taboada, J.; Blanco-Méndez, J.; García-Otero, X.; Varela-Fernández, R.; Herranz, M.; et al. Ophthalmic econazole hydrogels for the treatment of fungal keratitis. *J. Pharm. Sci.* **2018**, *107*, 1342–1351. [CrossRef]
42. European Medicines Agency. Background Review for Cyclodextrins Used as Excipients. EMA/CHMP/333892/2013. Available online: https://www.ema.europa.eu/en/documents/report/background-review-cyclodextrins-used-excipients-context-revision-guideline-excipients-label-package_en.pdf (accessed on 1 April 2019).
43. Segredo-Morales, E.; Martin-Pastor, M.; Salas, A.; Évora, C.; Concheiro, A.; Alvarez-Lorenzo, C.; Delgado, A. mobility of water and polymer species and rheological properties of supramolecular polypseudorotaxane gels suitable for bone regeneration. *Bioconjug. Chem.* **2018**, *29*, 503–516. [CrossRef]
44. McKenzie, B.; Kay, G.; Matthews, K.H.; Knott, R.M.; Cairns, D. The hen’s egg chorioallantoic membrane (HET-CAM) test to predict the ophthalmic irritation potential of a cysteamine-containing gel: Quantification using Photoshop(R) and ImageJ. *Int. J. Pharm.* **2015**, *490*, 1–8. [CrossRef]
45. Abdelkader, H.; Ismail, S.; Hussein, A.; Wu, Z.; Al-Kassas, R.; Alany, R.G. Conjunctival and corneal tolerability assessment of ocular naltrexone niosomes and their ingredients on the hen’s egg chorioallantoic membrane and excised bovine cornea models. *Int. J. Pharm.* **2012**, *432*, 1–10. [CrossRef]
46. Alvarez-Lorenzo, C.; Gomez-Amoza, J.L.; Martinez-Pacheco, R.; Souto, C.; Concheiro, A. Microviscosity of hydroxypropylcellulose gels as a basis for prediction of drug diffusion rates. *Int. J. Pharm.* **1999**, *180*, 91–105. [CrossRef]
47. Sun, C.Q.; Lalitha, P.; Prajna, N.V.; Karpagam, R.; Geetha, M.; O’Brien, K.S.; Oldenburg, C.E.; Ray, K.J.; McLeod, S.D.; Acharya, N.R.; et al. Association between in vitro susceptibility to natamycin and voriconazole and clinical outcomes in fungal keratitis. *Ophthalmology* **2014**, *121*, 1495–1500. [CrossRef]
48. Pescina, S.; Carra, F.; Padula, C.; Santi, P.; Nicoli, S. Effect of pH and penetration enhancers on cysteamine stability and trans-corneal transport. *Eur. J. Pharm. Biopharm.* **2016**, *107*, 171–179. [CrossRef]
49. Siefert, B.; Keipert, S. Influence of alpha-cyclodextrin and hydroxyalkylated beta-cyclodextrin derivatives on the in vitro corneal uptake and permeation of aqueous pilocarpine-HCl solutions. *J. Pharm. Sci.* **1997**, *86*, 716–720. [CrossRef]
50. PubChem. Natacyn. Available online: <https://pubchem.ncbi.nlm.nih.gov/compound/natamycin#section=Solubility> (accessed on 1 April 2019).
51. Amo, E.M.; Rimpelä, A.K.; Heikkinen, E.; Karia, O.K.; Ramsay, E.; Lajunen, T.; Schmitt, M.; Pelkonen, L.; Bhattacharya, M.; Richardson, D.; et al. Pharmacokinetic aspects of retinal drug delivery. *Progr. Retin. Eye Res.* **2017**, *57*, 134–185. [CrossRef]
52. Loch, C.; Zakelj, S.; Kristl, A.; Nagel, S.; Guthoff, R.; Weitschies, W.; Seidlitz, A. Determination of permeability coefficients of ophthalmic drugs through different layers of porcine, rabbit and bovine eyes. *Eur. J. Pharm. Sci.* **2012**, *47*, 131–138. [CrossRef]

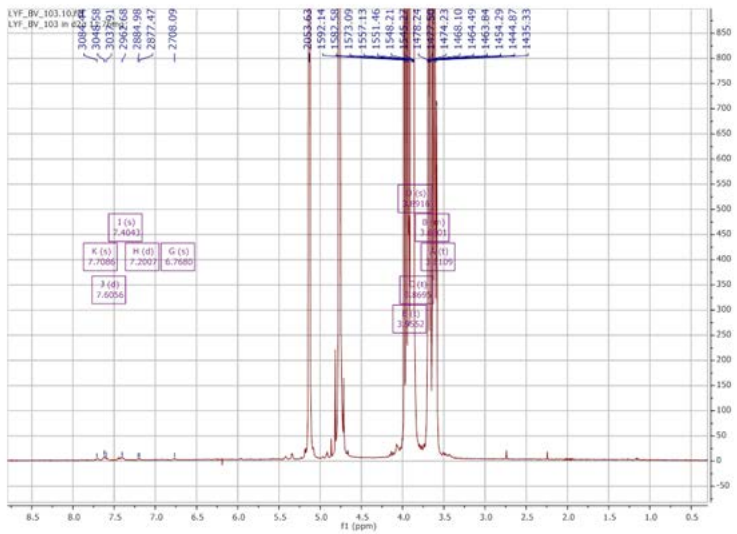
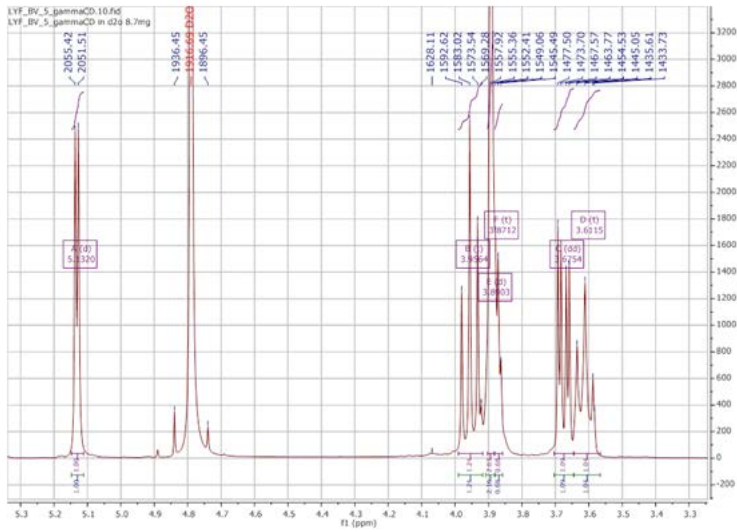


Appendix

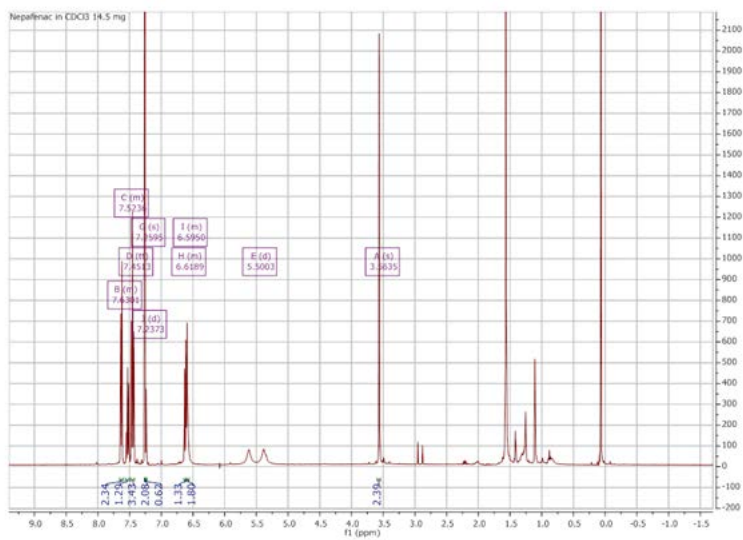
(a)



(b)



(c)



(d)

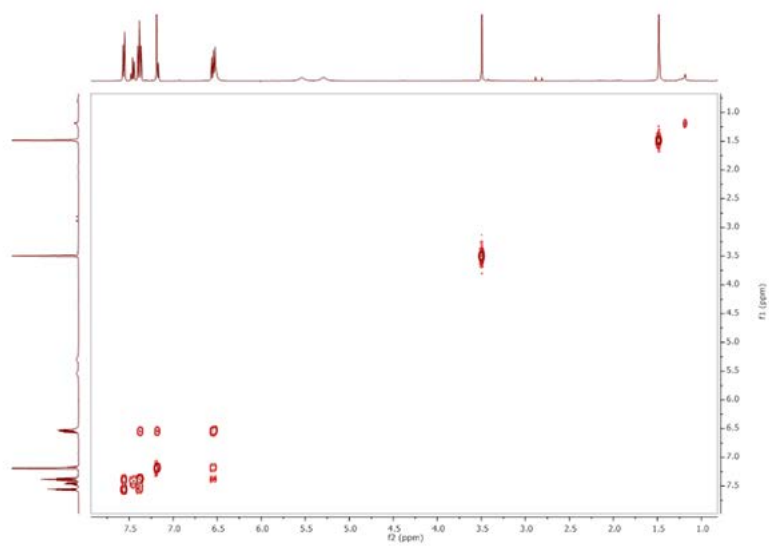


Figure A1. $^1\text{H-NMR}$ spectra corresponding to complexes of (a) nepafenac with γCD and (b) $\text{HP}\beta\text{CD}$ dissolved in D_2O , (c) nepafenac dissolved in CDCl_3 and (d) 2D COSY spectra of nepafenac in CDCl_3 .

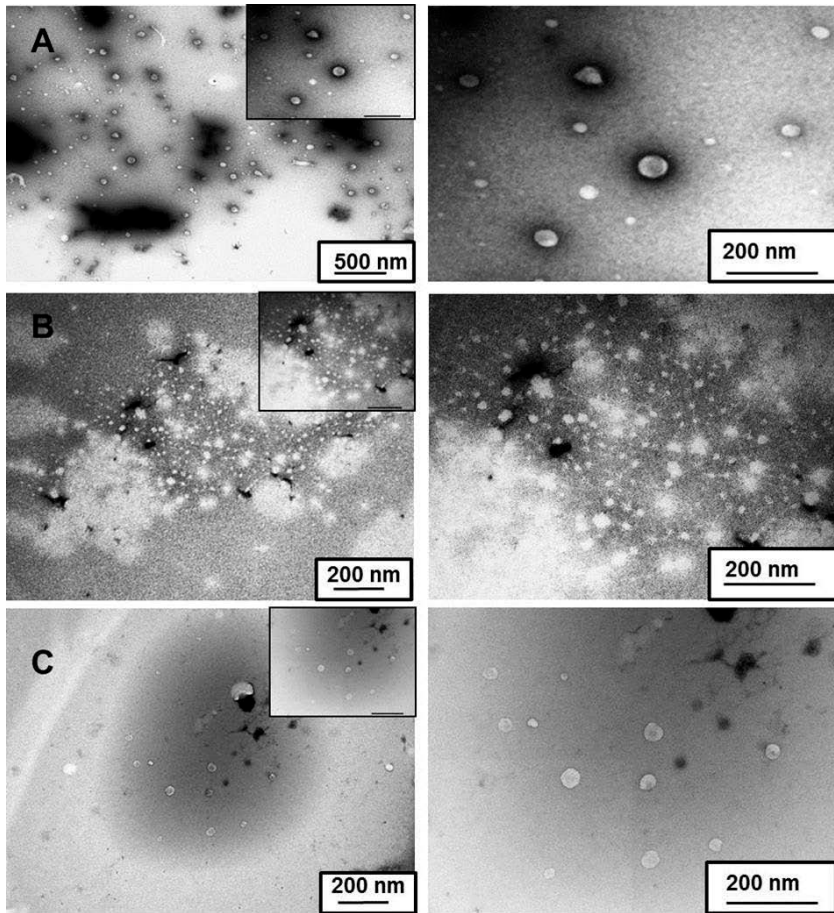


Figure A2. TEM images of (a) F2 magnified by 15k (left) and 60k (right), (b) F3 magnified by 30k (left) and 60k (right) and (c) F5 magnified by 30k (left) and 60k (right).

Table A1. Characteristics of 0.5% (w/v) eye drop formulations including solubility of nepafenac, proportion of solid drug fraction, osmolality, viscosity and aggregate size.

Formulations* (% w/v)	Solubility of nepafenac (mg/L)	Solid drug fraction (%)	Osmolality (mOsm/kg)	Viscosity (cP)	Size (nm)	
					Diameter (nm)	Vol (%)
F1 (2% PVA, 0.1 HPMC, 0.1% tyloxapol)	3.063 ±	61.26	198 ± 2	3.62	98	58.1
	0.108				424	41.9
F2 (1% CMC)	2.516 ± 0.014	50.32	338 ± 13	18.9 2 ± 2.16	212	55.4
					135	28.9
					427	13.7
					18	2
F3 (2% PVA, 1% CMC, 0.1% tyloxapol)	3.180 ± 0.066	63.60	410 ± 10	13.9 5 ± 0.36	247	88.5
					3.0	11.5
F4 (2% PVA, 0.1% tyloxapol)	3.119 ± 0.010	62.38	200 ± 2	4.17 ± 0.11	581	29
					241	28.8
					1127	23.4
					106	18.8
F5 (1% PVP, 1% CMC, 0.1% HPMC)	2.656 ± 0.074	53.12	400 ± 8	15.3 1 ± 0.88	310	50.1
					170	27.5
					13	22.4
F6 (1% PVP, 0.1% MC)	2.384 ± 0.172	47.08	186 ± 5	4.89 ± 0.31	350	77.4
					21	22.6
F7 (2% PVA, 1% CMC, 0.1% MC, 0.1% tyloxapol)	2.817 ± 0.015	56.34	390 ± 4	10.1 5 ± 0.47	208	89.4
					644	9.1
					54	1.5
F8 (1% PVP, 0.1% tyloxapol)	1.685 ± 0.054	33.70	193 ± 2	3.83 ± 0.16	17	74.5
					781	22.5
					1.0	3
F9 (2% PVA, 1% CMC, 0.1% MC)	2.422 ± 0.056	48.44	392 ± 7	13.5 6 ± 0.92	208	97.7
					28	2.3

Table A2. Properties of non-loaded Soluplus and Pluronic P103 micelle dispersions in 0.9% NaCl at 25°C (n.d.= non detectable).

Polymer concentration (%w/v)	Soluplus				Pluronic P103			
	pH	Mean diameter (nm)	PDI	Mean Zeta potential (mV)	pH	Mean diameter (nm)	PDI	Mean Zeta potential (mV)
5	3.45	73.66 ± 0.19	0.084 ± 0.004	-0.02 ± 0.05	6.30	14.77 ± 0.11	0.140 ± 0.023	-0.02 ± 0.05
4	3.54	71.04 ± 1.10	0.079 ± 0.006	-0.16 ± 0.08	6.33	15.47 ± 0.18	0.125 ± 0.019	-0.16 ± 0.08
3	3.60	69.41 ± 0.28	0.075 ± 0.005	-0.11 ± 0.07	6.26	15.44 ± 0.03	0.069 ± 0.016	-0.11 ± 0.07
2	3.69	67.55 ± 0.57	0.055 ± 0.012	-0.16 ± 0.19	6.25	17.21 ± 0.70	0.185 ± 0.016	-0.16 ± 0.19
1	3.89	69.27 ± 1.45	0.106 ± 0.034	-0.18 ± 0.08	6.24	23.81 ± 1.52	0.224 ± 0.027	-0.18 ± 0.08
0.1	4.86	68.04 ± 1.57	0.184 ± 0.066	-0.25 ± 0.04	5.70	n.d.	n.d.	-0.25 ± 0.04
0.01	5.20	70.00 ± 0.99	0.130 ± 0.034	-0.03 ± 0.18	5.57	n.d.	n.d.	-0.03 ± 0.18